

Title	The actinin family of actin crosslinking proteins: natural functions and potential applications in synthetic biology
Authors	Murphy, Anita Catherine Honor
Publication date	2016
Original Citation	Murphy, A. C. H. 2016. The actinin family of actin crosslinking proteins: natural functions and potential applications in synthetic biology. PhD Thesis, University College Cork.
Type of publication	Doctoral thesis
Rights	© 2016, Anita Catherine Honor Murphy. - http://creativecommons.org/licenses/by-nc-nd/3.0/
Download date	2025-09-08 01:20:42
Item downloaded from	https://hdl.handle.net/10468/3314

**The Actinin Family of Actin Crosslinking Proteins:
Natural Functions and Potential Applications in
Synthetic Biology**

By

Anita Catherine Honor Murphy, BSc

School of Biochemistry and Cell Biology

University College Cork, Ireland

A thesis presented to the National University of Ireland
for the degree of Doctor of Philosophy

April 2016

Supervisor: Dr. Paul Young

Head of Department: Prof. David Sheehan

Table of Contents

Declaration	5
Acknowledgements	6
List of Abbreviations	7
Abstract	10
Chapter 1: General Introduction	11
1.1 Spectrin Family Protein Members: α-Actinin and α-/β-Spectrin	12
1.1.1 Evolution	12
1.1.2 Structure	14
1.1.2.1 Actin Binding Domain	15
1.1.2.2 Calmodulin-like Domain	18
1.1.2.3 The Central Region of Spectrin Repeats	20
1.1.2.4 Pleckstrin Homology Domain	29
1.1.3 Regulation	29
1.1.3.1 Regulation of Actinin	29
1.1.3.2 Regulation of Spectrin	31
1.1.4 Function	33
1.1.4.1 Functions of Actinin Proteins	33
1.1.4.2 Functions of Spectrin Proteins: Erythrocyte Membrane Skeleton	52
1.1.5 Conclusion	55
1.2 Bionanotechnology and its Contributions to Synthetic Biology	56
1.2.1 Nucleic Acid Nanotechnology	57
1.2.1.1 Tile Based Approach	58
1.2.1.2 DNA Origami	59
1.2.1.3 RNA Nanostructures	62
1.2.2 Carbohydrate Nanotechnology	62
1.2.3 Lipid Nanotechnology	63
1.2.4 Peptide Nanotechnology	64
1.2.4.1 Dipeptides	64
1.2.4.2 Ionic Self-Complementary Peptides	65
1.2.4.3 Surfactant-like Peptides	65
1.2.4.4 Cyclic peptides	66
1.2.4.5 Coiled Coils	67
1.2.5 Proteins	69
1.2.5.1 Fusion-based Assembly	70
1.2.5.2 Ligand-mediated Assembly	71
1.2.5.3 Metal-directed	73
1.2.6 Conclusion	73
Chapter 2:	74
<i>Congenital Macrothrombocytopenia-linked Mutations in the Actin-Binding Domain of α-Actinin-1 Enhance F-actin Association</i>	74
2.1 Abstract	74

2.2 Introduction	75
2.2.1 Platelets	75
2.2.2. Platelet Production	75
2.2.3 Platelet Activation	77
2.2.4 Platelet Blood Disorders	81
2.2.4.1 A similar pathological mechanism may exist for Actinin-1 related CMTP and Actinin-4 related FSGS	83
2.3 Materials and Methods	87
2.4 Results	93
2.4.1 <i>In Vitro</i> Functional Analysis of the <i>ACTN1</i> -CMTP Associated Mutations	93
2.4.1.1 A Comparative Study on the Solubility of WT and CMTP-Associated Mutant Actinin-1 Proteins	93
2.4.1.2 A Comparative Study on Actin-Binding/Bundling Ability Between WT Actinin-1 and CMTP-Associated Mutant Actinin-1 Proteins	94
2.4.2 <i>In Cellula</i> Functional Analysis of <i>ACTN1</i> -CMTP Associated Mutations	103
2.4.2.1 Comparison of Actin Organization in WT Actinin-1 or Mutant Actinin-1 Expressing Cells	103
2.4.2.2 Comparison of the Stability of the Association of WT-Actinin-1 or Mutant-Actinin-1 with Actin	106
2.5 Discussion	111
2.6 Conclusion	117
Chapter 3:	118
<i>Assessment of the Actinin and Spectrin Dimerisation Domains in view of their use as Potential Nanostructure Building Blocks</i>	118
3.1 Abstract	118
3.2 Introduction	119
3.2.1 Actinin Dimerisation	119
3.2.1.1 The Staggered Model for the Actinin Rod Domain	119
3.2.1.2 The Aligned Model for the Actinin Rod Domain	121
3.2.2 Spectrin Dimerisation	122
3.2.3 Strategies for the Characterisation of Actinin and α -/ β -Spectrin Rod Domains	125
3.2.4 Strategies for Inducible Co-expression of Multiple Proteins in <i>E. coli</i>	126
3.2.4.1 P_{BAD} Expression System	127
3.2.4.2 The <i>T7lac</i> Expression System	130
3.2.4.3 Crosstalk between the <i>T7lac</i> Promoter and the P_{BAD} Promoter	131
3.2.5 Objectives	132
3.3 Materials and Methods	134
3.4 Results	145
3.4.1 Expression and Purification of Spectrin-like and Spectrin Repeat Containing Constructs from Actinin and Spectrin	145
3.4.2.1 Choosing a Bacterial Co-Expression Strategy	146
3.4.2.2 Optimizing Co-expression of Actinin Spectrin-like Repeat Constructs using a Two-Plasmid Co-expression System	148
3.4.2.3 Crosstalk Between the <i>T7</i> Expression System and the P_{BAD} Expression System	151

3.4.3 Heterodimer Purification	158
3.4.3.1 Actinin Dimer and α -/ β -Spectrin Heterodimer Purification	158
3.4.3.2 Improvement of Dimer/Protein Complex Purification Strategy	159
3.4.4 Actinin Spectrin-like Repeat Dimerisation Studies	160
3.4.4.1 Actinin spectrin-like repeat Interaction Assays	161
3.4.4.2 Assessment of Actinin spectrin-like repeat Dimers Using Native-PAGE	166
3.4.5 Dimeric Actinin spectrin-like repeat Stability Assay Studies	167
3.4.5.1 Investigating the Effect of Salt Concentration on the Structural Stability of Actinin Dimers	168
3.4.5.2 The Investigation of the Thermostability of Actinin Dimers	171
3.4.6 α -/ β -Spectrin Spectrin Repeat Dimerisation Studies	175
3.4.6.1 α -/ β -Spectrin spectrin repeat Interaction Assay	175
3.4.6.2 Assessment of α -/ β -Spectrin spectrin repeat Heterodimers Using Native-PAGE	176
3.4.7 Heterodimeric α -/ β -Spectrin spectrin repeat Stability Assays Studies	178
3.4.7.1 Investigating the Effect of Salt Concentration on the Structural Stability of Spectrin r1-r4/r18-21 Heterodimers	179
3.4.7.2 The Investigation of the Thermostability of Spectrin r1-r4/r18-21 Heterodimers	180
3.5 Discussion	183
3.5.1 Co-expression System	183
3.5.2 Heterodimer Purification	185
3.5.3 Actinin Spectrin-like Repeats and α -/ β -Spectrin Spectrin Repeats: Dimerisation Studies	186
3.5.4 Actinin Spectrin-like Repeat Dimers and α -/ β -Spectrin Spectrin Repeat Heterodimers: Stability Assays	189
3.6 Conclusion	192
Chapter 4:	193
4.1 Abstract	193
4.2 Introduction	194
4.2.1 Approaches and Principles for Designing Protein Nanostructures	195
4.2.2 Objectives	197
4.3 Materials and Methods	198
4.4 Results	204
4.4.1 Evaluation of Fusion-based Assembly Strategy Employing Two Homodimeric Oligomerisation Domains	204
4.4.1.1 Assessment of Fusion-protein Linkers	205
4.4.1.2 Analysis of Possible Protein Assemblies using Electron Microscopy	212
4.4.1.3. Generation of Orthogonal Homodimeric Actinin Rod Fusion Proteins	218
4.4.2 Evaluation of Fusion-based Strategy Employing Heterodimeric and Homodimeric Oligomerisation Domains	223
4.4.2.1 Connection of Heterodimeric and Homodimeric Oligomerisation Domains with Flexible Linkers	225
4.4.2.2 Connection of Heterodimeric and Homodimeric Oligomerisation Domains with Rigid Helical Linkers	226
4.4.3 Evaluation of Fusion-based Strategy Employing Three Protein Oligomerisation Domains	234
4.5 Discussion	237

4.5.1 Homodimeric Actinin Rod Fusion Proteins	237
4.5.2 Orthogonal Actinin Rod Fusion Proteins	238
4.5.3 Major Findings from Fusion-Protein Strategy: Using Homodimeric Protein Oligomerisation Domains	239
4.5.4 Heterodimeric to Homodimeric Fusion Proteins and Their Major Findings	240
4.5.5 Negative Stain Electron Microscopy for Homodimeric Actinin Rod Fusion-Proteins and Heterodimeric-to-Homodimeric Fusion Proteins	242
4.5.6 Molecular Modelling	244
4.6 Conclusions	246
5. Bibliography	247
6. Appendix	290

Declaration

This thesis is my own work and has not been submitted for another degree either at University College Cork or elsewhere.

Anita Murphy

Acknowledgements

Firstly, I would thank my supervisor Dr Paul Young for providing me with the opportunity to work in his lab and for his teaching, encouragement and guidance. I would next like to thank The Irish Research Council for their support of my work. My thanks to all members of the School of Biochemistry and Cell Biology, particularly Dr. Andrew Lindsay for his help with confocal microscopy and Ms Suzanne Crotty, from the Department of Anatomy and Neuroscience, for her experience with electron microscopy. A special mention to the technical staff; Pat, Noreen, Jenny and Tricia.

I must also thank Joan Lenihan, a great work colleague, and a brilliant friend. Finally, I would like to thank my parents for their care and kind words.

List of Abbreviations

ABD	Actin Binding Domain
ABS	Actin Binding Site
ALAD	Aminolevulinic Acid Dehydrogenase
APP	Amyloid Precursor Protein
ATP	Adenosine Triphosphate
BSA	Bovine Serum Albumin
BSS	Bernard-Soulier syndrome
CaCl ₂	Calcium Chloride
CaM	Calmodulin-like Domain
CB	Chicken Brain
CMTp	Congenital Macrothrombocytopenia
CRP	Cysteine Rich Protein
DCM	Dilated Cardiomyopathy
DHFR	Dihydrofolate Reductase
DTT	Dithiothreitol
ECM	Extracellular matrix
EGTA	Ethylene Glycol Tetra Acetic Acid
EMS	Erythrocyte Membrane Skeleton
FSGS	Focal Segmental Glomerulosclerosis
FRAP	Fluorescence Recovery After Photobleaching
GFP	Green Fluorescent Protein
GST	Glutathione-S-Transferase
H	Hydrophobic
HCM	Hypertrophic Cardiomyopathy
HE	Human Erythroid
HE	Hereditary Elliptocytosis
HPLC	High Performance Liquid Chromatography
IMS	Invaginated Membrane System
ICAM	Intracellular Adhesion Molecule

IPTG	Isopropyl- β -D-1-Thiogalactopyranoside
IR	Infrared
LB	Luria Broth
LCNEC	Large Cell Neuroendocrine Carcinoma
MCS	Multiple Cloning Site
MBP	Maltose Binding Protein
Mg ⁺²	Magnesium
MgCl ₂	Magnesium Chloride
MgSO ₄	Magnesium Sulphate
MLP	Muscle LIM Protein
MTX	Methotrexate
NaF	Sodium Fluoride
NaCl	Sodium Chloride
Na ₂ HPO ₄	Sodium Phosphate Dibasic
NaH ₂ PO ₄	Sodium Phosphate Monobasic
Na ₃ VO ₄	Sodium Orthovanadate
Ni	Nickel
NP-40	Nonyl Phenoxy polyethoxy ethanol
OSCC	Oral Squamous Cell Carcinoma
P	Polar
PBS	Phosphate Buffered Saline
PFA	Paraformaldehyde
PH	Pleckstrin Homology
PIP ₂	Phosphatidylinositol 4,5 bisphosphate
PIP ₃	Phosphatidylinositol 3, 4, 5 bisphosphate
PMSF	Phenylmethanesulfonyl fluoride
PS	Phosphatidylserine
PTA	Phosphotungstic Acid
r1r2	spectrin repeats 1 and 2
r2r3	spectrin repeats 2 and 3
r3r4	spectrin repeats 3 and 4

r1r2r3	spectrin repeats 1 to 3
r2r3r4	spectrin repeats 2 to 4
r1r2r3r4	spectrin repeats 1 to 4
r18r19r20r21	spectrin repeats 18-21
RBC	Red Blood Cell
SCLC	Small Cell Lung Cancer
SH3	SRC homology 3 domain
TEV	Tobacco Etch Virus
UA	Uranyl Acetate
vWF	von Willebrand Factor
WT	Wildtype
YFP	Yellow Fluorescent Protein

Abstract

Actinin and spectrin proteins are members of the Spectrin Family of Actin Crosslinking Proteins. The importance of these proteins in the cytoskeleton is demonstrated by the fact that they are common targets for disease causing mutations. In their most prominent roles, actinin and spectrin are responsible for stabilising and maintaining the muscle architecture during contraction, and providing shape and elasticity to the red blood cell in circulation, respectively. To carry out such roles, actinin and spectrin must possess important mechanical and physical properties. These attributes are desirable when choosing a building block for protein-based nanoconstruction.

In this study, I assess the contribution of several disease-associated mutations in the actinin-1 ABD that have recently been linked to a rare platelet disorder, congenital macrothrombocytopenia. I investigate the suitability of both actinin and spectrin proteins as potential building blocks for nanoscale structures, and I evaluate a fusion-based assembly strategy to bring about self-assembly of protein nanostructures.

I report that the actinin-1 mutant proteins display increased actin binding compared to WT actinin-1 proteins. I find that both actinin and spectrin proteins exhibit enormous potential as nano-building blocks in terms of their stability and ability to self-assemble, and I successfully design and create homodimeric and heterodimeric bivalent building blocks using the fusion-based assembly strategy.

Overall, this study has gathered helpful information that will contribute to furthering the advancement of actinin and spectrin knowledge in terms of their natural functions, and potential unnatural functions in protein nanotechnology.

Chapter 1: General Introduction

Actin is a fundamental constituent of the cytoskeleton. It functions in many cellular processes such as cell division, cellular motility, endocytosis and intracellular trafficking, and is also responsible for providing the cell with shape and strength (Winder & Ayscough 2005). As a result, the organisation and arrangement of actin filaments into bundles and networks is central to preserving the integrity of the cell (Winder & Ayscough 2005). Actin bundling and actin binding (Fig. 1.1) are the two main methods used to assemble and organise actin filaments (Winder & Ayscough 2005) and proteins known to have such functions can be found in the Spectrin Superfamily of Proteins (Broderick & Winder 2005).

This family includes the cytoskeletal proteins α -actinin, α - and β -spectrin, dystrophin and their homologues and isoforms. Proteins in this family all share common structural features and all perform the same basic function, that is to crosslink actin filaments to each other or to the cell membrane. But despite this, their differing number of homologous repeating units, spectrin repeats, imparts important functional differences between them (Yan et al. 1993).

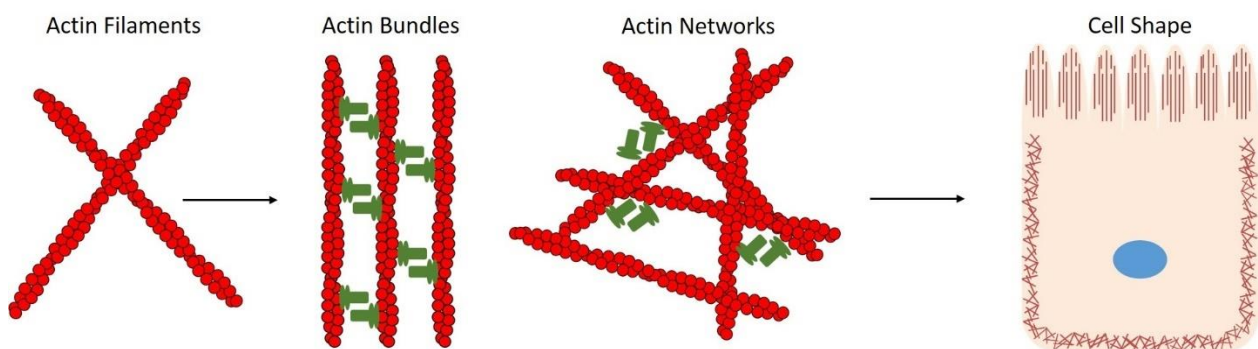


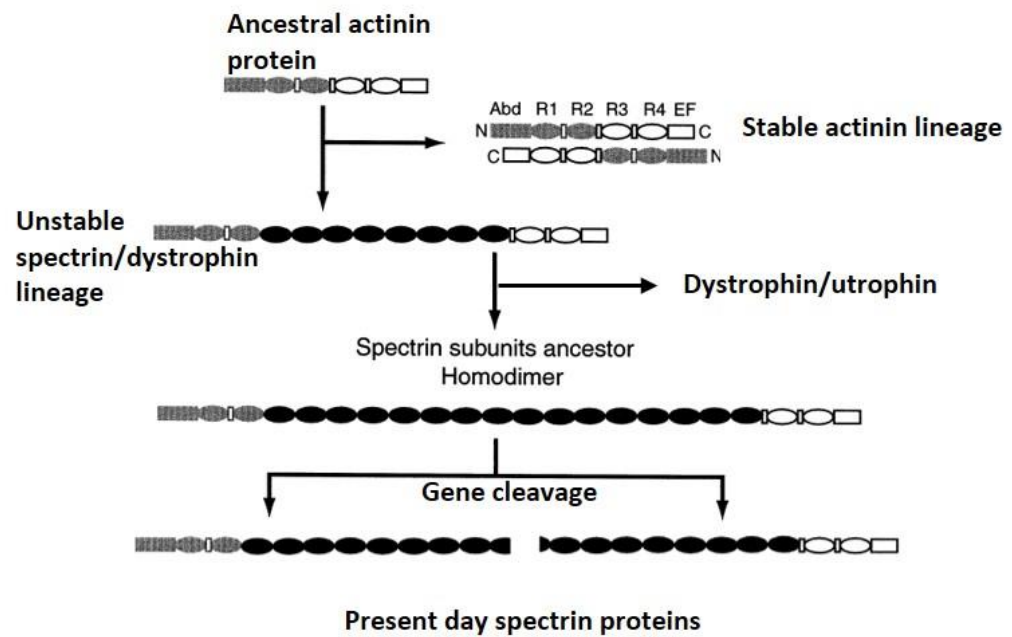
Figure 1.1: Actin Crosslinking Proteins. Such proteins are responsible for organising actin filaments into bundles and networks. These forms of organisation permit actin to function in many types of cellular process, and also provide the cell with shape (Winder & Ayscough 2005; Broderick & Winder 2005).

1.1 Spectrin Family Protein Members: α -Actinin and α -/ β -Spectrin

1.1.1 Evolution

It is believed that the members of this family evolved from a common ancestral actinin ancestor, but difficulties in aligning the dystrophin sequence to the actinin and spectrin sequences suggests that dystrophin/utrophin diverged from this path at a very early stage (Pascual et al. 1997). Sequence alignments between actinin and spectrin however have revealed that they share notable homology within their protein domains. The N-terminal of actinin shares sequence similarity to the N-terminal of β -spectrin (Byers et al. 1989) while the C-terminal of actinin shares sequence similarity to the C-terminal of α -spectrin (Dubreuil et al. 1989). Also, sequence alignments and phylogenetic tree analysis have reported the existence of a common ancestor for repeat 1 of actinin and repeat 1 of β -spectrin, the same has also been found for remaining repeats 2-4 of actinin and repeats 2 of β -spectrin and repeats 20-21 of α -Spectrin, respectively (Pascual et al. 1997). An 8-residue amino acid insertion has been conserved in the linker region between the four actinin spectrin-like repeats and the spectrin spectrin repeats β 1-2 and α 20-21 (Viel & Branton 1994). This insertion is responsible for specifying the correct lateral register between these repeats (Viel, 1999), of which is important for self-assembly (Viel & Branton, 1994).

One theory (Fig. 1.2) proposes that this ancestral actinin protein possessed four spectrin-like repeats, duplication of its gene sequence generated one stable actinin lineage and one unstable spectrin/dystrophin lineage. The stable actinin lineage brought about the development of the present day actinin genes, while the unstable spectrin/dystrophin lineage, through genetic rearrangements and unequal crossing-over events gained additional repeats, and developed into one very long gene. A gene cleavage event in this elongated gene sequence produced two functional genes, each encoding the α -spectrin subunit or the β -spectrin subunit (Viel 1999).



Adapted from Viel 1999

Figure 1.2: Evolution of the Spectrin Superfamily. Gene duplication of the actinin ancestral protein gave rise to one stable actinin lineage and one unstable spectrin/dystrophin. The stable lineage eventually gave rise to present day actinin genes. The unstable lineage gained additional repeats and formed one elongated actinin-like gene. The dystrophin lineage diverged from the model at this point. A gene cleavage event divided this elongated gene into two, leading to the generation of present day α - and β -spectrin proteins.

An alternative theory suggests that the original ancestral actinin possessed one spectrin repeat, not four (Viral & Backman, 2004). Early in invertebrate evolution, intragenic duplication generated a second repeat. Another round of intragenic duplication brought the total number of repeats to four (Viral & Backman, 2004).

Regarding evolution of the actinin family; two courses of genome duplication that occurred in vertebrate evolution, known as the 2R hypothesis (Hughes, 1999; Durand, 2003), gave rise to the two vertebrate actinin groups; the calcium sensitive non-muscle isoforms (actinin-1/-4) and the calcium insensitive muscle isoforms (actinin-2/-3) (Fig. 1.3) (Viral and Backman, 2004). Functional divergence occurred between these isoforms in respect of avoiding gene loss (Lek et al. 2010). Neo-functionalisation, where only one of the duplicates acquires specific functions (Lek et al. 2010), occurred between actinin-1 and actinin-4; actinin-4 appears to have unique functions in the kidney (Kaplan et al, 2000; Weins

et al, 2005), plays a role in cancer and acts as a transcriptional regulator (Honda 2015 and references therein). Sub-functionalisation, where both duplicates acquire specific changes (Lek et al. 2010), or neo-functionalisation between actinin-2 and actinin-3 has generated an actinin-2 isoform that is the principal actin crosslinker in the sarcomeric Z-disc, and an actinin-3 isoform whose function is specialised to type two fast glycolytic skeletal muscle fibres (Lek et al. 2010). A multiple sequence alignment of human actinin proteins (actinin-1,-2,-3 and -4) and actinin sequences from select model organisms is provided in Appendix at the back of this document.

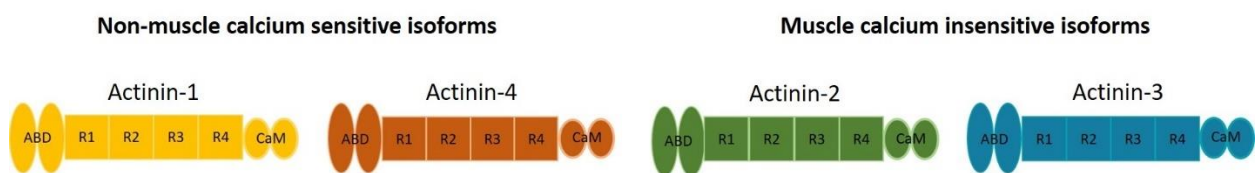


Figure 1.3: The α -Actinin Family. There are four actinin isoforms, two non-muscle isoforms (actinin-1; yellow, and actinin-4; brown) and two muscle isoforms (actinin-2; green, and actinin-3; blue). The non-muscle isoforms are expressed in most cell types (Foley & Young 2014). Their actin binding activity is regulated by calcium binding to their CaM domain (Sjöblom et al. 2008). The muscle isoforms are expressed in muscle cells (Beggs et al. 1992). Their actin binding activity is not calcium regulated (Blanchard et al. 1989). The colour scheme used for each isoform in this figure is used in subsequent figures through-out this document.

1.1.2 Structure

Actinin functions as a homodimer made up of two identical monomers. Each monomer comprises an N-terminal actin-binding domain (ABD), a rod domain composed of four spectrin-like repeats, and a C-terminal Calmodulin-like domain (CaM). Anti-parallel dimerisation positions an ABD at both ends of the molecule, this facilitates actin crosslinking (Sjöblom et al. 2008; Ribeiro et al. 2014). Within this dimer, the ABD of one actinin monomer is situated next to and opposite the CaM domain of the opposing actinin monomer (Ribeiro et al. 2014).

Spectrin is a heterodimeric protein complex that is made up of an α -spectrin and a β -spectrin protein subunit. The α -spectrin subunit comprises a CaM domain and 20 full length spectrin repeats, while the β -spectrin subunit comprises an ABD and 16 full length spectrin repeats. Dimerisation between both generates a

heterodimer in which the β -spectrin ABD lies opposite the α -spectrin CaM (Baines 2009).

1.1.2.1 Actin Binding Domain

The ABD allows for direct interaction with actin filaments, and is found at the N-terminal of both actinin and β -spectrin proteins. For both actinin and β -spectrin, the ABD is made up of two tandem calponin homology domains, CH1 and CH2 (Gimona et al. 2002). Four main α -helices (A, C, E and G) make up the principal structure of the CH domain, and together they form the core of the protein; helices C and G are parallel to each other and are wedged between helix A on one side and helix E on the other (Fig. 1.4) (Djinovic-Carugo et al. 1997; Franzot et al. 2005). β -spectrin CH domain structure contains three minor helices (B, D, and F) however only two of these, B and F, are present in the actinin structure (Fig. 1.4). Helix D, which normally connects helices C and E is absent in all CH domains in actinin (Djinovic-Carugo et al. 1997; Franzot et al. 2005).

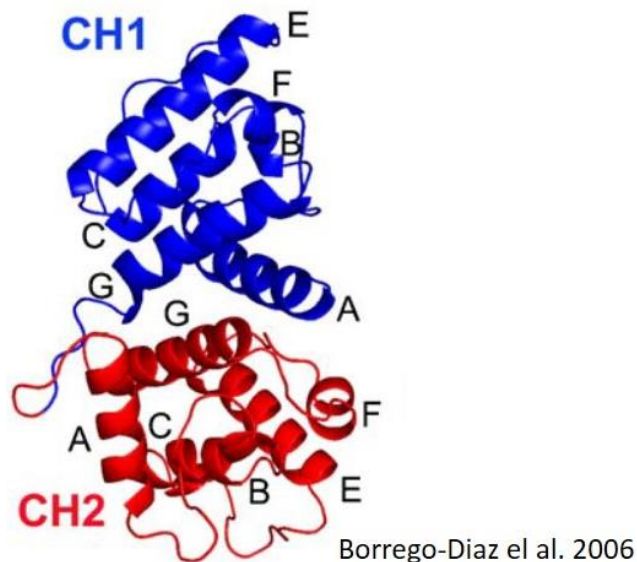


Figure 1.4: Structure of the actinin ABD. The actinin ABD is made up of two CH domains, CH1 (blue) and CH2 (red), each consisting of four main α -helices, A, C, E and G, and 2 minor α -helices, B and F. The "closed" conformation is achieved through extensive interactions between the two CH domains whereby the A and G helices of CH1 pack against the G and F helices of CH2 (Franzot et al. 2005; Borrego-Diaz et al. 2006).

Despite both types of CH domain (CH1 and CH2) having similar structures they have been found to be functionally inequivalent. CH1 alone displays affinity for actin, but CH2 has no affinity for actin filaments. However, actin affinity displayed by CH1 is much lower than the actin affinity displayed by the complete ABD, indicating that the presence of CH2 must contribute to the actin binding interaction (Way et al. 1992; Gimona et al. 2002). It may be that CH1 plays a role in making contact with the actin filaments, while CH2 enhances this binding (Bañuelos et al. 1998; Way et al. 1992). However, deletion of the first 20 amino acids of CH2 of β -spectrin was found to expose CH2 actin binding activity (An et al, 2005). In addition to strengthening actin binding, the CH2 domain is also the binding site for PIP₂ in the actinin protein (Ribeiro et al. 2014) (discussed further in section 1.1.3.1), and the binding site for protein 4.1 in the β -spectrin protein (An et al. 2005) (discussed further in section 1.1.3.2). Many older studies, such as these involving mutational (Hemmings et al. 1992; Kuhlman et al. 1992) and NMR spectroscopy (Levine et al. 1992; Levine et al. 1990) analyses of dystrophin and actinin, have identified three regions responsible for actin binding, actin binding sites 1, 2 and 3 (ABS1-3). Actinin crystal structures, and others, have reported their location to be; on the N-terminal A helix and C-terminal G helix of CH1, and on the region connecting both CH domains very near the N-terminal Helix A of CH2. Both ABS2 and ABS3 are located close to each other on the surface of the domain, while ABS1 is partially buried in the region between the two CH domains (Borrego-Diaz et al. 2006; Franzot et al. 2005).

There has been considerable questioning regarding the conformation of the ABD. The crystal structures of ABDs have been reported for dystrophin (Norwood et al. 2000), utrophin (Keep et al. 1999), fimbrin (Goldsmith et al. 1997) and all four isoforms of actinin (Lee et al. 2008; Franzot et al. 2005; Borrego-Diaz et al. 2006; Ribeiro et al. 2014). For each of these, CH1 and CH2 are reported to be in very close contact, a “closed” conformation, which is represented by a large amount of interactions between the two CH domains (Keep et al, 1999; Norwood et al, 2000; Lee et al. 2008; Franzot et al. 2005; Borrego-Diaz et al. 2006; Ribeiro et al. 2014). For both dystrophin and utrophin however, close contact between the CH domains (i.e. the “closed” conformation), occurs through the form of antiparallel dimers

where the CH1 domain of one ABD interacts with the CH2 domain of the other ABD, this may not have any biological relevance as this type of occurrence is generally regarded as an artefact associated with crystallography, it is known as domain swapping. Each dystrophin or utrophin ABD monomer contributing to the dimer however exhibits a “open” conformation (dumb-bell shape), in which both CH domains are uncoupled from each other via extension of the central connecting α -helix (Norwood et al. 2000; Keep et al. 1999). The solution structures of the utrophin and dystrophin ABDs have been found to be monomeric in solution in the “closed” conformation (Winder et al. 1995; Singh & Mallela 2012), this is supported by the observation that the utrophin ABD undergoes limited proteolysis when treated with chymotrypsin and trypsin; the cleavage products obtained are not as a result of cleavage of the central CH domain connecting α -helix (Moores & Kendrick-Jones. 2000). The compact “closed” conformation must protect this central α -helix from digestion (Moores & Kendrick-Jones. 2000). Studies involving cryo-EM reconstructions of actin filaments decorated with utrophin ABDs have reported that the utrophin ABD binds to actin in the “open” conformation (Moores et al. 2000). For the actinin ABD, cryo-EM studies of chicken gizzard actinin crystals have reported that each ABD at either end of the dimer display conformational diversity; the ABD at one end of the molecule displays a “closed” conformation, while the ABD at the other end displays the “open” conformation (Liu et al. 2004). As mentioned above, ABS1 is buried between the two CH domains, therefore, to efficiently bind actin, structural rearrangements of the CH domains may be required (Borrego-Diaz et al. 2006). Also, the interface between the two CH domains is moderately conserved and semi polar, suggesting that this interface is favourable to structural changes and rearrangements (Borrego-Diaz et al. 2006). Cysteine mutagenesis of the utrophin ABD has revealed that utrophin binds actin in the “open” conformation (Broderick et al. 2012) and cryo-electron microscopy reconstructions of actin filaments decorated with actinin ABDs have reported that the “closed” ABD conformation is not agreeable to actin binding (Galkin et al. 2010). This latter study suggests that a conformational rearrangement is necessary due to steric clash between CH2 and actin when the ABD is in the “closed” conformation, rather than exposure of another ABS1.

It may be however, that all actin binding proteins do not require structural rearrangements of their ABDs for effective actin binding. The crystal structure of fimbrin ABD and helical reconstructions of actin filaments decorated with fimbrin ABDs have reported that, for fimbrin, actin binding does not involve ABS1. Actin binding occurs when the fimbrin ABD is in the “closed” conformation and therefore involves only ABS2 and ABS3 (Hanein et al. 1998). Fimbrin has a much longer than usual central linker connecting the two CH domains, this may account for its different actin binding mechanism (Gimona et al, 2002).

Ribeiro et al (2015) have reported the crystal structure of the human actinin-2 dimer. This study has confirmed the closed conformation of the unbound actinin ABD and provides details on the intramolecular mechanisms that regulate actin binding for the actinin muscle isoforms. It is important to mention that it may be unreliable to focus all attention on the three ABSs in attempting to answer the “open” or “closed” debate on the conformation of the ABD. Studies identifying these sites (mentioned above) made use of peptides, rather than fully folded domains, and so residues on the domain surface that are not normally available for actin interaction may have been capable of actin interaction in peptide binding studies (Keep et al, 1999).

1.1.2.2 Calmodulin-like Domain

EF hand motifs are helix-loop-helix structures that function to chelate divalent ions such as calcium. They appear in pairs and form a globular domain (Ikura 1996). Two pairs of EF hands (EF1-2 and EF3-4; four EF-hands in total) make up the C-terminal CaM domain of α -spectrin and actinin (Trave et al. 1995; Sjöblom et al. 2008). In general, the binding of calcium to this globular domain induces in it a conformational change whereby it transitions from a closed to an open conformation, allowing it to interact with its targets (Ikura 1996).

1.1.2.2.1 Actinin CaM Domain

In non-muscle calcium sensitive actinins, this CaM domain serves to regulate actin binding. At a calcium concentration above 10^{-7} M, actin binding is impaired (Sjöblom et al. 2008).

Muscle isoforms have lost their ability to bind calcium due to several mutations in their EF hand motifs that are important for calcium co-ordination (Blanchard et al. 1989). This may have been an evolutionary adaption brought about to avoid the destabilising effect of calcium on the muscle architecture during times of calcium induced contractions (Blanchard et al. 1989). Cryo-electron microscopy studies of the full length actinin dimer from rabbit skeletal muscle (Tang et al. 2001) and chicken gizzard smooth muscle (Liu et al. 2004) reported that the CaM domain from one actinin molecule was positioned between the two CH domains of the opposite actinin molecule in the dimer, while the crystal structure of the human actinin-2 dimer (Ribeiro et al, 2014) has reported that the EF3-4 pair engages the helical linker that connects the actinin ABD to spectrin-like repeat 1 of the central rod domain. This helical linker contains an acknowledged calcium/calmodulin binding motif (Ribeiro et al, 2014). This interaction is stabilised by hydrogen bonds and stacking interactions between spectrin-like repeat 1 and the EF3-4 pair (Ribeiro et al, 2014).

These structural studies suggest that within the actinin dimer, the CaM domain of one monomer administers regulatory control over the actin binding of the adjacent and opposite ABD, this is discussed further in section 1.1.3.1.

1.1.2.2.2 α -Spectrin CaM Domain

Similar to actinin, close contact between the α -spectrin CaM domain and the β -spectrin ABD suggests that the α -CaM domain plays a role in regulating actin binding of the adjacent β -ABD (Broderick & Winder, 2005). Indeed, protein minispectrin complexes made up of truncated α -spectrin proteins (containing only spectrin repeats 18-21, the EF1-2 pair of the CaM domain and an abridged EF3-4 pair), and truncated β -spectrin proteins (containing CH1 and CH2 of the ABD and spectrin repeats 1-4) have a reduced ability to bind actin (Korsgren and Lux, 2010). Also, independent β -spectrin proteins do not bind actin (Cohen & Langley 1984) even in the presence of protein 4.1 (Cohen & Langley, 1984), the importance of this latter protein, protein 4.1, is discussed further in section 1.1.3.2. Therefore, the CaM domain, specifically the EF3-4 pair, must contribute to actin binding.

Within the α -spectrin CaM domain only one pair of EF-hand motifs are functional with regard to calcium binding; the EF1-2 (N-terminal) is calcium sensitive and responsive to calcium in the millimolar range, while the EF3-4 (C-terminal) is thought to be calcium insensitive (Trave et al. 1995). The functions of non-erythroid spectrin are believed to be calcium regulated, while the functions of erythroid spectrin are not; erythroid α -Spectrin has a calcium dissociation constant in the low millimolar range, 0.5mM, and therefore it is believed that the physiological micromolar concentrations of calcium that exist in erythrocytes have no effect on α -spectrin calcium binding (Korsgren & Lux 2010). In the body, non-erythroid Spectrin has many more varied roles compared to erythroid spectrin therefore, calcium regulation may be necessary to control and organise these different functions (Buevich et al, 2004). It is interesting to note, however, that one study has reported that the erythroid α -spectrin CaM is responsive to micromolar concentrations of calcium *in vitro* (Korsgren et al, 2010). This is discussed further in section 1.1.3.2.

1.1.2.3 The Central Region of Spectrin Repeats

Spectrin repeats are one of the protein units which Nature has used to build long protein molecules, such as those in the Spectrin Family of Proteins. They act as spacers to separate protein interaction domains, such as the ABDs of dimeric members of the Spectrin Superfamily. However, this does not seem to be the only function of these repeats. They are commonly found in cellular structures that experience great stress, such as the erythrocyte membrane skeleton (EMS) or the muscle sarcomere. The mechanical properties needed to withstand such stresses are provided by the important structural role of the spectrin repeats (Djinovic-Carugo et al. 2002). An extremely versatile protein unit, these repeats have developed a high specificity to form dimers, and some also specialise in binding to many different proteins (Djinovic-Carugo et al. 2002). It is interesting to note that single spectrin repeats display a greater sequence identity to equivalent repeats in other species than with neighbouring spectrin repeats in the same protein chain. This suggests that each individual spectrin repeat has evolved to have its own particular and specific set of functions (Baines 2009; Thomas et al. 1997).

The first detailed structural analyses of the spectrin repeats came from both the crystal structure of the single 14th repeat from the *Drosophila melanogaster* α -spectrin (Yan et al. 1993) and from the solution structure of the single 16th repeat from chicken brain α -spectrin (Pascual et al. 1997). These studies revealed the core feature of each spectrin repeat to be a triple helical coiled-coil bundle (Pascual et al. 1997; Yan et al. 1993). Within this triple helical bundle, each of the three α -helices displays the heptad sequence of periodicity, with amino acid residues traditionally labelled *a* to *g* (Yan et al. 1993). Every two turns of each α -helix comprises the seven residues of the heptad (Le Rumeur et al. 2012). Hydrophobic residues are generally found in positions *a* and *d*, and charged residues are generally found at positions *e* and *g* (Pascual et al. 1997). Sequence alignment studies of spectrin repeats have revealed that these hydrophobic residues at positions *a* and *d* are conserved (Pascual et al. 1997) and further analysis of spectrin repeat crystal structures have reported that these residues are positioned on the inward-facing surface of the helix (Yan et al., 1993). Hydrophobic interactions between these *a* and *d* residues in each of the three α -helices bring about the formation of the triple helical coiled-coil bundle, while further electrostatic interactions between *e* and *g* residues in each of the three α -helices contribute to the stability of each repeat (Yan et al. 1993; Pascual et al. 1997).

1.1.2.3.1 The Actinin Rod Domain

The central region of the actinin protein (Fig. 1.5), length of 24nm and width of 4-5nm, contains four spectrin-like repeats, the region is commonly referred to as the actinin rod domain (Ylänne et al. 2001).

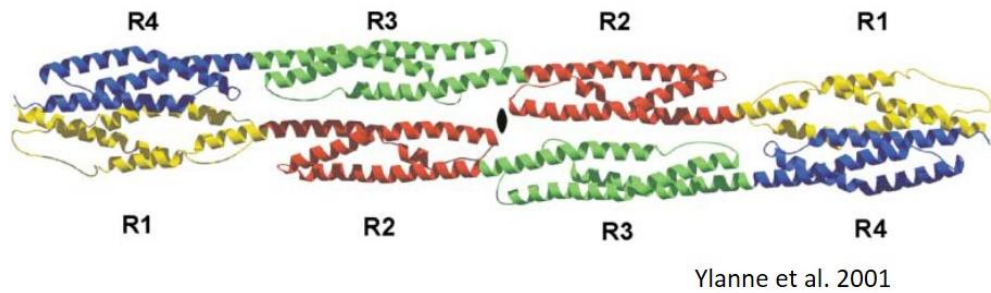


Figure 1.5: Structure of the α -Actinin Rod Domain. The actinin rod domain is made of four spectrin-like repeats (R1; yellow, R2; red, R3; green, R4; blue). Each repeat is a triple helical coiled coil bundle, separated with a helical linker. Intrahelical interactions contribute to the stability of each bundle while interhelical interactions bring about the formation of the dimer. This dimeric interface spans the length of the molecule, in which each repeat is perfectly aligned to its juxtaposing repeat (Djinovic-Carugo et al. 1999; Ylanne et al. 2001).

Dimerisation between actinin monomers is principally mediated by the rod domain (Ylänne et al. 2001; Imamura et al. 1988), however, the crystallographic structure of full length actinin-2 has revealed that a small number of polar interactions between the EF3-4 pair of the CaM domain of one actinin monomer and the helical linker between the ABD and spectrin-like repeat 1 of the opposing actinin monomer acts to stabilise the dimer (Ribeiro et al. 2014). The rod domain serves as a solid junction between the two ABDs of the actinin dimer, the exact distance of separation that this rod domain imposes between the two ABDs is crucial for correct organisation of the sarcomeric Z-disc and proper maintenance of its architecture during muscle contraction (discussed in section 1.1.4.1.3) (Djinovic-Carugo et al. 2002).

Crystal structures of multiple spectrin-like repeats from human muscle actinin-2 have reported a long and specific spectrin repeat dimeric interface where complementary electrostatic interactions between charged amino acid residues drive the formation of a very tight dimer (Ylänne et al. 2001). The electrostatic potential of this dimeric interface displays a gradient from basic in spectrin-like repeat 1 to acidic in spectrin-like repeat 4 (Ylänne et al. 2001). However, dimerisation is also brought about by solvent molecules that maintain the hydrogen bond network that connects both monomers (Djinović-Carugo et al. 1999). Within this tight dimer, both monomers are in contact with each other along their entire length (Djinović-Carugo et al. 1999; Ylänne et al. 2001). This structural analysis explains the high dimer formation affinity for the actinin rod domain (Ylänne et al.

2001), which has been calculated to be about 10pM (Flood et al. 1995; Flood et al. 1997).

Crystallographic studies have also revealed more information regarding the inter-repeat junction. The C-terminal helix of one spectrin-like repeat and the N-terminal helix of the following spectrin-like repeat are connected to each other through a helical linker. This helical linker remains continuous with the secondary structure of the spectrin-like repeats with no obvious break or discontinuity (Djinovic-Carugo et al. 2002; Djinović-Carugo et al. 1999). The helices connecting the different spectrin-like repeats in the rod domain have different amino acid compositions meaning that each can adopt different conformations. The linker connecting repeats two and three contains a proline residue, meaning that this linker is bent slightly at an angle of 21°. These linkers are structurally important as they dictate the orientation of the spectrin repeats (Djinović-Carugo et al. 1999) and are important for describing the lateral register of each repeat (Viel 1999). In general, for actinin, these helical linkers are described as being stiff, providing overall rigidity to the rod domain (Sjöblom et al. 2008). The helical linker connecting repeats 2 and 3 is probably the most important; the orientation that these repeats adopt determines the orientation of the entire actinin molecule (Djinović-Carugo et al. 1999). These studies have also reported that the dimeric actinin rod domain is twisted 90° to the left, with most of the tilting occurring at repeats 2 and 3. Importantly, this twist functions to stabilise the rod, and it prevents it from bending (Ylänne et al. 2001). The ABD is connected to spectrin-like repeat 1 via a six turn helical linker (Ribeiro et al. 2014). This linker is very flexible, being highly susceptible to proteolytic cleavage (Winkler et al. 1997). This flexibility permits the ABD to adopt many orientations to facilitate actin binding; crosslinking both parallel and anti-parallel actin filaments (Ribeiro et al. 2014). The rigidity of the rod domain, provided by the 90° twist, also functions to control the orientations the ABD (Ribeiro et al. 2014; Ylänne et al. 2001). In general, these studies, and more involving chemical crosslinking and analytical equilibrium sedimentation, suggest that the actinin dimeric rod, made up of eight spectrin repeats in total, forms a very stable and rigid junction between two very flexible ABDs (Imamura et al. 1988; Flood et al. 1997; Flood et al. 1995; Djinovic-Carugo et al. 2002). The actinin rod

domain offers more than just a structural role. While the overall charge of the dimeric interface runs from positive to negative (mentioned above) (Ylänne et al. 2001), the surface of the rod domain is acidic, the residues of which have been greatly conserved (Ylänne et al. 2001). The actinin rod domain can therefore act as a type of protein docking platform through interaction with the basic peptides of many different proteins (Djinovic-Carugo et al. 2002; Ylänne et al. 2001). Such interactions lead to the generation of multiprotein assemblies that are involved in developing cytoskeletal architectural complexes, or are involved in signal transduction pathways (Djinović-Carugo et al. 2002).

1.1.2.3.2 The Spectrin Central Region

While spectrin proteins contain more spectrin repeats than actinin, α -spectrin has 20 full repeats and β -spectrin has 16, the repeats in both α - and β -spectrin are shorter; actinin repeats are made up of 122 amino residues while spectrin protein repeats contain only 106 amino acids (Broderick & Winder 2005).

Heterodimerisation between α - and β -spectrin is also mediated by the spectrin repeats, and begins at a spectrin repeat nucleation site consisting of α -spectrin repeats 20 and 21 and β -spectrin repeats 1 and 2, in which α -21 interacts with β -1 and α -20 interacts with β -2. This initial interaction involves complementary electrostatic interactions where the α 20-21 repeats contribute the negatively charged residues and the β 1-2 contribute the positively charged residues. These primary steps align the remaining spectrin repeats, and also align the β -spectrin ABD with the α -spectrin CaM domain. Dimerisation then propagates in a “zipper-like” fashion down the length of protein molecules (Li et al. 2007). These two stages of dimerisation, initiation and propagation, have different thermodynamic properties. Through carrying out sedimentation equilibrium experiments with spectrin complexes in conditions of increasing salt concentrations, and thereby disrupting electrostatic interactions, Begg et al. (2000) found that recombinant α -/ β -spectrin complexes containing only those spectrin repeats that make up the nucleation site (α 20-21 and β 1-2) were more susceptible to salt induced dissociation than α -/ β -spectrin complexes containing additional spectrin repeats

outside of the nucleation site (α 18-21 and β 1-4). This suggests that hydrophobic interactions predominate in the second stage of dimerisation (Li et al. 2007; Begg et al. 2000). Overall, dimer initiation is directed by enthalpic interactions involving electrostatic interactions along with hydrogen bonds and many hydrophilic interactions. Subsequent dimer propagation is directed by entropic interactions including weak hydrophobic interactions (Li et al. 2007; Begg et al. 2000).

Spectrin repeat 1 at the N-terminus of α -spectrin and spectrin repeat 17 at its C-terminus of β -spectrin are both only partial repeats; of the triple helical coiled coil structure that makes up every other spectrin repeat, α -1 only comprises one of these α -helices, while β -17 only comprises two (Speicher et al. 1993). To form a closed dimer “hairpin” structure, the longer α -spectrin folds back on its N-terminal so that the α -1 partial repeat interacts with and forms an intradimer bond with the β -17 partial repeat. A triple helical coiled coil that is very similar to the usual complete triple helical coiled coil spectrin repeats is reformed (Speicher et al. 1993).

Spectrin repeat 9 of both erythroid and non-erythroid α -spectrins contains a SRC homology 3 domain (SH3) (Wasenius et al. 1989; Machnicka et al. 2014). The SH3 domain is a well-known protein interaction domain and is very commonly found in proteins involved in signal transduction pathways (Mayer 2001). Owing to the presence of this SH3 domain, spectrin has been found to play a role in signalling pathways, such as those involved in Rac activation (Bialkowska et al. 2004).

Spectrin repeat 10 of non-erythroid α -spectrin contains a 36 amino acid sequence that incorporates recognition sites for both calpain and caspase proteases, and a Ca^{+2} dependent calmodulin binding site (Harris et al. 1988; Harris & Morrow, 1988; Rotter et al. 2004). The close proximity of these sites suggests that a close relationship may exist between the activity of each protein (Harris et al. 1988), indeed Rotter et al. (2004) have reported that calcium dependent calmodulin binding regulates non-erythroid α -spectrin cleavage by caspases and calpains.

Spectrin repeat 15 of β -spectrin contains the ankyrin binding site (Kennedy et al. 1991). Ankyrin functions to attach the spectrin-actin network to the cell membrane (Bennett & Baines 2001).

While crystal structures have reported the dimeric actinin rod domain to be very rigid, studies of spectrin proteins have reported the spectrin central region to be quite flexible. Work carried out by Grum et al. (1999) has revealed that the spectrin central region has two models of flexibility; conformational rearrangement and bending at the linker region. This study solved four crystal structures of four closely related sections of repeats 16-17 of the chicken brain (CB) α -spectrin protein; one crystal structure contained an additional eight amino acid residues on the N-terminal side of repeat 16 and all four contained increasing amounts amino acid residues on the C-terminal side of repeat 17. In this study, the conformational rearrangement model is founded on the observation that, upon comparing two CB α 16-17 crystal structures, a loop undergoes a conformational change to a helix. Within repeat 17 of one crystal structure, a loop is centred between two helices, on comparing this structure to another one of the four crystal structures, this loop has transitioned to a helix, while the neighbouring helix has melted to replace the loop, in other words, the loop has moved. The authors suggest that, in nature, if many tandem repeats were to undergo such a conformational change in unison, the spectrin protein would change in length. The bending model is formed on the observation that the relative orientation of the two repeats varies on comparison of each of the crystal structures. Considering that all individual repeats within each crystal structure superpose well (with the exception of the crystal structure displaying movement of the position of the loop within spectrin repeat 17, mentioned above), implying no change in secondary structure, the authors suggest that all changes in orientation must be centred on the linker region connecting the two repeats, i.e. bending of the linker region. Crystal structures of human erythroid (HE) β -spectrin repeats 8 and 9 have also been solved by Kusunoki et al. (2004a). This study supports the bending model of flexibility. Through repetitive superpositioning of the two-repeat structures; HE β 8-9 repeats and CB α 16-17 repeats, the authors constructed hypothetical models of β -spectrin made up of 16 full length spectrin repeats and one partial repeat. A range of conformations form from each of the models constructed, the formation of which depends on the twist angle between the repeats in each of the models constructed. This study proves

that the linker between repeats is agreeable to a wide variety of different twist angles.

Studies have reported that β -spectrin repeats 8-9 exhibits very low thermal stability, unfolding at 33.8°C in the presence of physiological NaCl concentration (MacDonald & Cummings, 2004). In studying the HE β 8-9 crystal structure Kusunoki et al. (2004a) reported that repeat 9 is without two tryptophan residues which are highly conserved in spectrin repeats and are important for the formation of a very tightly packed spectrin repeat hydrophobic core and, as a result, confer conformational stability to the repeat. This finding explains why HE β 8-9 displays very such low thermal stability and both studies (MacDonald & Cummings, 2004; Kusunoki et al. 2004a) suggest that β -spectrin repeat 9 is partially unfolded in physiological conditions. Kusunoki et al. (2004a) also found that HE β 8-9 has a fewer number of canonical intrahelical hydrogen bonds compared to other spectrin repeats. They speculate that this finding may also explain the reduced thermal stability of HE β 8-9. Studies investigating the stability of folding to temperature of many pairs of spectrin repeats have found that some pairs are more stable than others. MacDonald & Cummings (2004) found that HE α 13-14, like HE β 8-9, exhibits low thermal stability, unfolding at 36°C., while repeat pairings such as HE α 1-2 and HE α 2-3 were found to have higher thermal stabilities and unfolded at 52.3°C and 57.9°C, respectively. Their study proposes that, within the spectrin tetramer formation, pairs of less stable spectrin repeats are located next to and opposite other pairs of unstable spectrin repeats and likewise for the more stably folded spectrin repeats; HE β 8-9 lies opposite HE α 13-14 on the same spectrin tetramer, while HE α 1-2 lies nearly opposite HE α 2-3 (MacDonald & Cummings 2004). They suggest that these clusters of unstable, partially unfolded spectrin repeats may function as a type of “hinge” region, providing the spectrin complex with flexibility (MacDonald & Cummings 2004). Crystal structures composed of three CB α -spectrin spectrin repeats, repeats 15, 16 and 17, solved by Kusunoki et al. (2004b) have also exposed the large conformational flexibility available to the spectrin proteins. This study found that the spectrin repeats at either end of this three repeat structure move independently of one another, and that the bending of one linker in between

two repeats does not have any impact or significance on the bending of the adjacent linker (Kusunoki et al. 2004b).

All crystal structures; CB α 16-17, HE β 8-9 and CB α 15-17, have reported that the linker connecting the spectrin repeats is helical (Grum et al. 1999; Kusunoki et al. 2004a; Kusunoki et al. 2004b).

1.1.2.3.3 A Comparison of the Crystal Structures of the Actinin and Spectrin Central Regions

The crystal structures of the actinin rod domain crystallised as an anti-parallel homodimer, as did the two spectrin-like repeat actinin structure (Ylänné et al. 2001; Djinić-Carugo et al. 1999). Interestingly, the three spectrin repeat α -spectrin structure, CB α 15-17, also crystallised as an anti-parallel dimer (Kusunoki et al. 2004a). Comparative studies on both the actinin rod domain dimeric crystal structures and the α -spectrin spectrin repeat 15-17 dimer crystal structure have been important in constituting the structural, and thereby functional, differences between actinin and spectrin proteins, namely rigidity versus flexibility respectively. Overall, it was found that the actinin spectrin-like repeats show greater dimer affinity than the spectrin spectrin repeats. The increased dimer affinity for actinin spectrin-like repeats is provided by the precise alignment of spectrin-like repeats 1 and 2 with spectrin-like repeats 3 and 4. This precise alignment guarantees maximum use of surface area for dimerisation, ensuring almost all of the entire length of the rod domain contributes to the dimeric interface. This is in contrast to the imprecise antiparallel alignment of the α -spectrin 15-17 repeats. This imprecise alignment provides a much smaller surface area for dimerisation, in this case only three quarters of each spectrin repeat are contributing to the dimeric interface. Points of no contact between the spectrin repeats promote movement of the repeats. Differences in the dimeric interface contribute to differences in the range of movements assigned to each protein (Kusunoki et al. 2004b). Overall, these repeats provide structure and rigidity to actinin, flexibility and elasticity to erythroid spectrin.

1.1.2.4 Pleckstrin Homology Domain

In addition to those domains mentioned above, β -spectrin proteins also contain a pleckstrin homology (PH) domain (Zhang et al. 1995). Differential mRNA splicing of erythroid and non-erythroid β -spectrin generates two splice forms; one form containing a long C-terminal region, about 230 amino acid residues, and the other form containing a shorter C-terminal region, about 52 amino acid residues (Winkelmann et al. 1990; Hayes et al. 2000). The longer splice variant, and not the short variant, contains the PH domain (Baines 2009; Machnicka et al. 2014). PH domains are normally involved in membrane targeting, cell signalling and cytoskeleton organisation via their ability to bind phosphoinositides (Lemmon & Ferguson, 2000; Lemmon et al. 2002). The β -spectrin PH domain binds phosphatidylinositol 4,5 bisphosphate (PIP₂) (Hyvonen et al. 1995), and Das et al. (2008) have reported that, in midgut copper cells, an epithelial cell type, spectrin targeting to the plasma membrane is dependent on phosphoinositide binding its PH domain.

The β -spectrin PH domain has been reported to bind PIP₂ with low affinity (Lemmon et al. 2002). Considering that α -/ β -spectrin proteins can assemble into oligomeric complexes, tetramers and larger (Morrow & Marchesi, 1981) (discussed in section 1.1.4.2), and that spectrin junctional complexes consist of many spectrin dimers bound to actin (Nans et al. 2011) (also discussed in section 1.1.4.2) it seems likely that spectrin PH domain-lipid mediated membrane association occurs through multivalent interactions with phosphoinositides (Lemmon et al. 2002).

The alternative β -spectrin splice variant with the shorter C-terminus contain, at this location, a stretch of amino acid phosphorylation sites (Baines, 2009).

1.1.3 Regulation

1.1.3.1 Regulation of Actinin

It is known that actin binding of non-muscle actinin isoforms is regulated by calcium binding to their EF-hand motifs in their CaM domain (Sjöblom et al. 2008). Cryo-electron microscopy studies carried out by Tang et al. (2000) have revealed

that dimerisation between actinin molecules oppositely aligns the N-terminal CH domains in the ABD of one monomer to the C-terminal EF-hand motifs in the CaM domain of the other. This study has speculated that the binding of calcium to the EF hand motifs in the CaM domain induces the EF3-4 pair to wrap itself around the linker region between the two CH domains. This linker contains large hydrophobic amino acid residues that are a common feature of calmodulin binding motifs (Tang et al. 2001). This action would serve to separate the two CH domains, preventing them from partaking in actin binding. Also, the bulk presence of the CaM domain between the two CH domains might act to sterically prevent actin binding.

Actin binding activity of muscle actinin isoforms is regulated by phosphatidylinositol 4,5 bisphosphate (PIP₂), whose binding site has been mapped to CH2 of both actinin-2 and -3 (Ribeiro et al. 2014). As confirmed by the recent crystal structure of dimeric actinin-2, in the aligned parallel dimer formation, the EF3-4 hands from one monomer interact with the neck region between the ABD and spectrin-like repeat 1 of the opposing monomer, a known calmodulin binding motif (Fig. 1.6A) (Ribeiro et al. 2014). Binding of PIP₂ disrupts this interaction. It has been proposed that the binding of PIP₂ at the CH2 site positions it in proximity to the neck region between the ABD and spectrin-like repeat 1. At such a distance, its long aliphatic chain can disturb the EF3-4 interaction with the neck region. This releases the EF3-4, making it available to interact with the protein titin and be targeted to the Z-disc of the sarcomere (Fig. 1.6B) (Ribeiro et al. 2014). PIP₂ binding has been reported by Fukami et al. (1992 and Fukami et al. (1996) to make actinin more receptive to actin binding (Fig. 1.6B). This may be explained by the fact the PIP₂ binding site is located near ABS3 on CH2 of the actinin ABD (Tang et al. 2001). Interestingly, for the non-muscle actinin isoforms, the binding of phosphoinositides, namely PIP₂ and phosphatidylinositol 4,5 bisphosphate (PIP₃), to the ABD have been reported to decrease actinin actin bundling activity (Fraley et al. 2003). It was later found that PIP₂ acts to inhibit actin bundling, while PIP₃ acts to both inhibit and disrupt actin bundling (Corgan et al. 2004). However, this study reported that PIP₃ only disrupted full length actinin actin bundling activity, i.e actin bundling activity of the actinin dimer, and not the actin bundling activity of the isolated actinin ABD

(Corgan et al. 2004). The intimate surroundings of the ABD may influence phosphoinositide regulation (Gimona et al. 2002).

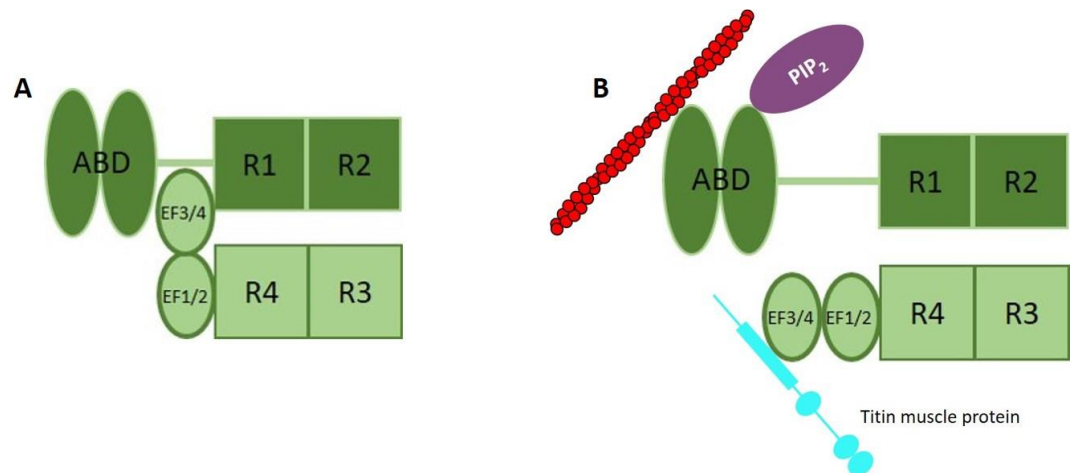


Figure 1.6: Phosphoinositide Regulation of Actinin-2. (A) In the unbound actinin ABD, the EF3-4 pair interacts with the helical linker between spectrin repeat 1 and the ABD (Ribeiro et al. 2014). **(B)** PIP₂ binding to the ABD disrupts this interaction and makes available the EF3-4 pair to interact with the muscle protein titin (Ribeiro et al. 2014). The binding of PIP₂ has also been reported to make the ABD of actinin-2 more sensitive to actin binding (Fukami et al. 1992; Fukami et al. 1996).

Actinin actin binding activity is also regulated through actinin phosphorylation by protein kinases. Phosphorylation of tyrosine residue 12 in the ABD of actinin-1 by the focal adhesion kinase (FAK) (Izaguirre et al. 2001) and phosphorylation of tyrosine residues 4 and 31 in the ABD of actinin-4, in response to epidermal growth factor (Shao et al. 2010), reduces their ability to bind actin. Another form of actinin regulation is calpain mediated proteolysis. This is modulated by the binding of the phosphoinositides PIP₂ and PIP₃ to actinin (Sprague et al. 2008).

1.1.3.2 Regulation of Spectrin

Despite being considered vestigial, reports have suggested that the α -spectrin EF hand motifs are functional in physiological calcium concentrations. Calcium binding to EF1-2 induces an interaction between EF3-4 and protein 4.2 (Korsgren et al. 2010), a very important protein involved in maintaining both the structure and flexibility of the EMS (Sung et al. 1992). In the presence of high

micromolar concentrations of calcium, calmodulin binding to EF1-2 inhibits the binding of protein 4.2 to EF3-4 (Korsgren et al. 2010).

β -spectrin contains two binding sites for protein 4.1 on its ABD; one on each CH domain (An et al. 2005). Binding of spectrin to protein 4.1 functions to anchor the spectrin-actin network to the cell membrane (Viel & Branton 1996), but the binding of protein 4.1 to β -spectrin has also been shown to increase spectrin binding to actin (An et al. 2005; Cohen & Langley 1984). However, it appears that the α -spectrin EF3-4 plays a vital role in β -spectrin ABD actin binding. Truncated α -spectrin proteins not containing EF3-4, complexed with β -spectrin, still retain the ability to bind protein 4.1, but their ability to bind actin is reduced (An et al. 2005). In addition, independent β -Spectrin proteins do not bind actin in the presence of protein 4.1 (Cohen & Langley 1984). Therefore, the EF3-4 must contribute to actin binding. An interaction between the α -spectrin EF3-4 and the β -spectrin ABD may be necessary to induce actin binding in the presence of protein 4.1 (An et al. 2005). Similar to actinin, heterodimerisation aligns the β -spectrin ABD with the α -spectrin CaM domain. Perhaps similar regulatory mechanisms are therefore involved; where EF3-4 interacts with either the short linker connecting CH1 and CH2, or, the longer linker connecting β -spectrin spectrin repeat 1 to the ABD, and in doing so, regulates actin binding through modulating conformation (Korsgren & Lux 2010).

The interaction between protein 4.1 and β -spectrin is regulated by PIP₂, the binding of PIP₂ to the β -spectrin ABD greatly increases protein 4.1 binding to β -spectrin (An et al. 2005).

For both actinin and spectrin, the exact role of the interaction between oppositely aligned CaM domains and ABDs in regulating actin binding is unclear.

1.1.4 Function

1.1.4.1 Functions of Actinin Proteins

1.1.4.1.1 *General Functions of Non-Muscle Actinins*

Within the cell, actin filaments can be fashioned into many different types of structures. Membrane protrusions called microvilli, which function to increase the surface area of a cell, are made up of ordered tight bundles of actin. Contractile structures called stress fibres are made up of actin bundles, and a web of actin filaments form the lamellipodia, which extend from the leading edge of a cell during migration (Lodish et al. 2008a).

Actinin plays an important structural role in organising actin filaments into some of these structures. In addition to binding actin, actinin has evolved to interact with many other different types of proteins; cytoskeletal proteins, signalling proteins, and transmembrane proteins. Through these additional interactions, actinin functions not only to crosslink the actin cytoskeleton to the plasma membrane, thus providing and maintaining structure and shape to the cell, but it also serves to regulate the actin cytoskeleton by acting as scaffold for proteins involved in signalling pathways (Djinovic-Carugo et al. 2002; Sjöblom et al. 2008). A number of many cellular structures and processes in which the non-muscle actinins play important roles are described below.

1.1.4.1.1.1 Microvilli

L-selectin is a cell-surface glycoprotein found on the microvilli of leukocytes (te Velthuis et al. 2007; Pavalko et al. 1995). L-selectin is involved in the primary stages of leukocyte activation at sites of inflammation; tethering and rolling. Through binding lectin ligands, L-selectin functions to attach (tether) the leukocyte to the endothelium of a blood vessel. The leukocyte then moves (rolls) slowly along the blood vessel wall (Dwir et al. 2001; Pavalko et al. 1995). Through its rod domain, actinin constitutively interacts directly with the cytoplasmic tail of L-selectin (Pavalko et al. 1995). This interaction has been found to be very important for L-

selectin function and subsequent leukocyte activation. Deletion of the L-selectin cytoplasmic domain abrogates leukocyte tethering and rolling to the endothelium (Dwir et al. 2001; Pavalko et al. 1995). In anchoring L-selectin to the actin cytoskeleton, actinin functions to stabilise the L-selectin bond tethering the leukocyte to the endothelium so that the leukocyte remains tethered during physiological shear flow. In connecting L-selectin to the actin cytoskeleton, actinin regulates the activity of L-selectin (Dwir et al. 2001).

1.1.4.1.1.2 Stress Fibres

Stress fibres are the contractile structures of non-muscle cells (Tojkander et al. 2012) of which both actin and myosin are the primary proteins. Contractile force is produced through the ATPase activity of myosin coupled with its interaction with actin filaments (Tojkander et al. 2012). Within this actomyosin structure, actinin functions to crosslink the actin filaments into a bipolar arrangement (Fig. 1.7) (Tojkander et al. 2012). Immunofluorescent staining reveals a periodic pattern of actinin in which it appears to alternate with myosin bands (Langanger et al. 1986). This arrangement resembles the sarcomeric contractile unit in muscle cells. However, the arrangement of actin filaments in stress fibres is less ordered than in muscle sarcomeres (Tojkander et al. 2012).

FRAP analysis has revealed that actinin in stress fibres does more than just arrange actin filaments. It has revealed that a very dynamic association exists between actinin and actin filaments (Peterson et al. 2004; Edlund et al. 2001; Fraley et al. 2005; Hotulainen & Lappalainen 2006). A dynamic cytoskeleton is important because it allows the cell to rapidly reorganise in response to signals (Fraley et al. 2005). It has been suggested that this dynamic dissociation/re-association is important because it could permit rotation of the actin filaments, which, when coupled with the ATPase activity of myosin, would allow for contraction (Hotulainen & Lappalainen 2006). Another possible reason for the importance of this dynamic dissociation/re-association is due to stress fibres not being as organised as muscle sarcomeres (Tojkander et al. 2012). In the latter, actinin is confined to the muscle Z-disc, but in stress fibres, actinin may also be localised in the equivalent of the I band

too. In this case, actinin must be constantly dissociated from the actin filament to allow for myosin movement and subsequent contraction (Peterson et al. 2004).

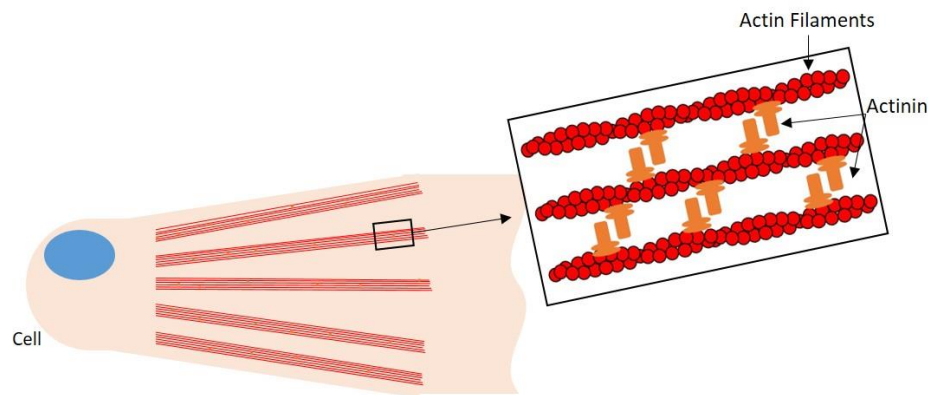


Figure 1.7: Actinin in Stress Fibres. The dynamic association between actinin and actin in stress fibres allows for a semi-ordered arrangement of actin filaments and permits for the rotation of actin filaments, providing a means of contraction (Tojkander et al. 2012; Hotulainen & Lappalainen 2006).

Apart from actin, several other proteins that are common to stress fibre regions have been reported to interact with actinin, providing actinin with various functions. In binding the proteins zyxin and cysteine-rich protein 1 (CRP1), proteins involved in actin filament organisation and cell differentiation respectively, actinin functions to target them to stress fibre regions, and to scaffold interactions between them (Reinhard et al. 1999; Pomies et al. 1997; Crawford et al. 1992; Crawford et al. 1994). In binding the CLP-36 PDLIM protein, a protein with the ability to bind protein kinases, actinin acts as a type of linker, connecting signalling pathways to the cytoskeleton (Vallénus et al. 2000; Vallénus & Mäkelä 2002).

1.1.4.1.1.3 Focal Adhesions

Terminating stress fibres can be attached to the plasma membrane at regions known as focal adhesions (Tojkander et al. 2012). Focal adhesions are contact points between the cell and its surrounding extracellular matrix (ECM) and they are important because they allow for communication between the cell and the ECM (Burridge & Chrzanowska-Wodnicka 1996). Integrins are transmembrane proteins and they are one of the main components of a focal adhesion (Burridge & Chrzanowska-Wodnicka 1996). Actinin, via its rod domain, binds to the cytoplasmic

tail of the β_1 integrin receptor, and in doing, so connects the actin cytoskeleton to the plasma membrane (Fig. 1.8). Consequently, in addition to crosslinking actin filaments, actinin also functions to anchor them (Otey et al. 1990).

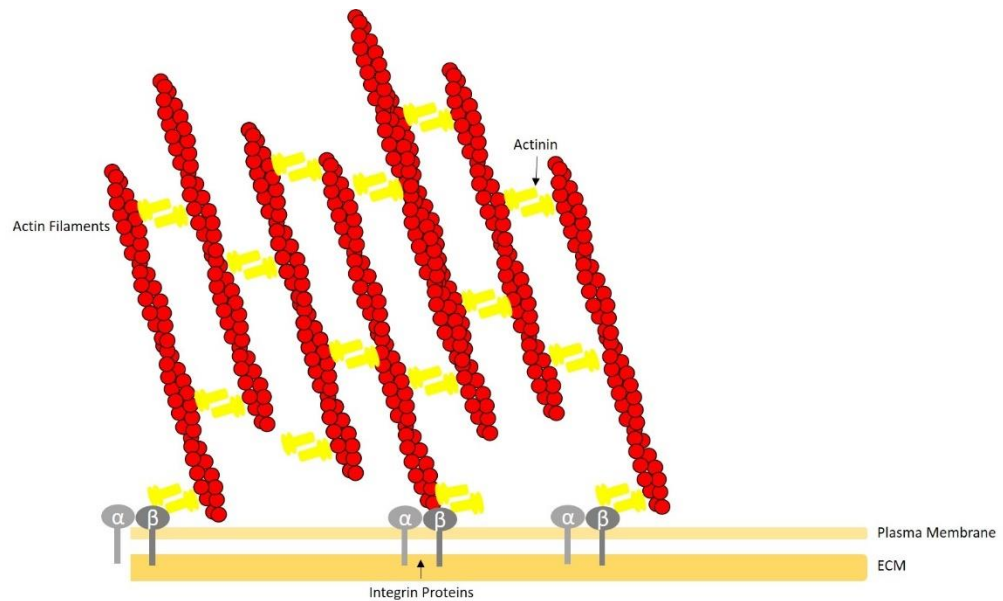


Figure 1.8: Actinin in Focal Adhesions. Through binding to transmembrane proteins such as integrin proteins, actinin functions to attach the actin cytoskeleton to the plasma membrane (Otey et al. 1990).

Communication between the cell and the ECM is by means of mechanical force or stress. The cell can apply force on the ECM and, in return, the ECM can apply force on the cell. Focal adhesions provide both the ECM and the cell the ability to “sense” mechanical cues from each other, and respond accordingly. Such responses could be cellular processes such as proliferation and differentiation (Ye et al. 2014; Roca-Cusachs et al. 2013; Tojkander et al. 2012). One of the main forces produced by a cell is that of a contractile force resulting from the movement of myosin proteins along actin filaments in stress fibres (Tojkander et al. 2012). With its ability to bind integrin receptors, two independent studies have shown that actinin is responsible for transmitting these mechanical contractile forces from the cytoskeleton to focal adhesions (Roca-Cusachs et al. 2013; Ye et al. 2014). In both studies, the transmission of force or tension through actinin resulted in maturation or growth of focal adhesions. With its ability to crosslink actin filaments, actinin may also be able to control the stiffness of these filaments by increasing or decreasing its actin binding. In doing so actinin could function to modulate the

transmission of this tension (Clainche & Carlier 2008). Roca-Cusachs et al. (2013) suggest that actinin may also be able to do this through increasing or decreasing its integrin binding.

Also, in addition to force transmission, in linking the actin cytoskeleton to receptors in the plasma membrane, actinin functions to maintain cell shape and structure, and regulate the activity of transmembrane receptors (Otey & Carpen 2004).

1.1.4.1.1.4 Cell Motility

Due to its considerable involvement in focal adhesions, actinin also contributes to cell motility. Lamellipodia are actin rich cell membrane protrusions which function to direct cell motility, propelling the cell across the substratum (Lodish et al. 2008a). These structures are generated through actin filament polymerisation at the leading edge of a cell and attach themselves securely to the underlying substratum through focal adhesions (Ridley et al. 2003). As mentioned in section 1.1.4.1.1.3, actinin plays a role in anchoring the actin cytoskeleton to the cell membrane through its interaction with integrin proteins (Otey et al. 1990). These focal adhesions serve to stabilise the lamellipod, but they also serve as traction sites that allow the cell to move forward; these tractional forces are transmitted to the focal adhesions and are generated through myosin interactions with actin filaments (Ridley et al. 2003). In order to finally permit cell movement, focal adhesions at the rear of the cell are disassembled. This disassembly involves separation of the actin cytoskeleton from the focal adhesion (Lodish et al, 2008a). Not only playing a role in focal adhesion formation, actinin may also be involved in focal adhesion disassembly. Inactivation of actinin in focal adhesions results in disruption of the interaction between actinin and integrin and separation of stress fibres from focal adhesions (Rajfur et al. 2002), while the introduction of actinin fragments containing only the ABD, or only the rod domain, also results in disruption in both stress fibres and focal adhesions (Pavalko & Burridge 1991).

Essentially, cell motility involves co-ordinating and balancing forces; the contractile forces generated by the actomyosin cytoskeleton and the resisting forces generated by the focal adhesion. Ultimately, no cell movement will occur if a

cell is too strongly attached to its underlying substratum (Lodish et al, 2008a). As already mentioned in section 1.1.4.1.1.3, actinin may play a role in modulating the transmission of tension through regulating its actin binding (Clainche & Carrier 2008) or integrin binding (Roca-Cusachs et al. 2013). Binding of integrins to the ECM via their extracellular domain triggers the activation of many signalling pathways that bring about protein tyrosine phosphorylation and changes in phospholipid biosynthesis (Ridley et al. 2003). Actinin actin binding activity is regulated by both tyrosine phosphorylation and phosphoinositide binding (section 1.1.3.1). This also suggests that actinin plays an active role in focal adhesion assembly and disassembly.

1.1.4.1.1.5 Endocytosis

Another dynamic cellular process where actinin plays a role is endocytosis, which is the internalisation of cell surface molecules into intracellular compartments (Le Roy & Wrana 2005). In motile cells, such as macrophages, actinin-4 is localised to circular ruffles on their dorsal surface (Araki et al. 2000). These circular ruffles are the precursor forms of macropinosomes, a variety of cellular chamber that form during macropinocytosis, a type of endocytosis (Lim and Gleeson 2011). Scrape loading cultured macrophages with anti-actinin antibodies, designed to recognise the actinin central rod region and hence disrupt actinin dimerisation and ultimately actin crosslinking, resulted in decreased macropinocytosis activity in these cells (Araki et al. 2000).

Also in the context of endocytosis, actinin interacts with the intracellular C-terminal of the G-protein coupled receptor Adenosine A_{2A} receptor (A_{2A}R). These interactions may function in internalising the receptor upon agonist induction. A truncated A_{2A}R without its intracellular C-terminal, and thereby not able to interact with actinin, was not internalised upon agonist induction in cultured cells. This study indicates that the attachment of the A_{2A}R to the actinin-actin cytoskeleton is necessary for receptor internalisation i.e. endocytosis (Burgueño et al. 2003).

1.1.4.1.1.6 Adherens Junctions

While actin filaments can be moulded into different cellular structures, the cells themselves can assemble into different tissues and be organised into different organs. This requires molecular interactions between cells in the form of cell:cell adhesions or junctions. These junctions confer strength and rigidity to a tissue or an organ, and also allow for communication between cells, regulating important processes, such as development (Lodish et al. 2008b). Several studies have identified actinin as a constituent of some of these junctions.

Adherens junctions are one such type of cell:cell adhesion. At the electron microscope level, these junctions are identified by very close contact between two interacting cells (Knudsen et al. 1995). Transmembrane proteins called cadherins are a common component of these junctions. Their extracellular domain functions to mediate cell:cell interactions through binding copies of themselves on neighbouring cells, while their intracellular domain promotes interactions with a group of proteins called catenins. Through its rod domain, actinin interacts with the α -catenin protein so that it indirectly tethers the actin cytoskeleton to these junctions (Fig. 1.9). The presence of two α -catenin binding sites on the actinin dimer greatly stabilises the complex (Nieset et al. 1997; Knudsen et al. 1995).

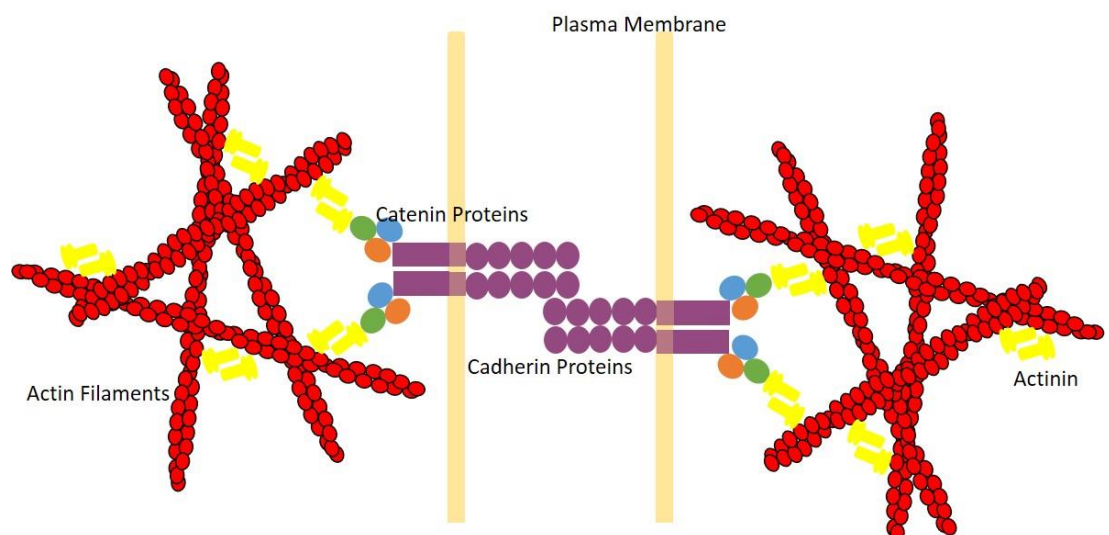


Figure 1.9: Actinin in Adherens Junctions. In binding to catenin proteins, actinin functions to indirectly link the actin cytoskeleton to cadherin protein complexes, and ultimately, to the actin cytoskeleton of neighbouring cells (Nieset et al. 1997; Knudsen et al. 1995).

A direct association has been reported between actinin and the transmembrane protein intracellular adhesion molecule-1 (ICAM-1), a ligand for leukocyte integrins (Carpén et al. 1992). This interaction may facilitate the extravasation of leukocytes through the cell junction (Celli et al. 2006).

1.1.4.1.2 Actinin-1/Actinin-4 Specific Functions

Both actinin-1 and actinin-4 share 86.7% amino acid identity, which suggests that they are very closely related (Honda et al. 1998). However, in motile cells, they each display a very different localisation pattern; actinin-1 is normally associated with focal adhesions, and adherens junctions while actinin-4 is usually associated with stress fibres and is distributed throughout the cytoplasm (Honda et al., 1998). Other studies have also reported actinin-4 to be associated with dorsal ruffles in motile cells (Araki et al. 2000). Different distribution patterns suggest different functions for both isoforms (Honda et al., 1998).

As an aside, it is interesting to note that these two isoforms form actinin-1/actinin-4 heterodimers. Even more surprising, these heterodimers predominate over homodimers in many cancerous cell lines (Foley & Young, 2013). The authors suggest that these heterodimers may have properties that differ from the actinin homodimers, speculating that the homodimers perform the isoform specific functions (that are discussed in the following sections 1.1.4.1.2.1 - 1.1.4.1.2.3).

1.1.4.1.2.1 Actinin-1 and Platelets

A role for actinin-1 in a human genetic disorder has become apparent in the past three years, with four independent studies showing *ACTN1* to be one of many causative genes implicated in dominantly-inherited congenital macrothrombocytopenia (CMTP) (Bottega et al. 2015; Guéguen et al. 2013; Kunishima et al. 2013; Yasutomi et al. 2016). This is a rare blood disorder characterised by a reduced number of platelets in the peripheral vascular system along with increased platelet size (Kunishima & Saito 2006). Initially Kunishima et al identified six variants that co-segregated with affected individuals in six Japanese families suffering from CMTP. Expression of these variants in Chinese hamster ovary cells and primary mouse fetal liver-derived megakaryocytes brought about

abnormal alterations in the actin cytoskeleton organisation. Gueguen et al subsequently reported an *ACTN1* variant, p.Arg46Gln, to be segregating with CMTP in a French family. This missense mutation had already been reported by Kunishima et al. Six novel *ACTN1* variants were reported by Bottega et al. Expression of these mutant actinin-1 proteins in human fibroblast cultured cells caused actin cytoskeleton disorganisation. Recently, Yasutomi et al. have reported a p.Leu395Gln mutation in a CMTP family. It has been suggested that a possible cause for macrothrombocytopenia is a deficiency in the regulation of platelet production (Thon & Italiano 2012). In support of this, primary mouse fetal liver-derived megakaryocytes transfected with *ACTN1* variants display altered pro-platelet formation and size (Kunishima et al. 2013). This finding is compatible with the increased platelet size that is characteristic of CMTP. A recent study has reported that several of these mutations that are located in the actnin-1 ABD cause increased binding of actinin-1 to actin filaments and enhance filament bundling *in vitro* (Murphy and Young 2016). Actinin-1 may play a specific role in platelet formation, possibly through actin binding or bundling ability, that is sensitive to mutational perturbation and cannot be compensated for by other actinin isoforms.

1.1.4.1.2.2 Actinin-4 and Cancer

Invasive cancer cells exhibit increased mobility performance and, during metastasis, make use of extensive structures such as invadopodia, which are similar to lamellipodia, to guide them through the ECM and through blood vessels (Yamaguchi & Condeelis 2007; Machesky 2008). The functions of non-muscle actinins, particularly with regard to cell motility and the localisation pattern of actinin-4, being mostly expressed moving structures, such as dorsal ruffles, (Araki et al., 2000) would suggest potential metastatic properties. Indeed, overexpression of actinin-4 in colorectal cancer cells induced their formation of membrane ruffles and lamellipodia, where the actinin-4 protein was largely localised. These cells also experienced increased cell mobility compared to control cells in wound healing assays (Honda et al. 2005). In a subsequent study, this group reported a reduction in cell motility and retraction of cellular protrusions in actinin-4 knockdown colon cancer cells (Hayashida et al. 2005). Of all four actinin isoforms, actinin-4 is

predominantly associated with cancer and overexpression of actinin-4 has been reported for a number of different cancer types (Honda 2015). Biopsy samples from patients with oral squamous cell carcinoma (OSCC) revealed large amounts of staining for actinin-4 at the growing edge of the tumours, while overexpression of actinin-4 was reported for all OSCC cell types. siRNA mediated knockdown of actinin-4 in one OSCC cell line resulted in a reduction in the cell mobility rate and invasiveness (Yamada et al. 2010).

In some cases, *ACTN4* gene amplification is the cause of protein overexpression, and the use of this observation can be helpful in determining patient outcome and deciding upon additional adjuvant therapies (Honda 2015). Gene amplification has been noted in ovarian cancer patients. In these studies, patients with a high *ACTN4* copy number (four copies or over) exhibited highly malignant, chemoresistant tumours and, in general, displayed a poorer prognosis for survival than those patients with normal copy number (less than four copies) (Yamamoto et al. 2009).

Apart from overexpression, expression of an alternative splice variant of actinin-4 has been found to be associated with some cancer types (Honda 2015). Actinin-4 splicing removes the 83bp exon 8 and replaces it with an exon of the same size, exon 8a is swapped for 8b. Three amino acid changes differentiate this new exon from the normal exon. This splice variant has been detected in biopsy samples from patients with small cell lung cancer (SCLC) and large cell neuroendocrine carcinoma (LCNEC) and in many SCLC cell lines (Honda et al. 2004; Miyanaga et al. 2013). The isolated ABD of this Actinin-4 8b variant has been reported to have a greater affinity for actin than the 8a variant, which may explain why SCLC cells are characteristically fragile and it may explain the irregular actin cytoskeleton that was observed in patient biopsy samples (Honda et al. 2004). Interestingly, the sites of the three amino acid changes within the exon map near the sites of two mutations that are known to cause the kidney disease focal segmental glomerulosclerosis (FSGS) (Honda et al., 2004). This disease is discussed further in section 1.1.4.1.2.3. Actinin-FSGS causing mutants also exhibit increased actin affinity (Weins et al. 2007; Weins et al. 2005; Kaplan et al. 2000). Reports regarding the activity of this splice variant in cancer promotion have been conflicting however. A subsequent

study has found that the dimeric actinin 8b variant has a similar actin binding affinity and calcium sensitivity to that of the 8a variant (Foley & Young 2013).

In addition to its structural properties in cancerous cells, there have been several reports which suggest that actinin-4 may also act as a transcriptional co-activator (Honda 2015). Actinin-4 displays nuclear localisation in many cancer cell lines (Honda et al. 1998). *In vitro* studies suggest that actinin-4 may function to regulate transcription from nuclear hormone receptors such as the oestrogen receptor (Khurana et al. 2011).

1.1.4.1.2.3 Actinin-4 and the Kidney

In addition to different localisation patterns within a cell, unique expression of actinin-4 in the kidney has been described, particularly within podocytes (Kaplan et al. 2000). Podocytes are highly differentiated epithelial cells that strengthen the glomerular basement membrane and participate in the formation and function of the glomerular filtration barrier. They have long extensions called foot processes with function to firmly attach the podocyte to the glomerular basement membrane via integrin receptors. The foot processes of many neighbouring podocytes interdigitate together and are connected to each other through an adherens junction-like structure called the slit diaphragm, the function of which is to maintain the permselectivity of the glomerulus. The correct organisation of actin filaments is vital to maintaining this complex architecture (Pavenstädt et al. 2003; Mundel & Shankland 2002; Cybulsky & Kennedy 2011; Michaud et al. 2009).

Human studies have identified five dominant *ACTN4* mutations that cause FSGS (Kaplan et al. 2000; Weins et al. 2005). This disease is characterised by decreasing kidney function with final progression to end stage renal failure (Feng et al. 2015). These five mutations have been mapped to the actinin-4 ABD (Fig. 1.10) (Weins et al. 2005; Kaplan et al. 2000), where they give rise to a gain-of-function phenotype; mutant actinin-4 proteins have a higher affinity for F-actin binding compared to WT actinin-4 (Weins et al. 2005; Kaplan et al. 2000; Weins et al. 2007). In addition, the p.Lys255Glu-actinin-4 mutant is no longer sensitive to calcium regulation (Weins et al. 2007).

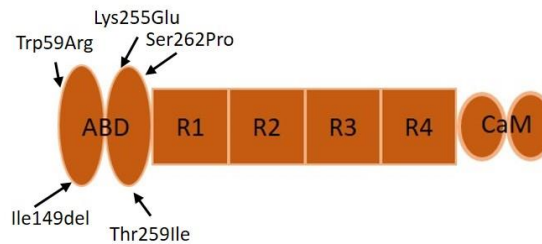


Figure 1.10: FSGS-associated Actinin-4 mutations. All five actinin-4-FSGS mutations have been mapped to its ABD.

The p.Lys255Glu mutation in the ABD resides on the CH2 domain. It was initially thought that its presence would bring about a more “open” conformation of the ABD because the replacement of a lysine residue with a glutamic acid residue disturbs an important stabilisation interaction between the two CH domains, an interaction that was thought to bring about a “closed” conformation (Lee et al. 2008). However, the crystal structure of the Lys255Glu actinin-4 ABD displayed the compact formation, which indicated that a structural change was not responsible for the increased actin binding (Lee et al. 2008). As mentioned in section 1.1.2.1, Ribeiro et al (2015) have reported the closed confirmation of the unbound actinin-2 ABD.

Many studies have suggested that actin disorganisation is the molecular mechanism by which these mutations operate to cause disease. Actin networks crosslinked with p.Lys255Glu actinin-4 and visualised using electron microscopy (Weins et al. 2007) or fluorescence microscopy (Yao et al. 2011) reveal abnormal actin organisation. WT actinin-4 induces the formation of uniform bundles of actin, while the p.Lys255Glu actinin-4 induces the formation of tight entangled networks. These Lys255Glu actinin-4-actin based networks were reported to be very fragile, this suggests that the increased actin binding may be altering the elastic properties of the actin network (Yao et al. 2011). Mouse models are also indicative of a cytoskeleton disorder. *Actn4* knock-out mice (*Actn4*^{-/-}) show altered podocyte morphology, with signs of glomerular kidney collapse and foot process effacement. They eventually develop FSGS. In mice, both actinin-1 and actinin-4 proteins are expressed in podocytes (Kos et al. 2003), however this result suggests that in mice, actinin-1 cannot compensate for actinin-4 (Kos et al. 2003). These mice also displayed a reduced podocyte number per glomerulus compared to WT mice. At

weeks 6-10 there was a 20% difference in podocyte number (Dandapani et al, 2007) and in culture, immortalised podocytes from knock-out mice were reported to be less adhesive to proteins that are commonly found in the glomerular basement membrane, such as collagen and laminin (Dandapani et al, 2007). It was found that the loss of actinin-4 resulted in a very weak linkage between the integrin receptor and the cytoskeleton, resulting in improper cell adhesion and therefore large cell loss (Dandapani et al. 2007). A knock in mouse model homozygous for the murine correlate of p.Lys255Glu-actinin-4 exhibited podocyte abnormalities such as foot process effacement, displayed signs of proteinuria and showed an altered localisation pattern of actinin-4 with protein aggregation (Yao et al. 2004).

In addition to actin disorganisation, it has been suggested that the molecular mechanism by which these mutations cause disease is through the development of protein aggregates, leading to eventual proteotoxicity in podocytes (Cybulsky & Kennedy 2011). In cell culture systems, p.Lys255Glu actinin-4 aggregates have been shown to impair the ubiquitin-proteasome system, leading to a build-up of proapoptotic stress in the endoplasmic reticulum. (Cybulsky & Kennedy 2011).

1.1.4.1.3 General Function of Muscle Actinins: The Sarcomere

The muscle actinins, actinin-2 and -3, are notable for their role in the sarcomeric Z-disc, where they crosslink and anchor actin filaments from adjacent sarcomeres (Squire 1997; Gautel & Djinoivic-Carugo 2016).

Muscle cells are made up of myofibrils, and each myofibril is composed of a chain of sarcomeres. These sarcomeres are responsible for both the structural integrity of the muscle cell, and its functionality; contraction. One sarcomere is the most basic unit of contraction in the muscle cell. The sarcomere cytoskeleton is made up of a series of thick and thin filaments, myosin and actin filaments respectively. Sarcomeres are separated from each other through a region called the Z-disc, which is made up of a network of cytoskeletal proteins and fibres. Actin filaments extend from this Z-disc structure down the sarcomere. Viewed under a light microscope, this region makes up part of the I band. Towards the centre of the sarcomere is a region of cross-linked myosin filaments, the M-band. Where both

the actin and myosin filaments overlap is a region called the A band. In the presence of calcium and ATP, these actin and myosin filaments slide past each other through a mechanism called the Sliding Filament Model, which involves myosin binding to and pulling the actin filaments towards the centre of the sarcomere. During this process both the actin and myosin filaments do not shorten in length, but simply overlap to a greater extent, i.e. the I band becomes narrower and the A band becomes wider, which results in the shortening of the sarcomere length (Lodish et al. 2008a). When a muscle contracts, this process is intensified; all the millions of sarcomeres within the entire muscle, work congruently together, over distances of millimetres to centimetres to bring about unidirectional force and movement that ultimately brings about whole muscle contraction (Gautel & Djinoivic-Carugo 2016). The steady and regular banding pattern seen for all sarcomeres under a light microscope is evidence of a highly organised collection of cytoskeletal proteins (Gautel & Djinoivic-Carugo 2016).

The sarcomere (Fig. 1.11) is considered to be a biological machine, made up of many different parts interacting together (Barral & Epstein 1999). The basic parts that make up this machine are the proteins myosin and actin, along with a host of accessory proteins such as titin, telethonin, actinin, tropomyosin, myomesin and nebulin, to name a few (Gautel & Djinoivic-Carugo 2016). Assembly of this highly organised machine occurs progressively, from the formation of premyofibrils to nascent myofibrils and eventually to mature myofibrils, with interactions between many of those aforementioned proteins. Premyofibrils are minisarcomeres, they contain Z bodies which are composed of actinin and cross-linked actin, while their A band region contains nonmuscle myosin II proteins. The addition of muscle myosin II and titin to the Z bodies alters the actinin organisation, and this signals the shift from premyofibrils to nascent myofibrils. Also, at this stage the premyofibrils start to align with each other. As maturation continues, the aligned Z bodies start to transform into Z-discs. Further proteins, such as telethonin and myomesin, are added to the complex to stabilize the core proteins (Sanger et al. 2010; White et al. 2014). Interactions between these proteins is mediated by a multitude of chaperone proteins (Willis et al. 2009). This highly organised protein assembly is a great example of how nature employs molecular assembly to generate well defined

protein complexes. The precision of molecular assembly is evident from the regularity that is observed between sarcomeres. This regularity is vital to muscle functionality (Gautel & Djinojic-Carugo 2016).

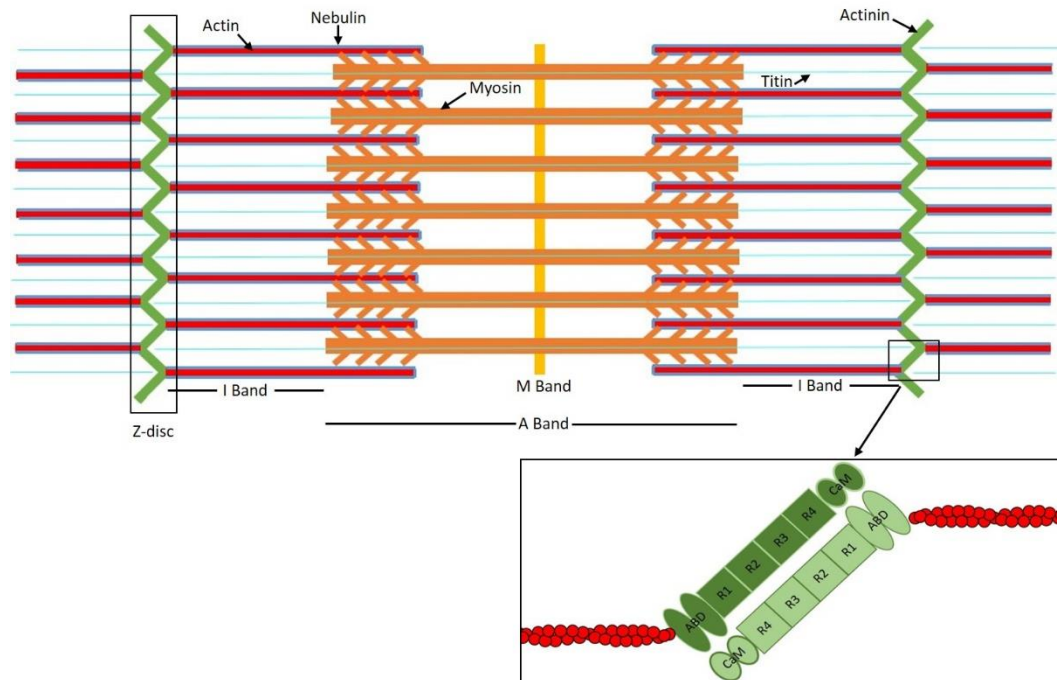


Figure 1.11: Schematic Diagram of the Sarcomeric Cytoskeleton. The M-band is made up of crosslinked myosin filaments. The Z-disc marks the end of the sarcomere and is made up of actinin mediated actin cross links. Actin filaments extend into the I-band. The A-band consist of overlapping myosin and actin filaments.

Muscle actinins are largely localised to the Z-disc of the mature sarcomere, in fact actinin it is one of its primary proteins. Here, actinin functions to cross-link anti-parallel actin filaments from two neighbouring sarcomeres to create a tetragonal lattice-like structure (Sjöblom et al. 2008). This tetragonal lattice is quite elastic and can adopt two different conformations, a small square lattice and a basket weave conformation (Luther 2009). These conformations are a symptom of the condition of the muscle; small square form takes precedence in relaxed muscle while the basket weave form takes precedence in contracting muscle (Goldstein et al. 1988). These conformations are permitted owing to inherent flexibility in the helical linker connecting the ABD to spectrin-like repeat 1, and the rigidity of the central rod region (discussed in section 1.1.2.3.1) (Ylänne et al. 2001; Ribeiro et al. 2014; Gautel & Djinojic-Carugo 2016).

Apart from flexibility, the functions of the Z-disc actinin-actin lattice suggest that it possesses huge mechanical and physical strength and stability; it stabilises the muscle contractile machinery (Sjöblom et al. 2008), it controls the assembly of actin filaments (Luther et al. 2002) and it permits the transmission of mechanical strain or force from one sarcomere to the other (Vigoreaux 1994).

Actinin also plays a principle role in determining muscle performance. The width of a Z-band differs among fibre types and muscle types; fast muscles fibres have narrow Z-bands, while cardiac and slow muscles fibres have wide Z bands. This represents an adaption of the muscle to its function, fast muscle fibres produce a very high contraction velocity with a strong force (Luther 2009). Overlap between the actinin-actin cross-links produce different amounts actinin-actin layers within the Z-band. The width of a Z-disc is known to correlate to the number of actinin-actin layers in that Z-disc. Fast muscle fibres usually exhibit two layers while slow muscle fibres exhibit six layers (Luther 2009). The muscle protein titin is known to also play a role here. Titin is a giant protein, the length of which runs from the M band to the Z-disc in the sarcomere (Luther 2009). 45 amino acid residue repeats, called Z-repeats, make up a region near its N-terminus. Actinin can bind these Z-repeats through its C-terminal CaM domain. In this way, titin acts as a 'molecular ruler', targeting actinin to the Z-disc and specifying its layout (Young et al. 1998). Alternatively spliced variants of titin are found in different muscle types and they contain different numbers of Z repeats (Gautel et al. 1996). This means that each variant binds a different number of actinin molecules, leading to a different number of actinin-actin cross links for each muscle type.

1.1.4.1.4 Actinin-3 Specific Functions

Both actinin-2 and actinin-3 are the non-muscle, calcium insensitive actinin isoforms. These isoforms both share 80% amino acid identity. Actinin-2 is expressed in all muscle fibre types while expression of actinin-3 is limited to type two fast glycolytic skeletal muscle fibres, the muscle fibres responsible for the generation of rapid and forceful contractions. This actinin-3 restricted expression would imply that actinin-3 is the most specialised of the mammalian actinins (Beggs et al. 1992; MacArthur & North 2007; Mills et al. 2001). Surprisingly, an *ACTN3* polymorphism,

causing the nonsense mutation p.Arg577X, was found to be very prevalent in many human populations (North et al. 1999). Approximately 16% of the world's population are homozygous for this sequence change that completely prevents the production of the actinin-3 protein, meaning that more than one billion people lack actinin-3 expression (Lek et al. 2010). This null genotype is not associated with any disease, suggesting that *ACTN3* is a non-essential gene in humans, and its loss compensated for by actinin-2 (North et al. 1999). Though absent in birds, the *ACTN3* gene is conserved in most other vertebrates, including fish, suggesting that it arose by gene duplication early in vertebrate evolution (Holterhoff et al. 2009). Actinin-3 must have had non-redundant functions through the course of vertebrate evolution in most lineages to explain its sequence conservation. In early humans however, it appears that the p.Arg577X mutation arose, was not detrimental, and was maintained for some time, before expanding under positive selection to achieve a very high frequency in specific populations (e.g. European and Asian), but not others (e.g. African)(Mills et al. 2001).

Yang et al. (2003) initially reported an overrepresentation of the wildtype *ACTN3* allele (p.Arg577Arg) in elite Australian sprint athletes, suggesting that its presence is advantageous in sprint and power activities. They also found the homozygous p.Arg577X genotype to be more common in female endurance athletes when compared to power athletes. This suggested that the *ACTN3* genotype is linked to normal variation in muscle function, with each genotype possibly conferring an advantage for different types of athletic performance. Numerous other studies have subsequently investigated the association between the *ACTN3* genotype and athletic performance, in both normal populations and various groups of elite athletes. Some studies support the basic findings of Yang et al. (2003), while others do not find significant associations. Overall, it can be concluded that at least in some populations (e.g. Caucasians), the association of the wildtype allele with sprint and power performance seems to hold true, while the association of p.Arg577X variant with enhanced endurance is not as clear cut (Alfred et al. 2011; Eynon et al. 2012). Notably though, in African populations, where the frequency of the p.Arg577X variant is very low, no association of *ACTN3* genotype with elite athlete status was found (Yang et al. 2007), despite Kenyans

and Ethiopians having dominated long-distance running in recent years (Larsen 2003). This suggests that we must consider not only the *ACTN3* genotype, but also other polymorphisms that may be working in combination with, or independently of, *ACTN3* to dictate performance (Alfred et al. 2011). In addition, athletic performance depends not just on an individual's genetic make-up, but also on environmental factors, training regimes and coaching expertise (Alfred et al. 2011; Eynon et al. 2012).

Studies of *Actn3* knockout mice provide further insights (MacArthur et al. 2007). These mice are viable and healthy. They do exhibit slight decreases in muscle mass and muscle strength, but these values are regarded as within the normal range and are not a sign of muscle dysfunction (Berman & North 2010). More significantly, these mice display muscle metabolism conversion from the anaerobic pathway, which is generally seen in slow muscle fibres (MacArthur et al. 2007). Activity of key enzymes associated with oxidative metabolism, such as citrate synthase and succinate dehydrogenase, and glycolysis, such as hexokinase, are increased, while indicators of anaerobic metabolism namely glycogen phosphorylase, showed decreased activity. The metabolic changes have a positive effect on endurance; knockout mice have a much greater running distance prior to experiencing fatigue compared to wildtype controls (MacArthur et al. 2007). The function of glycogen phosphorylase is to breakdown glycogen. In humans, activities such as sprinting rely on glycogen as a main source of energy, a reduction in glycogen breakdown would therefore be unfavourable to sprint athletes (Berman & North 2010). However, a reduced ability to breakdown glycogen might be beneficial to endurance athletes, as it allows them to utilise other fuels and conserve glycogen (Quinlan et al. 2010). Thus, metabolic changes observed in *Actn3* knockout mice might provide plausible explanations for the association of *ACTN3* genotypes with sprint/power versus endurance performance in humans. More efficient aerobic muscle metabolism may be the trait associated with p.Arg77X genotype that has been positively selected for in specific human populations. The frequency of this allele in human ethnic groups is correlated with latitude, with the p.Arg577X mutation is more prevalent further from the equator (Friedlander et al. 2013). Indeed, recently described alterations in the calcium kinetics of *Actn3* knockout

mice are consistent with cold acclimatisation and thermogenesis (Head et al. 2015; Quinlan et al. 2010)

The molecular mechanisms mediating these effects on actinin-3 are still unknown. Actinin-2 and actinin-3 serve as a scaffold to anchor many signalling proteins and metabolic enzymes to the Z-disc (Sjöblom et al. 2008). Most of these interactions are probably shared by both muscle actinin isoforms, though this has not been explicitly tested, nor have actual binding affinities been compared. Assuming there are some differential interactions of signalling proteins with actinin-2 versus actinin-3, then alterations in sarcomeric signal transduction in humans or mice lacking actinin-3 could drive a program of gene expression resulting in the actinin-3 null muscle phenotype. Calsarcin-2, a regulator of calcineurin signalling, displays just such a differential interaction (Seto et al. 2013). Actinin-3 deficient muscle in both mice and humans show enhanced calcineurin signalling, probably as a result of increased binding of calsarcin-2 to actinin-2 in the absence of actinin-3 (Seto et al. 2013). Calcineurin signalling is known to shift muscle fibres towards an oxidative phenotype (Long et al. 2007; Delling et al. 2000; Chin et al. 1998).

In the interest of completeness, a number of investigations have now linked dominantly-inherited *ACTN2* missense mutations to a range of myopathies. An *ACTN2* mutation was reported in a patient with dilated cardiomyopathy (DCM), a condition characterised by dilation of the left ventricle of the heart and a reduction in the heart's ability to contract (Mohapatra et al. 2003). This p.Gln9Arg mutation is found in the ABD of actinin-2 and abrogates an interaction of actinin-2 with the Z-disc component muscle LIM protein (MLP) (Mohapatra et al, 2003). Examining patients with hypertrophic cardiomyopathy (HCM), Theis et al. (2006) identified thirteen mutations in five Z-disk proteins, including three in actinin-2. Semsarian and co-workers found one of these same mutations (p.Thr495Met) as well as three novel mutations in Australian families affected by HCM and other heterogeneous cardiac conditions (Chiu et al. 2010; Bagnall et al. 2014). Similarly, an actinin-2 p.Met228Thr mutation was found to segregate with affected individuals in a large Italian family that had a history of HCM and juvenile atrial arrhythmias (Girolami et al. 2014). Eight *ACTN2* have thus far been linked to HCM, DCM and/or other cardiac

abnormalities. These mutations do not map to a particular region of actinin-2, with some located in the ABD, some in the central rod and one in the CaM domain. While mutations that map to the ABD and CaM domains may affect actin binding properties, those in the rod domain are more likely to affect the binding of other Z-disc proteins to actinin. However, the consequences of these mutations have not been examined experimentally.

1.1.4.2 Functions of Spectrin Proteins: Erythrocyte Membrane Skeleton

Spectrin fashions actin filaments in to ordered networks. In their most prominent role they are responsible for providing support and shape to the erythrocyte through their ability to crosslink actin filaments into a flexible 2D protein lattice known as the erythrocyte membrane skeleton (EMS) (Bennett & Baines 2001).

The essential function of the erythrocyte is to carry and offload oxygen from the lungs to the tissues of the body. This requires the erythrocyte to pass through not only blood vessels of the macrovasculature, but also thin, narrow blood vessel capillaries of the microvasculature, some of which are narrower than its own diameter, everyday throughout its 120-day life-cycle (Gratzer 1981). This means that, throughout the hundreds of miles that the erythrocyte travels in its lifetime, it undergoes considerable morphological revisions; from a biconcave, discoid shape in the macrovasculature to a parachute shape in the microvasculature, with regression back to the biconcave shape in the macrovasculature again (Uzoigwe 2006). This shape change is not only required for progression through the circulatory system, but it also maximises their functional performance; the biconcave shape encourages laminar flow and discourages turbulent flow, while the parachute shape encourages diffusion of oxygen molecules to the tissues through its increased surface area (Uzoigwe 2006). These mechanical and elastic properties are attributed to its membrane skeleton, the aforementioned 2D flexible protein lattice (Fig. 1.13) comprising of spectrin crosslinked with actin, and many other proteins such as, protein 4.1 and ankyrin, tropomyosin and protein 4,2 (Bennett & Baines 2001). This lattice has a well ordered hexagonal shape (Liu et al. 1987). The most basic aspect of this lattice formation is the self-association properties

displayed by spectrin. The functional unit of spectrin is the heterodimer (Fig. 1.12A) (Winkelmann & Forget 1993) however, anti-parallel association of two spectrin heterodimers through interaction between the N-terminal α -spectrin partial repeat 1 and the C-terminal β -spectrin partial repeat 17 forms a spectrin tetramer that consists of a long chain of uninterrupted spectrin repeats (Ipsaro et al. 2010). This formation places an ABD at both ends of the tetramer (Dubreuil et al. 1989). In this form, spectrin can crosslink actin filaments (Fig 1.12B) (Begg et al. 1997).

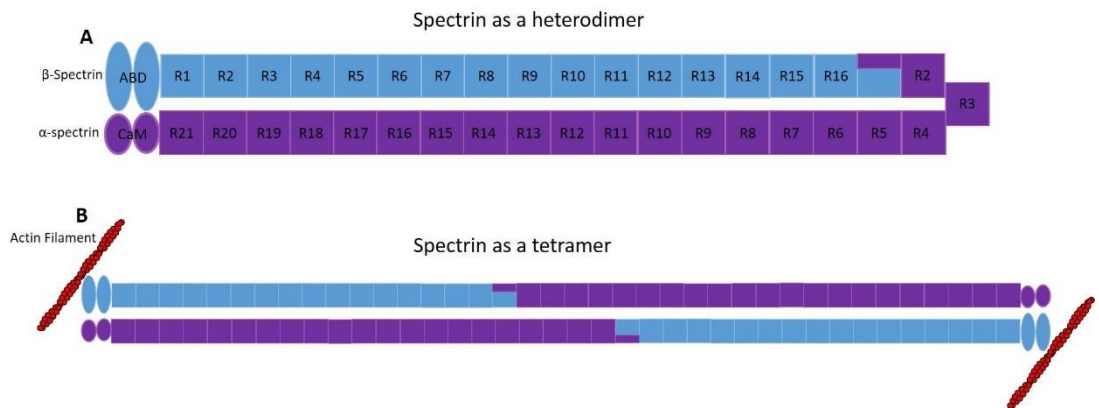


Figure 1.12: Heterodimeric Spectrin Complexes and Tetrameric Spectrin Complexes. (A) Spectrin can exist as a heterodimer made up of an α -spectrin subunit and a β -spectrin subunit. To form a closed “hairpin” dimer, the longer α -Spectrin folds back on its N-terminal so that the α -Spectrin partial repeat interacts with and forms an intradimer bond with the β -Spectrin partial repeat (Speicher et al. 1993). (B) Spectrin can also exist as a tetramer, made up of two α -spectrin proteins and two β -spectrin proteins. Tetramer formation is brought about with antiparallel association of two spectrin heterodimers through interactions between the α -spectrin and β -spectrin partial repeats. This tetramer formation places an ABD at either end of the structure, facilitating actin crosslinking (Ipsaro et al. 2010; Dubreuil et al. 1989; Begg et al. 1997).

The ability of the erythrocyte to resist mechanical stress are supplied by spectrin. Spectrin tetramers have the ability to convert and revert into dimers and tetramers respectively. The dissociation of tetramers to dimers accommodates the large amount of deformation needed for the erythrocyte to pass through small blood vessels (An et al. 2002). The importance of these elastic properties of spectrin is demonstrated by the finding that the spectrin dimer/tetramer self-association site is a very common target for mutations (Pascual et al. 1997) which cause haemolytic anaemias such as hereditary elliptocytosis (HE) (Dhermy et al. 1982; Nicolas et al. 1998; Delaunay 1995) The red blood cells (RBCs) of patients with this disease exhibit increased instability and fragility (Liu et al. 1982).

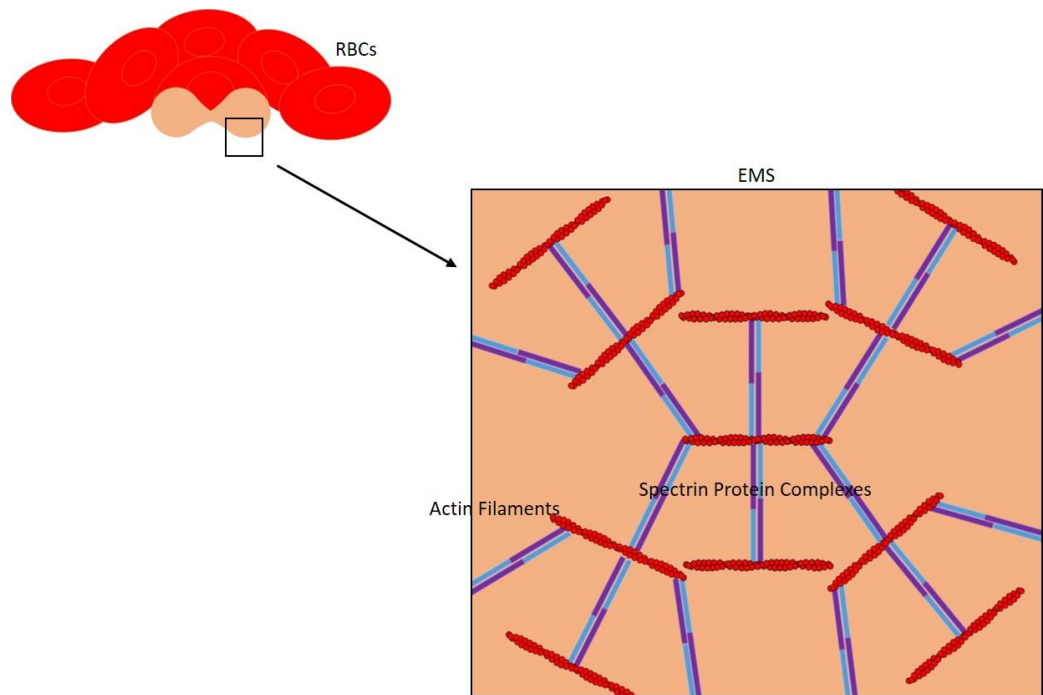


Figure 1.13: The Erythrocyte Membrane Skeleton. Tetrameric spectrin complexes function to crosslink actin filaments into a 2D protein lattice called the EMS which functions to provide RBCs with shape and support (Bennett & Baines 2001).

The protein ankyrin functions to tether this spectrin lattice to the RBC membrane bilayer through interaction with both β -spectrin, at spectrin repeat 15, and band 3, an integral membrane protein. Spectrin tetramers provide two ankyrin binding sites (Pascual et al. 1997). Protein 4.1 also has a similar function. It binds both β -spectrin, in the ABD, and the protein glycophorin C, another integral membrane protein (Workman & Low 1998). These interactions function to not only tether the cytoskeletal lattice to the cell membrane but they also stabilise the membrane. In binding to these membrane proteins, spectrin controls their distribution within the membrane. It also acts to prevent receptor aggregation and to prevent the formation of membrane regions devoid of proteins; such regions promote membrane fragmentation or vesiculation (De Matteis & Morrow 2000; Gratzer 1981). The spectrin lattice can also be attached to the lipid bilayer through direct interaction with phospholipids along the inner layer. Phosphatidylserine (PS) was found to bind to spectrin repeats from both α -spectrin and β -Spectrin; β -Spectrin repeats 12-14, which is close to the ankyrin binding site, and α -Spectrin repeats 8-10. PS was also reported to bind at a site close to the protein 4.1 binding site, near the ABD on β -spectrin (An et al. 2004a; An et al. 2004b). It has been

suggested that these interactions between spectrin and phospholipids act to stabilise the lipid bilayer with concern to the translocation of phospholipids from one leaflet of the membrane to the other (An et al. 2004a; Mohandas & Gallagher 2009).

Many other proteins play many other roles in this complex structure; protein 4.2 (as mentioned in section 1.1.3.2) acts to maintain the integrity of the EMS (Sung et al. 1992), adducin functions to cap the fast growing end of actin filaments, and tropomodulin, in a complex with tropomyosin, caps the slow growing end of actin filaments (Machnicka et al. 2014; De Matteis & Morrow 2000). The end result is a large multifunctional elastic and deformable self-assembled protein scaffold capable of binding to and organising cytoplasmic, structural and membrane proteins (De Matteis & Morrow 2000; An et al. 2002).

1.1.5 Conclusion

Both actinin and spectrin proteins display a remarkable array of capabilities. Nature has selected them as building blocks to create a wide variety of important cellular structures not only for their robust qualities, but also for their finely tuned molecular recognition properties. While both proteins are similar in terms of their domain content, their structural differences (i.e. number of spectrin repeats) and thereby functional differences are very apparent when comparing their EM micrographs. Actinin has been described as “rod-like” (Winkler et al. 1997) while spectrin has been described as “floppy” (Yoshino & Marchesi 1984). These observations emphasise the adaptability of the spectrin repeat. Such structures, or variations thereof, might also be useful in an unnatural setting, outside the cell.

Mutational studies involving actinin-4 and FSGS have revealed how simple missense mutations can give rise to new or altered properties. Such properties, although an obvious disadvantage to a natural system, such as the kidney, might be advantageous in the construction of an unnatural system or complex.

Many studies have documented successful efforts in using biomolecules as building blocks to create nanostructures with potential useful properties. The next section of this introduction I review some of these studies.

1.2 Bionanotechnology and its Contributions to Synthetic Biology

The definition of Synthetic Biology is two-part: firstly; it involves the use of unnatural molecules to construct or reproduce complexes from natural biology, secondly; it exploits natural components from living systems to produce complexes that assemble unnaturally, and have either comparable or different properties to those already seen in nature (Benner & Sismour 2005). It offers the potential to gain a better and deeper understanding of biological systems and to also develop novel molecules and systems (Benner & Sismour 2005). On review of the literature within this area of research, it is clear that Bionanotechnology has contributed to many of the advances in Synthetic Biology in recent times.

Nanotechnology concerns the research and development of materials, devices and systems whose structure is defined in the nanometre scale. Objects at this size and scale are termed 'nanoparticles', and they are very desirable because of their novel properties, providing great potential in the field of medicine and biology. By operating at the nanoscale, nanoparticles can pass through blood vessel walls and travel within the circulatory system of the host. They can also transverse many physiological barriers, such as the blood-brain-barrier and stomach epithelium (McNeil 2005). Their small size also disposes them to many non-therapeutic applications too. In electronic circuitry, for example, nanometre scale electronic connections are advantageous because they allow for a faster performance at a reduced weight and power consumption (Mishra 2015). Traditionally, nanoparticles have been prepared using top-down approaches such as photolithography (Xia & Whitesides 1998) and much study has been focused on the use of nanomaterials such as metals and carbon (Nayak & Andrew Lyon 2005). Biomolecules, such as DNA, lipids, polysaccharides and proteins, are nanoparticles that naturally exist in the nanometre range, and bionanotechnology employs their molecular recognition properties in the "bottom-up" fabrication and self-assembly of artificial nanostructures (Jungmann et al. 2008). Self-assembly is profuse in nature, where stable systems and complex organelles are assembled from simple building blocks of biological molecules. Structural compatibility and chemical complementarity provide the shape and surface properties to bring about this

instinctive, spontaneous and specific association of molecules, which is mediated through many non-covalent interactions such as hydrogen bonds, Van Der Waals and electrostatic interactions, the sum of which contribute to the overall stability of the complex (Whitesides et al. 1991; Goodsell & Olson 2000). Biomolecular self-assembly is an attractive bottom-up approach to nanoconstruction because it does not require the need to individually pattern building blocks. This approach therefore contains fewer design steps, making the whole process much faster and much more amenable to mass production in the long-term (Scheibel et al. 2003). Also, because assembly is initiated at the atomic or molecular level, construction using self-assembling biomolecules as building blocks provides a much greater degree of control over the construction process (Lee et al. 2010) and it allows for the manipulation of these building blocks, so as to functionalize the final structure.

While this study is primarily interested in protein-based bionanotechnology, a brief review of research carried out on all biological molecules (nucleic acids, lipids, carbohydrates and peptides and proteins) is important. It contributes to a better understanding of this scientific field, particularly with regard to techniques and theories, and it provides inspiration and ideas for similar bionanotechnology based projects.

1.2.1 Nucleic Acid Nanotechnology

Nucleic acids have been reassigned from their traditional use in molecular genetics and genetic manipulation and have now been described as materials with which to build nanostructures. Single strands of DNA can self-assemble into double stranded helices through complementary and precise hydrogen bonding Watson-Crick base pairing. This simple, specific, and most importantly, predictable bonding of DNA base pairs, adenine-thymine and guanine-cytosine, makes DNA highly programmable for construction (Krishnan & Bathe 2012). It has the ability to be processed with atomic precision and efficiency with DNA -modifying enzymes, such as endonucleases and ligases, and thus provides the researcher with a “toolbox” of biomolecular reagents (Niemeyer 2001). DNA synthesis is relatively cheap and DNA

amplification is a very straightforward process (Niemeyer 2001; Krishnan & Bathe 2012). Finally, the DNA double helix has been well characterised; the distance between each base pair is 3.4 Angstrom, it has a diameter of 20 Angstrom and it makes a complete turn about its axis every 10-10.5 base pairs, or every 3.5nm (Nelson & Cox 2005a). This knowledge should provide for control and calculation of the final arrangement of the structure.

1.2.1.1 Tile Based Approach

The tile based approach is one method used to construct DNA-based nanostructures. Structures are self-assembled from branched DNA structures which resemble branched DNA Holliday Junctions that form during cell division (Seeman 2003). Each branch point is designed to contain a complementary single stranded DNA overhang, called a “sticky-end” so that self-assembly of these branched structures is brought about through complementary sticky-end hybridisation (Seeman 2003). Initial building blocks consisted of four DNA strands, creating four way junctions, but more rigid building blocks have since been described consisting of double and multiple crossover motifs, and comprising of two DNA intertwined duplexes at each branch point (Seeman et al 1993; Shen et al. 2004).

Using this tile based approach Yan et al. (2003) created a DNA tile nanostructure comprising four four-branch junctions that could self-assemble into two different lattice forms, depending on the composition of the sticky ends; a nanoribbon or 2D nanogrid. The branched junctions were formed from nine single stranded DNA strands, with each branch point pointing North, South, East or West. Individual branch points were stabilised with interaction between two single strands of DNA, and with the participation one single strand in all four junctions. The distinctive feature of this structure was their inclusion of T4 DNA hairpin loops in each of the four inside corners of the tile. Their purpose was to allow the branch points to point in all four different directions, and to decrease interactions between the different branch points. While serving a very important structural role, in a follow-on study Park et al. (2005) found that, in the 2D nanogrids lattice formation, these DNA loops could serve to aid in functionalising the nanogrid with their ability to tether functional groups. This group found that this nanogrid could be useful as a

periodic protein array; they observed periodic streptavidin arrays when they incorporated biotin into the T4 loops. This report proves that it is possible to pattern DNA nanostructures, and that it may be possible to do so precisely. It represents a movement in the right direction for the eventual use of DNA lattices to scaffold the assembly of molecular complexes, for example.

1.2.1.2 DNA Origami

Another approach for generating DNA nanostructures is called DNA origami, developed by Paul Rothemund (Rothemund 2006). This new technique facilitates the rapid design and creation of DNA nanostructures and its development represents one of the most important advances in DNA nanotechnology (Nangreave et al. 2010; Rothemund 2006).

The DNA origami technique is very straightforward and is based on the folding of a long single strand of DNA, called the scaffold strand, Rothemund exploited from the M13 phage genome, into any desired shape or pattern with the aid of many, much shorter single strands, called staple strands (Rothemund 2006). Rothemund himself described the technique as a “one-pot” method (Rothemund 2006) in which the scaffold strand and the short staple strands are all mixed in a Mg^{+2} buffer and are then heat annealed to create the desired designed structure (Rothemund 2006). The staple strands are designed to be complementary to two or more different regions of the scaffold strand and they are also all of different lengths so that they all anneal at different temperatures. The initial attachment partly arranges the scaffold and makes it more feasible for the remaining strands to bind, making the folding process hierarchical and therefore coordinated. In general, 100-fold excess staple strands are used so that incorrect binding can be eliminated through strand invasion during the hierarchical folding process (Birkedal et al. 2011; Zadegan & Norton 2012; Rothemund 2006; Nangreave et al. 2010). It is believed that the long scaffold strand acts to enclose the staple strands in a small area, thereby increasing their concentration. Regardless of whether oligonucleotides are purified or not, this increase in concentration causes precise stoichiometry to form between staple and scaffold and, as a result, leads to the generation of correctly formed structures (Pinheiro et al. 2011).

In general, the DNA origami approach has taken precedence over the tile-based approach. The latter requires a considerable amount of knowledge on DNA geometry (Rothemund & Andersen 2012) and is very time consuming, requiring the precise design and exact stoichiometry of many oligonucleotides so that they assemble into the desired structure (Nangreave et al. 2010). Equimolar stoichiometric concentrations are not a concern using the DNA origami approach because the staple strands are not required to bind to each other and so their concentrations are not important (Nangreave et al., 2010).

Rothemund initially used his technique to produce random 2D planar shapes and structures, such as a smiley face, a star and dolphin (Andersen et al. 2008; Rothemund 2006). However, a leading study carried out by Ke et al. (2008) found that this technique was not limited to the production of arbitrary shapes and that it might have important applications in single molecule detection. In this study, Ke et al used the DNA origami method to create nucleic acid probe tiles that allowed for the label free detection of RNA hybridization. Short staple strands were designed to fold a long scaffold strand into a rectangular nucleic acid tile, from which single strands of DNA, each 20 nucleotides in length, protruded from. These protruding single strands were complementary to their RNA targets, *Rag-1*, *c-myc* and *β -actin*, and they worked together in pairs to bind 40 bases of their RNA target. The binding of the RNA target to the pair of half probes caused the strands to form a stiff V-shaped structure. After binding the tiles were then adsorbed onto mica and the new stiff V-shaped structure, signalling RNA hybridisation, was easily detected using atomic force microscopy (AFM). While this probe tile is not yet at the standard where it can compete with the more established techniques for low level gene detection, such as DNA microarrays that contain thousands of probes, its smaller size, and its potential to be made smaller, offers it the possibility of one day being used to detect low level gene expression in one single cell.

Another very exciting study using 2D DNA origami was reported by Endo et al. (2010). They used the DNA origami method to scaffold a study of enzyme activity. Their 2D DNA structure was designed to contain a centre vacant area. Through this vacant area they placed double stranded DNA molecules that each had a damaged nucleobase that was in need of repair. Onto this structure they then

planted DNA base excision repair enzymes and through AFM they were able to analyse and capture the motion of the enzymes as they processed the DNA. This study demonstrated the ability of a DNA-based structure to act as a support when studying complex interactions.

Apart from 2D structures, there have also been a number of studies describing their production and use of 3D origami nanostructures. Ke et al. (2009) reported construction of a closed tetrahedron container. In one step, 248 designed staple strands folded along the M13 scaffold DNA creating a tetrahedron with internal volume of $1.5 \times 10^{-23} \text{m}^3$. One of the most exciting structures arising from 3D DNA origami was the design and creation of a DNA box that remarkably had a controllable lid, opening in the presence of externally supplied “keys” (Andersen et al. 2009). Its assembly took place over two reactions, the first involved the folding of the M13 phage into six DNA origami sheets, and the second involved linking the edges of each sheet together to form the cuboid box shape. The DNA box had an external size of $42 \times 36 \times 36 \text{nm}^3$. Strand displacement was the technique used to bring about opening of the lid. The “lock” on the DNA box was made up of DNA duplexes with “sticky ends”. The “key” was a new strand, the displacement strand, that was designed to be complementary to the “sticky-ends” of the “lock”. Hybridization between the displacement strand and the “sticky-ends” of the DNA duplex, brought about branch migration which displaced the pre-hybridized strands, forming the “lock” (Andersen et al. 2009; Zadegan & Norton 2012). The addition of two fluorophores, one to the edge of the lid and the other to the edge of the face perpendicular to the lid, meant that the opening of the lid could be monitored through FRET (fluorescence resonance energy transfer) analysis; when the lid is closed, FRET occurs because the dyes are close to each other, but opening of the lid brings distance between the dyes, and FRET decreases (Andersen et al. 2009). The next important step with such a structure is to determine its ability to store cargo. 3D DNA structures that possess the ability to carry molecular cargo have enormous potential in future applications, especially as a delivery vehicle for the transport and release of cargo such as therapeutic agents.

1.2.1.3 RNA Nanostructures

To extend the utilisation of nucleic acids as building blocks in the construction of nanostructures RNA molecules are now being considered as a building material. RNA has many distinctive and special characteristics that also make it suitable for this purpose. Just like DNA, RNA molecules can also self-assemble through Watson-Crick complementary base pairing. However, RNA molecules also have alternative base pairing rules, non-Watson-Crick base pairing such as Wobble base pairing (Li et al. 2016), which allow RNA molecules to fold into structurally distinct motifs, such as loops, pseudoknots, bulges hairpins and stems (Li et al., 2016). The variety of structures that natural RNA molecules can form reveals a very impressive folding capability for nanoconstruction exploitation. Using hairpin loops and kissing loop RNA structures Chworos et al. (2004) constructed RNA “jigsaw pieces” or tectosquares which, through sticky tail connectors, could self-assemble into pre-designed patterns.

Not just limited to DNA, studies have also proven that RNA molecules are also amenable to the origami technique of nanoconstruction. In one such study a long single strand of RNA molecules, produced from an *in vitro* transcription reaction, was folded into a pre-designed shapes, such as rectangles and triangles, using DNA staple strands (Wang et al. 2013). This study noted however, that the RNA scaffold strand was less stable than a DNA scaffold strand. In fact, RNA instability is a factor that has interfered with the progression of RNA as a nanostructure building material (Guo 2010).

1.2.2 Carbohydrate Nanotechnology

A broad range of heterogeneity exists between different polysaccharides. This heterogeneity is brought about by the presence or absence of certain functional groups; amino, carboxyl, or hydroxyl groups, and the position of these groups, their chirality, and their ability to form linear or branched structures (Ghazarian et al. 2011). This diversity offers potential for the arrangement of unique nanostructures, and their functional groups are readily amenable to chemical modification (Swierczewska et al. 2016; Han et al. 2015).

The attachment of hydrophobic molecules, such as fatty acids, to the polysaccharide backbone has brought about self-assembly of carbohydrate nanoparticles, consisting of a hydrophobic cavity and a carbohydrate outer framework. These nanoparticles are capable of carrying the drug ibuprofen and so display remarkable potential for drug delivery and release therapies (Jiang et al. 2006). While the structural complexity of polysaccharides is regarded as their biggest potential for use in the nanotechnology industry, it may also be regarded as one their biggest deterrents. Their complexity complicates their preparation process and reduces the yields obtained (Han et al. 2015). Research carried out to identify and address these challenges will inspire more studies to consider polysaccharide molecules as tools for nanoconstruction (Han et al., 2015).

1.2.3 Lipid Nanotechnology

Lipid nanotechnology has not yet been acknowledged as a scientific discipline and this is surprising because lipids do exhibit some attractive properties that make them appealing as a building material and there are many studies describing their use as such (Mashaghi et al. 2013). Phospholipids are amphiphilic being made up of a hydrophilic polar head group and two hydrophobic hydrocarbon tails (Nelson & Cox 2005c). In an aqueous environment, hydrophobic interactions force these phospholipids to spontaneously self-assemble into lipid bilayer. An exposed edge in a lipid bilayer is forbidden, phospholipids will always rearrange themselves to close the edge, forming closed structures with internal cavities called liposomes (Nelson & Cox 2005d). These liposomes can be manipulated to enclose molecular reagents upon assembly (Mashaghi et al. 2013) and have proven popular as a form of nano-gene or drug carrier in the medicine and healthcare industry. Liposomes functionalised with monoclonal antibodies directed against the ErbB2 tyrosine kinase receptor, a receptor which plays a large role in the pathogenesis of many types of cancer, have served very well as nano-carriers of the drug Doxorubicin. In animal models, these liposomes were specifically targeted to and internalised in ErbB2 overexpressing cells, showing successful targeted delivery, and no drug leakage (Park et al. 2002). The utility and

benefit in using natural biomolecules as building blocks for nanostructures became apparent when, in 2007, the FDA approved the human use of Doxil, a liposomal formulation drug for the treatment of myelomas (Ning et al. 2007).

1.2.4 Peptide Nanotechnology

Peptides are simple structures which can be easily synthesised. They are capable of self-assembly and their amino acid side chains can be readily functionalised with both chemical and physical properties. For these reasons, peptides are attractive building blocks for nanoconstruction (Colombo et al. 2007; Gilead & Gazit 2005).

1.2.4.1 Dipeptides

In nature, polypeptide self-assembly is normally associated with disease. Amyloid fibres are an organised collection of self-associating polypeptides, of average diameter 4-11nm (Rambaran & Serpell 2008). The presence of amyloid fibres is the prevailing characteristic of several diseases, such as Alzheimer's Disease, in which these aggregations were found mostly to be made up a 4kDa β -amyloid peptide of 40-43 amino acids in length, a fragment of the transmembrane amyloid precursor protein (APP) (Tatarnikova et al. 2015; Rambaran & Serpell 2008). In studies to identify the molecular mechanism by which this aggregation was occurring, it was found that a core diphenylalanine recognition motif within this β -amyloid peptide was the minimum requirement to induce polypeptide aggregation. Remarkably, this dipeptide contained all the information required to self-assemble (Reches & Gazit 2006). The natural self-assemblies observed with this dipeptide were well-ordered distinct nanotubes of constant lengths that were brought about by stacking interactions between the phenylalanine residues (Reches 2003; Reches & Gazit 2006). These nanotubes were found to be highly stable and soluble in organic solvents (Reches 2003; Reches & Gazit 2006) and have been used as moulds for casting metal nanowires (Reches 2003). Ionic silver solution was added to the cavity of the nanotube, and was then reduced using citric acid. The diphenylalanine peptide mould was then removed via proteolytic degradation using

proteinase K. Individual silver nanowires were obtained, each ~20nm in length. These nanotubes may have further use as potential nanotube based biosensors or as tubing in nanofluidic circuits (Reches 2003). With the introduction of a thiol group (cysteine residue), these peptides were found to self-assemble into spheres 10-100nm in diameter (Reches & Gazit 2004), suggesting that these building blocks have great versatility.

1.2.4.2 Ionic Self-Complementary Peptides

In general, these peptides are made up of 16 amino acid residues arranged in an alternating polar and non-polar pattern which self-assemble to form β -sheets in which one side is hydrophilic and the other is hydrophobic (owing to the alternating polar and non-polar amino acid pattern). These peptides are carefully designed so that the hydrophilic side of the β -sheet is made up of regular repeats of alternating positively and negatively charged amino acids. In water, these β -sheets self-assemble to shield the hydrophobic residues, while the positively and negatively charged residues form complementary ionic bonds. Further self-assembly of the β -sheets leads to the formation of discrete nanofiber structures which further self-assemble into nanoscaffolds. Similar to the porosity of the ECM, these nanoscaffolds also contain pores of sizes 5-200nm and so offer potential for use as 3D cell culture systems (Zhang 2003). Indeed, the attachment of biologically active motifs, such as the RGD cell adhesion motif, which is found in many ECM proteins, to such nanoscaffolds has been shown to allow for cell attachment to these scaffolds. Such functionalised nanoscaffolds have already been used in studies involving cell growth, differentiation and tissue formation (Kisiday et al. 2002; Holmes et al. 2000; Zhang et al. 1995). One ionic self-complementary peptide consisting of arginine, alanine and aspartate amino acid residues is now a commercially available under the name of PuraMatrix. It is actively used in research to culture and differentiate many different types of cells (Zhao & Zhang 2007).

1.2.4.3 Surfactant-like Peptides

Another type of amphiphilic peptide being utilised as a nanoconstruction unit are surfactant-like peptides. The design of these peptides was inspired by

phospholipids; they all consist of a hydrophilic head group, made up of one to two positively or negatively charged amino acids, and a hydrophobic tail, made up of many successive hydrophobic amino acids (Zhao 2009). In water, electrostatic repulsion within the head group induces the self-assembly of nanotubes of diameter 30-50nm, with a peptide bilayer thickness of 4-5nm (Zhao 2009). Such amphiphilic peptides can also self-assemble into micelles or nanospheres (Zhao 2009). Surfactant-like peptides have found a role in solubilising and stabilising membrane proteins. By interacting with the hydrophobic domain of these membrane proteins, they act to surround the protein, preventing its interaction with water (Zhao & Zhang 2007). They therefore offer great potential in the determination of structures of many more transmembrane proteins.

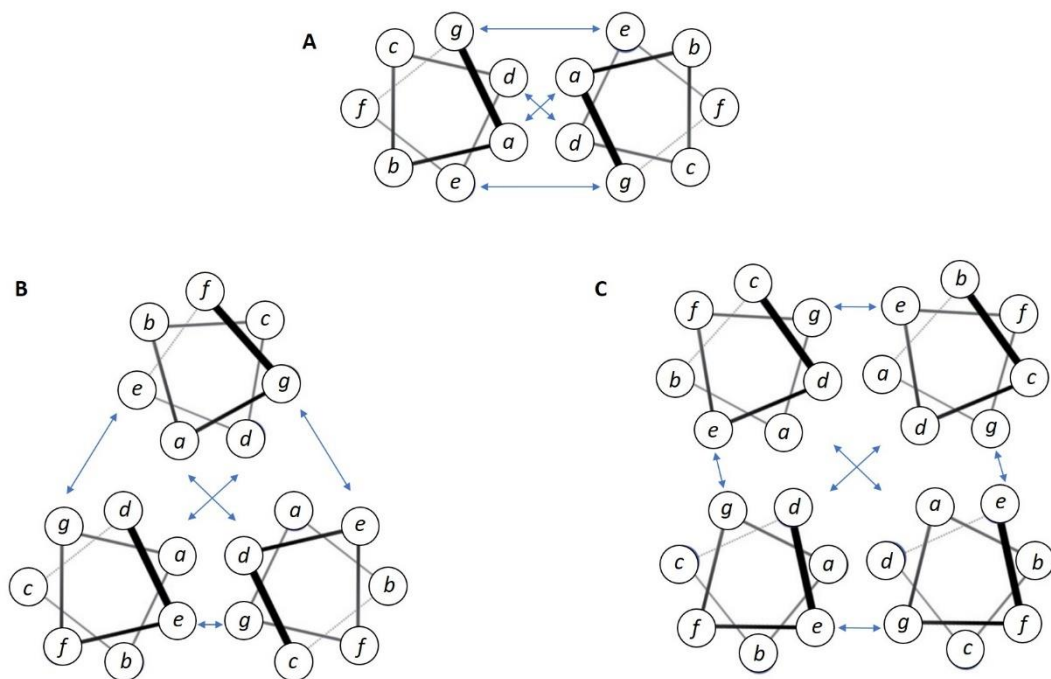
Bola-amphiphilic peptides have two hydrophilic head groups which are linked together with a hydrophobic alkyl spacer. In water, amphiphilic peptides were observed to self-assemble into nanofibers and nanospheres that have both a hydrophilic core and surface. Diameters of these structures were measured to be very narrow at 10nm. Their small size and unique characteristics offers massive potential for their use as nano-carriers of hydrophilic substances such as nucleic acids or drugs (Zhao 2009).

1.2.4.4 Cyclic peptides

Cyclic peptides are comprised of even numbers of alternating D- and L- amino acids. Interactions between these amino acids leads to the self-assembly of nanotubes, the diameter of which can be manipulated through altering the length of the peptide (Reches & Gazit 2006). The amino acid side chains determine the surface of the nanotubes and this can be manipulated through altering the amino acid composition of the peptide. The ability to adjust and modify the outer surface of the nanotubes permits their formation in a wide variety of environments. Cyclic peptide based nanotubes have already been shown to form in bacterial cell membranes where they function to increase cell permeability, ultimately causing cell death. This offers a hopeful alternative to antibiotics, aiding in the treatment of infectious diseases (Fernandez-Lopez et al. 2001).

1.2.4.5 Coiled Coils

Coiled coils are a common type of interaction motif made up of two or more α -helices wrapped around each other (Mason & Arndt 2004). These motifs are interesting because their formation appears to rely a few certain rules and commonalities. Each helix contributing to the coil is amphipathic, made up of a contiguous pattern of seven hydrophobic (H) and polar (P) amino acid residues that generally follows the sequence $(HPPHPPP)_n$ (where n is the number of times the pattern is repeated within the helix). This repeating pattern is known as the heptad repeat and, conventionally, the residues within the repeat are labelled *abcdefg*, where hydrophobic amino acids reside at *a* and *d* sites (Woolfson et al. 2012). In general, α -helices turn every 3.6 amino acid residues. This periodicity brings the *a* and *d* residues close together and creates an *a/d* hydrophobic face which twists its way around the α -helix. Owing to the hydrophobic effect (i.e. to ensure complete burial of hydrophobic amino acids), two or more α -helices associate via these hydrophobic faces and, in doing so, wrap around each other forming a left-handed supercoil, a coiled coil (Woolfson et al. 2012). The hydrophobic effect is non-specific and, as a result, coiled coils can adopt a variety of different oligomerisation states, dimeric, trimeric, tetrameric etc. (Woolfson et al. 2012). The *e* and *g* residues are generally charged and interhelical interactions between these residues act to stabilise coiled coil formation (Woolfson 2005). The *b*, *c* and *f* residues are exposed to the solvent, contribute to the intrahelical interactions, are hydrophilic and helix forming (Mason & Arndt 2004). In summary, each individual amino acid within the heptad performs to maintain the α -helical structure (intrahelical interactions) or to promote particular oligomeric states and orientations (interhelical interactions) (Fig. 1.14).



Adapted from Armstrong et al. 2009

Figure 1.14: Helical Wheel Representations of Coiled-coil Structures. The relative positions and type of residues at each site of the heptad sequence dictates the type of oligomeric coiled-coil that will form (Mason & Arndt 2004; Woolfson et al, 2012), **(A)** dimeric, **(B)** trimeric **(C)** tetrameric. Blue arrows represent interactions between residues.

Pioneering work by Harbury et al. (1993) involving the coiled coil GCN4 yeast transcription factor found that it is possible to program the overall structure of the coiled coil motif. The 33 amino acid crystal structure of the naturally occurring GCN4 reveals a dimeric parallel coiled coil that is made up of four full heptad repeats in which position *a* is normally occupied by a valine and position *d* is normally occupied by a leucine (O'Shea et al. 1991). Harbury et al manipulated the hydrophobic core of the GCN4 dimer and simultaneously mutated the four *a* residues (normally valine) and the four *d* residues (normally leucine) to leucine, valine or isoleucine. They found that different combinations of each of the amino acids in these two sites induced the formation of different oligomeric coiled coil structures; a leucine at the *a* site and an isoleucine at the *d* site induced the formation of a tetramer, an isoleucine at both sites induced the formation of a trimer, while an isoleucine at the *a* site and a leucine at the *d* site generated a dimeric structure (Harbury et al. 1993). This study was exciting as it represented one of the first steps in rational protein design; there was a very clear relationship

between the amino acid sequence, the coiled coil folding, and the eventual end structure. Since this time, many groups have built upon these broad principles to use coiled coils in protein engineering and synthetic biology projects. Linking a pair of complementary coiled coils together via a flexible linker of various lengths, each made up of different amounts of glycine and asparagine residues, Boyle et al. (2012) reported the formation of a diverse range of nanostructures. Identifying steric constraints imposed by residues in the linker, Boyle et al. found that short linkers induced the formation of rigid nanofibres, while longer linkers induced the formation of large insoluble aggregates. The optimum linker length was four residues long, and it induced the formation of closed structures. Drawing inspiration from the DNA origami technique (section 1.2.1.2), Gradišar et al. (2013), documented their formation of a tetrahedron structure whose formation was brought about by the self-assembly of a polypeptide chain composed of 12 coiled coil segments. Self-assembly of this structure was brought about by designed interactions between the coiled coil segments, which allowed for the correct pairing and orientation of each segment. Therefore, the final shape of the structure, i.e. tetrahedron, was defined by the order and individual design of each coiled coil segment. This study represents one of the first in *de novo* protein fold design.

1.2.5 Proteins

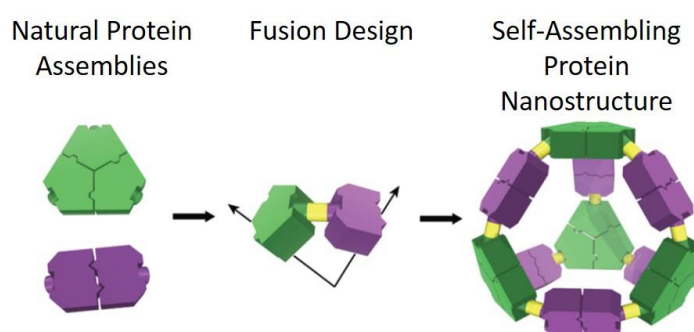
Possessing large conformational variability and a range of functionality, proteins are a particularly attractive building block for nanoconstruction. They naturally self-assemble into intricate 3D structures and are most commonly used by nature to form large and complicated protein machines consisting of remarkably co-ordinated moving parts. All the information that is required to fold a protein along a particular folding pathway into its natural and functional shape is encoded in its primary amino acid sequence, a sequence which contains varying ratios of 20 amino acids. This large repertoire of amino acids makes possible the unique structural architecture exhibited by natural protein complexes. This indicates that a large amount of information can be encoded in this primary sequence. The considerable variety of chemical moieties displayed on each of these amino acids in

the primary sequence facilitates the addition of functionality to the structure. This versatility can be used to create new protein assemblies with capabilities unseen in nature (Whitesides et al. 1991; Gradišar & Jerala 2014; Alberts 1998). Proteins, being larger than peptides, make it possible to disconnect the self-assembly process of the nanostructure from the eventual function of the nanostructure. Thus, in theory, the architecture of the nanostructure should not be compromised with the addition of functionality (Bruning et al. 2010).

Thus far, protein-based nanoconstruction has been dominated by the exploitation of ferritin proteins and viral capsid proteins. This is because, in nature, these proteins are known to instinctively self-assemble into cage-like structures with interior cavities and so, offer the potential for use as drug-delivery carrier systems. (MaHam et al. 2009; He & Marles-Wright 2015). However, various approaches have been established to manipulate the self-assembly and molecular recognition properties of different types of proteins to bring about the formation of higher order nanostructures.

1.2.5.1 Fusion-based Assembly

The fusion strategy involves genetically fusing two protein oligomerisation domains into a single protein chain (King & Lai 2013), (Fig 1.15)



Adapted from Lai et al., 2012

Figure 1.15: Protein Fusion Strategy: A short peptide linker (yellow) is used to fuse two oligomeric domains from two different proteins (green and purple) into one protein chain. Self-assembly between the oligomerisation domains drives the formation of complex structures.

This strategy was first introduced by Padilla et al. (2001) in which they created a fusion protein containing one domain of the trimeric bromoperoxidase protein linked to one domain of the dimeric M1 matrix protein of the influenza virus, by way of a rigid alpha-helical linker. 12 copies of this fusion protein self-assembled to generate a cage structure. Careful design of the linker region between the two protein domains allowed for precise control of the orientation of these domains, leading to the production of homogenous protein assemblies (Lai et al. 2013).

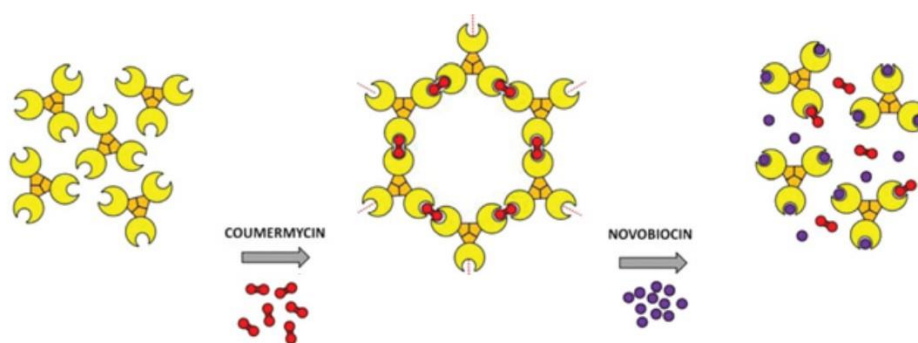
A deviation on this method fuses together protein oligomerisation domains with rotational symmetry, which was pioneered by Sinclair et al (2011). The use of higher order symmetry increases the area of the interaction interface of each fusion protein and, in doing so, allows for the formation of two or more connections between fusion proteins, providing that the two domains within the fusion protein are connected along the same order of symmetry (Sinclair et al. 2011). Self-assembly of such fusion proteins brings about the formation of unbounded protein lattices. In their study, Sinclair et al designed two protein fusions, one fusion protein comprised one domain of the D_4 symmetric aminolevulinic acid dehydrogenase (ALAD) fused to either one of two “Velcro-like” peptides, the Lac21E synthetic peptide or the Lac21K synthetic peptide {these form heterotetramers through ion pair interactions (Fairman et al. 1996)}. Upon mixing, these two fusion proteins self-assembled together to form a protein lattice.

1.2.5.2 Ligand-mediated Assembly

Ligand-mediated assembly is another approach used to bring about the formation of protein structures. This approach exploits the high affinity of small molecules for their specific binding sites in proteins. This approach is attractive because it can sometimes provide a means to regulate both assembly and dis-assembly of the building blocks (King & Lai 2013). Ligand-mediated assembly was also utilised by Sinclair et al in their generation of protein lattices (this group also used fusion-based assembly, section 1.2.5.1). They created two fusion proteins each consisting of two protein oligomerisation domains with rotational symmetry. The first fusion protein comprised one domain of the D_2 symmetric tetrameric

protein DsRED fused to the D₂ symmetric streptag I, and the second fusion protein comprised one domain of the ALAD octameric protein fused to the D₂ symmetric streptag I. With the addition of streptavidin, both of these fusion proteins self-assembled into 2D protein lattices. The successful attachment of a calmodulin domain to the N-terminus of each subunit of ALAD without any disruption to the self-assembly of the protein lattice is an indication that these structures have the capacity to be functionalised, which indicates a broad range of possible future applications.

Another study prepared a fusion protein consisting of one subunit from the gyrase protein and one subunit from the trimeric bacterial CutA1 protein. Self-assembly into a hexagonal lattice occurred with the addition of the antibiotic coumermycin, and disassembly of the lattice was promoted with the addition of novobiocin. Coumermycin can simultaneously bind two gyrase subunits, leading to the formation of a gyrase dimer, while novobiocin competes with and displaces coumermycin and in doing so dissociates the gyrase dimer (Doles et al. 2012) (Fig. 1.16).



Adapted from Doles et al., 2012

Figure 1.16: Ligand-Mediated Assembly/Disassembly Strategy. Fusion proteins consisting of protein gyrase (crescent shape) and one domain of naturally trimeric CutA1 protein. Coumermycin simultaneously binds two gyrase binding sites, inducing gyrase dimerisation and formation of protein lattice. Novobiocin displaces coumermycin, promoting disassembly of lattice.

A different study reported the formation of nanoring structures through the self-assembly of fusion proteins made up of two dihydrofolate reductase (DHFR) molecules fused together with a flexible linker (DHFR₂). Assembly only occurred in the presence of a methotrexate (MTX) molecule that was previously manipulated

be divalent, consisting of two MTX molecules connected with a dodecanediamine linker (bisMTX), and therefore able to bind two DHFR molecules. The nanoring size could be manipulated through altering the composition and length of the flexible linker separating the two DHFR molecules (Carlson et al. 2006). Further studies on these nanorings found them capable of being functionalised with single chain antibodies via the DHFR₂ (Li et al. 2010) and fluorophores via the bisMTX (Fegan et al. 2012). With their ability to be endocytosed into T-cells, they show great potential for future therapeutic applications (Fegan et al. 2012; Li et al. 2010).

1.2.5.3 Metal-directed Assembly

Metal-directed protein assembly exploits the natural affinity of metal ions to certain amino acid residues to direct the folding and assembly of protein complexes (Salgado et al. 2010). This approach was used by (Bai et al. 2013) to make protein nanorings. They modified the glutathione S transferase (GST) homodimer so that it displayed two His tag motifs. Self-assembly was brought about by the addition of Ni⁺² metal ion and its binding to two His tags, each from a separate GST protein. The location of the His tags on the GST homodimer dictated the shape of the final structure formed.

1.2.6 Conclusion

Overall, these studies demonstrate the effectiveness of the self-assembly approach in the engineering of biological based nanoconstructions. The success demonstrated by these studies indicate that such research is worthwhile and beneficial. The structure and function of actinin and spectrin proteins offer potential in such studies.

Chapter 2:

Congenital Macrothrombocytopenia-linked Mutations in the Actin-Binding Domain of α -Actinin-1 Enhance F-actin Association

2.1 Abstract

Mutations in the actin crosslinking protein actinin-1 were recently linked to dominantly inherited congenital macrothrombocytopenia, a rare platelet disorder. Here I report that several disease-associated mutations that are located within the actinin-1 actin-binding domain cause increased binding of actinin-1 to actin filaments and enhance filament bundling *in vitro*. These actinin-1 mutants are also more stably associated with the cytoskeleton in cultured cells, as assessed by biochemical fractionation and fluorescence recovery after photobleaching experiments. This study might contribute to a more comprehensive understanding of the function of the cytoskeleton in platelet production.

2.2 Introduction

2.2.1 Platelets

Platelets are small anucleate blood cells that circulate in the bloodstream and function in haemostasis. They are discoid in shape, a shape which is preserved by a unique and highly specialised cytoskeletal system, comprising of tubulin-spectrin-, and actin-based cytoskeleton proteins (Semple et al. 2011). They have the ability to store numerous biologically active substances in their secretory organelles, of which they have three; α -granules, dense granules and lysosomes (Semple et al. 2011). They specialise in preventing bleeding by clumping together and clotting injuries to blood vessels to create a thrombus, or blood clot (Semple et al. 2011; Machlus et al. 2014).

2.2.2. Platelet Production

A human adult contains about one trillion circulating platelets in their bloodstream. The lifespan of each of these platelets is around eight to ten days, therefore, in order to keep these normal platelet levels, about 100 billion platelets must be produced daily (Semple et al. 2011).

Platelets develop from the cytoplasm of megakaryocytes, which reside in bone marrow (Thon & Italiano 2012). Platelet production begins when the maturing megakaryocyte undergoes a process called endomitosis by which the megakaryocyte becomes polyploid. In its polylobulated nucleus the megakaryocyte can acquire DNA content of $4n$, $8n$, $16n$, $32n$, $64n$ and $128n$. The maturing megakaryocyte also begins to develop an extensive membrane system called the invaginated membrane system (IMS). This consists of a series of cisternae and tubules. It is continuous with the plasma membrane of the megakaryocyte, and is also dispersed through-out its cytoplasm. The purpose of this system is to function as a membrane protein reserve for platelet formation. It has been suggested that megakaryocytes are polyploid so that they can produce the considerable amount of proteins required to produce this IMS, and also to yield the large amount of

proteins required by the developing platelet, such as platelet specific granule proteins and cytoskeletal proteins (Machlus et al. 2014).

The membrane of the megakaryocyte then evaginates to create blunt, thick protrusions called pseudopodia (Thon & Italiano 2012). This morphological change is brought about a re-organisation of the microtubule cytoskeleton. In immature megakaryocytes, the microtubules diverge from the nucleus to the cortex. With the development of the pseudopodia, cortical microtubules gather themselves into thick bundles positioned beneath the now protruding plasma membrane (Thon & Italiano 2012). These bundles are initially composed of hundreds of microtubules (Hartwig & Italiano 2006), however the blunt pseudopodia soon elongate into long tube-like extensions called proplatelet shafts, and as this occurs, the bundles get smaller and contain fewer numbers of microtubules (Thon et al. 2010; Hartwig & Italiano 2006). This elongation is powered by the growth of microtubules from their free plus ends (Hartwig & Italiano 2006), and through the sliding mechanism of the dynein motor protein that positions itself with these microtubules (Machlus et al. 2014). At the tip of the proplatelet shaft, the growing microtubule loops beneath the plasma membrane and re-enters the shaft. This creates a tear-shaped swelling called the proplatelet, and it is from this structure that platelets are formed (Machlus et al. 2014).

In order to increase the number platelets produced per megakaryocyte, branching of the proplatelet shaft occurs, with each branch terminating with its own tear-shaped proplatelet (Thon & Italiano 2012; Hartwig & Italiano 2006). Through this mechanism, one megakaryocyte can produce hundreds of platelets (Italiano et al. 1999).

The proplatelet shaft plays the part of an assembly line in which the microtubules behave as the molecular tracks on which material required by the developing platelet, such as cellular organelles, e.g. mitochondria, granules, and their granular content, are carried (Hartwig & Italiano 2006; Thon et al. 2010). The proplatelet shafts extend into the sinusoidal vessels of the bone marrow (Thon & Italiano 2012), ensuring the release of the platelets into the vasculature. A recent study has provided evidence for the existence of podosomes on the outer surface of the megakaryocyte plasma membrane. They have shown that these podosomes

play an important role for the projection of the proplatelets across the basement membrane into the vascular space, via their ability to degrade the ECM with their matrix metalloproteinase activity (Schachtner et al. 2013).

It has been proposed that shear stress induced by the blood flow in the vascular space acts to detach the proplatelet from the proplatelet shaft (Machlus & Italiano 2013). The fragment released has been termed the preplatelet. Once the whole megakaryocyte cell body has been reformed into proplatelets the nucleus is expelled and degraded (Machlus & Italiano 2013; Machlus et al. 2014). From this point, platelet formation continues in the bloodstream. These preplatelets have the ability to reversibly convert back into proplatelets and, through a series of fission events, promoted by vascular shear forces and abscission, platelets are finally created (Machlus & Italiano 2013; Machlus et al. 2014).

Platelet formation is one of the most complex haematopoietic cellular differentiation pathways (Schwartz et al. 2010), in which the cytoskeleton plays a fundamental and primary role (Machlus & Italiano 2013).

2.2.3 Platelet Activation

Once a tear appears in a blood vessel, collagen, which is normally located below the endothelium (Furie & Furie 2008), and tissue factor, normally present in the vessel wall (Brass 2003), both come into contact with the flowing blood. The exposed collagen initiates the accumulation of platelets at the site of injury (Furie & Furie 2008), while the exposed tissue factor triggers a coagulation cascade that ultimately ends with the generation of thrombin (Monroe et al. 2002). Platelet adhesion to collagen is facilitated through three interactions; direct binding of collagen to the platelet glycoprotein VI or the platelet integrin protein $\alpha_2\beta_1$, and indirect collagen binding through von Willebrand factor (vWF) bound glycoprotein Ib-V-IX complex, where vWF acts as a bridge between collagen and platelets (Furie & Furie 2008; Dubois et al. 2006). Both glycoprotein VI and thrombin play essential roles in activating platelets (Furie & Furie 2008; Brass 2003); the interaction of glycoprotein VI with collagen, and the cleavage of the PAR receptors on the platelet

surface by thrombin, both trigger a signal transduction cascade which ultimately leads to the “activation” of the platelet (Brass 2003; Furie & Furie 2008).

Platelet activation involves the release of chemical mediators from their three secretory organelles. These mediators act to increase the signals for the activation of more platelets - an increase in the number of activated platelets will ultimately lead to a thrombus formation; a plug that will seal the site of injury (Furie & Furie 2008). The α -granules are the largest of the three secretory granules. They contain large molecules (Rendu & Brohard-Bohn 2001) such as: the blood clotting factors V, VII, XI and XIII, cellular mitogens, such as platelet derived growth factor, which promotes wound healing (Semple et al. 2011), and adhesive glycoproteins, such as fibronectin and vWF, which function to adhere platelets to the site of injury (Beumer et al. 1995). Dense granules contain much smaller, mostly non-protein molecules (King & Reed 2002), such as adenosine diphosphate (ADP), which functions to activate nearby platelets through interaction with the two ADP platelet surface receptors, P2Y1 AND P2Y12 (Furie & Furie 2008) and serotonin, which promotes coagulation (Semple et al. 2011). Lysosomes contain digestive enzymes, such as proteases and glycohydrolases. It is thought that these enzymes function to remove the thrombus to restore the extracellular matrix (Rendu & Brohard-Bohn 2001).

Along with the release of these biological mediators, platelet activation also involves a morphological change, in which platelets transition from a discoid shape to a spherical shape with the extrusion of finger-like filapodia and pseudopods (Semple et al. 2011; Kamath et al. 2001). It has been speculated that this shape change induces a very stable attachment of the platelets to the endothelium (Kuwahara et al. 2002) while also providing an increased cell surface area for the platelet to display the higher number of receptors and molecules that are expressed upon its activation, such as ephrin-Eph and P-selectin molecules, both of which enhance platelet-platelet affinity and recruit more platelets to the injury site (Furie & Furie 2008; Kamath et al. 2001). This shape change is brought about by an actin cytoskeleton re-organisation brought about by the action of many different actin-binding proteins (Bearer et al. 2002). One very important receptor that is stimulated upon platelet activation is the integrin, $\alpha_{IIb}\beta_{IIIa}$. During activation, it

undergoes a conformational change in which it transitions from a bent conformation to a more straightened one (Nurden & Nurden 2011). This conformational change increases its affinity for its two ligands; fibrinogen and vWF, both of which act as crosslinking proteins, crosslinking platelets together by co-binding the $\alpha_{IIb}\beta_{IIIa}$ on each platelet (Fig. 2.1C) (Furie & Furie 2008; Kamath et al. 2001). $\alpha_{IIb}\beta_{IIIa}$ is thus considered to be the main receptor in bringing about platelet aggregation (Jennings 2009).

Actinin-1 has a potential role in platelet activation and aggregation. In a resting platelet, tyrosine residue 12 of actinin-1 is phosphorylated and actinin-1 is associated with the β_{III} cytoplasmic tail of this $\alpha_{IIb}\beta_{IIIa}$ integrin complex (Fig. 2.1A). This interaction maintains the $\alpha_{IIb}\beta_{IIIa}$ integrin complex in its inactive conformation. On platelet activation, the cleavage products of thrombin mediated PAR receptor cleavage promote dephosphorylation of tyrosine residue 12 of actinin-1. This dephosphorylation disrupts the interaction between actinin-1 and the $\alpha_{IIb}\beta_{IIIa}$ complex and dissociation of actinin-1 promotes the $\alpha_{IIb}\beta_{IIIa}$ complex to adopt its active conformation (Fig. 2.1B) (Tadokoro et al. 2011). Actinin may be a regulator of platelet activation. Platelet activation results in a tyrosine phosphorylation cascade. The phosphorylation of actinin-1 may promote its re-association to the $\alpha_{IIb}\beta_{IIIa}$ complex, thus reversing activation (Tadokoro et al. 2011).

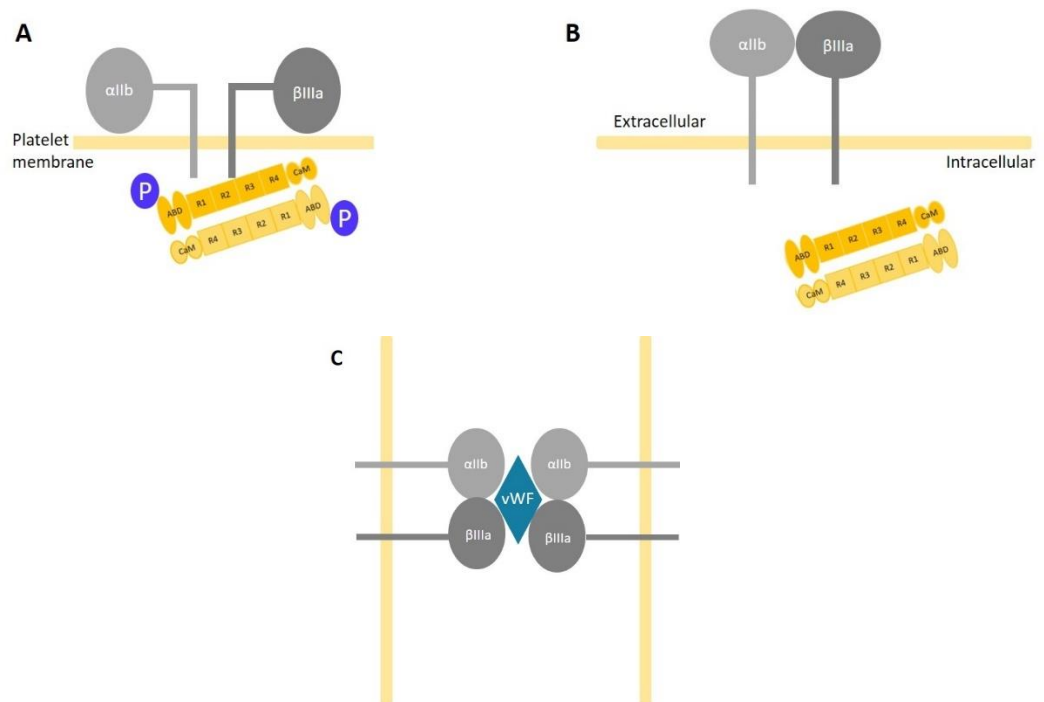


Figure 2.1: Actinin-1 in Platelet Activation. One very important platelet adhesion receptor that is stimulated upon platelet activation is the integrin $\alpha_{IIb}\beta_{IIIa}$ complex (Nurden & Nurden 2011). Actinin-1 has a potential role in the stimulation of this receptor. **(A)** Phosphorylated actinin-1 associates with the cytoplasmic tail of the β_{IIIa} portion of this complex. In doing so, it retains the complex in its inactive bent conformation. **(B)** Signalling cascades during platelet activation promote dephosphorylation of actinin-1. Dephosphorylated actinin dissociates from β_{IIIa} and this promotes the integrin complex to adopt a straight active conformation (Tadokora et al. 2011). **(C)** This conformational change facilitates its binding to its ligand vWF. vWF acts to crosslink platelets by co-binding the $\alpha_{IIb}\beta_{IIIa}$ complex on two separate platelets. This brings about platelet aggregation and the eventual formation of a platelet plug (Furie & Furie 2008; Kamath et al. 2001; Jennings 2009).

Once platelet aggregation has occurred, creating a platelet plug, the next step is stabilisation of this plug, preventing platelet retraction and disaggregation (Brass 2003). Here, thrombin again plays a role, converting fibrinogen to fibrin (Furie & Furie 2008). This fibrin acts to stabilise the platelet plug. It does this through its interaction with platelet cell surface receptors glycoprotein Ib, another receptor which is stimulated during platelet activation (Heemskerk et al. 2002), and the $\alpha_{IIb}\beta_{IIIa}$ integrin receptor (Brass 2003). The end result is a fibrin-strengthened platelet plug, the presence of which prevents blood loss and ensures haemostasis.

Along with their ability to facilitate haemostasis, platelets have also been shown to have many immuno-functions, which can be attributed to their ability to store biologically active substances in their aforementioned secretory organelles, substances that, unlike above, have non-haemostatic functions, and work to promote the clearance of invading pathogens or insults (Semple et al. 2011; Smyth

et al. 2009; Franco et al. 2015). Platelets also express receptors on their cell surface, that upon ligand binding, promote activation of either the innate or adaptive immune response (Semple et al. 2011; Franco et al. 2015). Surface membrane glycoproteins involved in platelet thrombus formation, such as $\alpha_{IIb}\beta_{IIIa}$ and Ib-X, have also been shown to have the ability to recognise and bind invading pathogens (Franco et al. 2015). Platelets have been proven to be a multipurpose cell.

2.2.4 Platelet Blood Disorders

Certainly haemostasis is a very important process and, as such, inherited platelet disorders are quite rare (Gregg 2003). However, genetic defects of platelet production and function have been identified and these defects have given rise to a series of thrombocytopathies, defined by the presence of large platelets in the peripheral bloodstream, thrombocytopenia, and a variable bleeding tendency (Kunishima & Saito 2006).

The *MYH9* gene, encoding for the non-muscle myosin II A heavy chain is the most commonly affected gene (Kelley et al. 2000; Balduini et al. 2011). Platelet disorders such as the May-Hegglin anomaly, the Epstein syndrome and the Sebastian syndrome are all caused by various different mutations of this gene and are all therefore collectively known as *MYH9*-related diseases (Balduini & Savoia 2012). These disorders are all characterised by the presence of large platelets, as well as variable degrees of severity of nephritis, hearing loss and sight failure (Balduini & Savoia 2012; Kunishima & Saito 2006). A distinguishing feature of all *MYH9*-related diseases is the presence of inclusion-bodies in the granulocytes, in fact, *MYH9*-related diseases are discriminated from each other through ultrastructural differences in their inclusion bodies (Savoia et al. 2010).

One of the very early thrombocytopenias to be studied was Bernard-Soulier syndrome (BSS). Like the previously mentioned platelet disorders, BSS is characterised with the presence of large platelets, and a severe tendency to bleed (Balduini & Savoia 2012). This disorder is caused by mutations in the genes *GP1BA*, *GP1BB* or *GP9*, which encode for the proteins GPIb α , GPIb β and GPIX. These proteins make up the GP Ib-V-IX receptor complex (Balduini & Savoia 2012), which,

as mentioned above in section 2.2.3, functions to adhere the platelet to the site of injury through its ability to bind vWF (Furie & Furie 2008), but may also play a role in platelet formation (Balduini et al. 2008). Mutations in these genes cause qualitative or quantitative defects in the GP Ib-V-IX complex (Kunishima & Saito 2006), which result in defective platelet adhesion to the site of injury, giving patients their severe tendency to bleed (Kunishima & Saito 2006). A disrupted IMS has been observed in the bone marrow megakaryocytes of patients suffering with BSS. This observation suggests that the large platelets observed in this syndrome are the result of altered megakaryopoiesis (Kunishima & Saito 2006).

Mutations in the *FLNA* gene, encoding for the filamin A protein, are associated with a wide variety of rare diseases, of which thrombocytopenia and a bleeding tendency appear as symptoms (Berrou et al. 2013).

Despite being considered rare (Gregg 2003), there is an exhaustive list of platelet disorder causative genes. Glanzmann Syndrome is brought about by mutations in genes encoding the $\alpha_{IIb}\beta_{IIIa}$ complex receptor proteins, *ITGA2B* or *ITGB3* (Nurden et al. 2011) and Gray Platelet Syndrome results from mutations in the *NBEAL2* gene, a gene encoding a for protein involved in granule trafficking in platelets. This syndrome is characterised with the absence of α -granules in platelets (Gunay-Aygun et al. 2011).

Platelet disorders seem to be very difficult to categorise, only some exhibit altered platelet numbers and morphology, however all experience some type of platelet dysfunction and all have a variable bleeding tendency.

In recent times, four independent studies have identified 13 actinin-1 mutations implicated in congenital macrothrombocytopenia (CMTP) (Yasutomi et al. 2016; Kunishima et al. 2013; Guéguen et al. 2013; Bottega et al. 2015). Kunishima et al. (2013) first identified six *ACTN1* variants (p.Gln32Lys, p.Arg46Gln, p.Val105Ile, p. Glu225Lys, p. Arg738Trp and p.Arg752Gln) to be co-segregating with affected individuals in six Japanese families suffering from CMTP. Subsequently Guegeun et al. (2013) reported one of these same mutations, p.Arg46Gln, to be co-segregating with CMTP in a French family. The appearance of this p.Arg46Gln mutation in two independent disconnected cohorts provides reliable evidence for the definite involvement of *ACTN1* in CMTP. Bottega et al. (2015) linked nine *ACTN1*

variants to CMTP in families from Italy and the United Kingdom. Six of these were novel mutations (p.Asp22Asn, p.Arg46Trp, p.Gly251Arg, p.Thr737Asn, p.Gly764Ser and p.Glu769Lys) and three had previously been identified by Kunishima et al (p.Glu225Lys, p.Arg738Trp and p.Arg752Gln). Again, their re-occurrence strengthens the involvement of *ACTN1* in CMTP. Yasutomi et al. (2016) have very recently described one more *ACTN1* variant (p.Leu395Gln) in a CMTP family.

Based on the symptoms displayed by the individuals in these families examined in these four studies, we can characterise *ACTN1*-related thrombocytopenia with moderate macrothrombocytopenia and a low bleeding tendency. No additional platelet defects were observed in each of the patients; platelet aggregation and clot formation were normal (Kunishima et al. 2013; Guéguen et al. 2013; Bottega et al. 2015; Yamamoto et al. 2012). Overall, *ACTN1* - related thrombocytopenia appears to be a very mild syndrome.

In the aforementioned studies, mutant actinin-1 proteins promoted dis-organisation of the actin and actinin cytoskeleton when expressed in cell lines (Bottega et al. 2015; Guéguen et al. 2013; Kunishima et al. 2013; Yasutomi et al. 2016), and in primary mouse fetal liver-derived megakaryocytes (Kunishima et al. 2013). These primary mouse-derived megakaryocytes also experienced disrupted platelet formation (Kunishima et al. 2013). The molecular mechanisms underlying these effects have not yet been explored.

2.2.4.1 A similar pathological mechanism may exist for Actinin-1 related CMTP and Actinin-4 related FSGS

Both actinin-1 and actinin-4 are the non-muscle calcium sensitive isoforms in the actinin family (Foley & Young 2014). These non-muscle actinins are expressed in nearly all cells and, to a great extent, their expression is overlapping (Foley & Young 2014). They do exhibit different expression patterns in motile cells however (Honda et al. 1998), and actinin-4 appears to have a unique function in the kidney (Weins et al. 2005; Kaplan et al. 2000). In general however, they function to crosslink and anchor actin filaments to structures such as cell:cell and cell:matrix junctions (Otey & Carpen 2004). They share 86.7% sequence similarity (Honda et al.

1998) and have similar actin binding properties (Foley & Young 2013). Also, platelets express large amounts of actinin-1 and actinin-4 (Foley & Young 2013).

Of the 13 aforementioned actinin-1 mutations, 12 have been mapped adjacent to or within the ABD and the CaM domain (Kunishima et al. 2013; Bottega et al. 2015; Guéguen et al. 2013). Only one of these mutations has been mapped to the central rod domain (Yasutomi et al. 2016), even though the rod encompasses half the actinin protein sequence (Fig. 2.2).

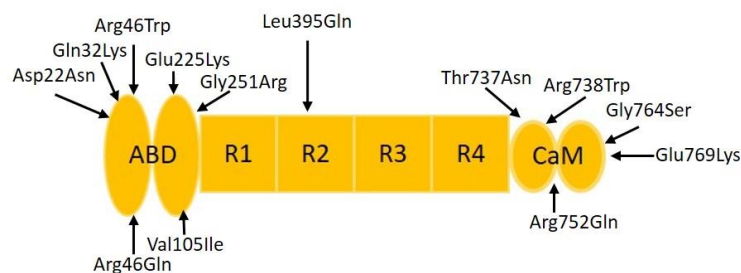


Figure 2.2: CMTP-associated Actinin-1 Mutations. 13 actinin-1 mutations have been identified to cause CMTP. Seven have been mapped to the ABD, five have been mapped to the CaM domain, and one to the central rod region (Yasutomi et al. 2016; Kunishima et al. 2013; Guéguen et al. 2013; Bottega et al. 2015). The R46 site is a particular mutational hotspot, with two different mutations of the same residues reported (Kunishima et al. 2013; Guéguen et al. 2013; Bottega et al. 2015).

These observations have connotations to the five actinin-4 mutations (p.Trp59Arg, p.Ile149Del, p.Lys255Glu, p.Thr259Ile and p.Ser262Pro) that have been identified to cause the kidney disease FSGS (Weins et al. 2005; Kaplan et al. 2000) since all five of these mutations have been mapped to the ABD of actinin-4 (Weins et al. 2005; Kaplan et al. 2000). *In vitro* actin filament co-sedimentation assays show that these mutant actinin-4 proteins have increased actin-binding ability compared to the WT actinin-4 protein (Kaplan et al. 2000; Weins et al. 2005; Weins et al. 2007). Remarkably the binding affinity of p.Lys255Glu actinin-4 for actin was found to be three times greater than the WT actinin-4 actin binding affinity, as assessed through fluorescence recovery after photobleaching (FRAP) (Ehrlicher et al. 2015). In relation to their actin binding ability, both actinin-1 and actinin-4 proteins are regarded as the non-muscle calcium sensitive isoforms; at intracellular calcium concentrations of above 10^{-7} M their actin binding ability is decreased (Condeelis & Vahey 1982). Interestingly, despite the fact that all *ACTN4* FSGS-causing mutations reside in the ABD, the addition of calcium to actin-binding assays

involving the p.Lys255Glu actinin-4 had no effect on its actin binding ability, suggesting that this mutant actinin-4 protein is no longer sensitive to calcium regulation (Weins et al. 2007). Cryo-electron microscopy studies (Tang et al, 2001) have reported that dimerisation between actinin molecules oppositely aligns the N-terminal CH domains in the ABD of one monomer to the C-terminal EF-hand motifs in the CaM domain of the other. The proximity between these two domains suggests that the CaM domain may influence the activity of the opposite ABD. Tang et al. (2001) speculate that the binding of calcium to the EF hand motifs in the CaM domain induces the EF3-4 pair to wrap itself around the linker region between the two CH domains in the opposite ABD. This interaction may cause a decrease in actin binding ability in either one of two ways; it would separate the two CH domains, or the presence of the CaM domain between the two CH domains would sterically prevent actin binding (discussed in section 1.1.3.1). Taking this study into account, it is easy to understand how a mutation in the ABD of a non-muscle actinin protein could affect its calcium sensitivity.

Expression studies of p.Trp59Arg and p.Ile149Del actinin-4 in cultured podocytes reveal their abnormal localization and the formation of large aggregates (Weins et al. 2005). Mutant *Actn4* knock-in mouse models, homozygous for the murine correlate of Lys255Glu, also display these large aggregates in their kidneys (Yao et al. 2004). Podocytes, derived from this mouse model, transfected with p.Lys255Glu actinin-4 also exhibit actin aggregates (Yao et al. 2004). Immunostaining of fibroblasts, also derived from this knock-in mouse model, reveal that endogenously expressed mutant *Actn4* proteins do not incorporate themselves in focal adhesions, but instead form large actin aggregates (Weins et al. 2007). All of these investigations suggest that dysregulation in the actinin-actin cytoskeleton in podocytes is involved in the pathogenesis of FSGS.

From these actinin-4 studies, I speculated that dysregulation of actinin-1 association with the actin cytoskeleton might also contribute to the pathogenesis of CMTP in platelets, it again presenting itself through altered F-actin binding and disrupted intracellular localization.

I have tested this hypothesis directly and find that several CMTP-linked mutations within the ABD increase the association of actinin-1 with actin filaments

both *in vitro* and *in cellula*. These studies identify the impact that these actinin-1 mutations have on the cytoskeletal system of platelets and might provide essential insight into the pathophysiology of *ACTN1* related thrombocytopenias disorders or lead to a better understanding of the possibly exclusive functions of actinin-1 in platelets.

2.3 Materials and Methods

2.3.1 Antibodies and Reagents

Sources of antibodies and stains were as follows: anti-FLAG, anti-GAPDH, anti- β -actin, and rhodamine-conjugated Phalloidin were from Sigma-Aldrich, Arklow, Ireland (Catalog numbers: #F3165, #G9545, #A5441 and #77418 respectively); IRDYE®800CW conjugated anti-mouse secondary antibody was from LI-COR Biosciences, Cambridge, UK (#926-32210); horseradish peroxidase-conjugated anti-rabbit and Cy3 conjugated anti-mouse secondary antibodies were from Jackson ImmunoResearch Suffolk (#111-035-003 and #715-165-150 respectively).

All other reagents and chemicals used were obtained from Sigma-Aldrich (Arklow, Ireland) unless otherwise stated.

2.3.2 Actinin-1 cDNA Constructs and Plasmid Construction

The calcium sensitive (non-muscle, exon 19a-containing) splice variant of human actinin-1 was used in all experiments (Accession number: NM_001102).

For actin co-sedimentation assays the *ACTN1* cDNA sequence was cloned into a modified pET24 bacterial expression vector (Novagen, Quintin, France), pET24-6xHis-GST-TEV, that encodes an N-terminal 6xHistidine (6xHis) tag followed by the glutathione-S-transferase (GST) sequence and a recognition site for TEV protease. This served as the template into which the CMTP-associated mutations were introduced, using the Quikchange site-directed mutagenesis kit (Agilent Technologies). The veracity of all constructs was verified by DNA sequencing.

For cytoskeletal purification experiments, these actinin-1 constructs were sub-cloned into the mammalian expression vector pCMV-NFLAG, to add an amino-terminal FLAG epitope tag to actinin-1.

For FRAP experiments, WT and p.Arg46Gln Actinin-1 were sub-cloned into the pEGFP-N1 mammalian expression vector (Clontech, Saint-Germain-en-Laye, France) to produce these proteins with a C-terminal GFP tag.

2.3.3 Bacterial Protein Expression and Purification

Constructs encoding 6xHis-GST-TEV actinin-1 were transformed into *E. coli* [DE3] (Novagen, Quintin, France). Protein expression was induced at 37 °C by addition of 0.2mM isopropyl- β -D-thiogalactopyranoside (IPTG) and cells were harvested 4 hours post induction. Cell pellets were resuspended in PBS, 0.2% triton, 20mM β -mercaptoethanol and 1mM phenylmethylsulfonyl fluoride (PMSF). Cells were lysed by sonication and addition of 0.1mg/ml lysozyme for 30 min at 4 °C. Lysates were cleared by centrifugation at 39,000xg for 40 min at 4 °C. For solubility comparison of WT versus mutant actinin-1 proteins the pellet generated during this centrifugation step was retained and resuspended in a 1% SDS lysis buffer. Both supernatant and pellet fractions were then analysed.

For GST-based purification, proteins were loaded onto a glutathione column (GE Healthcare) pre-equilibrated with wash buffer (PBS, 0.1% triton, and 5mM β -mercaptoethanol). The column was then washed twice with 12ml of wash buffer. Bound proteins were then eluted with 10mM glutathione in a solution of 50mM Tris-HCl, pH8.0. Eluted proteins were incubated overnight at 4 °C with TEV-protease (1mg TEV protease/100mg protein) in dialysis tubing immersed in a dialysate buffer (20mM Tris-HCl pH7.5, 50mM NaCl, and 5mM β -mercaptoethanol).

For consequent Ni-column purification to remove cleaved tags, proteins were loaded onto a Nickel-NTA column pre-equilibrated with dialysate buffer. Untagged actinin-1 proteins were collected in the flow through fraction. Purified proteins were concentrated using Amicon Ultra centrifugal filters (Millipore, Cork, Ireland).

2.3.4 Actin Co-Sedimentation Assays

Human platelet actin (Cytoskeleton Inc., Denver, USA) was mixed in G-actin buffer (5mM Tris pH 8.0, 0.2mM MgCl₂, 0.2mM ATP, 0.5mM Dithiothreitol (DTT)), which was then cleared by ultracentrifugation at 112,000xg for 30min at 4 °C. Actin was polymerised by addition of 1/100 volume of 100x polymerisation buffer (2M NaCl, 0.1M MgCl₂) and incubated overnight at 4 °C. Purified actinin-1 proteins were cleared by ultracentrifugation at 162,000xg for 1 hour at 4 °C.

For actin binding and bundling assays, 2µM actin was mixed with 1µM actinin in F-actin buffer (10mM Tris-HCl pH7.5, 100mM NaCl, 10mM NaN₃, 10mM MgCl₂, 1mM ATP, and 1mM DTT). With the exception of section 2.4.1.2.4, all assays were performed in the presence of 0.2mM ethylene glycol tetra-acetic acid (EGTA), to maintain Actinin-1 in an uninhibited (calcium unbound) state with regard to actin binding. In section 2.4.1.2.4, EGTA is replaced with 0.1mM CaCl₂. Samples were then incubated for 30 min at 30 °C. In studying actin binding, polymerised actin was separated by ultracentrifugation at 112,000xg for 30min at 30 °C. In the case of actin-bundling, cross-linked actin was separated by centrifugation at 10,000xg. Pellets and supernatants were brought to the same total volume with SDS sample buffer, boiled, and equal volumes loaded on 10% SDS-polyacrylamide gels. SDS-PAGE gels were stained in GelCode™ BlueSafe Protein Stain (Thermo Scientific, Waltham, USA) for 1 hour, and de-stained in deionised water for 1 hour.

As controls, to account for the non-specific trapping of proteins in the F-actin pellet, all actin co-sedimentation assays were carried out with an actinin-1 only sample and an initial actin co-sedimentation assay was carried out with non-actin-binding proteins. No significant trapping of non-actin binding proteins in F-actin pellets was observed under assay conditions. A very small amount of protein of interest (whether actinin or non-actin-binding control proteins) were recovered in the pellet fraction in assays performed in the absence of F-actin. This represents either supernatant carryover, or the non-specific binding of the protein of interest to the assay tube, and if significant, was subtracted in calculations of bound actinin. Densitometry analysis was performed using Odyssey Image Studio Software (LI-COR Biosciences, Cambridge, UK).

To determine the dissociation constant (K_d) for actin binding, 2 μ M actin was used per assay along with a range of actinin concentrations (0.25-30 μ M). A single ligand-binding site was assumed, and rectangular hyperbolic curves were fitted to plots of bound versus free actinin with GraphPad Prism software using the equation: $Y = (B_{\max} * X)/(K_d + X)$, where B_{\max} is the maximal binding.

2.3.5 Cell Culture and Transfections

HeLa cells, a gift from Prof. Rosemary O' Connor (University College Cork, Ireland), were cultured in Dulbecco's Modified Eagle Media (Sigma-Aldrich D6429), 10% Foetal Bovine Serum (FBS), 1% penicillin/streptomycin, and 1% L-glutamine. Cells were maintained routinely at 37 °C, 100% humidity and 5% CO₂. For cytoskeleton purification, FRAP and immunofluorescence studies, HeLa cells were seeded so as to be 80-90% confluent for transfection in 6-well dishes, 35mm glass bottomed imaging dishes (Ibidi, Planegg, Martinsried, Germany) or glass coverslips, respectively.

Transfections relating to cytoskeleton purification and FRAP were carried out using Lipofectamine 2000 reagent (Invitrogen, Life Technologies Carlsbad, California, USA). Cells were washed with 1xPBS and were then covered with 1.7ml DMEM without antibiotics. For each transfection two solutions were made; one containing 1 μ g DNA made up to a volume of 150 μ l with Opti-MEM reduced serum, the other containing 2 μ l of Lipofectamine and 148 μ l of Opti-MEM reduced serum. Both solutions were mixed and incubated at room temperature for 20minutes. The resulting 300 μ l was added to the cells to be transfected and left incubate for 24-36hours at 37 °C.

For immunofluorescence studies, HeLa cells were transfected with 2 μ g of DNA using a calcium phosphate precipitation protocol. Transfected cells were left incubate for 24hours at 37 °C.

2.3.6 Purification of Cytoskeletal Fractions

Cytoskeletal fractions enriched for F-actin and intermediate filaments were purified as described by Choi et al (2014). Briefly, 24hours post transfection, cells were rinsed twice with ice cold 1xPBS. Lysis buffer (50mM PIPES pH6.9, 50mM NaCl, 5% glycerol, 0.1% NP-40, 0.1% Triton X-100, and 0.1% Tween 20) was added to the dish, on ice, for 1.5min. The lysate was collected and retained, while the dish was rinsed with wash buffer (50mM Tris-HCl, pH7.5) and then incubated with nuclease buffer (10mM MgCl₂, 2mM CaCl₂, and 10U/ml benzonase in 50mM Tris-HCl, pH7.5) for 10min at room temperature. The pre-collected lysates were then re-added to the dish for 30 seconds, on ice. The dish was then rinsed twice with wash buffer. Cytoskeletal proteins that remained on the dish were then collected in 1% SDS buffer. Lysis, wash and nuclease buffers all contained protease (Roche protease inhibitor cocktail) and phosphatase inhibitors (5mM sodium fluoride and 2mM sodium orthovanadate).

Protein concentration was determined using the BCA protein assay (Thermo Scientific, Waltham, USA) and equivalent amounts of proteins (5µg) from both the cytosolic and cytoskeletal fractions were analysed by SDS gel electrophoresis and western blotting. Detection was carried out with both the Odyssey Infrared Imaging System and on X-ray films (Thermo Scientific, Waltham, USA) using enhanced chemiluminescence substrate (Thermo Scientific, Waltham, USA) for peroxidase tagged secondary antibodies. Quantification of actinin was normalised to β-actin levels.

2.3.7 Fluorescence Recovery after Photobleaching (FRAP)

FRAP experiments were performed on a Zeiss LSM 510 META confocal microscope. Images were acquired every two seconds for a period of two minutes. After capturing 10 images, a circular region of interest (ROI) in each cell was bleached with 4sec using 60 iterations of 100% laser power. The average fluorescence intensity in the ROI was measured at each time point and normalised against the average fluorescence intensity of the whole cell using the FRAP profiler

Plug-In for Image J software. The degree of bleaching of the baseline fluorescence achieved was slightly greater for the p.Arg46Gln mutant than the wildtype protein. Fluorescence recovery curves were fitted to the data in Kaleidograph software using the equation: $\tau_{1/2} = \frac{\ln 0.5}{-\tau} f(t) = A (1 - e^{-\tau t})$, where A is the mobile fraction. The half time fluorescence recovery ($\tau_{1/2}$) was calculated using the equation $\tau_{1/2} = (\ln 0.5)/-\tau$. Three independent experiments were performed with 9-12 cells images for each condition per experiment.

2.3.8 Immunofluorescence Cytochemistry

24hours post transfection, cells were washed with 1xPBS and fixed with 4% paraformaldehyde (PFA) for 10min at 4 °C. Cells were incubated in blocking buffer (0.1% triton x-100, 5% goat serum, and 2% bovine serum in PBS) for 1 hour at room temperature prior to antibody incubation. All wash steps were carried out using 1xPBS in the wells of a 6-well cell-culture dish. All antibodies were diluted in 5% goat serum and 2% bovine serum in PBS, were added to cells and left to incubate overnight at 4 °C. Coverslips were mounted onto glass slides using Fluoromount mounting media.

Images were obtained using a Leica DMI 3000 microscope using 10x, 20x and 40x objectives. Fluorescent images taken with different light channels were merged using Adobe Photoshop Software.

2.3.9 Statistical Analysis

Comparisons of actin binding/bundling and FRAP for WT versus p.Arg46Gln Actinin-1 was analysed using a two-tailed Student's T-test (Microsoft Excel software). Experiments comparing WT Actinin-1 with multiple mutants were analysed using a one-way ANOVA, followed by a Dunnett t post-hoc test (2-sided). ANOVA was performed using SPSSv22 or GraphPad Prism software.

2.4 Results

2.4.1 *In Vitro* Functional Analysis of the *ACTN1*-CMTP Associated Mutations

2.4.1.1 A Comparative Study on the Solubility of WT and CMTP-Associated Mutant Actinin-1 Proteins

To identify if protein misfolding was the molecular mechanism through which these mutant actinin-1 proteins were acting, I set out to assess their solubility.

When expressed as recombinant proteins in *E. coli* cells, approximately equal amounts of all proteins were seen in both the soluble and insoluble fractions. There was no obvious difference in solubility between WT and mutant actinin-1 proteins (Fig. 2.3).

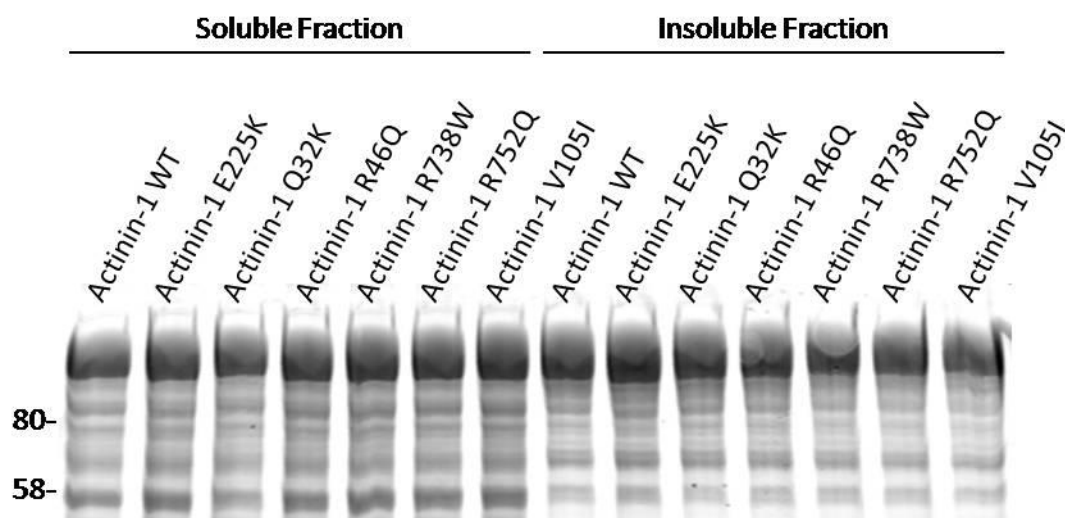


Figure 2.3: Assessing WT and Mutant Actinin 1 Protein Solubility. Soluble and insoluble protein fractions of *E. coli* cells expressing WT or mutant actinin-1 proteins were analysed using SDS protein gel electrophoresis. Proteins were visualised using Coomassie Brilliant Blue staining. Proteins of interest and the sizes (in kDa) of the relevant molecular weight markers are indicated. n=2

Single amino acid code is used for actinin-1 mutations in the labelling of this figure and in the labelling of subsequent figures.

2.4.1.2 A Comparative Study on Actin-Binding/Bundling Ability Between WT Actinin-1 and CMTP-Associated Mutant Actinin-1 Proteins

Based on their location predominantly within the ABD and CaM domains, and prompted by the increased actin binding ability of the actinin-4 FSGS associated mutations (Kaplan et al. 2000; Weins et al. 2005), I reasoned that CMTP-associated mutations may affect the interaction of actinin-1 with F-actin. To examine this possibility directly, I performed *in vitro* actin binding and bundling assays using purified recombinant WT and mutant actinin-1 proteins. Supernatants and pellets from actin co-sedimentation assays were analysed on Coomassie Blue-stained polyacrylamide gels and the proportion of actinin in both fractions was quantified.

2.4.1.2.1 Purification of Actinin-1 Proteins

6xHis-GST-TEV-WT/mutant full-length actinins were recombinantly expressed in *E. coli* cells. Purified untagged full-length actinins were achieved using sequential purification, which involved GST-column purification, followed with overnight TEV protease treatment to remove the 6xHis-GST affinity tag, and completed with His-column purification to separate the 6xHis-GST affinity tag from the untagged actinin protein, which was collected in the flow-through (Fig. 2.4).

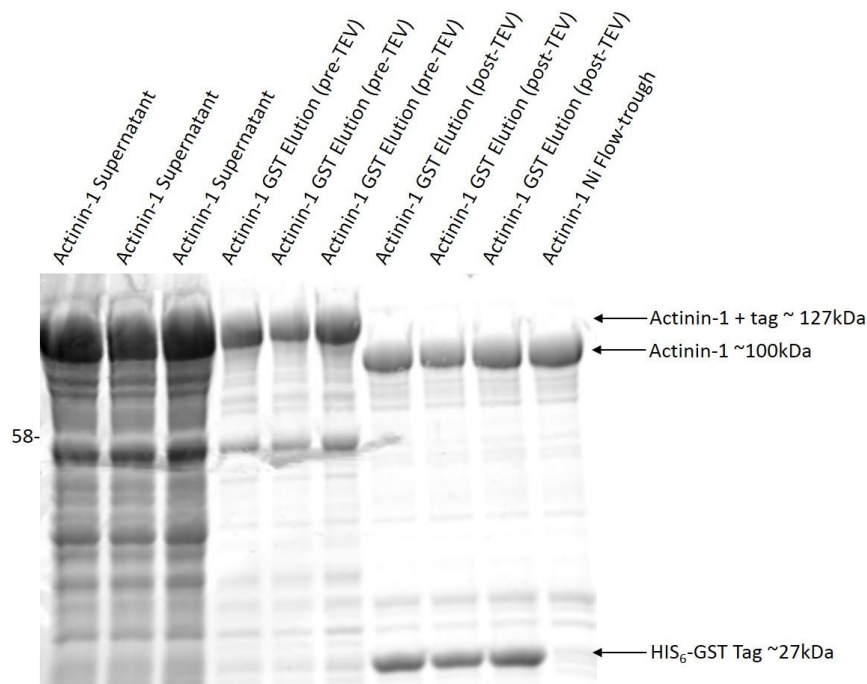


Figure 2.4: Purification of Full-Length Actinin-1. A Coomassie stained gel that is representative of the steps involved in purifying full-length WT or mutant actinin-1 proteins. Full Length 6xHis-GST-actinin-1 proteins (WT or mutant) were recombinantly expressed in *E. coli* cells with IPTG. Expression was carried out on a large scale (one litre cultures) and so three 2ml GST-columns and three 2ml Ni-columns were required to accommodate the large volume of protein. GST-column purification was followed with overnight TEV treatment to cleave the 6xHis-GST affinity tag. Ni-column purification was then carried out to separate the tag from the untagged actinin protein. Purified actinin was obtained from the Ni-column flow-through and combined. Proteins of interest and the sizes (in kDa) of the relevant molecular weight markers are indicated.

2.4.1.2.2 Comparison of Actin-Binding Ability of WT Actinin-1 and p.Arg46Gln

Actinin-1

My analysis initially focused on the p.Arg46Gln mutation, particularly because three separate studies had found it to be co-segregating with CMT1 (Kunishima et al. 2013; Guéguen et al. 2013; Bottega et al. 2015). Also, this site had proved itself to be a mutational “hotspot” with one study, (Bottega et al. 2015), reporting a different mutation of this same residue (p.Arg46Trp).

Firstly, in order to account for the non-specific trapping of proteins in the F-actin pellet under high speed centrifugation, all co-sedimentation assays were carried out with an actinin-1 protein only control and an initial actin co-sedimentation assay was carried out with three different non-actin binding proteins; bovine serum albumin (BSA), two spectrin-like repeats from the central

region of the actinin-2 rod domain (repeats 2 and 3 (r2r3)), and polyhistidine-tagged glutathione-S-transferase (GST).

The very small amount of these non-actin-binding proteins detected in the F-actin pellet fraction is no greater than the amount observed in the pellet fractions from assays performed in the absence of F-actin. This indicates that there is no detectable trapping of proteins in the F-actin pellet. Any protein detected in the fraction represents supernatant carryover, or the non-specific binding of the protein of interest to the assay tube, either of which is then eluted upon the addition of SDS gel loading buffer to the tubes to recover the pellet (Fig. 2.5). When present, this non-specific signal was subtracted in calculations of bound proteins of interest, i.e. mutant/WT actinin-1.

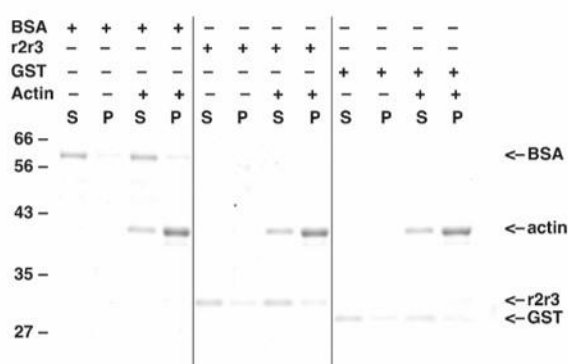


Figure 2.5: Analysis of Trapping in Actin Co-Sedimentation Assays. Co-sedimentation assays with the indicated proteins were performed in the absence and presence of F-actin. Supernatant (S) and pellet (P) fractions were analysed by SDS protein gel electrophoresis and proteins were visualised using Coomassie Brilliant Blue staining.

Quantity of non actin-binding protein in F-actin pellet samples are comparable to quantity of non actin-binding protein in equivalent sample in the absence of F-actin. This indicates no detectable trapping of protein in F-actin pellet.

Proteins of interest and the sizes (kDa) of the relevant molecular weight markers are indicated.

In actin co-sedimentation assays performed at 112,000g, p.Arg46Gln actinin-1 showed significantly increased actin binding compared to the WT protein (Fig. 2.6).

In samples containing actinin protein only (free from actin) no detectable amount of actinin, either WT actinin-1 or p.Arg46Gln actinin-1, was sedimented. This indicated that neither WT nor p.Arg46Gln actinin-1 were aggregating.

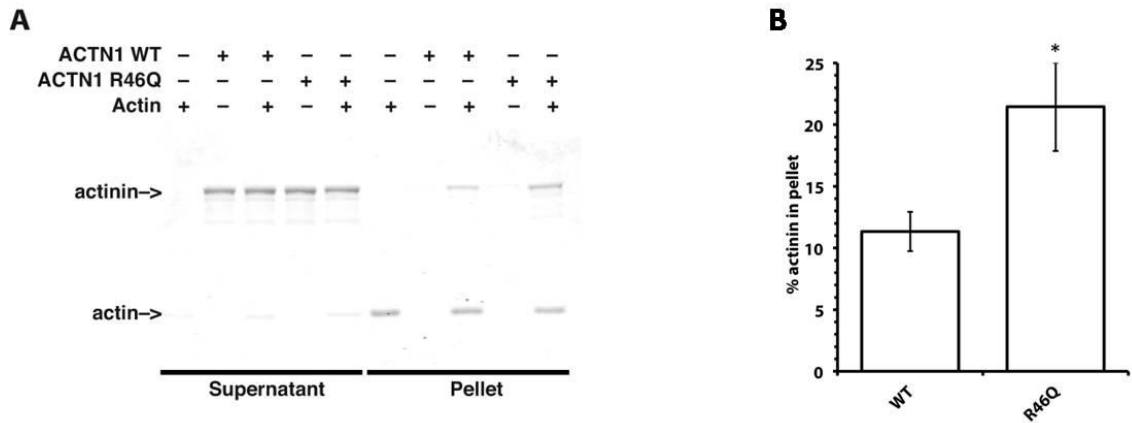


Figure 2.6: Effects of CMTP-associated R46Q Mutation on Actin Binding Properties of Actinin-1 *in vitro*.

(A) The supernatants and pellets from actin binding assays performed with the indicated combinations of proteins were analysed by SDS protein gel electrophoresis and Coomassie staining. Proteins of interest are indicated.

(B) Quantification reveals significantly increased co-sedimentation of the p.Arg46Gln (R46Q) mutant protein with actin compared to WT actinin (* $P < 0.05$). $n = 9$

2.4.1.2.2.1 Comparison of Dissociation Constants of WT Actinin-1 and p.Arg46Gln Actinin-1

To quantitatively measure this increased actin-binding ability I determined the dissociation constants (K_d) of both WT actinin-1 and p.Arg46Gln actinin-1. Actin-binding assays using increasing concentrations of actinin (WT or p.Arg46Gln) and fixed concentrations of actin were set up. When calculating the K_d , a single ligand binding site was assumed and rectangular hyperbolic curves were fitted to plots of bound versus free actinin. The results obtained were in agreement with those seen for Fig. 2.6; the (K_d) for the interaction of the p.Arg46Gln mutant with F-actin was calculated to be $0.72 \pm 0.18 \mu\text{M}$ compared to $2.53 \pm 1.28 \mu\text{M}$ for WT Actinin-1 (Fig. 2.7 and 2.8).

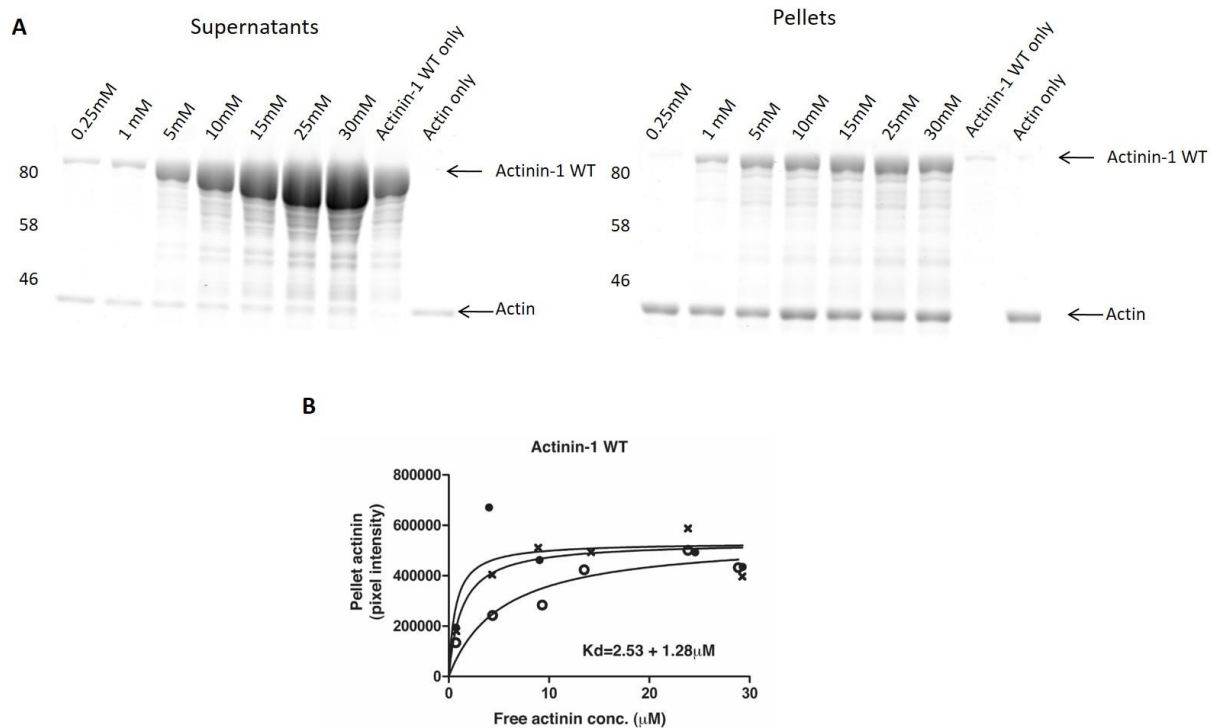


Figure 2.7: Actin Binding Affinity (K_d) Assays of WT Actinin-1.

(A) Actin binding assays were set up with increasing concentrations of WT actinin-1 (0.25–30 μ M) and a fixed concentration of F-actin. Supernatants and pellets were analysed by SDS protein gel electrophoresis and Coomassie staining, with densitometry. Representative gel shown.

Proteins of interest and the sizes (in kDa) of the relevant molecular weight markers are indicated.

(B) Plots of bound actinin versus free actinin concentrations were used to calculate the indicated dissociation constant (K_d) values for the interaction of WT actinin-1 with F-actin.

Three independent experiments were averaged to obtain the K_d value shown (\pm S.E.M). The experimental data and fitted curves for all three replicates are shown.

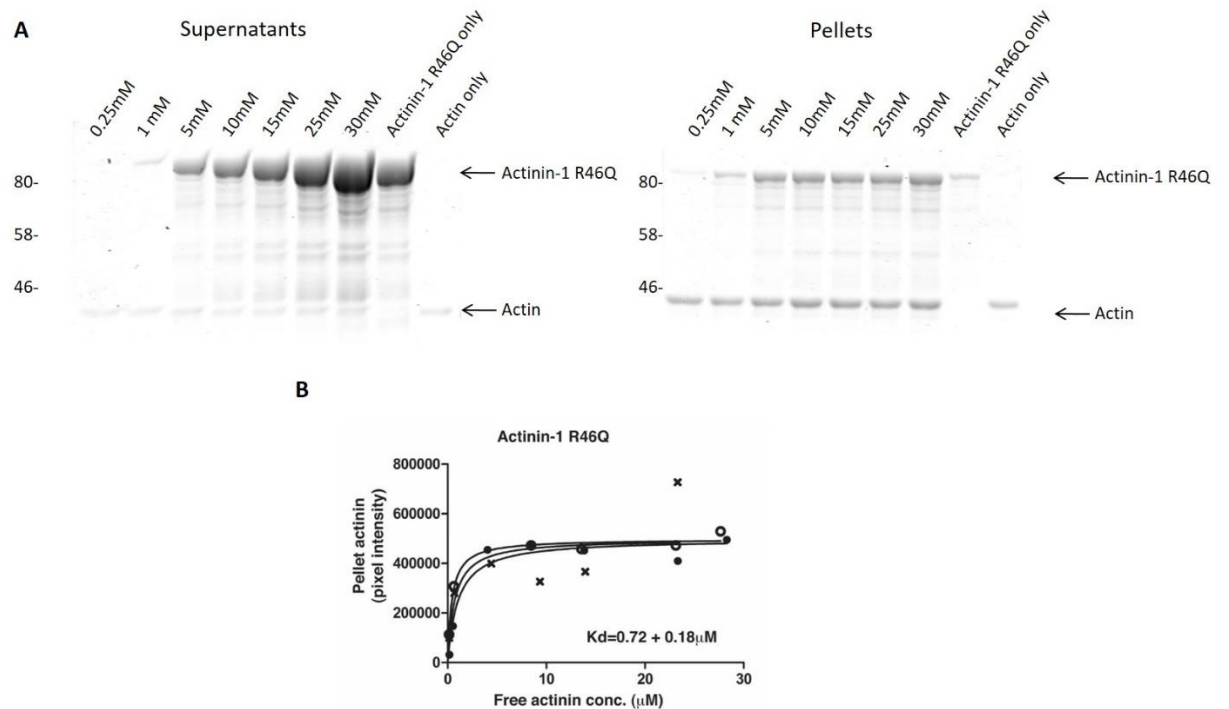


Figure 2.8: Actin Binding Affinity (K_d) Assays of R46Q Actinin-1.

(A) Actin binding assays were set up with increasing concentrations of p.Arg46Gln (R46Q) actinin-1 (0.25-30 μ M) and a fixed concentration of F-actin. Supernatants and pellets were analysed by SDS protein gel electrophoresis and Coomassie staining, with densitometry. Representative gel shown.

Proteins of interest and the sizes (in kDa) of the relevant molecular weight markers are indicated.

(B) Plots of bound actinin versus free actinin concentrations were used to calculate the indicated dissociation constant (K_d) values for the interaction of p.Arg46Gln (R46Q) actinin-1 with F-actin. Three independent experiments were averaged to obtain the K_d value shown (\pm S.E.M).

The experimental data and fitted curves for all three replicates are shown.

2.4.1.2.3 Comparison of Actin-Bundling Ability of WT Actinin-1 and p.Arg46Gln Actinin-1

Actin bundling assays were performed at 10,000g, a centrifugal force at which non-crosslinked actin filaments do not sediment. Supernatants and pellets were analysed on Coomassie Blue stained polyacrylamide gels and the proportion of both actin and actinin in each fraction was quantified. In these bundling assays increased binding, as well as an increased ability to bundle, was observed for the p.Arg46Gln mutant (Fig. 2.9).

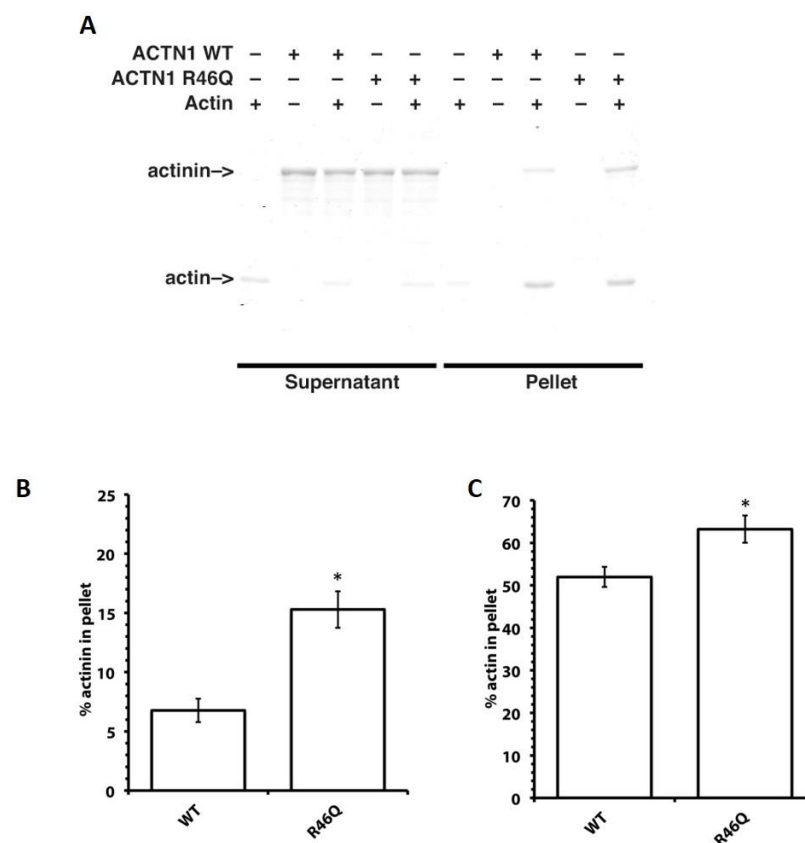


Figure 2.9: Effects of CMTP-associated R46Q Mutation on Actin Binding and Bundling Properties of Actinin-1 *in vitro*.

(A) Representative results of an actin bundling assay performed at 10,000g are shown. Proteins of interest are indicated.

(B) Quantification reveals significantly increased co-sedimentation of the p.Arg46Gln (R46Q) mutant protein with actin compared to WT actinin-1 (* $P < 0.05$). n=6

(C) Quantification shows significantly increased actin bundling by p.Arg46Gln (R46Q) actinin-1 compared to WT actinin-1. (* $P < 0.05$) n=6

2.4.1.2.4 Comparison of the Calcium Sensitivity of Actin-Binding for WT Actinin-1, p.Arg46Gln Actinin-1 and p.Glu225Lys Actinin-1

The p.Arg46Gln mutation was mapped to the ABD of actinin-1 (Kunishima et al. 2013), and is therefore not directly involved in the binding of calcium, however, considering the dimeric anti-parallel orientation of actinin monomers (Ribeiro et al. 2014), I thought it worthwhile to investigate if its presence altered the calcium sensitivity of this calcium sensitive isoform. Also, studies investigating the effect of the p.Lys255Glu FSGS-associated mutation on protein function found that this mutant actinin-4 was no longer sensitive to calcium regulation, despite the fact that this mutation resided in the ABD of actinin-4 (Weins et al. 2007).

The physiological levels of free calcium in a resting cell are normally approaching 100nM (Clapham 2007). Previous work to determine the calcium sensitivity of actin-binding for actinin-1 found that at free calcium concentrations of above 10 μ M there was a decrease in actin-binding ability (Foley & Young 2013). Therefore, to ensure calcium saturation, actin co-sedimentation assays, performed at 112,000g, were carried out in the presence of 0.1mM CaCl₂. Supernatants and pellets were analysed on Coomassie Blue stained polyacrylamide gels and the proportion of actinin in each fraction was quantified.

Increased actin binding is observed for both p.Arg46Gln and p.Glu225Lys actinin-1 proteins compared to WT in assays carried out in the absence of calcium, reconfirming my previous observation regarding pArg4Gln actinin-1 (section 2.4.1.2.2).

Actin binding in the presence of calcium is reduced to a similar extent for all three proteins, p.Arg46Gln, p.Glu225Lys and WT actinin-1. These mutations don't affect calcium regulation. (Fig 2.10).

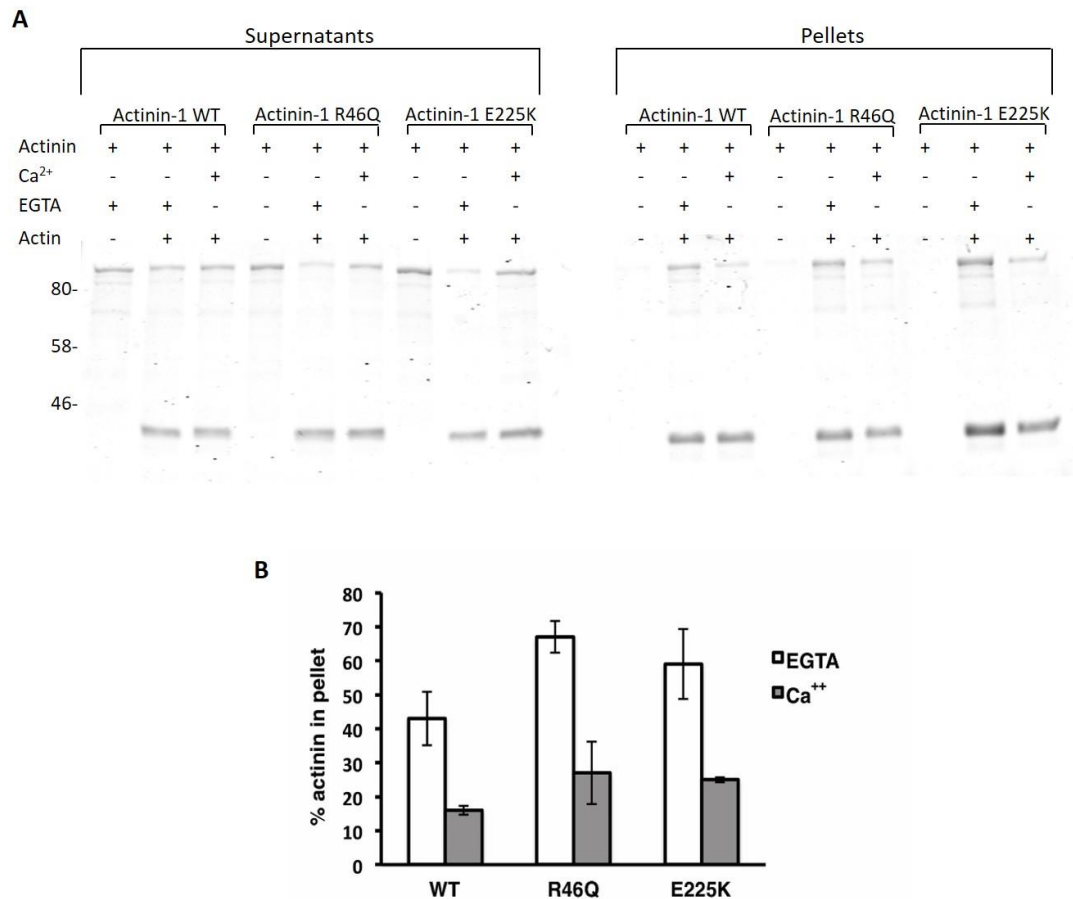


Figure 2.10: Effects of Calcium on Actin Binding Properties of WT, R46Q and E225K Actinin-1 proteins.

(A) The supernatants and pellets from actin binding assays performed, with the indicated combinations of proteins and in the presence of either 0.2mM EGTA or 0.1mM CaCl₂, were analysed by SDS protein gel electrophoresis and Coomassie staining.

Proteins of interest and the sizes (in kDa) of the relevant marker bands are indicated.

(B) Quantification confirms that the p.Arg46Gln (R46Q) and p.Glu225Lys (E225K) actinin-1 mutants exhibit increased co-sedimentation with actin compared to WT actinin-1 in the absence of calcium. Actin co-sedimentation is diminished to a similar extent for all three proteins in the presence of calcium. n=3.

Proteins of interest and the sizes of the relevant molecular weight markers are indicated.

2.4.1.2.5. Comparison of the Actin Bundling Ability of WT Actinin-1 and p.Val105Ile/p.Glu225Lys/p.Arg738Trp/p.Arg752Gln CMTP-associated Actinin-1 Mutations

I further investigated the actin bundling activity of four other CMTP-associated mutant proteins. All these mutant proteins exhibited both increased actin binding and bundling compared to WT actinin-1, though this only reached

statistical significance in the case of actin binding for p.Arg46Gln, p.Val105Ile and p.Glu225Lys Actinin-1. (Fig. 2.11).

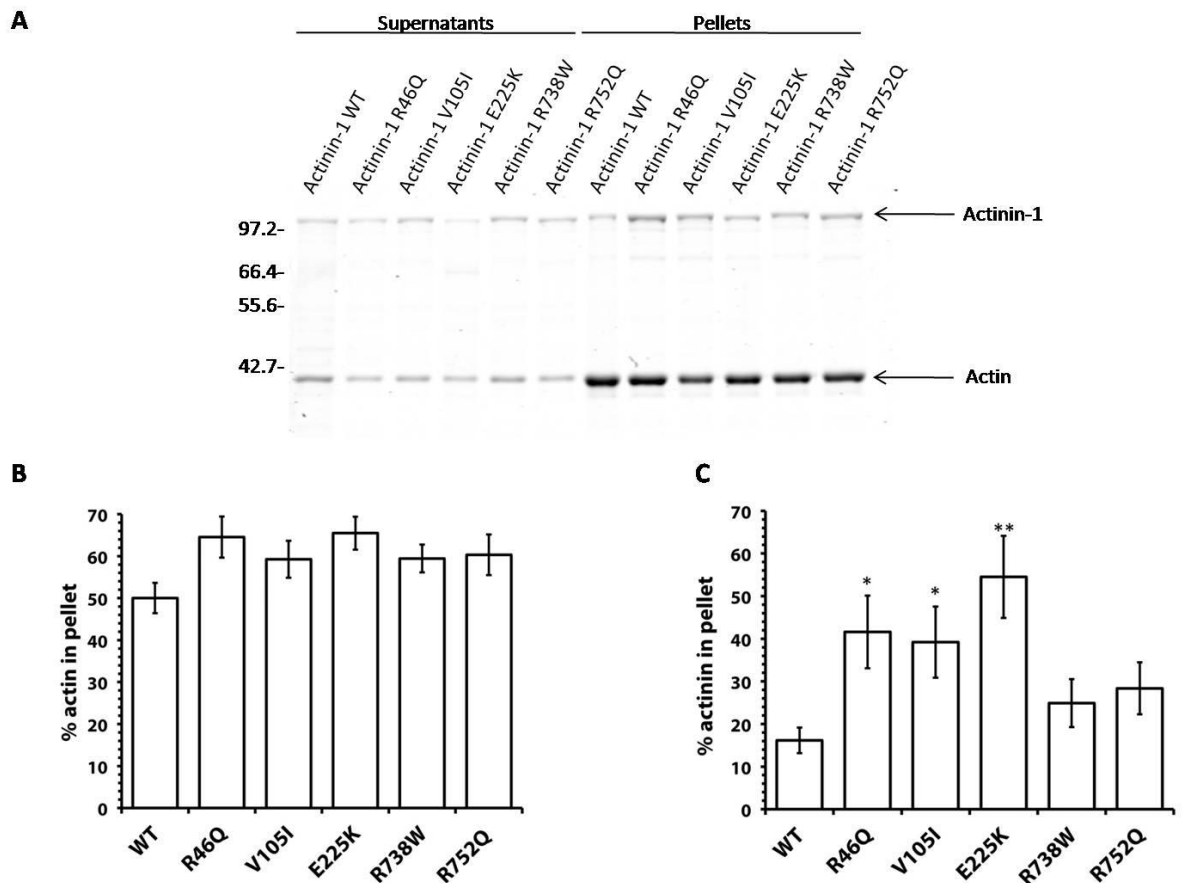


Figure 2.11: Effects of CMTP-associated Mutations on Actin Bundling and Binding Properties of Actinin-1 *in vitro*.

(A) Representative results of an actin bundling assay performed at 10,000g are shown. Proteins of interest and the sizes (in kDa) of the relevant molecular weight markers are indicated. (B) Quantification reveals increased actin bundling for all mutants compared to the WT protein. (C) Quantification reveals increased actin binding for all mutants compared to the WT protein. This reaches statistical significance in the case of p.Arg46Gln, p.Val105Ile (* $P < 0.05$) and p.Glu225Lys (** $P < 0.01$). n=7

2.4.2 *In Cellula* Functional Analysis of ACTN1-CMTP Associated Mutations

2.4.2.1 Comparison of Actin Organization in WT Actinin-1 or Mutant Actinin-1

Expressing Cells

Previous studies carried out to analyse the functional effect of some of the actinin-1 CMTP-associated mutations found that they induce actin disorganisation

when expressed in various cell lines, such as CHO cells (Yasutomi et al. 2016; Kunishima et al. 2013), human fibroblast cells (Bottega et al. 2015) and COS-7 cells (Guéguen et al. 2013). To investigate and evaluate these effects for myself, I examined HeLa cells transfected with FLAG-epitope tagged mutant or WT actinin-1 by immunofluorescence microscopy, in which Phalloidin staining was performed to reveal F-actin structures.

In contrast to what had previously been documented in the literature, I observed no actin cytoskeleton disruption (Fig. 2.12) In examining F-actin staining alone in a blinded fashion, transfected cells could not be consistently distinguished from neighbouring untransfected cells in terms of actin organisation for either WT or any of the mutants. In the vast majority of transfected cells, the mutant actinins co-localised with F-actin in a similar manner to the WT protein. Both WT and mutant exhibited a regular striated staining pattern in cells that had extensive stress fibre-like structures.

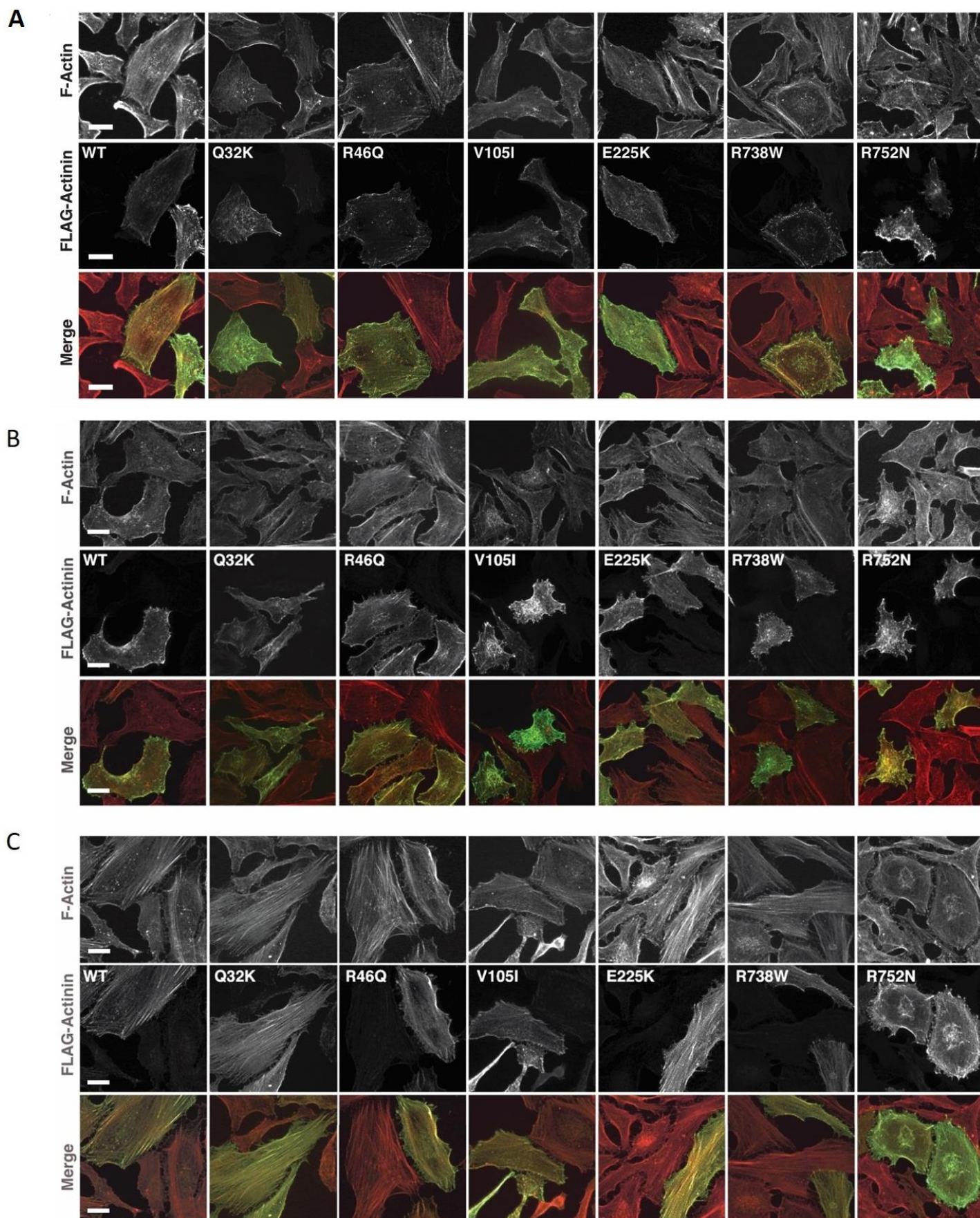


Figure 2.12: Assessing Mutant Behaviour in Cells. The indicated FLAG epitope-tagged actinin-1 proteins were detected by immunostaining following transient expression in HeLa cells (middle row of panels; green in merged image). F-actin was labelled using rhodamine Phalloidin (top row of panels; red in merged image).

(A) No major disruption of the actin cytoskeleton was observed in cells expressing moderate levels of either WT or mutant actinin-1.

(B) Further examples of cells with similar actin organisation to those shown in (A). Examining F-actin staining alone in a blinded fashion, transfected cells alone could not be consistently distinguished from neighbouring untransfected cells in terms of actin organisation for either WT or any of the actinin-1 mutants. Sometimes transfected cells did exhibit a degree of actin disorganisation (as discernible here for the p.Val105Ile (V105I) or p.Arg752Gln (R752Q) mutants), this may be related to actinin overexpression rather than the presence of the CMTF-linked mutations.

(C) Examples of cells that had extensive stress-fibre like structures. The mutant actinins generally co-localised with F-actin in a similar manner to the WT protein, and both WT and mutant actinins exhibited a regular, striated staining pattern along stress fibres in a subset of cells in which these structures were prominent.

Scale bar=20µm.

2.4.2.2 Comparison of the Stability of the Association of WT-Actinin-1 or Mutant-Actinin-1 with Actin

Since the mutant proteins did not appear to cause major disruption of F-actin organisation, I next examined whether the enhanced stability of the association of mutant actinin-1 with F-actin that was observed *in vitro* could also be observed *in cellula*.

The actin cytoskeleton is insoluble in nature and, on binding to the cytoskeleton, cytoskeleton regulatory proteins also become insoluble (Choi et al. 2014). Through separation of insoluble cytoskeletal fraction from the soluble cytoplasmic fraction from WT or mutant Actinin-1 transfected HeLa cell lysate, and quantifying the amount of WT/mutant actinin in each, I was able to confirm the increased binding of mutant actinin-1 for actin in a cell culture model.

2.4.2.2.1 Cytoskeletal Purification Protocol – Trial Run

I first tested the cytoskeleton purification protocol on untransfected HeLa cell lysates. For detailed description of the procedure see Materials and Methods Section, this protocol was adapted from Choi et al. (2014). Briefly, live HeLa cells were treated with a cell lysis buffer containing a combination of phosphatase and protease inhibitors, and detergents that function to remove the soluble cytoplasmic

proteins. Once this buffer was collected, cells were treated with a nuclease buffer containing benzonase, which functioned to remove DNA/RNA molecules and their associated proteins. In between these steps, proteins that remained bound to the dish were washed with a wash buffer, also containing phosphatase and protease inhibitors, to remove any remaining soluble proteins. Under these conditions, the insoluble actin cytoskeleton remained attached to the cell culture dish. These remaining cytoskeletal proteins were then solubilised and collected in 1% SDS solubilisation buffer (Choi et al. 2014). Fractions were then separated and analysed using SDS-PAGE electrophoresis, followed by western blotting.

Western blot analysis detected a small amount of β -actin in the soluble cytoplasmic fraction, G-actin. However, the cytoskeletal fraction was enriched with β -actin, F-actin. This result validated the overall approach, and proved that the protocol was effective in cleanly separating the soluble from the insoluble fraction in cell lysates. The detection of endogenous actinin-1 in both the soluble cytoplasmic fraction and the insoluble cytoskeletal fraction was verification that it would be possible to go forward and compare the amount of WT or p.Arg46Gln actinin-1 in each (Fig. 2.13)

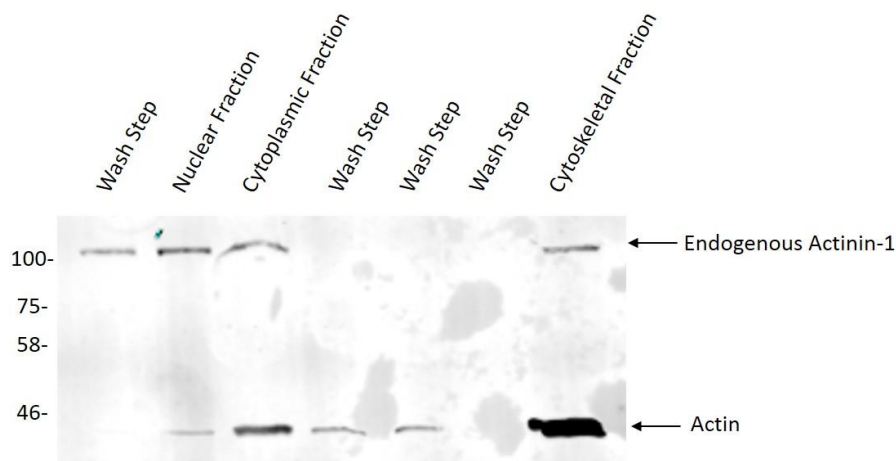


Figure 2.13: Western Blot Analysis of Indicated Proteins in the Cytoplasmic, Nuclear and Cytoskeletal Fractions.

Fractions were prepared from untransfected HeLa cell lysates using lysis buffer, nuclease buffer and solubilisation buffer respectively.

Actinin-1 and actin were detected via western blotting with anti-actinin-1 and anti- β -actin antibodies respectively.

Proteins of interest and the sizes (in kDa) of the relevant molecular weight markers are indicated.

2.4.2.2.2 Cytoskeletal Purification to Assess the Stability of the Association of WT Actinin-1 or Mutant Actinin-1 with Actin

Quantification of fractions obtained from HeLa cells overexpressing WT actinin-1 or mutant actinin-1 revealed that the amount of FLAG-actinin in the cytoskeletal fraction was increased for all tested mutant proteins compared to WT actinin-1. This increase in cytoskeletal association reached statistical significance for p.Gln32Lys and p.Arg46Gln actinin-1 mutant proteins. Variations in the levels of the mutant actinins in the cytosolic/nuclear fraction were not significantly different from WT protein. Western blot analysis showed that, as expected, β -actin was detected in both the cytosolic/nuclear fractions (G-actin) and cytoskeletal fractions (F-actin), while the cytosolic marker, GAPDH, was confined to the cytosolic/nuclear fraction (Fig. 2.14).

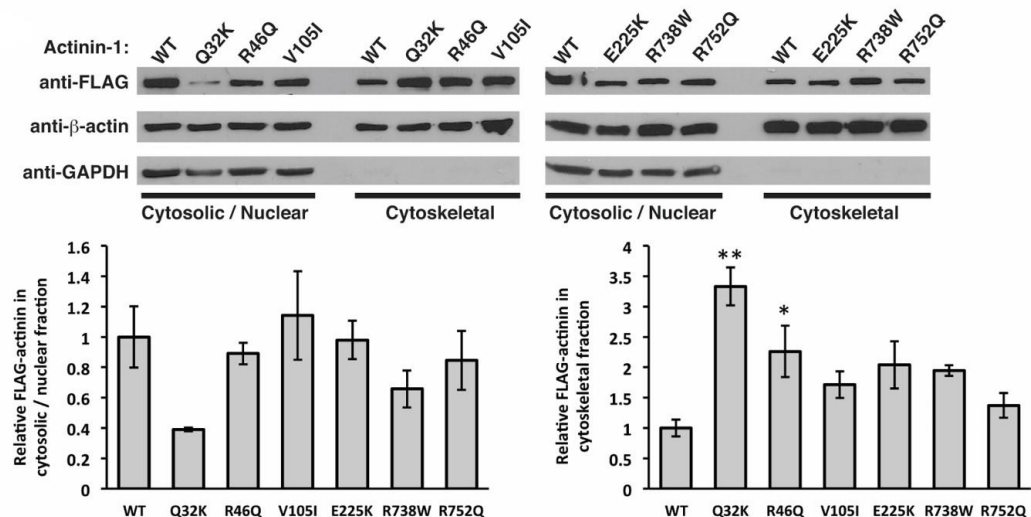


Figure 2.14: Effects of CMTP-associated Mutations on the Actin Association Properties of Actinin-1 in cellula.

Cytosolic/nuclear and cytoskeletal fractions were prepared from HeLa cells expressing the indicated FLAG-tagged actinin-1 proteins, and analysed by western blot. Successful purification of an F-actin containing cytoskeletal fraction is indicated by the presence of β -actin and the absence of the cytosolic marker GAPDH. Quantification of FLAG-actinin in both fractions (normalised to β -actin levels) is shown beneath the western blots. More actinin is found in the cytoskeletal fraction for all CMTP-associated mutants compared to the WT protein, and this reaches statistical significance for the p.Gln32Lys (Q32K) and p.Arg46Gln (R46Q) mutants. n=4.

2.4.2.2.3 Quantitative Comparison of WT Actinin-1 and p.Arg46Gln Actinin-1 Actin Association

To examine and quantitatively measure this mutation-induced increased actin association more directly in living cells I performed fluorescence recovery after photobleaching (FRAP) experiments employing WT and p.Arg46Gln GFP-tagged actinin-1 transiently transfected into HeLa cells.

2.4.2.2.3.1 Expression of GFP-Tagged WT/p.Arg46Gln Actinin-1 Constructs

Firstly, protein expression of each construct was confirmed by western blot (Fig. 2.15)

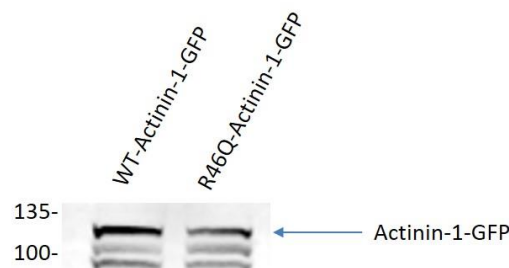


Figure 2.15: Expression of GFP Tagged WT and p.Arg46Gln Actinin-1 Proteins.

Anti-GFP Western blot detection of HeLa cell lysates transfected with GFP-tagged WT or p.Arg46Gln (R46Q) actinin-1 proteins.

Proteins of interest and the sizes (in kDa) of the relevant molecular weight markers are indicated.

2.4.2.2.3.2 FRAP Analysis to Quantitatively Assess Association of WT Actinin-1 or p.Arg46Gln Actinin-1 with Actin

FRAP was carried out 36 hours after HeLa cells had been transfected with GFP conjugated WT or p.Arg46Gln actinin-1 constructs. Concisely, after establishing the baseline fluorescence, a small region of interest was bleached and the recovery of fluorescence was monitored for 100 seconds (Fig. 2.16). Setting the intensity immediately post bleach as zero the recovery curves were fitted using the equation $f(t)=A(1-e^{-t/\tau})$. The mobile fraction was not significantly different for WT actinin-1 and p.Arg46Gln actinin-1 ($46\pm3\%$ and $49\pm5\%$ respectively). However, the calculated half time ($\tau_{1/2}$) for fluorescence recovery for the p.Arg46Gln mutant ($\tau_{1/2} = 15.5 \pm 0.9$ sec) was significantly slower than for the WT protein ($\tau_{1/2} = 7.0 \pm 1.7$ sec; $P<0.01$). This is in agreement with the p.Arg46Gln mutant being bound more tightly to F-actin structures in cells.

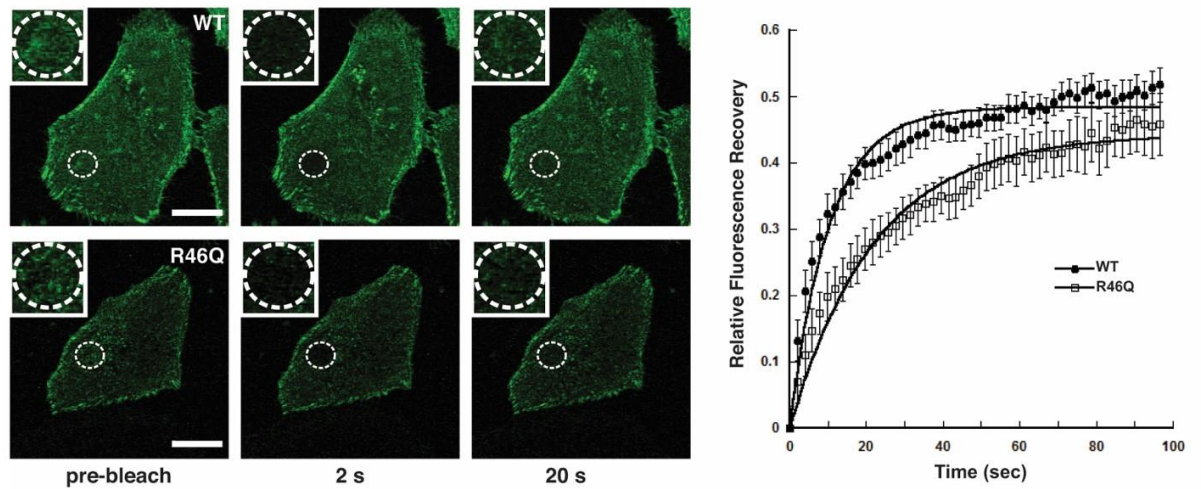


Figure 2.16: FRAP Analysis to Assess WT and R46Q-Actinin Association in Cells.

FRAP experiment using GFP-tagged WT and Arg46Gln (R46Q) actinin-1 expressed in HeLa Cells.

Images of representative cells, single confocal sections, taken immediately before and after bleaching, as well as after 20 seconds after recovery, are shown (left). Dashed circles and the insets indicate the bleached area. Representative plots of fluorescence recovery data and fitted curves are shown to the right (9-12 cells per experiment). The half time ($\tau_{1/2}$) for fluorescence recovery, averaged from the three independent experiments, was 7.0 ± 1.7 sec for WT actinin-1 and 15.5 ± 0.9 sec for the p.Arg46Gln mutant (\pm S.E.M).

Scale bar = $20\mu\text{m}$.

See appendix Fig 6.1 for projection confocal z-stack of whole HeLa cell (rather than single confocal section as displayed here).

2.5 Discussion

Congenital macrothrombocytopenias are a very rare group of platelet disorders. An accurate diagnosis is often very difficult to make because their clinical presentation can be very heterogeneous, ranging from asymptomatic patients, to patients suffering with a serious, life-threatening bleeding tendency. As a result, patients are sometimes misdiagnosed, receiving inappropriate, and sometimes harmful, treatments (Kunishima & Saito 2006). Advances in molecular genetics has led to progress in exposing some of the responsible genes for many CMTP (Kunishima & Saito 2006; Bolton-Maggs et al. 2006). To date, many genes have been identified (Kunishima & Saito 2006), however for about 50% of patients, the molecular cause remains unknown (Kunishima & Saito 2006). This may be partly due to a deficiency in our level of understanding of the various stages of platelet formation (Thon et al. 2010; Kunishima & Saito 2006). Owing to the characteristic symptoms normally ascribed to congenital macrothrombocytopenias, abnormal platelets size and a reduced platelet count (Kunishima & Saito 2006), we can speculate that the mutations arise in genes with unknown functions in megakaryocytes and/or platelets. Studies that identify the impact of these mutations will lead to a better understanding of the steps and stages of normal platelet production and/or function (Kunishima & Saito 2006).

The *ACTN1* gene has very recently been exposed as a CMTP causative gene (Guéguen et al. 2013; Bottega et al. 2015; Kunishima et al. 2013; Yasutomi et al. 2016). However, the molecular defects associated with mutant actinin-1 have not been explored.

Here, I have characterised the biological effect of several of these mutations, through biochemical assays and cell based studies, and describe a putative molecular basis for the deleterious effects of several of these CMTP-linked actinin-1 mutations. I provide evidence that these mutations, which localise within the ABD, increase actinin-1 binding to, or bundling of, actin filaments *in vitro*, and/or enhance actinin-1 association with the actin cytoskeleton in cultured cells.

In contrast to previous studies, (Guéguen et al. 2013; Bottega et al. 2015; Kunishima et al. 2013; Yasutomi et al. 2016), I did not observe major disruption of

the F-actin organisation in heterologous cells expressing moderate levels of CMTP-linked actinin mutant proteins. However, this finding agrees with the observation that patients carrying these mutations have a mild phenotype that seems to be restricted to platelet formation or maturation. Mutations causing widespread disruption of F-actin would be expected to yield a broader, more severe phenotype.

The increased actin-binding ability observed for these CMTP-associated mutant actinin-1 proteins lead me to speculate that the disorder operates through a “gain-of-function” mechanism. This gain-of-function phenotype fits with the dominant inheritance pattern of actinin-linked CMTP.

The biochemical mechanism, increased actin binding affinity, underlying this gain-of-function phenotype is one that has been seen before. Studies carried out to identify the mechanical impact of FSGS-associated mutations on actinin-4 observed increased actin binding affinity (Kaplan et al. 2000; Weins et al. 2007; Weins et al. 2005). The functional changes in the actinin-4 protein, due to the presence of these mutations, affect the structural organisation of the podocyte actin cytoskeleton, leading to podocyte abnormalities, making them more susceptible to damage or insult, eventually causing glomerulopathy (Kaplan et al. 2000; Weins et al. 2005). In this case, the cytoskeleton, or rather abnormalities in the cytoskeleton, play a definite role. It is no surprise that changes to the cytoskeletal structure and system can give rise to a pathological condition, given that cell division, stability, morphology and mobility, intracellular transport and communication cascades all originate and involve various aspects of the cell cytoskeleton (Ramaekers & Bosman 2004). The similar gain-of-function phenotype for actnin-1 associated CMTP as observed for actinin-4 associated FSGS suggests that similar molecular mechanisms may underlie these two different disorders This may help us to explain, and eventually understand, the pathological mechanism of *ACTN1*-CMTP related mutations.

From the results presented here, and through my review of other actin binding domain mutations, I support the hypothesis that *ACTN1* related CMTP is caused by a defect in the actin cytoskeleton, which presents itself during the stages of megakaryocyte differentiation and platelet production; this defect being increased actinin-actin binding ability. Even though actin is known to be the most

abundant protein in platelets (Hartwig & Italiano 2006), very little information is known about the exact role of actin in platelet production (Thon & Italiano 2012). What is known is that, ultimately, the crucial steps in this production rely on both the actin and microtubule cytoskeletons (Poulter & Thomas 2015; Thon & Jr 2012).

To begin, platelet biogenesis begins when megakaryocytes enter endomitosis (Machlus & Italiano 2013; Machlus et al. 2014). Just as actin plays an important role in the cell cycle and cell division (Heng & Koh 2010), it appears to also play an essential role in endomitosis. To start with, for the megakaryocyte to be able to enter into this process, it is vital that the actin cytoskeleton is correctly and tightly regulated (Poulter & Thomas 2015). Another function for actin in platelet production and formation is its involvement in podosomes. These are actin rich structures that exhibit matrix metalloproteinase activity which allow them to degrade the ECM, thereby facilitating the extension of proplatelets shafts across the basement membrane of a sinusoidal vessel for the eventual release of preplatelet and platelets in to the bloodstream (Schachtner et al. 2013). Once released into the blood system, platelet development continues through fission events promoted by vascular shear forces and abscission (Machlus & Italiano 2013; Machlus et al. 2014). This fission resembles the cleavage furrow that forms during cytokinesis (Thon et al. 2010; Schwertz et al. 2010), a process in which actinin is involved. Indeed, overexpression of actinin in dividing epithelial cells induces a failure in cytokinesis (Mukhina et al. 2007). It may be that a similar situation arises in these CMT platelets; actinin being more stably attached to the actin filaments might make these pro or preplatelets more resistant to fission events. “End Amplification” is another proposed role for actin in platelet production. Through branching and bifurcating of the proplatelet shaft, this mechanism increases the number proplatelet tips, and with that, increases the number of final platelets that are produced (Hartwig & Italiano 2006). This process involves the bending of the proplatelet shaft into a u-shape, which then folds back on itself to form a loop. A new process develops from this loop, and elongates. Actin-based forces drive these bending forces, and while the finer details of this reaction are unknown, it is believed that the actin filaments behave as “muscles” and bend the microtubules that comprise the proplatelet shaft (Hartwig & Italiano 2003; Hartwig & Italiano

2006). Through these important roles that actin plays in platelet formation, it is easy to comprehend how a mutation affecting the actin cytoskeleton regulation or/and stability could lead to the production of a reduced number of platelets.

This is not the first study to implicate an actin-binding protein and actin cytoskeleton abnormalities, as the causing factor and pathological mechanism of a platelet disorder. *MYH9*-disorders result through mutation of the *MYH9* gene, which encodes for the actin binding non-muscle myosin II protein (Kunishima & Saito 2006). This protein is believed to be responsible for actin organisation (Pertuy et al. 2014). While the impact of its mutations are not yet well defined, it is known that patients who have mutations affecting the head domain of this protein, the domain responsible for actin-binding, display a more severe thrombocytopenia than those patients with mutations affecting the tail domain, which has the ability to polymerise molecules. (Balduini & Savoia 2012; Pecci et al. 2008). Also, *myh9* knockout mice display premature proplatelets in their bone marrow and their megakaryocytes display a disrupted actin cytoskeleton and organelle distribution (Pertuy et al. 2014).

Filaminopathy A is another macrothrombocytopenia. The causative gene in this case the *FLNA* gene, encoding for cytoskeletal protein filamin A (Nurden et al. 2011). While this gene has been found to be mutated in patients displaying thrombocytopenia, the thrombocytopenia is usually seen as a symptom to one of the many rare diseases that *FLNA* mutations are known to produce, such as periventricular nodular heterotopia and the otoplatatodigital syndrome spectrum disorders (Berrou et al. 2013). Although it has also been known to cause thrombocytopenia as an isolated Filaminopathy A syndrome (Nurden et al. 2011). Filamin A is an actin binding protein (Tyler et al. 1980). It is richly expressed in platelets (Goubau et al. 2014). It stabilises actin filaments and connects them to the cell membrane via its ability to interact with major platelet integrin receptors (Stossel et al. 2001), such as the glycoprotein Ib α , of the Ib-V-IX complex (Nakamura et al. 2006). This interaction is vital platelet integrity (Williamson et al. 2002). Patients with Filaminopathy A exhibit abnormal platelet adhesive function, reduced platelet counts (Goubau et al. 2014) and altered platelet morphology (Nurden et al. 2011). Mouse model studies display reduced actin cytoskeleton integrity due to

disturbed filamin-integrin interaction (Falet et al. 2010). Interestingly, research carried out to characterise the effect of filamin A mutations implicated in otopalatodigital skeletal disorders, which are located in the filamin A ABD, have also reported increased actin binding ability as the molecular mechanism through which these disorders operate (Clark et al. 2009).

Studies carried out with cell culture models promote the importance of the actin cytoskeletal integrity in platelets. Mouse derived megakaryocytes, when cultured with actin polymerisation inhibitors such as the cytochalasins, display an altered and disrupted actin cytoskeleton and exhibit reduced proplatelet branching (Italiano et al. 1999). These results mirror some of the observations reported in investigations previously carried out with CMTP-associated actinin-1 mutant proteins. They also advocate the definite involvement of the actin cytoskeleton in the development of macrothrombocytopenia (Kunishima et al. 2013).

Referring back to this study and CMTP-associated actinin-1 mutations; the mechanism through which this increased actin binding ability affects the actin cytoskeleton system still remains unknown. However, in a study undertaken to address the physical changes that occur in podocytes expressing the FSGS-associated p.Lys255Glu actinin-4 protein (Ehrlicher et al. 2015) it was found that an increased actinin dissociation time from actin reduces cell motility and cytoplasmic mobility. Overall, this increased actinin-actin association time inhibits actin filament sliding, which leads to a relatively immobile cell that is unable to respond to its surrounding forces. In a subsequent study, they found that this increased dissociation time meant that cross-linked actin networks were under stress for longer periods of time (Yao et al. 2011). This might make the podocyte more susceptible to damage. Through my FRAP analysis, I observed a two-fold increase in mutant actinin-1 actin binding ability compared to WT protein. Perhaps the CMTP-associated mutations are also disrupting platelet cellular forces and dynamics through alterations of the cytoskeleton.

Although this study has described a similar gain-of-function phenotype for CMTP as has been observed for FSGS, by contrast, I found that calcium regulation of p. Arg46Gln actinin-1 actin-binding was unaffected, unlike the FSGS p.Lys255Glu actinin-4, which was shown to have no calcium sensitivity (Weins et al. 2007).

Calcium sensitivity of actin binding is also another important aspect of actinin-1 function that might be affected by CMTP-causing mutations that are located in the C-terminal calmodulin-like domain. While I observed that both p.Arg738Trp and p.Arg752Gln actinin-1 proteins exhibited increased F-actin binding both *in vitro* and in cultured cells, this did not reach statistical significance. However, it could be that these two mutations, and the other three, p.Thr737Asn, p.Gly764Ser and p.Glu769Lys, all of which have been mapped in or near the actinin-1 CaM domain (Bottega et al. 2015), affect actinin-1 calcium regulation. Similarly, it is conceivable that the p.Leu395Gln actinin-1 mutation mapped to the rod domain (Yasutomi et al. 2016) might affect actinin-1 homodimerisation, or indeed, heterodimerisation with other actinin isoforms that expressed in platelets, such as actinin-4 (Foley & Young 2013). It is interesting to note that of the five mutations mapped to the ABD, only the Gln32, Arg46 and Gly251 residues are conserved in actinins, while the Val105 and Lys225 residues are conserved across the spectrin family and in the ABD of calmin, plectin and dystonin proteins. Neither Val105 and Lys225 are conserved in fimbrin and only Val105 is conserved in filamin proteins (Borrego-Diaz et al. 2005).

2.6 Conclusion

Studies have described a potential role for actinin in platelet activation (Tadokoro et al. 2011), but no known role has been assigned to actinin in relation to platelet formation. It has been suggested that the actinins and their actin-cross linking activity are, to some degree, involved in nearly every actin-dependent process (Foley & Young 2014). Combining that statement with this study, and other previous studies carried out on *ACTN1*-related thrombocytopenia, particularly those carried out by (Kunishima et al. 2013), it would not be unreasonable to speculate that actinin-1, through its actin bundling and binding activity, does indeed play a role in platelet formation, a role that is sensitive to mutational disturbance.

Chapter 3:

Assessment of the Actinin and Spectrin Dimerisation Domains in view of their use as Potential Nanostructure Building Blocks

3.1 Abstract

Protein bionanotechnology is an emerging area of research that involves the use of proteins as building blocks in the construction of novel nanostructures. The functional and physical properties of proteins make them an appealing choice as a material with which to build and, in my opinion, the cellular cytoskeleton is a particularly attractive source for such protein building blocks.

The two most important properties to consider when choosing a protein-based building block are; stability and ability to self-assemble. Here, in relation to these two properties, I have investigated the suitability of the spectrin repeat domains from the actin crosslinking proteins, actinin and spectrin, as building blocks for nanoscale structures. Such an assessment was carried out through the use of dimerisation and protein stability assays. Proteins were produced through a bacterial co-expression system and purification system that I designed and optimised.

Both actinin and spectrin dimers show remarkable robustness in high salt and high temperature conditions, and I find that the minimum requirement for actinin dimer formation to be the presence of repeats 2 and 3 from its central region. Overall, this study demonstrates that spectrin repeats have many desirable properties supportive of their use in protein bionanotechnology.

3.2 Introduction

In theory, actinin dimers and α/β -spectrin heterodimers would be perfect components with which to build a protein nanostructure. In muscle cells, actinin acts to stabilize the muscle contractile apparatus machinery (Sjöblom et al. 2008), while spectrin is responsible for maintaining the shape and structure of RBCs (Zhang et al. 2013). In relation to this project, their most attractive feature is their ability to form dimers; actinin forms antiparallel dimers with itself (Ylänne et al. 2001), and spectrin forms antiparallel heterodimers composed of an α -spectrin subunit and a β -spectrin subunit (Speicher et al. 1992). I propose that this inherent property of “self-assembly” makes them amenable to bottom up fabrication, a popular construction approach in protein bionanotechnology in which small units assemble to form larger units (Zhang 2003).

3.2.1 Actinin Dimerisation

Actinin dimerisation is mediated by the four spectrin-like repeats that make up its central rod region (Djinović-Carugo et al. 1999; Ylänne et al. 2001). The arrangement of these spectrin-like repeats within the dimer has been the subject of much consideration and many studies have been set up to discriminate between the two models that have been proposed; the aligned model and the staggered model.

3.2.1.1 The Staggered Model for the Actinin Rod Domain

The staggered model predicts that only three of the four spectrin-like repeats are paired. In this model, the two actinin monomers contributing to the dimer are “staggered” relative to one another by one repeat, leaving either repeat 1 or repeat 4 unpaired and without a corresponding partner. Repeats 1, 2 and 3 of one monomer are paired with repeats 3, 2 and 1 of the opposing monomer, or alternatively, repeats 2, 3 and 4 are paired with repeats 4, 3 and 2. Depending on the arrangement, either repeat 1 or repeat 4 is unpaired or interacting with the non-homologous calmodulin-like domain (CaM) or actin binding domain (ABD), respectively (Fig. 3.1) (Winkler et al. 1997; Taylor & Taylor 1993)



Figure 3.1: Staggered Model of Actinin Rod Domain Structure.

(A) Staggered arrangement of spectrin-like repeats in which repeats 1, 2 and 3 of one monomer interact with repeats 3, 2, and 1 of the opposing monomer, leaving repeat 4 unpaired or interacting with the ABD.

(B) Alternative staggered arrangement of spectrin-like repeats in which repeats 2, 3 and 4 of one monomer interact with repeats 4, 3 and 2 of the opposing monomer, leaving repeat 1 unpaired or interacting with the CaM domain.

Using chicken gizzard actinin Taylor & Taylor (1993) reported that the dimeric structure of actinin was staggered. Utilising the lipid layer crystallization technique, Taylor & Taylor (1993) formed large two-dimensional actinin chicken gizzard protein crystals. Using electron microscopy, they used these crystals to produce low resolution three-dimensional projection images of actinin. These images revealed eight density peaks within the central rod region of actinin. They were arranged as three central pairs bordered with a single peak at either end, and were assumed to be the eight spectrin-like repeats of the actinin dimer. The single peak was interpreted to be repeat 1 and the three pairs of density peaks were interpreted to be the pairwise interactions of repeats 2-4 with repeats 4-2.

Winkler et al. (1997) also reported the actinin dimeric structure to be staggered. Images of purified actinin chicken gizzard protein were obtained using transmission electron microscopy. The overall general morphology of the central rod region in these images was that of three large central masses, assumed to be the three pairwise interactions between repeats 2-4 and 4-2. Repeat 1 was suspected to be the smaller mass that sometimes appeared in the images, or was assumed to be part of the larger mass defined as the actin binding domain.

One flaw with this staggered arrangement was that it positioned the CaM of one actinin monomer distant to the ABD of the other opposing monomer, making it very difficult to comprehend how calcium regulation could be accomplished in the calcium sensitive actinin isoforms.

3.2.1.2 The Aligned Model for the Actinin Rod Domain

The aligned model predicts the pairing of all four repeats, in which the repeats of one monomer are in symmetry, but opposite polarity, with the repeats in the opposing monomer. Repeats 1 and 2 are paired with repeats 4 and 3 respectively (Ylännä et al. 2001; Djinović-Carugo et al. 1999) (Fig. 3.2).

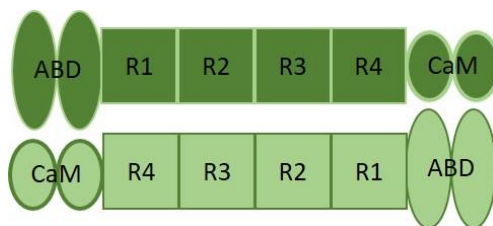


Figure 3.2: Aligned Model of Actinin Rod Domain Structure.

Aligned arrangement of spectrin-like repeats in which repeats 1 and 2 interact with repeats 4 and 3, respectively, from the opposing monomer.

In this model, four pairwise spectrin-like repeat interactions are contributing to the dimer formation. Therefore, dimers formed between full length rod domain monomers should be more stable than the dimers formed between terminally truncated rod domain monomers; the elimination of either of the terminal spectrin-like repeats, should result in a loss of two of these pairwise interactions, leaving only two to contribute to the dimer formation. This differs to the staggered model where three pairwise spectrin-like interactions are contributing to the dimer formation. Here, the elimination of either of the terminal spectrin-like repeats should not disrupt these three pairwise interactions, and so, for this aligned model to be true, one would expect the dimer stability between full length rod domain monomers to be equal to the dimer stability between terminally truncated rod domain monomers. Investigations carried out by Flood et al. (1995), using chemical cross-linking and sedimentation equilibrium studies with full length and truncated rod domain chicken gizzard actinin constructs, show that that full length actinin rod domain, repeats 1-4, can self-associate and form a very stable dimer. Truncated actinin rod domain constructs, consisting of repeats 1-3 (r1r2r3) or repeats 2-4 (r2r3r4), created through the removal of either repeat 4 or repeat 1 respectively, can also self-associate and form homodimers, but this self-association is much

weaker than that for the full length rod domain. This data disagrees with the staggered model and suggests that all repeats contribute to the dimer.

Isolated chicken gizzard actinin dimeric rod domain alone has been shown to be very stable (Imamura et al. 1988). This high stability indicates that the spectrin-like repeats are sufficient for actinin dimerisation, although interactions of the CaM domain with the “neck” region of the ABD and rod domain may also contribute to dimerisation of full length actinin (Young & Gautel 2000; Ribeiro et al. 2014).

Studies involving a yeast 2 hybrid system and two spectrin-like repeat truncated human actinin-2 constructs also support the aligned model. Here, constructs comprising repeats 1 and 2 (r1r2) were capable of dimerising with constructs comprising repeats 3 and 4 (r3r4), but each of these two repeat constructs were not capable of interacting with themselves or with constructs comprising repeats 2 and 3 (r2r3). These yeast 2 hybrid studies also showed that constructs comprising repeats 2 and 3 were only able to dimerise with copies of themselves (Young & Gautel 2000). In the staggered model, one would expect r2r3 to be able to interact with either r1r2 or r3r4.

The crystal structure of r2r3 of human actinin-2 has been determined to be an aligned anti-parallel dimer (Djinović-Carugo et al. 1999). This study provides near certainty that the aligned model is the correct one.

The crystal structure of the human actinin-2 rod domain (r1r2r3r4) has revealed that the rod domain is twisted 90° to the left (Ylänne et al. 2001). This feature may have been responsible for electron micrograph misinterpretation. As a result of the twist, the two repeats at one end the dimer, repeat 1 and repeat 4, might eclipse. In an electron micrograph, this might look like one single mass (a single repeat).

3.2.2 Spectrin Dimerisation

Unlike actinin, spectrin is an antiparallel heterodimer. It is composed of both an α - and β -spectrin subunit (Speicher et al. 1992). The spectrin repeats that make up the basic structure of both of these α - and β - spectrin subunits mediate

dimerisation between them (Ursitti et al. 1996; Harper et al. 2001; Speicher et al. 1992). Full length α - and β -spectrin contain 21 and 17 spectrin repeats respectively (Harper et al. 2001). Evaluation of these spectrin repeats through dimerisation studies have revealed the principal contributors to α -/ β -spectrin heterodimer formation. Initial dimerisation studies involved investigating the assembly of peptide fragments from each of the spectrin subunits (α -spectrin or β -spectrin) with their complementary full-length subunit. Through HPLC gel filtration chromatography, it was found that of the fragments produced when β -spectrin was cleaved with trypsin, only those containing the β IV domain, which includes the first four spectrin repeats (r1r2r3r4) at the N-terminal, could associate with full-length α -spectrin. Additionally, of the α -spectrin fragments produced, only those containing the α V domain, which includes spectrin repeats 19-21 (r19r20r21) at the C-terminal, could associate with full-length β -spectrin monomers (Speicher et al. 1992). Further characterization of α -/ β -spectrin heterodimerisation was carried out by Begg et al. (2000) and Ursitti et al. (1996). They found that the minimum number of spectrin repeats necessary to be present to initiate heterodimer formation is four; spectrin repeats β 1 and β 2 from β -spectrin and spectrin repeats α 20 and α 21 from α -spectrin. This site is commonly referred to as the dimer initiation site or the nucleation site. Ursitti et al. (1996) also found that the β 1 repeat alone is insufficient to induce heterodimer formation with α -spectrin monomers, but its presence is vital to the initialisation of heterodimerisation; truncated constructs not containing this β 1 repeat (β 2- β 4) could not induce heterodimer formation with α -spectrin monomers. Subsequent investigations thereafter found that while a minimum of two repeats from each spectrin monomer was necessary to induce heterodimerisation, the addition of more repeats was found to increase the salt stability of the heterodimer (Begg et al. 2000). This result revealed that complementary electrostatic interactions between α - and β - repeats in the dimer initiation site are contributing to this initial high affinity binding step, while dimerisation of additional repeats outside of the dimer initiation site thereafter is through low affinity hydrophobic interactions (also discussed in section 1.1.2.3.2) (Begg et al. 2000). The α 20-21 repeats contribute the majority of the negatively

charged residues and the β 1-2 contribute the majority of the positively charged residues (Li et al. 2008)

Harper et al. (2001) set out to assess the contribution of both the ABD and the CaM domain to heterodimer formation. Their studies compared the binding affinities between two repeat α -spectrin and two repeat β -spectrin recombinant proteins containing the EF-hand motifs from the CaM domain and the ABD respectively (α 20-21EF and β ABD1-2) with two-repeat α - and β -spectrin recombinant proteins lacking these domains (α 20-21 and β 1-2). Overall, they found no significant difference in binding affinity between α 20-21EF with β ABD1-2 and α 20-21 with β 1-2. Both pairs were able to form high affinity heterodimers, which suggested that both the ABD and the EF hand CaM domain do not contribute to heterodimer initiation.

Overall, a comprehensive model for the role of the spectrin repeats in α -/ β -spectrin heterodimer formation is as follows: an initial high affinity association of α 20-21 with β 1-2, mediated by complementary electrostatic interactions (Fig. 3.3A), aligns the α EF hand motifs with the β ABD (Fig. 3.3B) and aligns the remaining α -spectrin repeats with their remaining complementary β -spectrin repeats (Fig. 3.3C). Heterodimerisation then occurs in a “zipper-like” fashion, through lateral association of remaining spectrin repeats involving weaker hydrophobic interactions, to create a strong dimeric complex (Li et al. 2007).

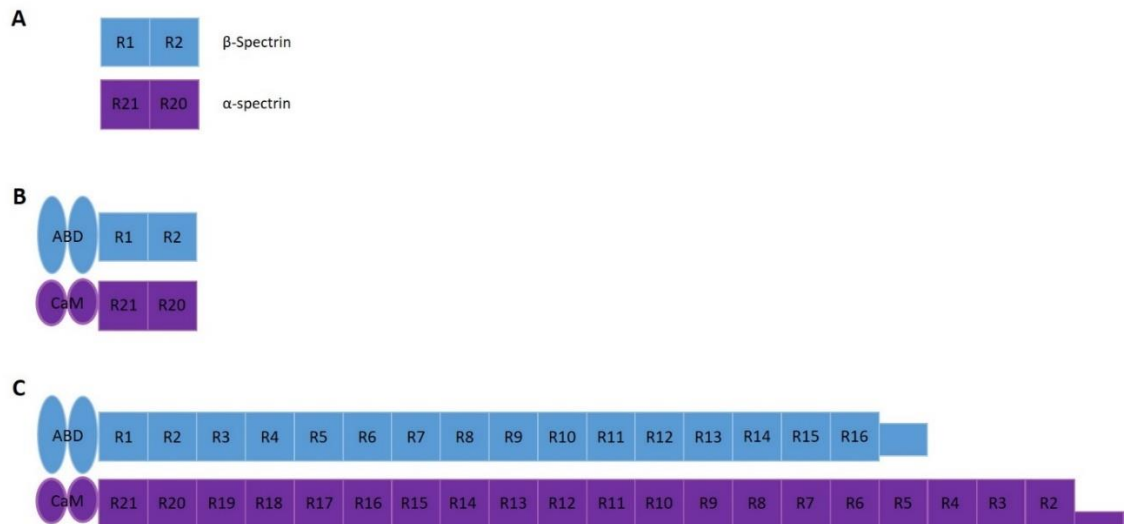


Figure 3.3: Spectrin Heterodimerisation. (A) Spectrin heterodimerisation begins with initial electrostatic interactions between β -spectrin spectrin repeats 1-2, and α -spectrin spectrin repeats 20-21. (Begg et al 2000; Ursetti et al 1996). (B) These primary interactions align the β ABD with the α CaM domain (Harper et al. 2001). (C) Dimerisation continues through hydrophobic interactions between the remaining α and β spectrin spectrin repeats in a "zipper-like" fashion down the length of the protein molecule (Begg et al. 2000).

3.2.3 Strategies for the Characterisation of Actinin and α -/ β -Spectrin Rod

Domains

From a nanoconstruction point of view, I considered stability and the ability to self-assemble the two most important attributes to a protein when considering it as a potential building block.

As we have seen, actinin and spectrin dimerisation have been well studied from a structural and biochemical point of view. In general, for both actinin and spectrin, it appears that isolated single repeats interact very weakly, if at all, and that pairing of two consecutive repeats are required to achieve appreciable dimerisation. It also appears that the addition of further interacting repeats to this core dimeric structure will add further stability. However, from the standpoint of using spectrin repeats in synthetic biology, further investigation into the structural foundations and conditions pertaining to the formation of these dimers is desirable. Specifically, it would be important to determine and establish:

- Which pairs of spectrin repeats are capable of inducing dimer formation?
- Is the context of consecutive repeats important, or can they be "mixed and matched"?

- What conditions disrupt dimer formation?

Ultimately, this study involved the investigation of the stability and self-assembly (dimerisation), properties of both the actinin rod domain and truncated α -/ β -spectrin proteins, each containing only four spectrin repeats, for potential use as nanostructure building blocks. These studies would primarily provide information that would allow for the exploitation of these proteins for protein-based nanoconstruction, but they would also provide more information regarding the physiological function and physical attributes of these proteins.

The general strategy for such an investigation employed in this chapter first involves expression and purification of various spectrin-like and spectrin repeat constructs that contain combinations of affinity, epitope or fluorescent protein tags that would allow both stability and dimerisation to be assessed through "pulldown" type assays or, in the case of dimerisation only, through native gel electrophoresis. I anticipated that in order to study actinin homodimerisation in particular, co-expression of differentially tagged constructs would be necessary. This is because certain constructs when expressed individually might be expected to form very stable homodimers, precluding their use in interaction or stability assays. However, I envisioned a secondary use for this co-expression system, a use that focused on the nanosynthetic aspect of the project. In order to build a structure using the bottom-up assembly technique I thought it important to have a system in which I could simultaneously produce several different "building blocks" and independently control the expression levels of each one. For these reasons, strategies for tunable co-expression of two or more constructs in *E. coli* were evaluated.

3.2.4 Strategies for Inducible Co-expression of Multiple Proteins in *E. coli*

Various co-expression strategies for protein production in *E. coli* have been described and several plasmid systems are available commercially. One potential approach is the expression of multiple proteins from a bicistronic mRNA. Another is the use of a two-promoter-one-plasmid system, and an alternative approach is the use of two plasmids. Both bicistronic and two-promoter-one-plasmid approaches use only a single plasmid into which both genes of interest are cloned. A bicistronic

plasmid contains only a single promoter. This promoter regulates the expression of multiple genes, and all genes are transcribed in one long mRNA strand. The two-promoter-one-plasmid approach consists of a plasmid that has two promoters. The expression of both genes of interest is controlled by its own promoter, and each gene is transcribed in its own short mRNA strand (Busso et al. 2011). In the two plasmid approach each plasmid carries a single gene. With this method, each plasmid must carry a different antibiotic resistance gene, and both plasmids must be compatible with each other, meaning they must each carry different origins of replication (Busso et al. 2011).

Out of the three co-expression strategies, the two plasmid approach might be considered to be the most flexible. Two popular bacterial expression systems are the T7 system, and its derivatives, and the P_{BAD} system (Studier & Moffatt 1986; Guzman et al. 1995).

The plasmids that I chose were the pBAD plasmid, purchased from Invitrogen (Life Technologies, Carlsbad, California, USA), containing the P_{BAD} promoter, and the pCDF/pRSF-duet plasmids, purchased from Merck (Novagen, Quintin, France), containing the *T7lac* promoter.

3.2.4.1 P_{BAD} Expression System

Along with the P_{BAD} promoter, the pBAD vector also contains the *araC* gene. This gene encodes for the AraC protein. This AraC protein regulates the activity of the P_{BAD} promoter (Guzman et al. 1995). It is a dimeric protein made up of a C-terminal DNA binding domain, a N-terminal dimerisation domain from which an 18 amino acid arm protrudes from, and an arabinose binding pocket (Fig. 3.4) (Schleif 2003).

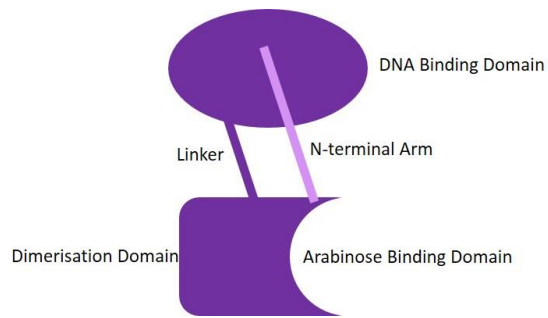


Figure 3.4: The AraC Protein. A multi-domain protein consisting of a C-terminal DNA binding domain and an N-terminal dimerisation domain with an 18 amino acid residue arm extension and an arabinose binding pocket (Schleif 2003).

In the absence of arabinose transcription is prevented (Fig. 3.5A). The N-terminal arm binds to the DNA binding domain. This interaction brings about an AraC orientation that encourages its binding to two half sites, *araI*₁ and *araO*₂, that are upstream of the P_{BAD} promoter. These sites are separated from each other by a great distance, and AraC binding to both generates a DNA loop (Schleif 2003), a widely used method to regulate gene expression (Matthews 1992). When arabinose is bound to AraC in the arabinose binding pocket binding (Fig. 3.5B) the N-terminal arm binds over the arabinose. The DNA binding domain is no longer constrained, and the dimeric AraC protein can now bind to two neighbouring half sites, *araI*₁ and *araI*₂ (Schleif 2003). This new interaction causes the DNA loop to open, which facilitates transcription (Schleif 2003; Schleif 2010). This regulatory mechanism is referred to as “The Light Switch Mechanism” (Schleif 2003).

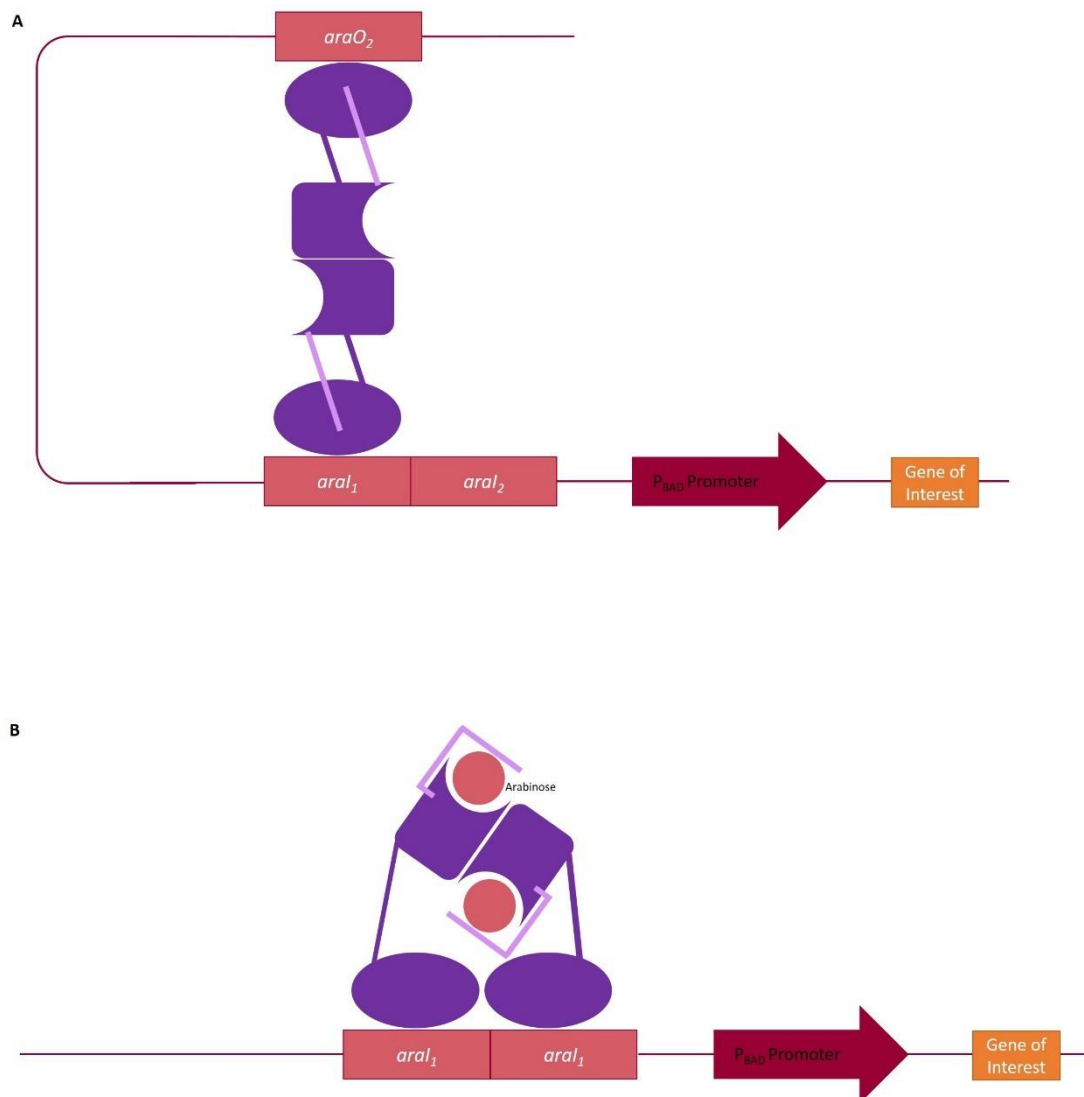


Figure 3.5: The Promoter and AraC Binding Sites on the Regulatory Region of the pBad Vector.

(A) In the absence of arabinose, the N-terminal arm interacts with the DNA binding domain. This permits the AraC protein to adopt a restricted conformation that allows it to bind to two well-separated AraC binding sites upstream of the *P*_{BAD} promoter, the *araO*₂ half site and the *araI*₂ half site. A DNA loop forms and this prevents transcription.

(B) When arabinose (depicted here as red circle) is present in the arabinose binding pocket, the N-terminal arm repositions itself, and no longer binds to the DNA binding domain. This allows the DNA binding domains to re-organise themselves and bind to two adjacent half sites, *araI*₁ and *araI*₂ half sites. This interaction opens the DNA loop and facilitates transcription (Schleif 2003; Schleif 2010).

Both the DNA binding domain and the dimerisation domain of the AraC protein can function independently of each other; *in vivo* and *in vitro* experiments with a chimeric protein made up of the AraC dimerisation domain and the DNA binding domain from the transcriptional repressor protein LexA report that this fusion protein can dimerise and can bind to the LexA operator sequence, while *in vivo* and *in vitro* experiments with a chimeric protein made up of the AraC DNA binding domain and the dimerisation domain, a leucine zipper motif, of the C/EBP

transcriptional activator protein report that this fusion protein can bind the *araI* site and stimulate transcription from the P_{BAD} promoter, and dimerise (Bustos & Schleif 1993). The AraC DNA binding domain is very flexible in terms of its DNA binding specificity; it can bind to repeat half sites and inverted repeat half sites (Carra & Schleif 1993). This suggests that the arabinose induced loop breaking is not a consequence of increased or decreased affinity for each of the half sites, but rather a protein conformational change that favours binding to two non-adjacent or adjacent sites, depending on the absence or presence of arabinose respectively. This mechanism relies upon the structure of the AraC protein (Lobell & Schleif 1990).

3.2.4.2 The T7/*lac* Expression System

Both the pCDF/ pRSF-Duet plasmids carry the T7/*lac* promoter and, as their name suggests, they contain the T7 promoter. The T7 expression system makes use of the T7 RNA polymerase that comes from the T7 bacteriophage (Studier & Moffatt 1986). The gene needed to encode T7 RNA polymerase is not contained on either of the duet plasmids, nor is it naturally expressed in *E. coli* cells (Studier & Moffatt 1986; Francis & Page 2010). For this reason, when using this promoter, it is necessary to choose a bacterial expression strain whose genome has been manipulated to encode for the T7 RNA polymerase. BL21 [DE3] *E. coli* cells are one such strain. In these cells expression of T7 RNA polymerase is under the control of the *lacUV5* promoter. Transcription from this *lacUV5* promoter is regulated with the presence or absence of IPTG. Transcription occurs when IPTG is present in the system (Francis & Page 2010). The T7 RNA polymerase specifically recognizes the T7 promoter (Studier & Moffatt 1986) and, once transcribed, in the presence of IPTG, the T7 RNA polymerase can go forward and activate transcription of the target construct (Studier & Moffatt 1986) (Fig. 3.6)

T7/*lac* promoters present on the pCDF/ pRSF-Duet plasmids in this study have additional regulatory features that help to minimise basal expression. They have a *lac* operator sequence downstream of the T7 promoter, and they contain the *lacI* gene sequence that encodes for the *lac* repressor. Binding of the *lac* repressor to the *lac* operator sequence reduces transcription and, in doing so, helps to decrease background expression (Novagen Duet Vector User Protocol).

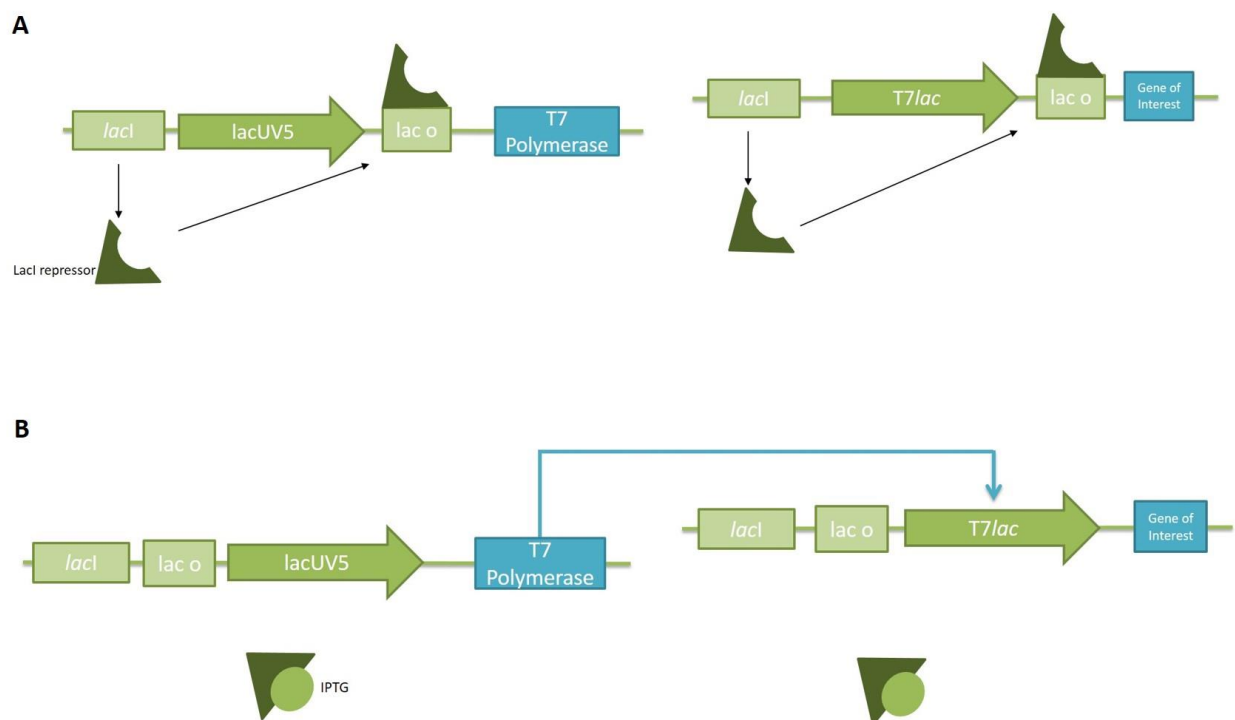


Figure 3.6: The T7 Expression System. Target constructs are cloned into an expression plasmid with the T7 promoter. Constructs are then transformed into *E. coli* cells whose genome has been altered to contain the T7 RNA polymerase. **(A)** When no IPTG is present there is no T7 RNA polymerase transcribed and therefore there is no transcription of the gene of interest. **(B)** When IPTG is present, the *lacUV5* promoter is activated to transcribe the T7 RNA polymerase. This T7 RNA polymerase can then activate transcription from the T7 promoter (Francis & Page 2010).

3.2.4.3 Crosstalk between the T7/*lac* Promoter and the P_{BAD} Promoter

One drawback in using the two plasmid co-expression approach is that sometimes the two promoters can disrupt each other's activity, i.e. engage in promoter crosstalk when the inducer of one promoter disturbs expression from the other promoter (Lee et al. 2007). A study undertaken by Lee et al. (2007) showed that IPTG inhibited expression from the P_{BAD} system. It was suggested that the binding of IPTG to AraC, the transcriptional regulator of the P_{BAD} system, was interfering with arabinose induction (Lee et al. 2007; Schleif 2010). Through directed evolution they were able to derive a P_{BAD} expression system that was more responsive to the presence of arabinose and, as a result, no longer sensitive to the presence of IPTG. This modified version of the P_{BAD} system contains a mutated variant of the *araC* gene that causes the production of a truncated AraC protein at its C-terminal (C280*). They found this new AraC protein to be IPTG-insensitive,

and, as a result, this new version of the P_{BAD} system to be more compatible with IPTG-induction systems.

This study also found that three mutations in the AraC N-terminal dimerisation domain collectively gave the same phenotype as the AraC protein truncated at its C-terminal. It is unclear why these mutations decrease the sensitivity of the P_{BAD} system to IPTG. The affected amino acid residues were found to reside outside of the arabinose binding pocket, and were found not to be any of the residues involved in DNA binding or involved in the binding of the N-terminal arm. This suggests that these mutations do not affect the binding of each domain to its corresponding ligand (Lee et al. 2007). The fact that both sets of mutations resulted in the same phenotype, even though they reside on different domains of the protein, suggests that these mutations take effect when both the dimerisation domain and the DNA binding domain need to work together.

Focusing on the C280* mutation, in their study, Lee et al (2007) compared expression from the WT P_{BAD} system with expression from their new C280* P_{BAD} system in the presence of IPTG; in all tests carried out, only one protein expression system was present and, therefore, only one protein was to be expressed.

To better determine the usefulness of this new C280* P_{BAD} system going forward, examination of expression from the C280* P_{BAD} system in a co-expression situation would need to be carried out; where one protein would be expressed from the C280* P_{BAD} system, induced by the presence of arabinose, together with expression of another protein from the T7/*lac* promoter, induced by the presence of IPTG.

3.2.5 Objectives

In conclusion, the overarching objectives of this chapter were to:

1. generate a co-expression system and purification strategy that would enable us to:
 - verify and produce actinin dimers and spectrin heterodimers.

- produce different “building blocks” for the self-assembly of a pre-designed protein nanostructure.
 - Accessory aims of this section were to:
 - further the investigation started by Lee et al. (2007) and compare expression between the WT P_{BAD} system and the C280* P_{BAD} system in a co-expression environment with the *T7/lac* system.
 - shorten the purification strategy of these dimers in view of making it a more attractive method for generating protein complexes.
- 2. study and learn more about the actinin rod domain dimerisation process (i.e self-assembly properties), with the intention of:
 - widening the knowledge of this dimerisation process in a biological context.
 - exploiting this dimerisation process to create potential biosynthetic building blocks.
- 3. determine the conditions that disrupt dimer association and induce dissociation between actinin dimers and α/β -spectrin heterodimers (i.e. stability properties).

3.3 Materials and Methods

3.3.1 Antibodies and Reagents

Sources of antibodies were as follows: anti-FLAG, from Sigma-Aldrich, Arklow, Ireland (Catalog Number: #F3165) and anti-MPB, from New England Biolabs, Hitchin, UK (Catalog Number: # E8030S); IRDYE®800CW conjugated anti-mouse and anti-rabbit secondary antibodies were from LI-COR Biosciences (Catalog Numbers: #926-32210 and #926-3221, respectively). All other reagents and chemicals used were obtained from Sigma-Aldrich, unless otherwise stated.

3.3.2 cDNA constructs

The cDNA constructs, for protein expression and subsequent self-assembly and stability analysis, were amplified by PCR.

All actinin constructs are the human muscle actinin-2 (calcium insensitive) isoform. Primer design was based on the GeneBank sequence NM_001103. All α -Spectrin constructs are the human erythrocytic α -Spectrin and all β -Spectrin constructs are the human erythrocytic β -spectrin transcript variant 1. Primer design was based on the GeneBank sequences; NM_003126 and NM_001024858, respectively.

The constructs used, with amino acids residues in brackets, are as follows. Actinin: r1-r4 (274-746); r1-r3 (274-637); r2-r4 (371-746), r1-r2 (274-501), r2-r3 (371-637) and r3-r4 (502-746). α -Spectrin: r18-r21 (1818-2259). β -Spectrin: r1-r4 (293-743).

Of special interest, two sets of primers (Integrated DNA Technologies, Inc., Leuven, Belgium) were designed for actinin r1-r4 construct amplification; one set to yield a product with an EcoRI site at its 5' end, and XhoI and HindIII sites at its 3' end. The other set, to yield a product with EcoRI and SacII sites at its 5' end, and KpnI and SalI sites at its 3' end (Fig. 3.7)

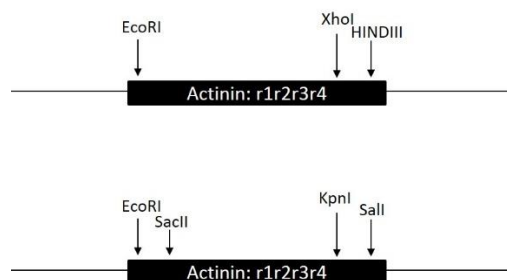


Figure 3.7: Strategy for Cloning Actinin cDNA Constructs. Restriction sites employed for the cloning of Actinin-2 constructs.

The primers to amplify the α -spectrin: r18-r21 construct were designed to yield a product with BglII and AscI sites at its 5' end and SalI and XhoI sites at its 3' end. The primers to amplify the β -spectrin: r1-r4 construct were designed to yield a product with a EcoRI site at its 5' end, and SalI and HindIII sites at its 3' end (Fig. 3.8).

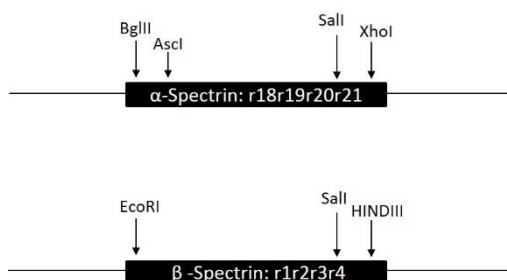


Figure 3.8: Strategy for Cloning Spectrin Constructs. Restriction sites employed for the cloning of α -Spectrin and β -Spectrin constructs.

For remaining constructs, restriction sites included in amplicon design were those used to introduce amplicon to plasmid, and are mentioned in Plasmid Construction section.

3.3.3 Plasmid Construction

3.3.3.1 Cloning of Actinin Constructs

The actinin r1-r4 construct was introduced into the commercially available pCDF-Duet plasmid (see appendix for plasmid map) twice as two separate preparations, as follows (restriction sites in brackets):

MCS1 (EcoRI and HindIII), so to be fused to a 6xHis tag at its N-terminal. This construct preparation was later modified to contain a FLAG epitope tag at the C-terminus of the 6xHis tag. MCS2 of the pCDF-Duet vector (EcoRI and Sall; making use of compatible cohesive end ligation with plasmid sites Mfe I and XhoI, respectively), so as to be fused to a S- tag at its C-terminal. From hereafter, actinin r1-r4 was sub-cloned into: MSC1 of a modified pCDF-Duet plasmid (EcoRI and HindIII), encoding a N-terminal 6xHis tag with a yellow fluorescent protein (YFP) tag sequence, a modified pBAD plasmid (EcoRI and HindIII), encoding a N-terminal HIS₆ tag followed by a maltose binding protein (MBP) tag sequence. A second modified pBAD plasmid (EcoRI and HindIII), encoding a N-terminal MBP tag sequence, which had previously been genetically manipulated, using the Quikchange site-directed mutagenesis kit (Agilent Technologies) to contain the C280* *araC* gene, encoding for the truncated version of the AraC regulatory protein.

The following actinin constructs were introduced into the commercially available pRSF-Duet plasmid (using restriction sites in brackets) so that each would be fused to a 6xHis tag at their N-terminal: r1-r3 (EcoRI and HindIII), r2-r4, r1-r2, r2-r3 and r3-r4. These construct preparations were later modified to contain a FLAG epitope tag at the C-terminus of their HIS₆ tag. From here, these actinin constructs were sub-cloned into the modified pBAD plasmid to be fused to a HIS₆MBP at their N-terminal.

3.3.3.2 Cloning of Spectrin Constructs

The α -spectrin r18-r21 construct was introduced into MSC1 of the pCDF-Duet plasmid (BglII and XhoI; making use of compatible cohesive end ligation with plasmid sites BamHI and Sall respectively), so as to be fused to a 6xHis tag at its N-terminal. From here, α -Spectrin r18-r21 was sub-cloned MCS1 of a modified pCDF-Duet plasmid (AscI and Sall), encoding a N-terminal 6xHis tag with a mCherry fluorescent protein tag.

The β -Spectrin r1-r4 construct was introduced into MSC1 of the pRSF-Duet plasmid (EcoRI and HindIII), so as to be fused to a 6xHis tag at its N-terminal. From hereafter, β -Spectrin r1-r4 was sub-cloned into a modified pRSF-Duet plasmid

(EcoRI and Sall), encoding a N-terminal 6xHis tag with a mCherry fluorescent protein tag, and sub-cloned into the C280* pBAD plasmid (EcoRI and Sall), with N-terminal MBP sequence.

3.3.3.3 Construction of Bicistronic Plasmid

The pRSF bicistronic expression plasmid was produced through multiple sequential cloning steps and is derived from the commercially available Duet plasmids. The pRSF-Duet plasmid was enzymatically digested with HindIII and MfeI. Intermediary segment, containing second promoter sequence and transcription start site was replaced with short oligonucleotide of 43 base pairs. The two MCSs from the original pRSF still remained. Actinin r1r2r3r4 was sub-cloned into MCS2 using restriction sites EcoRI and Sall; making use of compatible cohesive end ligation with plasmid sites Mfe I and XhoI, respectively. Resulting plasmid was enzymatically digested with KpnI and HindIII, to create a fragment containing the Actinin r1r2r3r4 sequence and the 43 base pair oligonucleotide. This fragment was introduced to a KpnI and HindIII digested modified pRSF-Duet plasmid encoding for YFP-r1r2r3r4 in MCS1, yielding a bicistronic YFP-r1r2r3r4 and r1r2r3r4-S tag expression plasmid.

The veracity of all constructs was verified by restriction digest, followed by DNA sequencing. A list of all constructs and the studies each was utilised in can be found in table 3.1; section 3.3.4.

3.3.4 Protein Expression

For single protein expression: All constructs listed in table 3.1 were transformed into *E. coli* [DE3] (Novagen, Quintin, France). All actinin constructs were induced at 37 °C by addition of 0.2mM IPTG and cells were harvested 4 hours post induction. All spectrin constructs were induced at 30 °C by addition of 0.2mM IPTG and cells were harvested 6 hours post induction.

For protein co-expressions using the two-plasmid-two-different-promoter co-expression system: Compatible plasmid combinations used were pRSF/pCDF-

Duet with pBAD/pBAD C280*. Each pair of recombinant actinin/spectrin constructs were co-electroporated into electro-competent *E. coli* [DE3]. All combinations were grown in LB media containing the two appropriate antibiotics (resistance markers for each plasmid are mentioned in table 3.1). Co-expression of actinin constructs was induced at 37 °C with the introduction of IPTG and arabinose (relevant concentrations listed in table 3.2). Cells were harvested 4 hours post induction. Co-expression of spectrin constructs was induced at 30 °C with the introduction of IPTG and arabinose (relevant concentrations listed in table 3.2). Cells were harvested 6 hours post induction.

For all expressions, a 1ml sample was removed from each culture before and after the induction period, pelleted, and resuspended in H₂O, for inspection by SDS-PAGE. Harvesting of remaining culture was through centrifugation, and pellet was stored at -20 °C.

For protein co-expressions using both the bicistronic and two-promoter-one-plasmid systems, two-plasmid-same-promoter: plasmids were transformed into *E. coli* [DE3] and expression was induced at 37 °C by addition of 0.2mM IPTG and cells were harvested 4 hours post induction. Analysis was carried out on 1ml pre and post induction samples.

Spectrin Repeat Containing Constructs from Actinin and Spectrin								
Actinin	Plasmid	Inducer	Conc.		Spectrin	Plasmid	Inducer	Conc.
<u>Self-Assembly Studies</u>					<u>Self-Assembly Studies</u>			
His r1r2r3r4	pCDF-Duet (Sm ^R)	IPTG	0.2mM		His α-r18r19r20r21	pCDF-Duet (Sm ^R)	IPTG	0.2mM
His MBP r1r2r3r4	pBAD (Amp ^R)	Arabinose	0.5%		His β-r1r2r3r4	pRSF-Duet (Kn ^R)	IPTG	0.2mM
His FLAG r1r2r3r4	pCDF-Duet (Sm ^R)	IPTG	0.2mM		His mCherry α-r18r19r20r21	pCDF-Duet (Sm ^R)	IPTG	0.2mM
His MBP r1r2r3	pBAD (Amp ^R)	Arabinose	0.5%		His mCherry β-r1r2r3r4	pRSF-Duet (Kn ^R)	IPTG	0.2mM
His MBP r2r3r4	pBAD (Amp ^R)	Arabinose	0.5%		MBP β-r1r2r3r4	pBAD C280* (Amp ^R)	Arabinose	0.5%
His FLAG r1r2r3	pRSF-Duet (Kn ^R)	IPTG	0.2mM					
His FLAG r2r3r4	pRSF-Duet (Kn ^R)	IPTG	0.2mM					
His MBP r1r2	pBAD (Amp ^R)	Arabinose	0.5%					
His MBP r2r3	pBAD (Amp ^R)	Arabinose	0.5%					
His FLAG r1r2	pRSF-Duet (Kn ^R)	IPTG	0.2mM					
His FLAG r2r3	pRSF-Duet (Kn ^R)	IPTG	0.2mM					
His FLAG r3r4	pRSF-Duet (Kn ^R)	IPTG	0.2mM					
<u>Stability Assays</u>					<u>Stability Assays</u>			
His r1r2r3r4	pCDF-Duet (Sm ^R)	IPTG	0.2mM		His α-r18r19r20r21	pCDF-Duet (Sm ^R)	IPTG	0.2mM
MBP r1r2r3r4	pBAD C280* (Amp ^R)	Arabinose	0.5%		MBP β-r1r2r3r4	pBAD C280* (Amp ^R)	Arabinose	0.5%
<u>Co-expression Strategies</u>								
S-tag r1r2r3r4	All co-expression strategy plasmids	0.2mM						
YFP r1r2r3r4	All co-expression strategy plasmids	0.2mM						

Table 3.1: List of Constructs Designed. Those constructs pertaining to this chapter and the studies they were utilised in (some constructs were used in more than one study; hence these are listed twice). Table includes the plasmid that each construct was cloned into, including the antibiotic resistance marker of that plasmid. Also listed is the inducer, and inducer concentration required, to activate the expression of each construct. Amp^R=ampicillin resistance; Kn^R=kanamycin resistance; Sm^R=Spectinomycin.

Co-Expression Combinations with Inducer Concentrations		
Construct Combinations	IPTG Concentrations	Arabinose Concentrations
<u>Actinin Self-Assembly Studies</u> (using T7lac system and WT pBAD system)		
His FLAG r1r2r3r4	0.2mM	-
His MBP r1r2r3r4	-	0.2%
His FLAG r1r2r3	0.0625mM	-
His MBP r1r2r3	-	1.25%
His FLAG r1r2r3	0.0625mM	-
His MBP r2r3r4	-	1.25%
His FLAG r2r3	0.0625mM	-
His FLAG r2r3	-	1.25%
<u>Actinin Stability Assays</u> (using T7lac system and C280* pBAD system)		
His r1r2r3r4	1mM	-
MBP r1r2r3r4	-	0.2%
<u>Spectrin Stability Assays</u> (using T7lac system and C280* pBAD system)		
His α-r18r19r20r21	1mM	-
MBP β-r1r2r3r4	-	0.1%

Table 3.2: Co-Expression Protein Combinations with Optimum Inducer Concentrations. Combinations of protein pairs co-expressed and co-purified for various studies carried out throughout this chapter and the optimum inducer concentrations required to bring about co-expression. Mentioned also are the two systems that were used to bring about co-expression.

3.3.4.1 Promoter Cross-Talk Study Co-expressions

Promoter cross-talk study was performed with the compatible plasmid combination pRSF-Duet and pBAD/pBAD C280*, expressing YFP and MBP proteins respectively. Expression was performed as described above; constant IPTG concentrations were at 0.2mM, with increasing IPTG concentrations being 0.2, 0.5 and 1mM. Constant arabinose concentrations were at 0.5%, with increasing arabinose concentrations being 0.01, 0.05, 0.2 and 0.5%. For expression of one protein, in a culture containing both plasmids, only the relevant inducer is introduced to the culture,

either 0.2mM IPTG or 0.5% arabinose only. Analysis was carried out on 1ml pre and post induction samples

3.3.5 Protein Purification

Frozen cells were thawed on ice and resuspended in PBS, 0.2% triton, 20mM β -mercaptoethanol and 1mM PMSF. Cells were lysed by sonication and addition of 0.1mg/ml lysozyme for 30min at 4 °C. Lysates were cleared by centrifugation at 39,000xg for 40min at 4 °C.

For Ni-based purification, proteins were loaded onto a Ni-column pre-equilibrated with Ni-wash buffer (0.5M NaCl, 50mM KPO₄ pH 8.0, 20mM β -mercaptoethanol, 5mM imidazole, 0.1% triton). Columns were washed three times with 10ml wash buffer. Bound proteins were eluted in 200mM imidazole pH7, with 20mM β -mercaptoethanol.

For amylose-based purifications, proteins were loaded onto an amylose column pre-equilibrated with amylose wash buffer (20mM Tris pH7.5, 150mM NaCl, 1mM DTT). Columns were washed three times with 10ml wash buffer. Bound proteins were eluted in 10mM maltose, with 20mM Tris pH7.5, 150mM NaCl, 1mM DTT. Protein dimers were purified using sequential chromatography steps; Ni-based purification followed by amylose based purification. Eluted proteins/dimers were incubated overnight at 4 °C in dialysis tubing immersed in a dialysis buffer (20mM Tris-HCl pH7.5, 50mM NaCl, and 5mM β -mercaptoethanol). Purified proteins were concentrated using Amicon Ultra centrifugal filters (Millipore, Cork, Ireland).

3.3.6 Actinin Spectrin-like Repeat and Spectrin Spectrin-Repeat

Dimerisation Assays

Actinin: His FLAG tagged with His MBP tagged actinin four-/three-/two-spectrin-like repeat constructs were co-expressed as previously described above. Consequent cell lysate of comparable concentrations was incubated with 30 μ l of amylose resin for 30min at 4 °C with continuous mixing. A separate sample using His MBP tag cell lysate was incubated with amylose resin as a control. The resin was collected with low speed centrifugation, 1800xg for 3min, and unbound proteins

were removed with three 1ml x 5min washing steps with amylose wash buffer. His MBP tagged proteins were eluted with 65µl amylose elution buffer. Eluted and pull-down proteins were analysed with SDS-PAGE followed by anti-FLAG western blot detection. For actinin two-spectrin-like repeat dimerisation assays, both co-expression and single expression cell lysates were used. For those assays involving mixing of single expression cell lysate: for each combination, comparable amounts of each expression lysate are mixed. Remainder of protocol is as per those assays carried out with co-expression lysate.

Spectrin: 1µM of each purified protein, His α -r18r19r20r21 and MBP β -r1r2r3r4, were mixed together for 20min at 4 °C. Protein mix was then incubated 60µl amylose resin and left to rock continuously for 20min at 4 °C. A separate sample in which only the His α -r18r19r20r21 protein was incubated with amylose resin was set up as a control. The resin was collected with low speed centrifugation, 1800xg for 3min, and three 1ml x 5min washing steps were carried out with amylose wash buffer. MBP β -r1r2r3r4 tagged proteins were eluted with 120µl amylose elution buffer. Eluted and pull-down proteins were analysed with SDS-PAGE.

3.3.7 Native Protein Gel Electrophoresis

Native protein gel electrophoresis set up was as per the standard polyacrylamide gel electrophoresis protocol, with the exception that SDS, β -mercaptoethanol and boiling steps were omitted.

Actinin: Comparable amounts of purified His MBP r1r2r3r4 and His r1r2r3r4 proteins were mixed. Single protein controls were also prepared; His MBP r1r2r3r4 only and His r1r2r3r4 only.

Spectrin: The following protein mixes were prepared, with comparable amounts of each protein: His mCherry α -r18r19r20r21 and His β -r1r2r3r4, His α -r18r19r20r21 and His mCherry β -r1r2r3r4. Control mixes included His α -r18r19r20r21 and His mCherry α -r18r19r20r21, His β -r1r2r3r4 and His mCherry β -r1r2r3r4. Single protein controls included His α -r18r19r20r21 only, His mCherry α -r18r19r20r21 only, His β -r1r2r3r4 only, and His mCherry β -r1r2r3r4 only.

Gel loading buffer (without β -mercaptoethanol and SDS) was added to all Actinin and Spectrin samples on ice. Samples were then loaded onto 5% native gels (prepared without SDS). Samples were run in native gel running buffer (without SDS) at 4 °C. Both the separating gel and gel running buffer were designed to have an approx. pH8-9, as per standard denaturing protocol.

3.3.8 Actinin spectrin-like repeat and Spectrin spectrin repeat Salt Stability Assays

1.5 μ M of actinin pseudoheterodimers (His r1r2r3r4:MBP r1r2r3r4) or 1.5 μ M of spectrin heterodimers (His α -r18r19r20r21:MBP β -r1r2r3r4) were each incubated with 10 μ l Ni-resin in a buffer containing 20mM Tris pH7.5, 5mM β -mercaptoethanol, 5mM imidazole and varying concentration of NaCl; from 150mM to 4.5M (150mM, 500mM, 1M, 1.5M, 2M, 2.5M, 3M, 3.5M, 4M and 4.5M) for actinin pseudoheterodimers, and 150mM to 2M (150mM, 500mM, 1M, 1.5M and 2M) for spectrin heterodimers. Separate samples containing either actinin MBP r1r2r3r4 only or spectrin MBP β -r1r2r3r4 were prepared as controls and were also subjected to all the same salt concentrations as their corresponding pseudoheterodimers or heterodimer. Samples were left for 1hr at 4 °C. The resin was collected with low speed centrifugation, 1800xg for 3min, and three 1ml x 5min washing steps were carried out with Ni-wash buffer. His tagged proteins were eluted with 40 μ l Ni-elution buffer. Eluted and pull-down proteins were analysed with SDS-PAGE, followed by anti-MBP western blot detection.

3.3.9 Actinin spectrin-like repeat and Spectrin spectrin-repeat Thermostability Assays

Thermostability assays were carried out as per salt stability assays, with a few variations: assays used 1 μ M of actinin pseudoheterodimers or spectrin heterodimers, each pseudoheterodimer or heterodimer sample was incubated in temperatures between 4 °C and 70 °C (4°, 27°, 50° and 70 °C) for 30 min prior to incubation with 10 μ l Ni-resin in a buffer containing 20mM Tris pH7.5, 5mM β -

mercaptoethanol, 5mM imidazole and 150mM NaCl. All incubation and wash steps for each sample were carried out at that sample's given temperature.

For actinin dissociation and re-association studies 1 μ M of His r1r2r3r4 and 1 μ M of MBP r1r2r3r4 were mixed and incubated at temperatures of between 37.7 °C and 57.4 °C (37.7°, 40.7°, 45.6°, 50.9°, 55.7° and 57.4 °C) for 10min and were then cooled slowly to 4 °C. Remainder is as per previous salt and thermostability assays, with all wash steps carried out at 4 °C.

3.4 Results

3.4.1 Expression and Purification of Spectrin-like and Spectrin Repeat Containing Constructs from Actinin and Spectrin

It was first necessary to design and clone the spectrin-like and spectrin repeat constructs from actinin and spectrin proteins respectively (see table 3.1 in Materials and Methods for exhaustive list of all dimerisation constructs), check if they expressed in *E. coli* cells, determine the optimum concentration of inducer to promote expression, and adopt a protein purification strategy.

Those constructs that were designed to have an MBP tag were cloned into the pBAD plasmid. All other constructs, those without an MBP tag, were cloned into either the pCDF- or pRSF-Duet plasmids.

Fig. 3.9 is presented as a representative figure to illustrate that all individual constructs could be expressed at a high level upon induction, and could also be purified with a high yield.

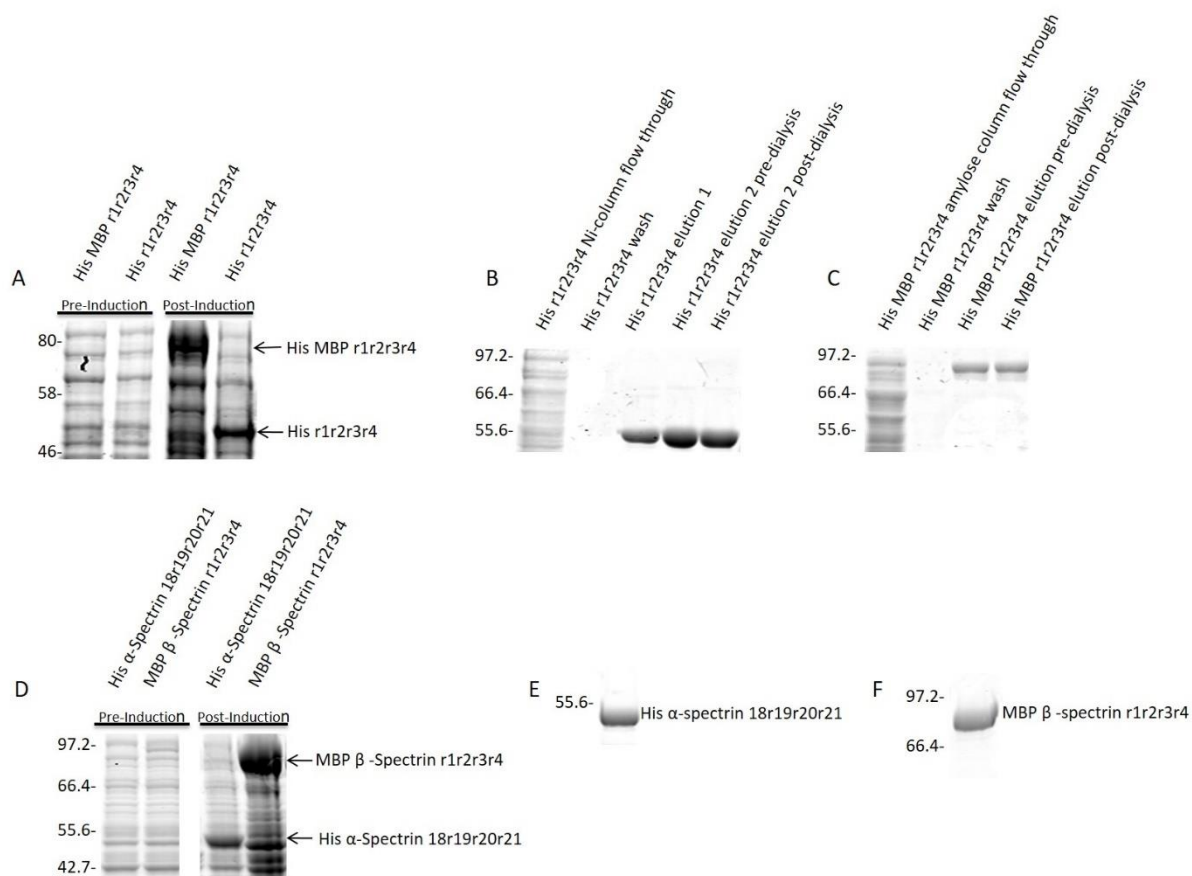


Figure 3.9: Representative Gel Demonstrating Successful Expression and Purification Strategies of Repeat Constructs.

All protein constructs were recombinantly expressed in *E. coli* cells. All protein expression and purification steps were analysed using SDS protein gel electrophoresis. Proteins were visualised using Coomassie Brilliant Blue staining.

(A) Total cell protein samples, both pre and post induction of protein expression with arabinose or IPTG.

(B) Fractions taken at each step of nickel column affinity chromatography purification.

(C) Fractions taken at each step of amylose column affinity chromatography purification.

(D) Total cell protein samples, both pre and post induction of protein expression with arabinose or IPTG.

(E) Purified His α -spectrin r18r19r20r21. Purification was carried out as per (B).

(F) Purified MBP β -spectrin r1r2r3r4. Purification was carried out as per (C).

Proteins of interest and the sizes (in kDa) of the relevant molecular weight markers are indicated on each gel.

3.4.2 Co-expression System

3.4.2.1 Choosing a Bacterial Co-Expression Strategy

The aim here was to investigate which co-expression strategy (bicistronic, two-promoter-one-plasmid or two-plasmid) would be best to produce the actinin dimers and α -/ β -spectrin heterodimers. A benchmarking study consisting of two

target constructs, S-tagged and YFP-tagged actinin rod domain constructs (spectrin-like repeats 1-4, r1r2r3r4), was set up. Both target constructs were cloned into a bicistronic plasmid, that I designed myself, and a commercially available two-promoter plasmid. One copy of each target constructs was cloned into a single separate plasmid for single expression (Fig. 3.10).

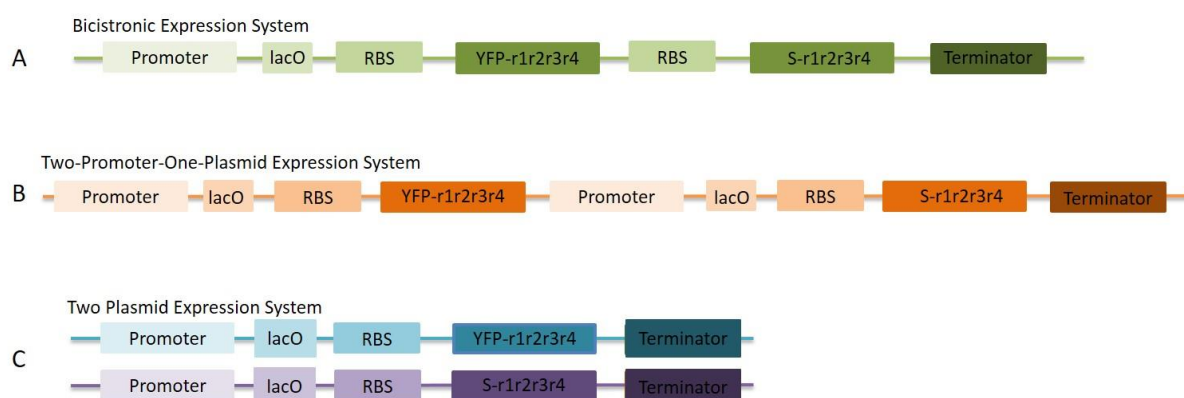


Figure 3.10: Schematic Representation of the Genetic Design (DNA sequences) of the Co-expression Constructs to Produce the YFP-ROD:S-ROD dimers. (A) pRSF bicistronic expression plasmid. **(B)** pCDF two-promoter-one plasmid expression plasmid. **(C)** pRSF and pCDF single gene expression plasmids for two plasmid expression approach.

In examining protein co-expression from each of these strategies a difference was observed. Co-expression of each of the target constructs was noted using both the two-promoter-one-plasmid strategy and the two plasmid strategy. There was no co-expression noted with the bicistronic strategy, only expression of the gene positioned closest to the promoter on the plasmid (Fig. 3.11).

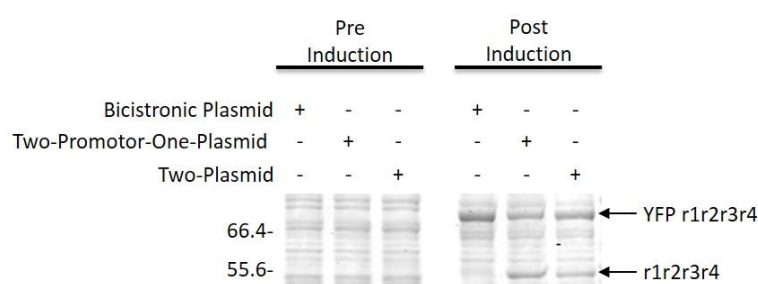


Figure 3.11: SDS-PAGE Analysis of Co-expression Strategies.

Total cell protein samples, both pre and post induction of protein expression with IPTG, were analysed using SDS-protein gel electrophoresis. Proteins were visualized using Coomassie Brilliant Blue staining.

Co-expression of both proteins of interest is only observed for two of the three strategies; the two-promotor-one-plasmid strategy and the two plasmid strategy.

Proteins of interest and the sizes (in kDa) of the relevant molecular weight markers are indicated.

n=1

3.4.2.2 Optimizing Co-expression of Actinin Spectrin-like Repeat Constructs using a Two-Plasmid Co-expression System

For reasons explained in the discussion section of this chapter I decided to progress with the two plasmid co-expression system.

For the benchmarking study on protein co-expression strategies, in the preceding section, the two-plasmid co-expression system (Fig.3.10C) made use of two plasmids that both had the *T7/ac* promoter, meaning that gene expression from both plasmids was regulated with the absence or presence of the same inducer, IPTG. Going forward, I adapted the two-plasmid co-expression system so that each plasmid carried a different promoter, either the *T7/ac* promoter or P_{BAD} promoter, meaning that expression of each target construct was regulated with a different inducer; IPTG and arabinose, respectively. This amendment was made with the intention that the expression of both genes of interest could be activated independently of each other, and that their expression levels could be altered separately.

Recombinant constructs consisting of the entire actinin rod domain (His MBP r1r2r3r4 and His FLAG r1r2r3r4) were used to establish if it was possible to observe co-expression using the, now modified, two-plasmid approach, where each plasmid now carried a different promoter. The His MBP r1r2r3r4 construct was cloned into the pBAD vector, meaning its expression was under the control of the P_{BAD} promoter, and the His FLAG r1r2r3r4 construct was cloned into the pCDF vector, meaning its expression was under control of the *T7/ac* promoter. Fig. 3.12 is a representative gel image which illustrates how the use of various combinations of concentrations of arabinose and IPTG yielded varying expression levels of each protein of interest.

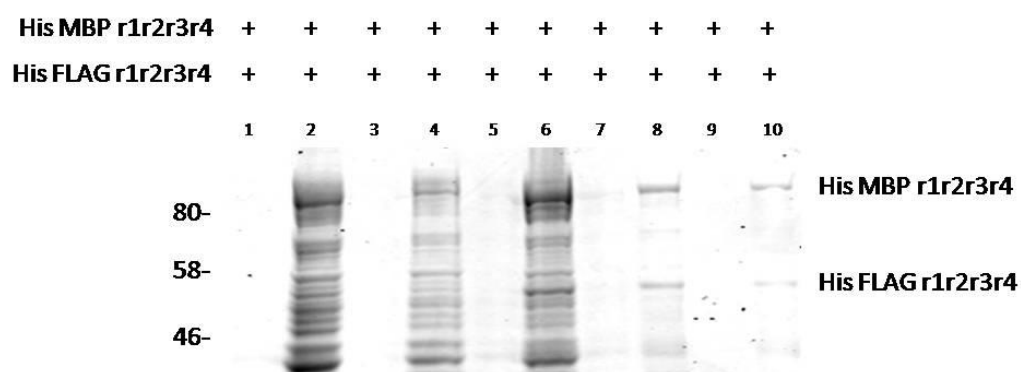


Figure 3.12: Preliminary Two-Plasmid Co-expression Trials Involving Two Different Promoters. Total cell protein samples, both pre and post induction of protein expression, were analysed using SDS protein gel electrophoresis followed with Coomassie Brilliant Blue staining. Odd numbered lanes (lanes 1, 3, 5, 7, 9) refer to pre-induction samples. Even numbered lanes (lanes 2, 4, 6, 8, 10) refer to post-induction samples. Lane 2: 0.5% arabinose and 0.025mM IPTG; Lane 4: 2% arabinose and 0.025mM IPTG; lane 6: 1.25% arabinose and 0.025mM IPTG; lane 8: 0.5% arabinose and 0.2mM IPTG; lane 10: 2% arabinose and 0.2mM IPTG. Different combinations of inducer concentrations yield varying expression levels of each protein. Proteins of interest and the sizes (in kDa) of the relevant molecular weight markers are indicated.

Studies investigating dimerisation and stability of both entire and truncated actinin rod domains, and truncated α -/ β -spectrin proteins, required co-expression of the monomeric proteins in equimolar amounts.

For dimerisation, or self-assembly studies, proteins were paired as per table 3.2 in Materials and Methods section (section 3.3.4.), and through optimisation, an optimal concentration of inducers that yielded near equimolar co-expression of both proteins in each pair was established, also listed in table 3.2. This near equimolar co-expression can be observed in Fig. 3.13 and 3.14.

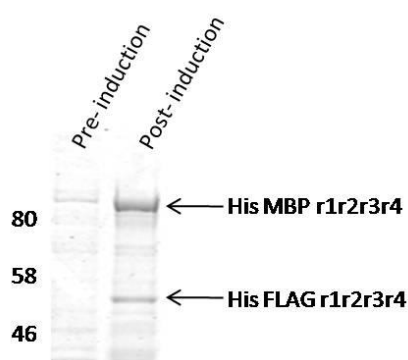


Figure 3.13: Equimolar Co-expression of His MBP r1r2r3r4 and His FLAG r1r2r3r4. Total cell protein samples, both pre and post induction of protein expression with 0.2% arabinose and 0.2mM IPTG, were analysed using SDS protein gel electrophoresis. Proteins were visualized using Coomassie Brilliant Blue staining. Approximately equimolar expression levels of both proteins of interest are observed using this combination of inducer concentrations. Proteins of interest and the sizes (in kDa) of the relevant molecular weight markers are indicated.

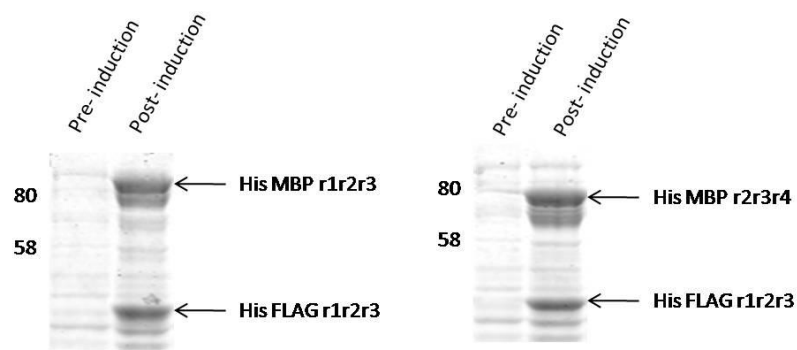


Figure 3.14: Equimolar Co-expression of Pairings of His MBP and His FLAG Tagged Actinin Three-Spectrin-like Repeat Constructs.

Total cell protein samples, both pre and post induction of protein expression with 1.25% arabinose and 0.0625mM IPTG, were analysed using SDS protein gel electrophoresis. Proteins were visualized using Coomassie Brilliant Blue staining.

This combination of inducer concentrations generated near equimolar expression of both proteins in each pairing.

Proteins of interest and the sizes (in kDa) of the relevant molecular weight markers are indicated on each gel.

However, equimolar co-expression of two-spectrin-like repeat actinin constructs was not achieved with any combination of IPTG or arabinose concentrations (Fig. 3.15). In these cases, strong expression of one protein and weak expression of the other protein in each pairing was noted.

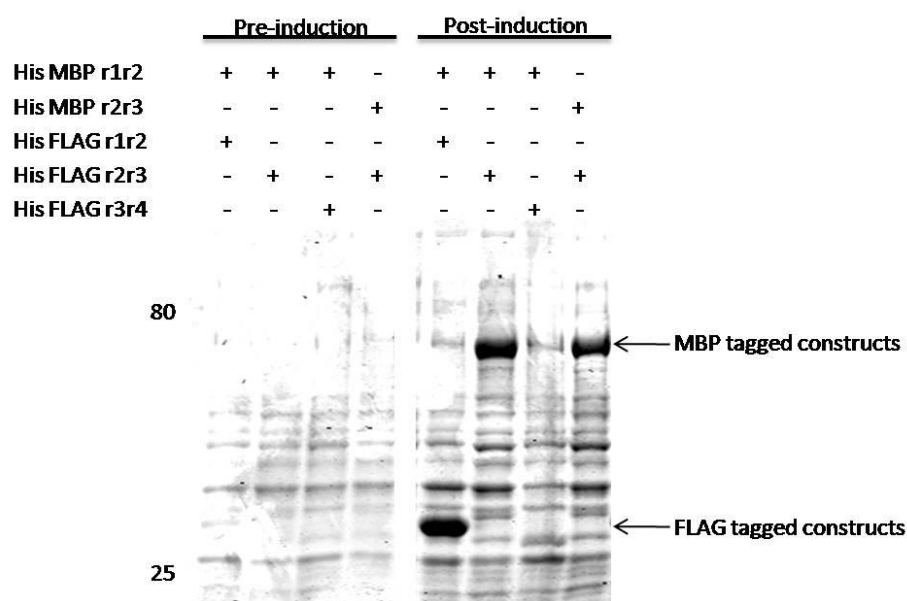


Figure 3.15: Uneven Co-expression of Pairings of His MBP and His FLAG Tagged Actinin Two-Spectrin-like Repeat Constructs.

Total cell protein samples, both pre and post induction of protein expression, were analysed using SDS protein gel electrophoresis. Proteins were visualized using Coomassie Brilliant Blue staining. Varying concentrations of arabinose and IPTG were added to each co-expression culture in an attempt to achieve equal co-expression. Arabinose and IPTG concentration combinations for each co-expression are as follows: His MBP r1r2 and His FLAG r1r2; 1.25% and 0.2mM, His MBP r1r2 and His FLAG r2r3; 1.25% and 0.0625mM, His MBP r1r2 and His FLAG r3r4; 0.5% and 0.2mM, His MBP r2r3 and His FLAG r2r3; 1.25% and 0.0625mM.

No equimolar co-expression was observed for any of the two-spectrin-like repeat pairings. Proteins of interest and the sizes (in kDa) of the relevant molecular weight markers are indicated.

3.4.2.3 Crosstalk Between the T7 Expression System and the P_{BAD} Expression System

I wondered whether difficulties in achieving equimolar co-expression of certain construct pairings could be due to crosstalk between the T7/*lac* promoter and the P_{BAD} promoter, as described by Lee et al. (2007) (Section 3.2.4.3). I decided to investigate if the fine tuning of expression levels would be easier using the IPTG-insensitive truncated AraC (C280* AraC) that Lee et al had described.

I chose two widely used proteins on which to conduct this comparative study; YFP and MBP. YFP was cloned into the pRSF-Duet plasmid meaning that its expression was regulated by the T7/*lac* promoter and hence IPTG. A pBAD plasmid with the C280* *araC* truncation was generated using site-directed mutagenesis. MBP was cloned into the previously used wildtype (WT) *araC* pBAD plasmid (WT) and this new C280* *araC* pBAD plasmid (C280*). In both plasmids, the P_{BAD} promoter and arabinose controlled MBP expression.

I first wanted to verify the observations seen by Lee et al. (2007); that the WT P_{BAD} system was inhibited by the presence of IPTG, and that their mutated P_{BAD} system was no longer affected by IPTG.

Bacterial cultures containing either the MBP WT *araC* pBAD plasmid only (WT) (Fig. 3.16; lanes 1-4) or the MBP C280* *araC* pBAD plasmid only (C280*) (Fig. 3.16; lanes 5-8) were prepared.

In cultures containing the MBP WT *araC* pBAD plasmid only, high expression of MBP is observed when IPTG is not present (lane 1). MBP expression then decreases when increasing IPTG concentrations are present (lanes 2-4).

In cultures containing the MBP C280* *araC* pBAD plasmid only, relatively high and stable expression of MBP is observed across all IPTG conditions (i.e IPTG being present or absent) and concentrations.

Ultimately, expression of MBP from the WT *araC* pBAD plasmid reduces when IPTG is present in the culture. By contrast expression of MBP from C280**araC* pBAD plasmid remains relatively stable across all inducer conditions. This is in agreement with Lee et al.

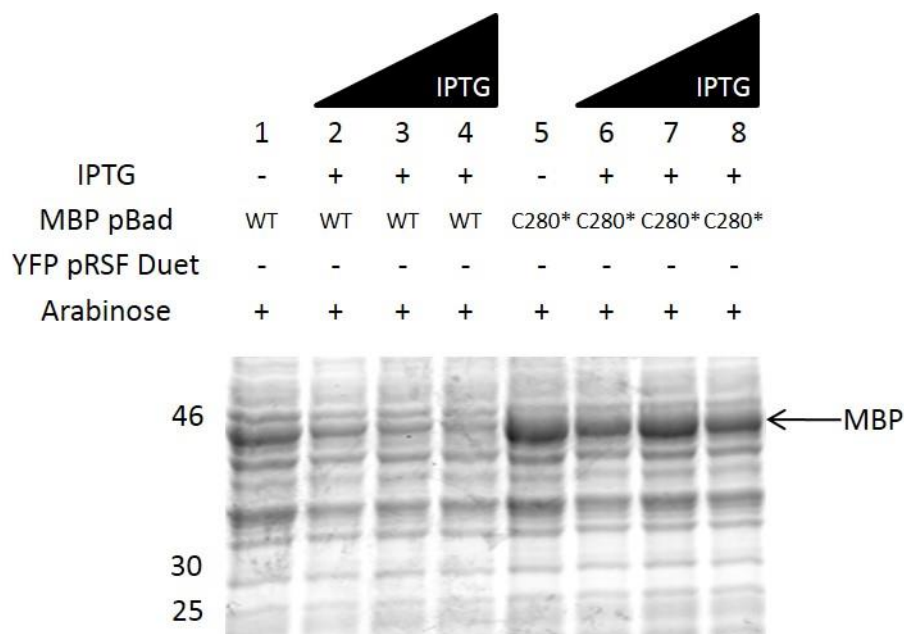


Figure 3.16: Inhibition of Expression from WT P_{BAD} System and Improved Expression from C280* P_{BAD} System in the presence of IPTG Inducer.

E. coli cells were transformed with either the MBP WT *araC* pBAD plasmid (WT) or the MBP C280* *araC* pBAD plasmid (C280*), from which bacterial cultures were prepared. MBP expression was induced with a constant concentration of arabinose in all cultures (0.5%). Increasing IPTG concentrations used (lanes 2-4 and 6-8) ranged from 0.2-1mM (0.2mM, 0.5mM, and 1mM). Total cell protein samples, post induction, were analysed using SDS protein gel electrophoresis. Proteins were visualised using Coomassie Brilliant Blue staining.

Expression of MBP from the WT *araC* pBAD plasmid reduces when IPTG is present in the culture (lanes 1-4). By contrast expression of MBP from C280* *araC* pBAD plasmid remains relatively stable across all inducer conditions (lanes 5-8).

Proteins of interest and the sizes (in kDa) of the relevant molecular weight markers are indicated.
n=5

Next I wanted to extend the work of Lee et al and examine expression from the C280* P_{BAD} system in a co-expression situation; where MBP is expressed from the C280* P_{BAD} system, in the presence of arabinose, and YFP is expressed from the T7/*lac* system, in the presence of IPTG. To do this I compared the effect that IPTG was having on the expression of MBP from both the WT and C280* P_{BAD} systems in cultures that are also expressing YFP, under the control of the T7/*lac* promoter.

Bacterial cultures containing the YFP pRSF plasmid with either MBP WT *araC* pBAD plasmid (WT) (Fig. 3.17; lanes 1, 3-5, and 9) or the MBP C280* *araC* pBAD plasmid (C280*) (Fig. 3.17; lanes 2, 6-8 and 10) were prepared.

In cultures wherein YFP was co-expressed with MBP from the WT *araC* pBAD plasmid, expression of MBP is observed when IPTG is not present (lane 1).

Expression of MBP reduces when IPTG is present (lanes 3-5). YFP is expressed

across all IPTG concentrations and arabinose conditions i.e. arabinose being absent or present (lanes 3-5 and 9)

In cultures wherein YFP was co-expressed with MBP from the C280* *araC* pBAD plasmid, expression of MBP is observed in all samples across all IPTG concentrations and conditions (lanes 2 and 6-8). YFP is highly expressed when no arabinose is present (lane 10), but these expression levels are reduced dramatically when arabinose is present, and are not regained as IPTG concentration increases (lanes 6-8).

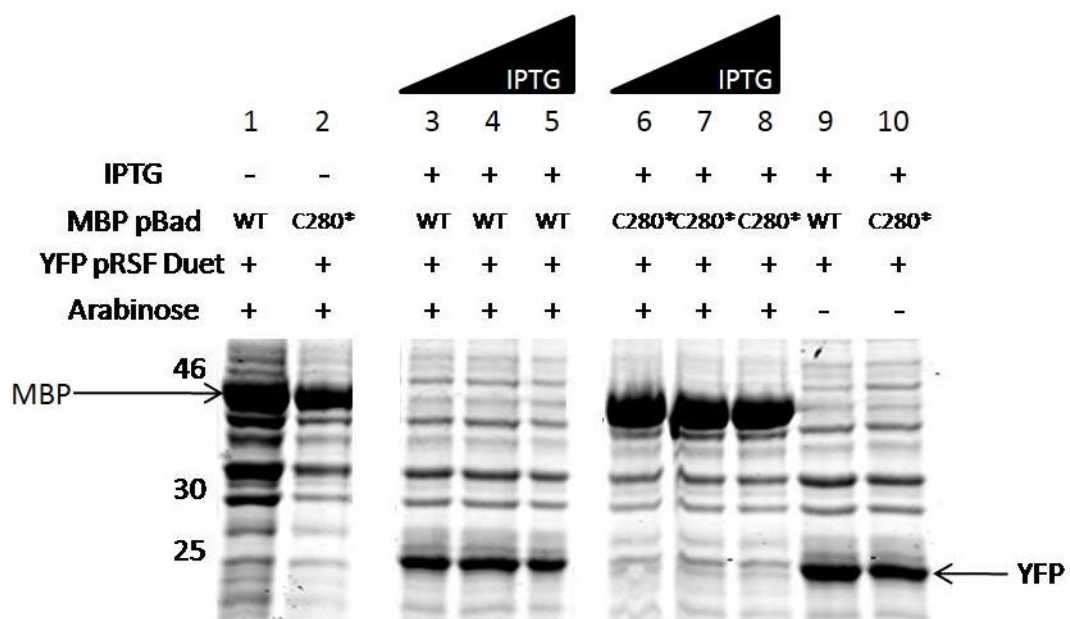


Figure 3.17: Effect of Increasing IPTG Concentrations on both WT *araC* and C280* *araC* P_{BAD} Systems in the presence of T7lac regulated expression plasmid.

E. coli cells were co-transformed with the YFP pRSF plasmid and either MBP WT *araC* pBAD plasmid (WT) or the MBP C280* *araC* pBAD plasmid (C280*), from which bacterial cultures were prepared. MBP expression was induced with a constant concentration of arabinose (0.5%), to those cultures indicated. Increasing IPTG concentrations used (lanes 3-5 and 6-8) ranged from 0.2-1mM (0.2mM, 0.5mM, and 1mM). Expression of YFP only was carried out at 0.2mM IPTG (lanes 9 and 10). Total cell protein samples, post induction, were analysed using SDS protein gel electrophoresis. Proteins were visualised using Coomassie Brilliant Blue staining.

When co-expressed with YFP, expression of MBP from the WT *araC* pBAD plasmid reduces when IPTG is present in the culture (lanes 1 and 3-5). YFP is expressed in all samples where IPTG is present. By contrast, expression of MBP from C280**araC* pBAD plasmid remains relatively stable across all inducer conditions (lanes 2 and 6-8). YFP is not expressed in those cultures where IPTG is present. Proteins of interest and the sizes (in kDa) of the relevant molecular weight markers are indicated. n=2

Experiments thus far used a fixed and relatively high concentration of arabinose. I next wanted to observe the effect that varying arabinose concentrations would have on both the WT and C280* P_{BAD} systems, and the T7lac system (Fig. 3.18).

Bacterial cultures containing the YFP pRSF plasmid with either MBP WT *araC* pBAD plasmid (WT) (Fig. 3.18; lanes 1, 3-6, and 11) or the MBP C280* *araC* pBAD plasmid (C280*) (Fig. 3.18; lanes 2, 7-10 and 12) were prepared.

In cultures wherein YFP was co-expressed with MBP from WT *araC* pBAD plasmid, expression of MBP is observed when IPTG is not present (lane 11). Expression of MBP reduces when IPTG is present, and are not regained as arabinose concentrations increase (lanes 3-6). YFP is expressed across all arabinose concentrations and conditions.

In cultures wherein YFP was co-expressed with MBP from C280* *araC* pBAD, expression of MBP is observed in all samples, regardless of the presence or absence of IPTG. As arabinose concentration increases, so too does MBP expression (lanes 7-10 and 12). YFP is highly expressed when no arabinose is present (lane 2), but these expression levels are reduced dramatically when arabinose is present. As arabinose concentration increases, YFP expression decreases (lanes 7-10).

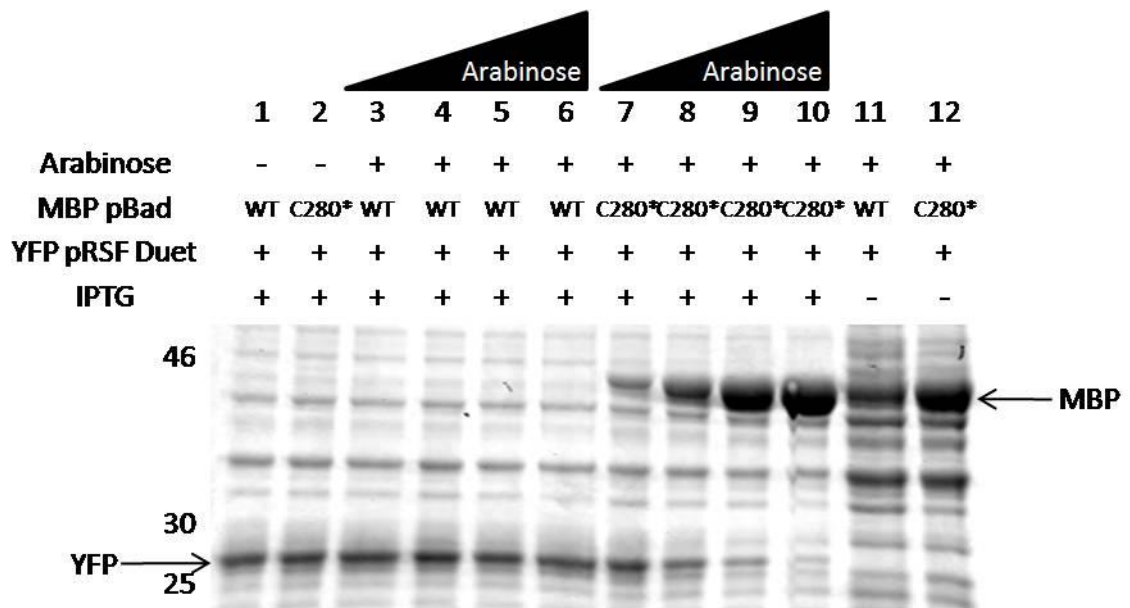


Figure 3.18: Effect of Increasing Arabinose Concentrations on both the WT *araC* and C280* *araC* P_{BAD} Systems in the presence of T7lac regulated expression plasmid.

E. coli cells were co-transformed with the YFP pRSF plasmid and either MBP wt *araC* pBAD plasmid (WT) or the MBP C280* *araC* pBAD plasmid (C280*), from which bacterial cultures were prepared. YFP expression was induced with a constant concentration of IPTG (0.2mM) to those cultures indicated. Increasing concentrations of arabinose (lanes 3-6 and 7-10) ranged from 0.01-0.5% (0.01, 0.05, 0.2 and 0.5%). Expression of MBP only was carried out at 0.5% arabinose (lanes 11 and 12). Total cell protein samples, post induction, were analysed using SDS protein gel electrophoresis. Proteins were visualised using Coomassie Brilliant Blue staining. When co-expressed with YFP, high concentrations of arabinose fail to circumvent the reduction in expression of MBP from the WT *araC* pBAD plasmid when IPTG is present in the culture. YFP is expressed in those cultures where IPTG is present (lanes 3-6). By contrast, expression of MBP from C280**araC* pBAD plasmid increases as arabinose concentration increases, despite the presence of IPTG in the culture (lanes 7-10). YFP expression decreases as arabinose concentration increases. Proteins of interest and the sizes (in kDa) of the relevant molecular weight markers are indicated. n=3

Fig. 3.18 suggests that the C280* P_{BAD} system was negatively affecting the T7lac system (Fig. 3.18, lanes 7-10). Subsequently, in Fig. 3.19, I wanted to answer the question; was the arabinose molecule itself interfering with the T7lac system?

Bacterial cultures containing either the YFP pRSF plasmid only (Fig. 3.19; lanes 1-5) or both the YFP pRSF and the MBP C280* *araC* pBAD plasmids (Fig. 19; lanes 6-10) were prepared.

In cultures containing the YFP pRSF plasmid only, the YFP protein is stably expressed in the presence of increasing arabinose concentrations.

In cultures wherein YFP is co-expressed with MBP from the C280* *araC* pBAD plasmid, high expression of YFP is observed when no arabinose is present (lane 6), or at very low arabinose concentrations (lane 7). However, as the

arabinose concentration increases, YFP expression levels decrease (lanes 7-10). Also, as seen before, under these conditions (Fig 3.18), as the arabinose concentration increases, so too does MBP expression.

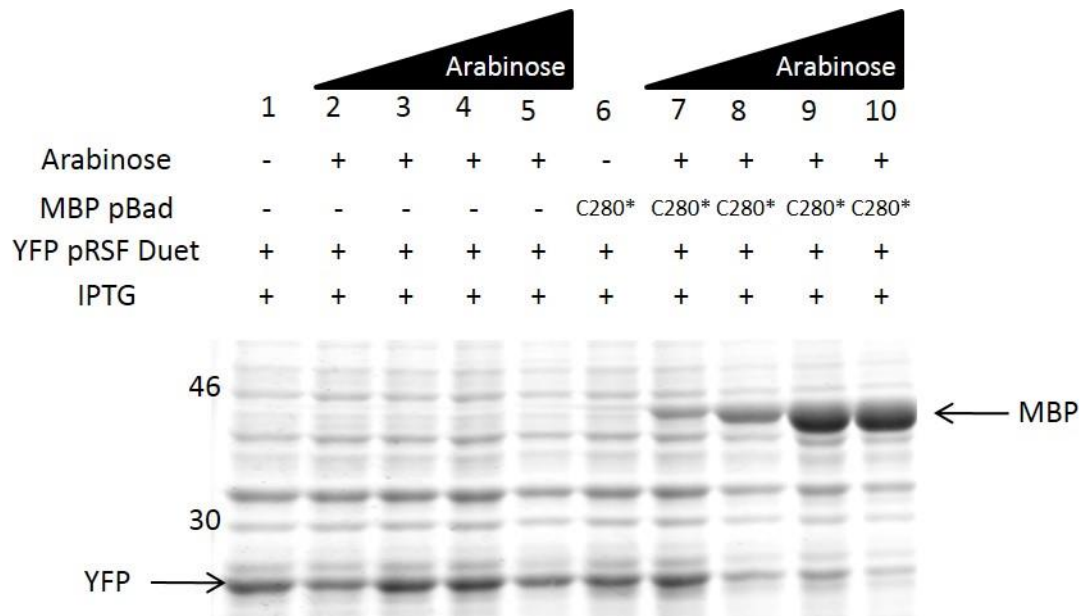


Figure 3.19: Arabinose does not Directly Interfere with the T7/lac Promoter:

E. coli cells were transformed with the YFP pRSF plasmid only and co-transformed with both the YFP pRSF and the MBP C280* *araC* pBAD plasmids, from which bacterial cultures were prepared. YFP expression was induced with a constant concentration of IPTG (0.2mM) to all cultures. Increasing concentrations of arabinose (lanes 2-5 and 7-10) ranged from 0.01-0.5% (0.01, 0.05, 0.2 and 0.5%). Total cell protein samples, post induction, were analysed using SDS protein gel electrophoresis. Proteins were visualised using Coomassie Brilliant Blue staining.

In cultures containing YFP pRSF plasmid only (lanes 1-5), the addition of increasing arabinose concentrations is not affecting expression levels of YFP. In cultures where YFP is co-expressed with MBP (lanes 6-10), the increasing expression of MBP is affecting the expression levels of YFP. Proteins of interest and the sizes (in kDa) of the relevant molecular weight markers are indicated. n=2

Since the presence of the arabinose inducer does not appear to be affecting expression from the T7/lac system, but rather expression from the C280* P_{BAD} system, it would appear that, in this situation, promoter crosstalk is not occurring. Perhaps, the C280* P_{BAD} system is much stronger than the T7/lac system, dominating the protein synthesis machinery of the bacterial cell.

3.4.3 Heterodimer Purification

3.4.3.1 Actinin Dimer and α -/ β -Spectrin Heterodimer Purification

Using this two-plasmid co-expression system, two actinin rod domain proteins (repeat 1 to repeat 4; r1r2r3r4) were co-expressed, one was fused to a His tag only and was expressed from the T7/*lac* promoter system. The other had a MBP tag only and was expressed from the C280* *araC* P_{BAD} promoter system (Fig. 3.20A). As each actinin rod domain protein had a different tag, the actinin pseudo-heterodimers (pseudo-heterodimers in the sense that each monomer contributing to the dimer had a different tag; His or MBP) could be purified using sequential affinity chromatography; nickel column chromatography followed by amylose column chromatography (Fig. 3.20B).

An identical expression and purification strategy was used to generate truncated α / β -spectrin heterodimers; a truncated α -spectrin protein (repeat 18-repeat 21; r18r19r20r21) was fused to a His tag and a truncated β -Spectrin protein (repeat 1-repeat 4; r1r2r3r4) was fused to a MBP tag.

Fig. 3.20 relates to actinin proteins only.

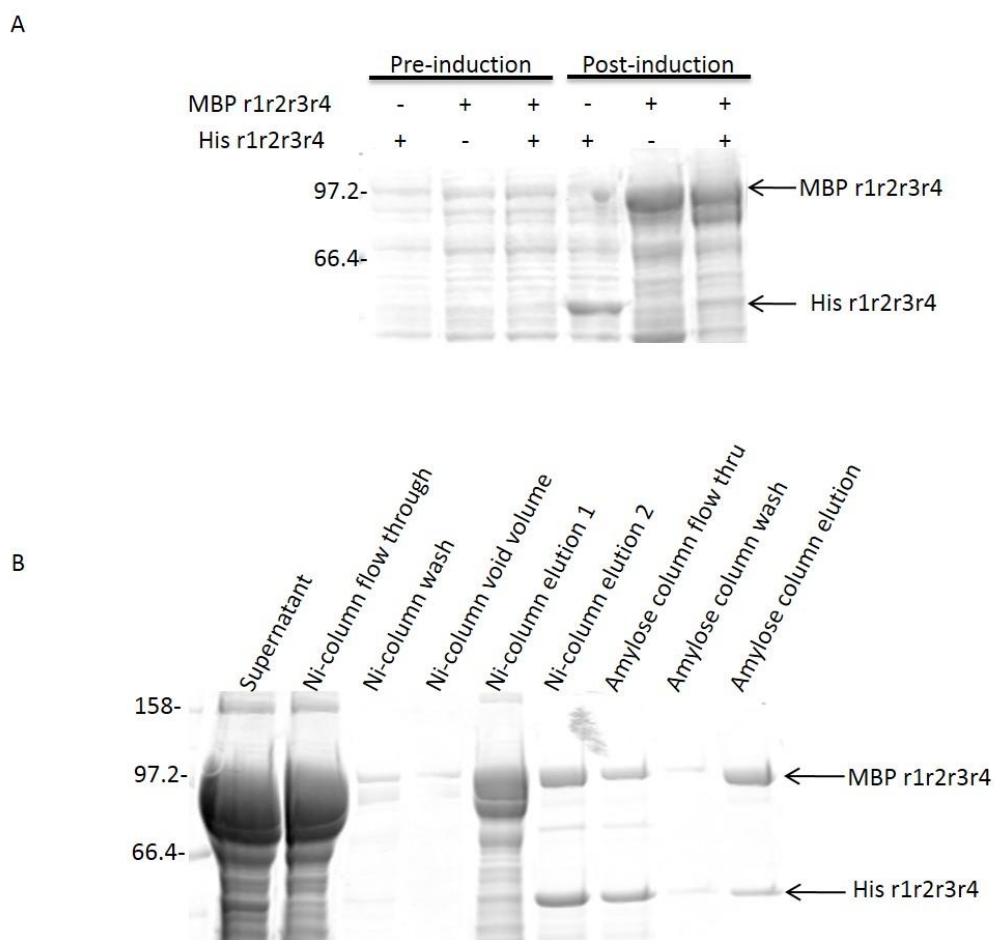


Figure 3.20: Expression and Purification of Actinin Pseudo-Heterodimers for Stability Assays.

His r1r2r3r4 and MBP r1r2r3r4 were both singly expressed and co-expressed in *E. coli* cells. All protein expression and purification steps were analysed using SDS protein gel electrophoresis. Proteins were visualised using Coomassie Brilliant Blue staining.

(A) Total cell protein samples, both pre and post induction of protein expression with IPTG or/and arabinose.

(B) Fractions taken at each step of sequential purification strategy to purify MBP r1r2r3r4: His r1r2r3r4 pseudo-heterodimers; nickel column chromatography followed by amylose column chromatography. Proteins of interest and the sizes (in kDa) of the relevant molecular weight markers are indicated on each gel.

3.4.3.2 Improvement of Dimer/Protein Complex Purification Strategy

To streamline this heterodimer purification technique and turn the purification process into a one day rather than two-day procedure, the necessity of dialysing out the imidazole from the nickel column protein elution before loading the protein onto the amylose column was investigated.

The potential disruption that the presence of imidazole could have on the binding of MBP to amylose was examined. I found MBP to still be able to bind amylose in the presence of imidazole. Densitometric analysis revealed that quantities of MBP r1r2r3r4 pull-downed from amylose in the presence of imidazole

were comparable to quantities pulled-down in the absence of imidazole (Fig. 3.21). This indicated the presence of imidazole does not interfere with the binding of MBP to the amylose column and therefore, the overnight dialysis is not a necessary step.

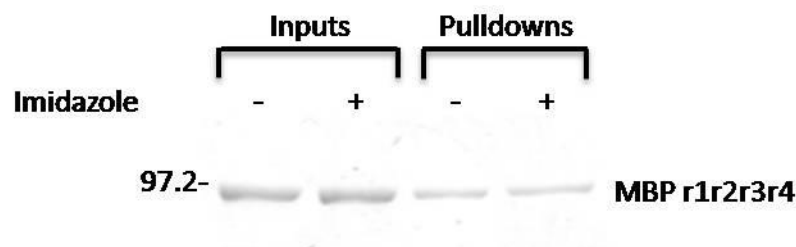


Figure 3.21: Potential Disruption of Amylose Column Binding Ability.

Purified MBP r1r2r3r4 protein was mixed in one of two solutions; one that did not contain any imidazole and one that contained 200mM imidazole. These two samples were incubated for a short period with amylose resin and after several wash steps MBP r1r2r3r4 was pulled-down with 10mM maltose. Resulting input and pull-down fractions were analysed using SDS protein gel electrophoresis followed by Coomassie Brilliant Blue staining.

MBP r1r2r3r4 was successfully pulled-down under both conditions. Comparable quantities of MBP r1r2r3r4 were pulled-down in each case, confirmed with densitometric analysis.

Proteins of interest and the sizes (in kDa) of the relevant molecular weight markers are indicated. n=1

3.4.4 Actinin Spectrin-like Repeat Dimerisation Studies

One of several attractive features of the actinin rod domain (r1r2r3r4) that prompted it to be considered as a possible building block in this study, was the fact that it could form anti-parallel dimers with itself (Ylänne et al. 2001) making it agreeable to bottom up assembly.

In looking for additional accessory building materials, I considered dividing this entire rod domain into segments consisting of just three- or two-spectrin-like repeats; essentially, the entire rod domain (r1r2r3r4) was divided into two three-spectrin-like repeat proteins: r1r2r3 and r2r3r4, and into three two-repeat proteins: r1r2, r2r3 and r3r4.

To consider these four-, three- and two-spectrin-like repeat proteins as potential building blocks it was necessary to investigate if they were capable of interacting with each other, i.e. engaging in self-assembly through dimerisation. Fig. 3.22 illustrates the possible outcomes that could occur with three- and two-spectrin-like repeat proteins.

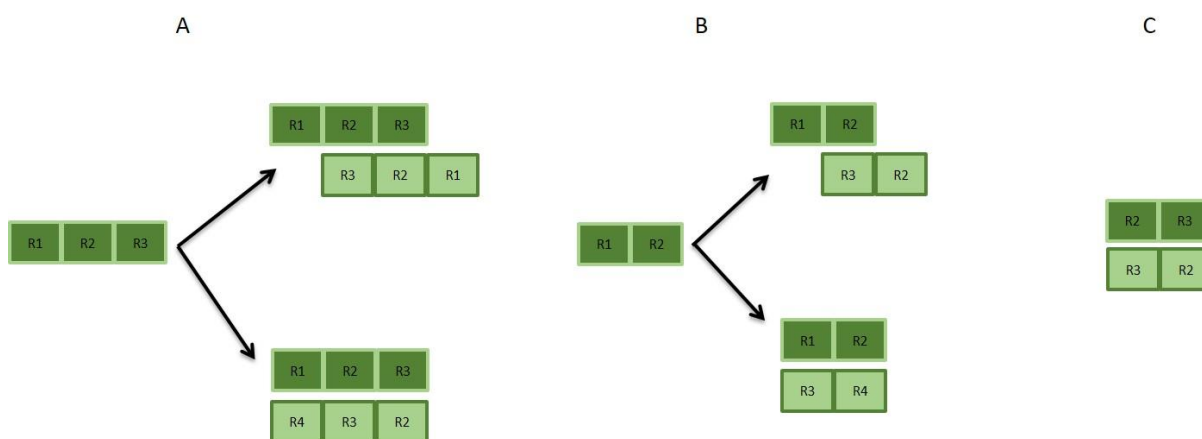


Figure 3.22: Possible Outcomes Resulting from Three- and Two- Spectrin-like Repeat Dimerisation Assay.

(A) r1r2r3 monomers might dimerise with themselves in a form of staggered arrangement where only repeats 2 (r2) and 3 (r3) from both monomers are mediating the dimerisation. Alternatively, r1r2r3 monomers might dimerise with r2r3r4 monomers in an aligned arrangement where all repeats are mediating the dimerisation.

(B) r1r2 monomers might dimerise with r2r3 monomers in a staggered arrangement, where only repeat 2 (r2) from one monomer and repeat 3 (r3) from the other monomer are mediating the dimerisation. Alternatively, r1r2 monomers might dimerise with r3r4 monomers in an aligned arrangement where all of the repeats are mediating the dimerisation.

(C) An aligned dimer could form between two r2r3 monomers, where all repeats are mediating dimerisation.

In this section, through a series of MBP pull-down spectrin-like repeat interaction assays and native gel electrophoresis, I explore the dimerisation, or self-assembly, properties of the actinin spectrin-like repeats, assessing their suitability as potential building blocks.

The two-plasmid co-expression strategy, using the WT P_{BAD} system and the T7/lac system is utilised to produce four-, three-, and two-spectrin-like repeat dimers (all mentioned in table 3.2 in Materials and Methods section 3.3.4.) to be utilised in these studies.

3.4.4.1 Actinin spectrin-like repeat Interaction Assays

An MBP pulldown approach was utilised to carry out the actinin spectrin-like repeat interaction assays. The two plasmid co-expression strategy for these actinin spectrin-like repeat proteins was as follows; those proteins to be expressed from the T7/lac system were designed to have a FLAG tag so that western blot analysis could be used to certify their identity, and verify that protein bands observed were not impurities, or the degradation products of MBP tagged proteins, or the result of

His FLAG tagged proteins binding non-specifically to the amylose resin, i.e. to ensure that the presence of a His MBP tagged actinin spectrin-like repeat protein is required for His FLAG tagged actinin spectrin-like repeat protein binding.

This MBP pulldown approach first needed to be validated by re-confirming that the entire actinin rod domain (r1r2r3r4) could dimerise with another copy of itself. Interaction was confirmed with the detection of His FLAG r1r2r3r4 in pull-down assay sample (Fig. 3.23). Co-expression samples for this assay were obtained using the WT P_{BAD} expression system with the T7/*lac* expression system. With this plasmid combination I was unable to achieve an ideal equimolar expression of His FLAG r1r2r3r4 with His MBP r1r2r3r4. With the levels of co-expression that were obtained however, I was still able to detect pseudo-heterodimerisation.

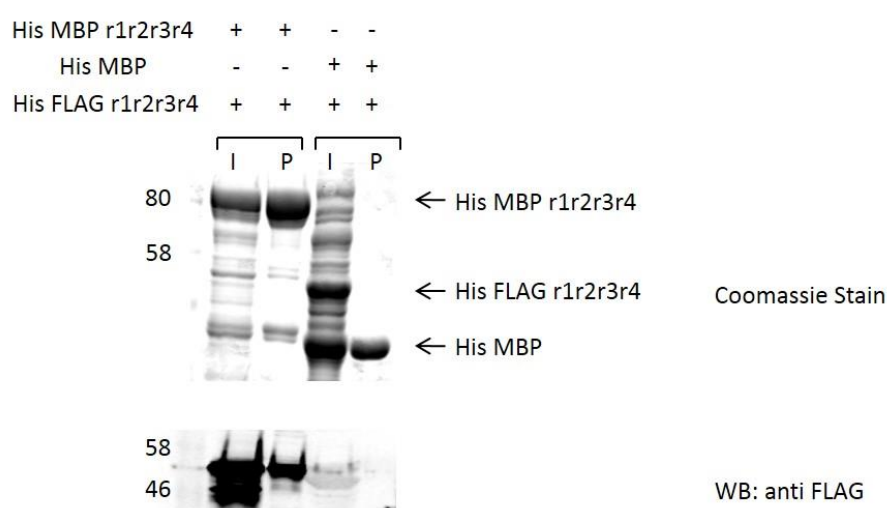


Figure 3.23: Full Length Rod Domain of Actinin Dimerisation Assay.

His MBP r1r2r3r4 and His FLAG r1r2r3r4 were co-expressed in *E. coli* cells. Cells were lysed and resulting lysate was subject to an MBP pull-down assay. A control assay involving a His MBP tag and His FLAG r1r2r3r4 co-expression lysate was carried out in parallel. Resulting input and pull-down fractions were analysed using SDS protein gel electrophoresis followed by Coomassie Brilliant Blue staining, in conjunction with western blotting using anti-FLAG.

Pull-down assays demonstrated interaction between His FLAG r1r2r3r4 and His MBP r1r2r3r4, and no interaction between His FLAG r1r2r3r4 and His MBP tag.

I=input samples; P=pull-down samples.

Proteins of interest and the sizes (in kDa) of the relevant molecular weight markers are indicated.

n=1

Once the MBP pull-down approach was validated, next was to investigate if a dimer would form from two actinin monomers each consisting of only three-

spectrin-like repeats. Binding of spectrin-like repeats 1-3 (r1r2r3) to copies of itself and to spectrin-like repeats 2-4 (r2r3r4) were examined. Interaction was confirmed in these pairings of three-spectrin-like repeats indicated by the detection of His FLAG r1r2r3 pull-downed along with His MBP r1r2r3 or His MBP r2r3r4. (Fig.3.24). Results indicate that interaction between r1r2r3 and r2r3r4 may be stronger than interaction between r1r2r3 and r1r2r3.

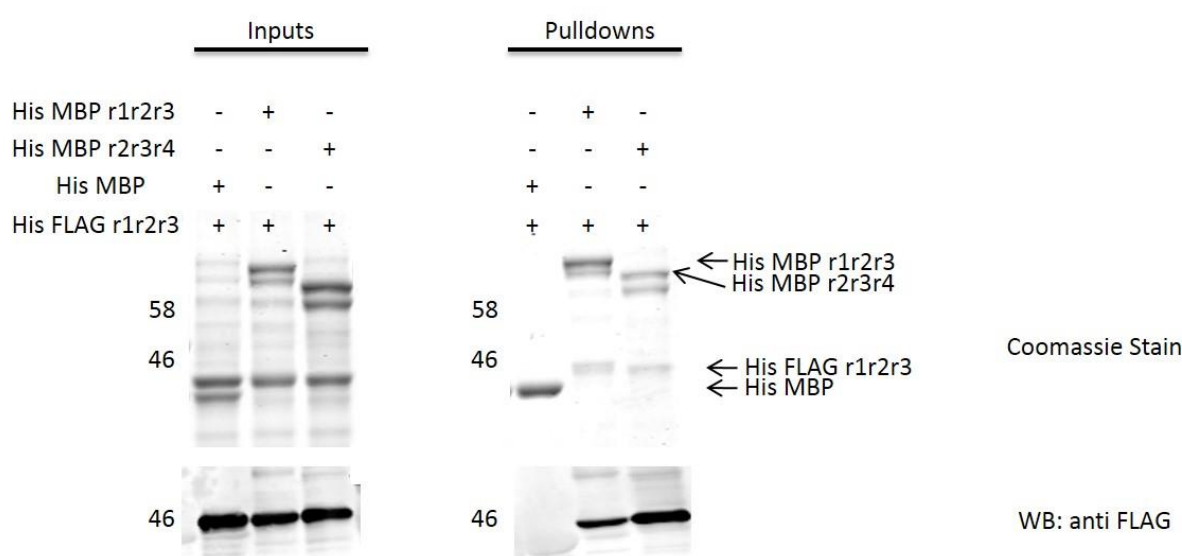


Figure 3.24: Actinin Three-Spectrin-like Repeat Dimerisation Assay.

His MBP r1r2r3 with His FLAG r1r2r3 and His MBP r2r3r4 with His FLAG r1r2r3 were co-expressed in *E. coli* cells. Cells were lysed and resulting lysate was subject to an MBP pull-down assay. A control assay involving an expression lysate mix consisting of His MBP only expression lysate and His FLAG r1r2r3 only expression lysate was carried out in parallel. Resulting input and pull-down fractions were analysed using SDS protein gel electrophoresis followed by Coomassie Brilliant Blue staining, in conjunction with western blotting using anti-FLAG.

Pull-down assays demonstrated incomparable interactions between His FLAG r1r2r3 with His MBP r1r2r3 and His FLAG r1r2r3 with His MBP r2r3r4. No interaction was detected between His FLAG r1r2r3 and His MBP tag.

Proteins of interest and the sizes (in kDa) of the relevant molecular weight markers are indicated. n=2

In investigating the dimerisation potential between the actinin two-spectrin-like repeat proteins, a lysate mix of single expressions rather than a co-expression lysate was used. This choice was made due to the difficulty experienced in co-expressing these two-spectrin-like repeat proteins. At that time in which these experiments were carried out I was using the WT P_{BAD} expression system with the T7/lac expression system, and not the more sensitive C280* P_{BAD} expression system.

Binding of spectrin-like repeats 1-2 (r1r2) to copies of itself, to spectrin-like repeats 2-3 (r2r3) and to spectrin-like repeats 3-4 (r3r4) were examined. The binding of r2r3 to copies of itself was also examined. No interaction in any of these pairings was detected (Fig. 3.25A).

I decided to carry out the r2r3 two repeat spectrin-like interaction pull-down assay again, this time using a co-expression lysate of His FLAG r2r3 with His MBP r2r3 (Fig. 3.25B; Inputs: lanes 1 and 2, Pulldowns: lanes 5 and 6) in tandem to a pull-down assay with His FLAG r2r3 expression lysate mixed with His MBP r2r3 expression lysate (Fig. 3.25B; Inputs: lanes 3 and 4, Pulldowns: lanes 7 and 8). Interaction with this pairing was confirmed indicated by the detection of His FLAG r2r3 pulled-down along with His MBP r2r3. However, His FLAG r2r3 was only detected in the pull-down fraction from the sample for which a co-expression of the proteins had been used. His FLAG r2r3 was not detected in pull-down sample pertaining to assay where lysate mix, rather than lysate co-expression, had been used. This observation suggested that r2r3 homodimers (e.g. His r2r3:His r2r3) were forming in single expression lysates and preventing further interactions with His MBP r2r3.

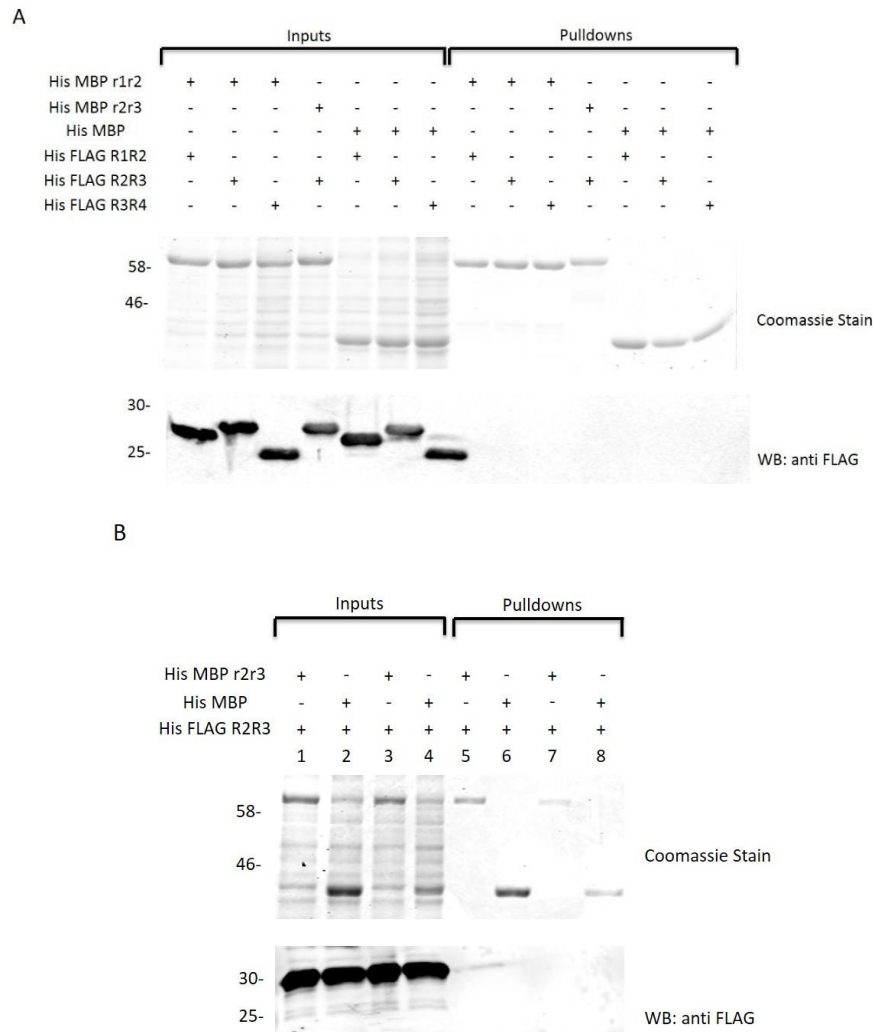


Figure 3.25: Actinin two-spectrin-like repeat Dimerisation Assay.

(A) His MBP r1r2, His MBP r2r3, His FLAG r1r2, His FLAG r2r3 and His FLAG r3r4 were each singly transformed and expressed in *E. coli* cells. Cells were lysed and resulting lysates were mixed to produce the following combinations; His MBP r1r2 and His FLAG r1r2, His MBP r1r2 and His FLAG r2r3, His MBP r1r2 and His FLAG r3r4, His MBP r2r3 and His FLAG r2r3. Control assays consisted of lysate mixes of His MBP with His FLAG r1r2 and His MBP with His FLAG r2r3 and His MBP with His FLAG r3r4. These lysate mixes were subjected to an MBP pull-down assay. Resulting input and pull-down fractions were analysed using SDS protein gel electrophoresis followed by Coomassie Brilliant Blue staining, in conjunction with western blotting using anti-FLAG.

No possible interactions were detected in any of the two-repeat pairings.

n=1

(B) His MBP r2r3 and His FLAG r2r3 were co-expressed in *E. coli* cells. Cells were lysed and resulting lysate was subject to an MBP pull-down assay (input sample: lane 1; pulldown sample: lane 5). A tandem pull-down assay involving a lysate mix of singly expressed His MBP r2r3 and His FLAG r2r3 (Input sample: lane 3; Pulldown sample: lane 7). Control assays, also with a co-expression lysate (Input sample: lane 2; Pulldown sample: lane 6) and single expression lysate mix (Input sample: lane 4; Pulldown sample: lane 8), in which His MBP r2r3 is substituted with His MBP was carried out in parallel. Resulting input and pull-down fractions were analysed using SDS protein gel electrophoresis followed by Coomassie Brilliant Blue staining, in conjunction with western blotting using anti-FLAG. Pull-down assays demonstrated interaction between His FLAG r2r3 and His MBP r2r3, but only where a co-expression lysate had been used as the input sample. No interaction detected between His FLAG r2r3 and the His MBP tag

n=3

Proteins of interest and the sizes (in kDa) of the relevant molecular weight markers are indicated.

3.4.4.2 Assessment of Actinin spectrin-like repeat Dimers Using Native-PAGE

At the outset of this project, I decided that native gel electrophoresis (non-denaturing conditions) would be the technique of choice when screening and characterizing potential building blocks and nanostructures.

In native PAGE, proteins are separated according to not only their size and shape, but also their net charge (Fanarraga et al. 2010). The recombinant actinin and spectrin proteins pertaining to this project had pI values of between 4.9 and 5.9. Gel running buffer was designed to have a pH of approximately 8-9, so that all proteins should have a net negative charge as they ran through the gel. The actinin and spectrin constructs consisting of four spectrin repeats have all very similar molecular weights of approximately 50kDa. However small differences in their overall negative charge may cause them to migrate at somewhat different rates on a native gel. Nevertheless, we expected that differences in migration pattern would be observed for protein complexes assembled from these building blocks, making it possible to screen for possible interactions.

In order to gain familiarity with this migration pattern of each of the actinin rod domain proteins, and to screen for potential interactions, they were expressed, purified, and subjected to native gel electrophoresis.

Earlier in this project, I had demonstrated that dimerisation could occur between two actinin rod domain (r1r2r3r4) proteins (Fig. 3.23). Native gel electrophoresis re-confirmed this interaction. Both homodimers and pseudo-heterodimers were generated in co-purified His MBP r1r2r3r4 with His r1r2r3r4 protein samples (Fig. 3.26; lane 2), from co-expressions, and homodimers were generated in each of the single purification samples; His MBP r1r2r3r4 and His r1r2r3r4 (Fig. 3.26; lanes 1 and 3), from single expressions.

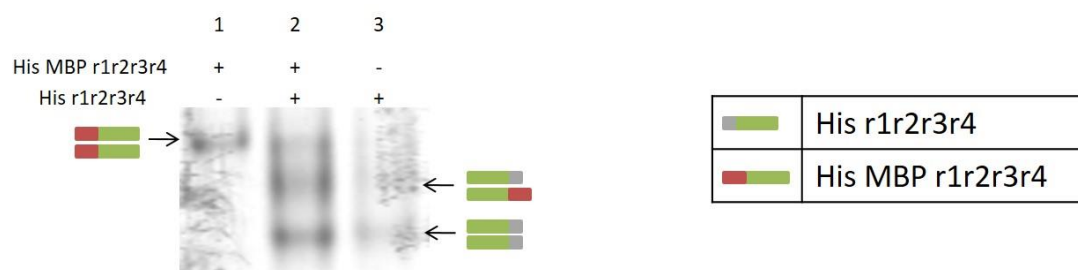


Figure 3.26: Observing Native Gel Migration Pattern of Actinin Dimeric Proteins.

Nickel column purification products from both single protein expressions (lanes 1 and 3) and co-expressions (lane 2) were analysed using Native protein gel electrophoresis followed by Coomassie Brilliant Blue staining.

Three possible dimer formations are observed; His MBP r1r2r3r4 homodimers (lanes 1 and 2), His r1r2r3r4 homodimers (lanes 2 and 3), and His MBP r1r2r3r4:His r1r2r3r4 pseudo-heterodimers (intermediate band in lane 2).

Migration pattern of each dimer is indicated with figure visuals.

n=3

3.4.5 Dimeric Actinin spectrin-like repeat Stability Assay Studies

Both actinins and spectrins have been extensively studied in terms of their structure and regulation. It is widely known, however, that buffers can have serious effects on both the tertiary and quaternary structure of proteins, causing denaturation, unfolding or aggregation (Ugwu & Apte 2004).

Neutral salts, such as NaCl are known to affect protein assembly (Sawyer & Puckridge 1973). Non-covalent interactions such as electrostatic attractions mediate dimerisation between two actinin monomers and between α - and β -spectrins (Begg et al. 2000; Djinoić-Carugo et al. 1999). I hypothesised that the addition of a high concentration of NaCl to the actinin rod domain dimers and to the truncated α -/ β - spectrin spectrin repeat heterodimers would cause them to dissociate, since salt can screen electrostatic interactions (Dumetz et al. 2007).

Heat, or temperature, is known to influence protein stability and structure by breaking up hydrogen bonds (Nelson & Cox, 2005b). The α -helical protein structure is stabilised through maximum use of hydrogen bonds (Nelson & Cox, 2005b). Since each spectrin repeat is made up of a triple helical coiled-coil conformation (Yan et al. 1993; Djinoić-Carugo et al. 1999), I put forward the idea that high temperatures would disrupt the actinin rod domain and the truncated α -/ β -spectrin central spectrin region.

From a synthetic biology point of view, with particular regard to preparing the buffers in which assembly of my putative nanostructures would occur, I thought it important to investigate the resistance, or stability, of both actinin spectrin-like repeat dimers and α -/ β -spectrin spectrin-repeat heterodimers to challenges, such as increasing salt concentrations and temperature conditions, through a series of stability assays. Such knowledge might be useful for preparing a buffer that would aid in the preparation of monomeric actinin or spectrin proteins, for example.

In this section, the co-expression strategy, using the C280* P_{BAD} system and the T7/*lac* system, and sequential purification strategy are used to yield actinin rod domain spectrin-like repeat dimers to be utilised in salt and thermostability studies.

To assess the effect of salt (NaCl) and heat on actinin spectrin-like repeat dimer stability, a His-tag pulldown approach was utilised. The two plasmid co-expression strategy for the generation of these actinin spectrin-like repeat proteins was as follows: those proteins to be expressed from the C280* P_{BAD} system were designed to have a MBP tag so that western blot analysis could be used to certify their identity, and verify that protein bands observed were not impurities, or the degradation products of His tagged proteins, or the result of MBP tagged proteins binding non-specifically to the resin, i.e. to ensure presence of His tagged r1r2r3r4 is required for MBP r1r2r3r4 binding.

3.4.5.1 Investigating the Effect of Salt Concentration on the Structural Stability of Actinin Dimers

Previous studies had reported that salt induced conformational changes in the actinin protein under different salt conditions. Winkler et al. (1997) found that the ionic strength affected the molecular length of the actinin protein. In solutions of low salt concentration, 0.05mM KCl, actinin was measured to be 29.3nm in length, while in solutions of higher salt concentration, 0.15mM KCl, actinin was measured to be longer, 32.6nm. Here, I assess the contribution of increasing NaCl concentrations on the stability of the actinin spectrin-like repeat dimer.

Purified actinin rod domain pseudoheterodimers (Hisr1r2r3r4:MBPr1r2r3r4) were incubated for 1 hour at 4° in increasing concentrations of NaCl, ranging from

150mM – 2M (Fig. 3.27A) and from 500mM-5M (Fig. 3.27B) with nickel resin. Interaction between this pairing was confirmed under all salt conditions, indicated by the detection of MBP r1r2r3r4 pulled-down along with His r1r2r3r4.

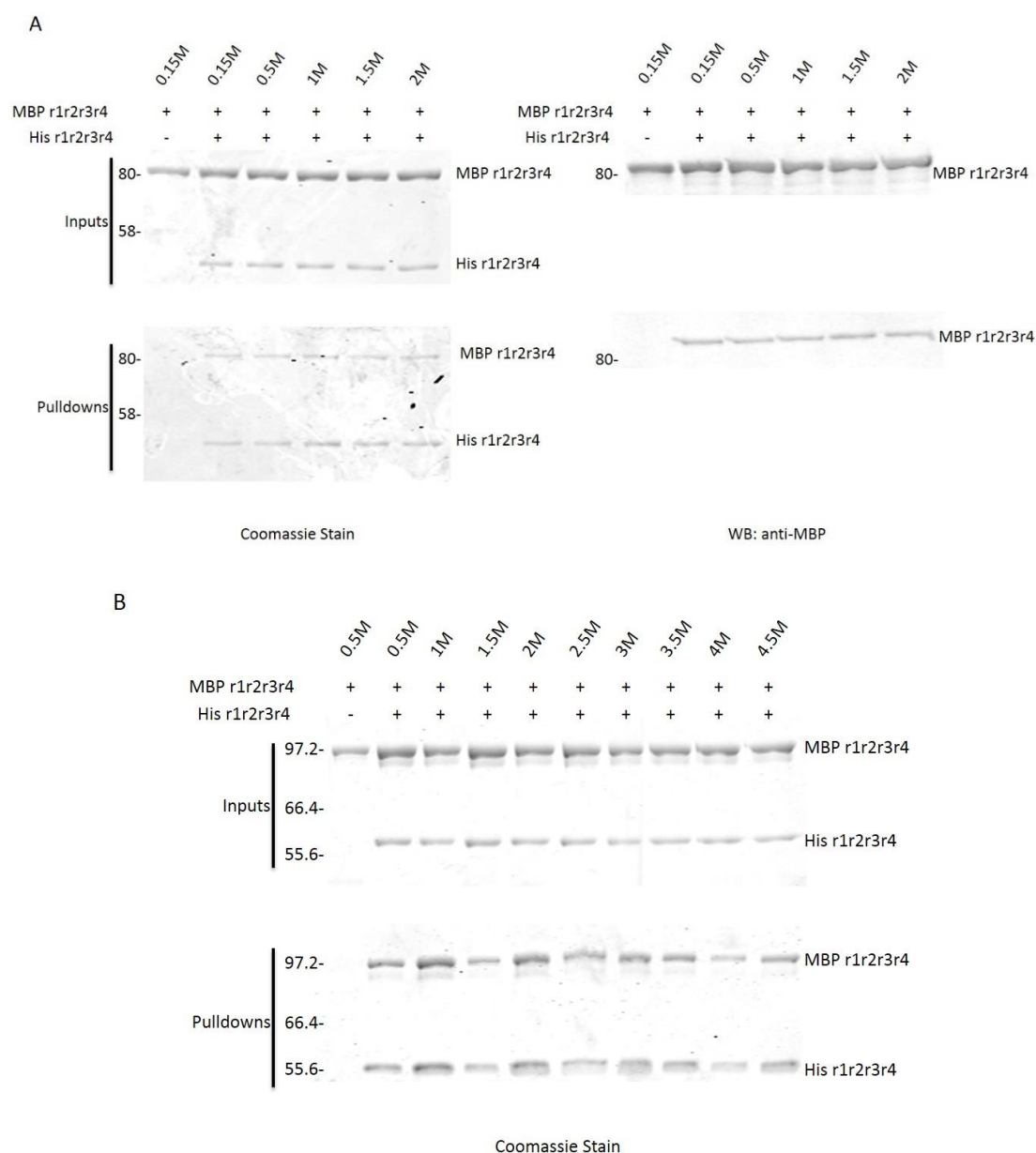


Figure 3.27: Stability of the Actinin Rod Domain Dimer under High Salt Concentrations:

MBP r1r2r3r4 and His r1r2r3r4 were co-expressed in *E. coli* cells, resulting pseudoheterodimers were purified using sequential affinity chromatography and subjected to a His tag pull-down assay under various NaCl concentrations. A control assay involving purified MBP r1r2r3r4 homodimers only was undertaken in parallel in all NaCl concentrations. (Full data not shown). Resulting input and pull-down fractions were analysed using SDS protein gel electrophoresis followed by Coomassie Brilliant Blue staining, in conjunction with western blotting using anti-MBP.

Pull-down assays demonstrated interaction between MBP r1r2r3r4 and His r1r2r3r4 under all salt conditions. No non-specific MBP r1r2r3r4 interactions were detected.

(A) Pseudoheterodimers were incubated with nickel resin under increasing salt concentrations (150mM – 2M). n=1

(B) Pseudoheterodimers were incubated with nickel resin under increasing salt concentrations (500mM-4.5M). n=1

Proteins of interest and the sizes (in kDa) of the relevant molecular weight markers are indicated.

3.4.5.2 The Investigation of the Thermostability of Actinin Dimers

Purified actinin rod domain pseudoheterodimers (Hisr1r2r3r4:MBPr1r2r3r4) were incubated in increasing temperatures for 30 min, from 4°C - 70°C. This short incubation period was to allow for possible dissociation between the pseudoheterodimers to occur. Each pseudoheterodimer sample at each temperature was then mixed with nickel beads and allowed to further incubate at its sample temperature. All wash steps were carried out at each samples required temperature.

MBP r1r2r3r4 was detected in samples pulled-down with His r1r2r3r4 that were incubated at 4°C and 37°C (Fig. 3.28). A smaller amount of MBP r1r2r3r4 was detected in samples pulled-down with His r1r2r3r4 that were incubated at 50°C. An unsatisfactory pull-down is achieved from samples incubated at 70°C. Coomassie stain reveals, for His r1r2r3r4, a very faint band, unequal in intensity to those bands observed for lower temperatures, while the corresponding western blot detects a large amount of MBP r1r2r3r4. This may suggest that, at this higher temperature, protein aggregation is occurring.

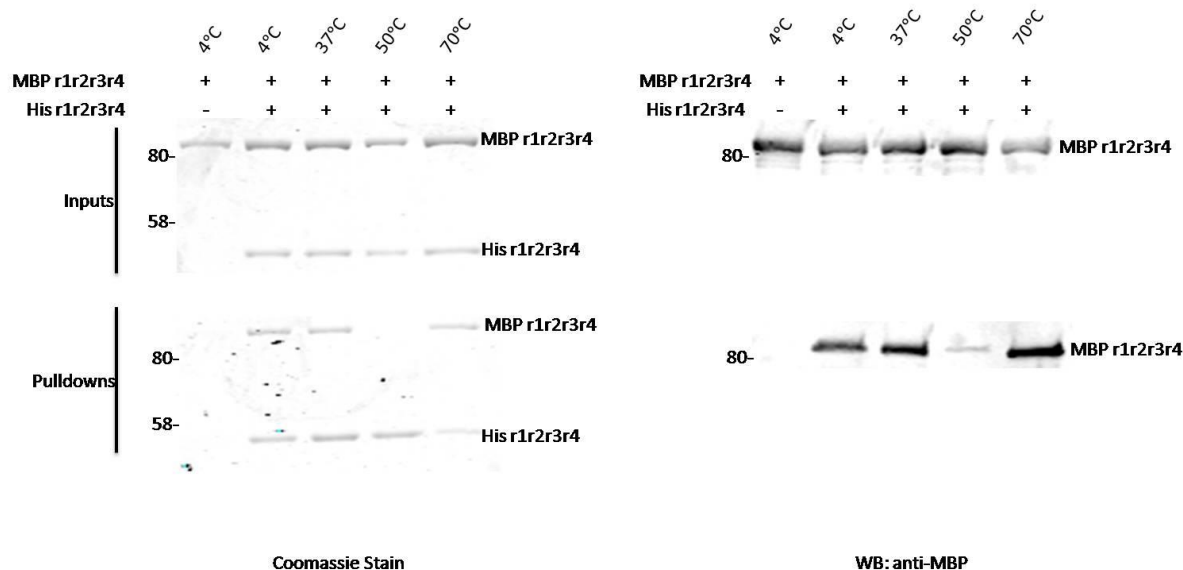


Figure 3.28: Stability of the Actinin Dimer under Increasing Temperatures.

MBP r1r2r3r4 and His r1r2r3r4 were co-expressed in *E. coli* cells, resulting pseudoheterodimers were purified using sequential affinity chromatography and subjected to a His tag pull-down assay under various temperatures of between 4 and 70°C. Control assay involving purified MBP r1r2r3r4 homodimers only was undertaken in parallel in all temperatures. (Full data not shown). Resulting input and pull-down fractions were analysed using SDS protein gel electrophoresis followed by Coomassie Brilliant Blue staining, in conjunction with western blotting using anti-MBP.

Pull-down assays demonstrated a maintained interaction between MBP r1r2r3r4:His r1r2r3r4 pseudoheterodimers in temperatures of 4° and 37°C, and dissociation of these pseudoheterodimers at 50°C. No non-specific MBP r1r2r3r4 interactions were detected.

Proteins of interest and the sizes (in kDa) of the relevant molecular weight markers are indicated.
n=2

Fig. 3.28 suggests that at 50°C the actinin pseudoheterodimers were dissociating to monomers. This finding complements the work carried out by Flood et al. (1997), in which they report that at 50°C the actinin rod domain starts to unfold, as measured using circular dichroism. I was interested in learning if it would be possible to re-associate these monomers to form dimers again.

The starting point for all of previous stability assays was with purified pseudo-heterodimers. For this next assay, however, the starting point was with singly expressed and purified His r1r2r3r4 homodimers and MBP r1r2r3r4 homodimers.

Equal concentrations of His r1r2r3r4 homodimers and MBP r1r2r3r4 homodimers were mixed together and incubated at different temperatures for 10 min ranging from 37.7°C-57.4°C. This range of temperatures was chosen because, drawing information from Fig. 3.28, dissociation of dimers should occur at some temperature above 37°C and below 70°C. His r1r2r3r4 and MBP r1r2r3r4 mixes

were then cooled to 4°C to re-associate the monomers, forming heterodimers. Mixes were then incubated with nickel resin for 30 min, also at 4°C. All wash steps were also carried out at 4°C.

Coomassie stain in Fig. 3.29A reveals that MBP r1r2r3r4 was only pulled-down with His r1r2r3r4 in samples that were incubated at 50.9°C, 55.7°C or 57.4°C. Western blot analysis (Fig. 3.29B) of two of these samples, 55.7°C and 57.5°C, verified the identity of the MBP r1r2r3r4, and that His tagged r1r2r3r4 was required for MBP r1r2r3r4 binding.

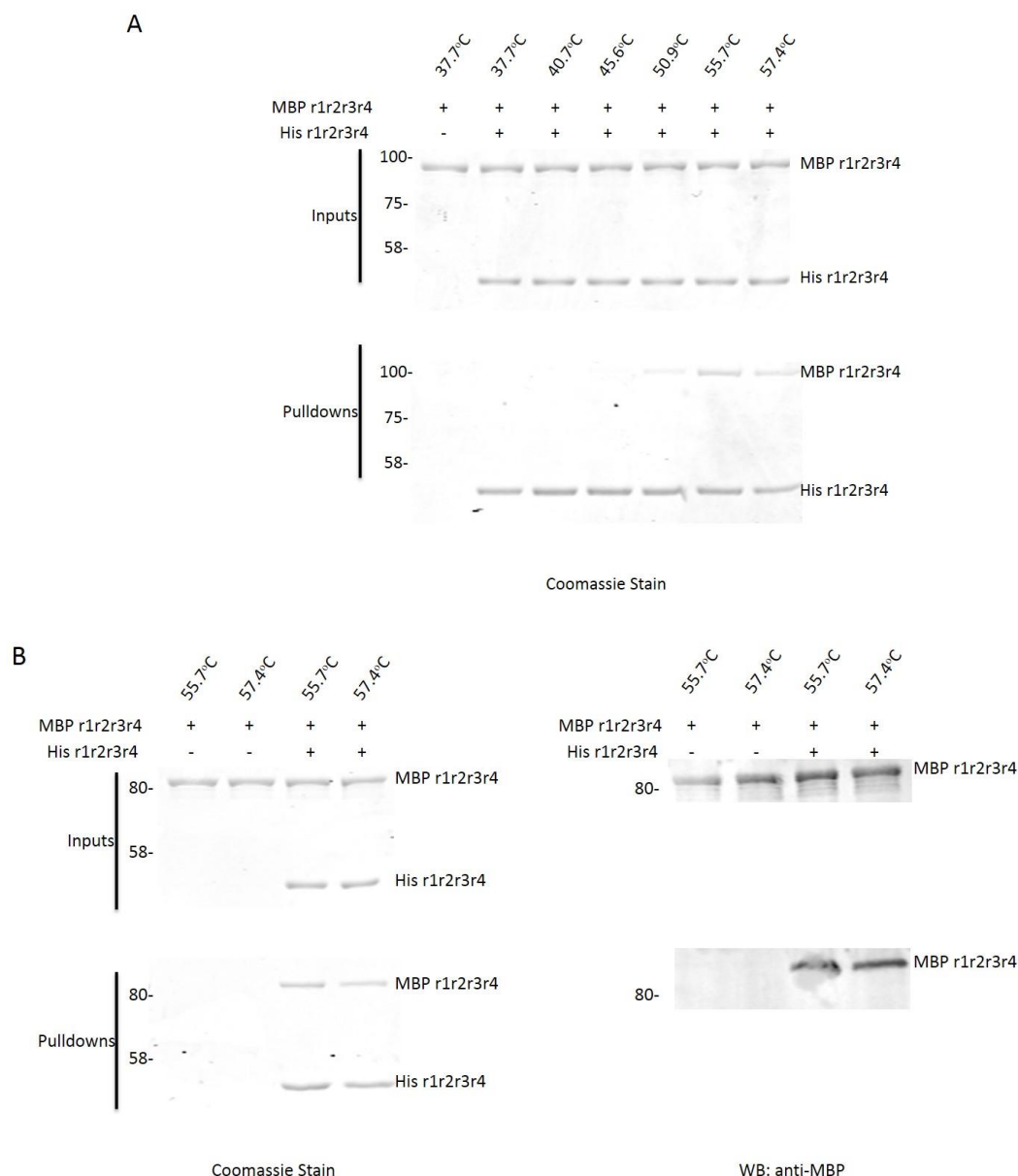


Figure 3.29: Dissociation and Re-association of Actinin Rod Domain Dimers.

His r1r2r3r4 and MBP r1r2r3r4 were each singly expressed in *E. coli* cells and purified to form homodimers. Equal concentrations of each homodimer were mixed and incubated at increasing temperatures ranging from 37.7°- 57.4°C. Mixes were then allowed to cool to 4°C and were then subjected to a His tag pull-down assay. Control assay involving purified MBP r1r2r3r4 homodimers only was undertaken in parallel in all temperatures. (Full data not shown). Resulting input and pull-down fractions were analysed using SDS protein gel electrophoresis followed by

(A) Coomassie Brilliant Blue staining, in conjunction with

(B) western blotting using anti-MBP.

Pull-down assays indicate re-association, at 4°C, of disassociated actinin rod domain monomers, at 55.7° and 57.4°C, verified with western blot. No non-specific interaction of MBP r1r2r3r4 is noted. Proteins of interest and the sizes (in kDa) of the relevant molecular weight markers are indicated.

n=2

3.4.6 α/β -Spectrin Spectrin Repeat Dimerisation Studies

I realized that one drawback of using actinin as a building block in certain contexts might be its strong ability to form homodimers with itself. These shortcomings are observed in chapter four of this document. Spectrin was appealing as an alternative or complementary building block because it is a heterodimer, composed of α -spectrin and β -spectrin subunits. The inability of the spectrin subunits to interact with themselves, but only with each other provides for a greater library of possible structures to design and create.

In this section, through MBP pull-down spectrin repeat interaction assays and native gel electrophoresis, I explore the dimerisation, or self-assembly, properties of the α/β -spectrin spectrin repeats, assessing their suitability as potential building blocks.

3.4.6.1 α/β -Spectrin spectrin repeat Interaction Assay

To assess the ability of α -spectrin spectrin repeats 18-21 and β -spectrin spectrin repeats 1-4 to self-assemble and form heterodimers, an MBP pull-down approach was utilised in which equal concentrations of purified His α -r18r19r20r21 and MBP β -r1r2r3r4 were mixed together with amylose resin. Interaction was observed, with His α -r18r19r20r21 pulled-down along with MBP β -r1r2r3r4 (Fig. 3.30).

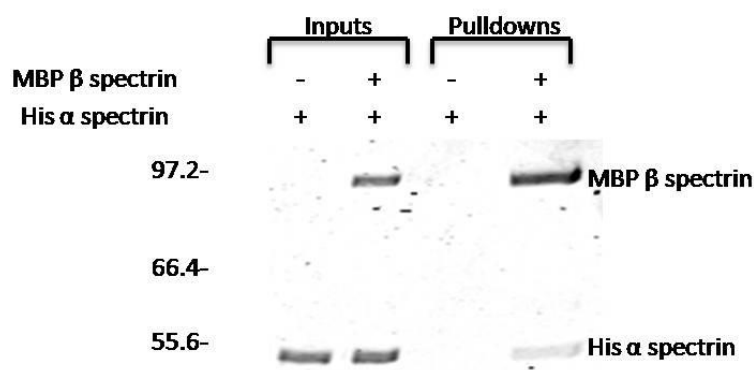


Figure 3.30: Dimerisation Between Truncated α - and β -Spectrin Constructs.

His α -r18r19r20r21 and MBP β -r1r2r3r4 were each singly expressed in *E. coli* cells and purified. Equal concentrations of each were mixed and subjected to a MBP pull-down assay. Control assay involving His α -r18r19r20r21 only was carried out in parallel. Resulting input and pull-down fractions were analysed using SDS protein gel electrophoresis followed by Coomassie Brilliant Blue staining. Pull-down assays indicate interaction between His α -r18r19r20r21 and MBP β -r1r2r3r4. No non-specific His α -r18r19r20r21 interaction is observed. Proteins of interest and the sizes (in kDa) of the relevant molecular weight markers are indicated. n=1

3.4.6.2 Assessment of α/β -Spectrin spectrin repeat Heterodimers Using Native-PAGE

Just as per the actinin dimeric proteins, it was also necessary to become familiar with the native gel migration pattern of the spectrin truncated proteins, and to screen for potential interactions.

His α -r18r19r20r21, His β -r1r2r3r4, His mCherry α -r18r19r20r21 and His mCherry β -r1r2r3r4 were each singly expressed in *E. coli* cells and purified using a nickel column. I had previously verified that dimerisation could occur between the truncated α - and β -Spectrin constructs (Fig. 3.30). Native gel electrophoresis re-confirmed this interaction.

For Fig. 3.31A, equal concentrations of His mCherry α -r18r19r20r21 and His β -r1r2r3r4 purified proteins were mixed together and subjected to native protein gel electrophoresis. For Fig. 3.31B equal concentrations of His α -r18r19r20r21 and His mCherry β -r1r2r3r4 purified proteins were mixed together and subjected to native protein gel electrophoresis. For both mixtures, controls investigating the possibility that these α - and β -Spectrin truncated proteins could form homodimers with themselves were also prepared. For Fig. 3.31A these included purified protein

mixes of His α -r18r19r20r21 with mCherry α -r18r19r20r21, and, for Fig 3.31B, these included purified protein mixes of His β -r1r2r3r4 with mCherry β -r1r2r3r4.

In Fig. 3.31A, the presence of His mCherry α -r18r19r20r21 only in lane 1 is confirmed using mCherry fluorescence detection. His β -r1r2r3r4 only is represented with one band in Lane 3. A mix of both these proteins is represented with one band only in lane 2, which appears to have the same migration pattern as that for His β -r1r2r3r4 only. mCherry fluorescence detection exhibits an altered migration pattern of His mCherry α -r18r19r20r21 from that seen in lane 1. This altered migration pattern and the presence of only one band suggests possible interaction between these two proteins. A mix of His mCherry α -r18r19r20r21 and His α -r18r19r20r21 purified proteins in lane 4 is represented with two bands, His mCherry α -r18r19r20r21 being one of these bands confirmed using mCherry fluorescence detection. The same migration pattern as that seen in lane 1 for this protein, and the presence of two bands suggests no interaction between these proteins.

In Fig. 3.31B the presence of His mCherry β -r1r2r3r4 only in lane 1 is confirmed using mCherry fluorescence detection. His α -r18r19r20r21 only is represented with one band in Lane 3. A mix of both these proteins is represented with two bands in lane 2. The top band is confirmed to be His mCherry β -r1r2r3r4 using mCherry fluorescence detection. Its migration differs from that in lane 1. while the bottom band is His α -r18r19r20r21-migrating at the same rate as that seen in lane 3. The presence of two bands does suggest no interaction between these two proteins, however the slightly altered migration pattern of His mCherry β -r1r2r3r4 between lanes 1 and 2 might indicate that interaction has occurred. The presence of two bands might mean that not all of the His α -r18r19r20r21 interacted. A mix of His mCherry β -r1r2r3r4 and His β -r1r2r3r4 purified proteins in lane 4 is represented with one band. The presence of mCherry β -r1r2r3r4 in this band is confirmed with mCherry fluorescence and its altered migration pattern from that seen in lane 1 is noted. This altered migration pattern and the presence of only one band suggests possible interaction between these proteins.

It may be that β -r1r2r3r4 has a slight tendency to form dimers with itself while α -r18r19r20r21 does not, as indicated with figure visuals in Fig. 3.31.

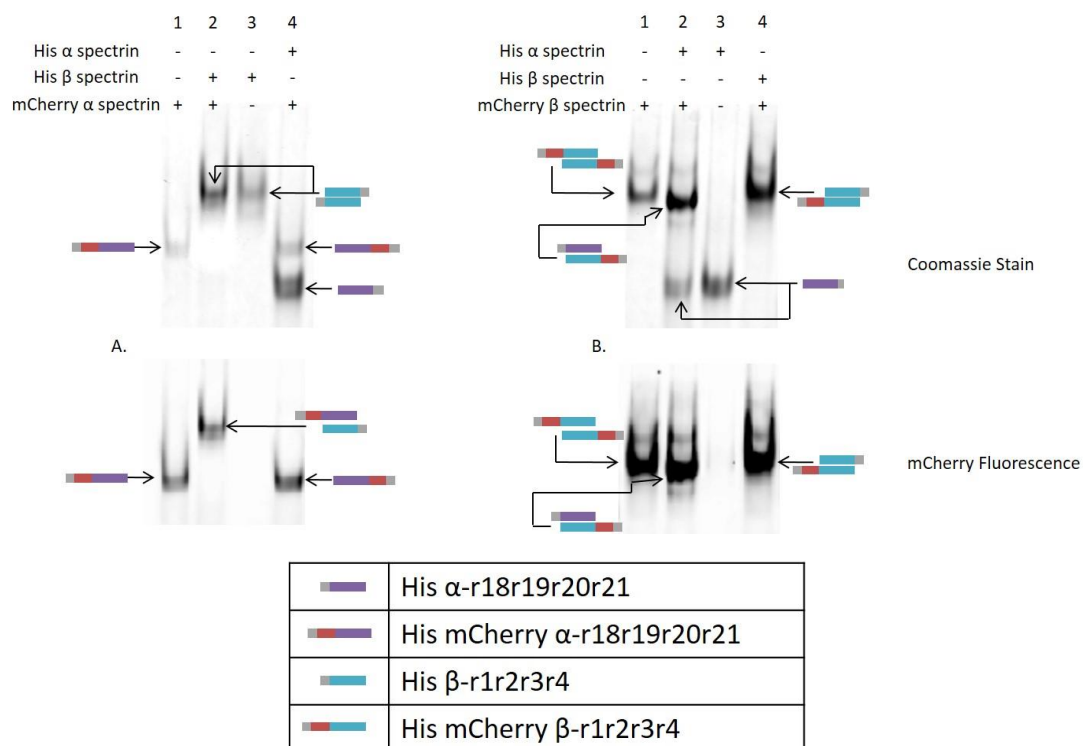


Figure 3.31: Observing Native Gel Migration Pattern of α -Actinin and α - β -Spectrin Proteins.

His α -r18r19r20r21, His β -r1r2r3r4 and His mCherry α -r18r19r20r21 and His mCherry β -r1r2r3r4 were each singly expressed in *E. coli* cells and purified using a nickel column. Protein mixes were prepared as indicated and subjected to native protein gel electrophoresis followed by Coomassie Brilliant Blue staining in conjunction with mCherry fluorescence detection.

(A) Native protein gel electrophoresis confirm interaction between His mCherry α -r18r19r20r21 and His β -r1r2r3r4 (lane 2). No interaction is detected between α -r18r19r20r21 proteins (lane 4).

(B) Native protein gel electrophoresis may suggest possible interaction between His α -r18r19r20r21 and His mCherry β -r1r2r3r4 (lane 2). Possible homodimeric interaction between β -r1r2r3r4 proteins is indicated (lane 4).

Migration pattern of each of the monomers and dimers is indicated with figure visuals.

n=3

3.4.7 Heterodimeric α - β -Spectrin spectrin repeat Stability Assays Studies

See section 3.4.5 for short introduction.

In this section, the co-expression strategy, using the C280* P_{BAD} system and the T7/*lac* system, and sequential purification strategy are used to yield α - β -spectrin spectrin repeat heterodimers to be utilised in salt and thermostability studies.

To assess the effect of salt (NaCl) and heat on spectrin spectrin repeat heterodimer stability, a His-tag pulldown approach was utilised. The two-plasmid

co-expression strategy for the generation of these spectrin spectrin-repeat proteins is as follows; those proteins to be expressed from the C280* P_{BAD} system were designed to have a MBP tag so that western blot analysis could be used to certify their identity, and verify that protein bands observed were not impurities, or the degradation products of His tagged proteins, or the result of MBP tagged proteins binding non-specifically to the resin, i.e. to ensure presence of His tagged α -r18r19r20r21 is required for MBP β -r1r2r3r4 binding.

3.4.7.1 Investigating the Effect of Salt Concentration on the Structural Stability of Spectrin r1-r4/r18-21 Heterodimers

Purified truncated α -/ β -spectrin heterodimers (His α -r18r19r20r21:MBP β -r1r2r3r4) were incubated for 1 hour in increasing concentrations of NaCl, ranging from 150mM – 2M with Nickel resin. Interaction between this pairing was confirmed under all salt conditions indicated by the detection of MBP β -r1r2r3r4 pulled-down with His α -r18r19r20r21 (Fig. 3.32). However, a weakening of association is occurring as the NaCl concentration is increasing.

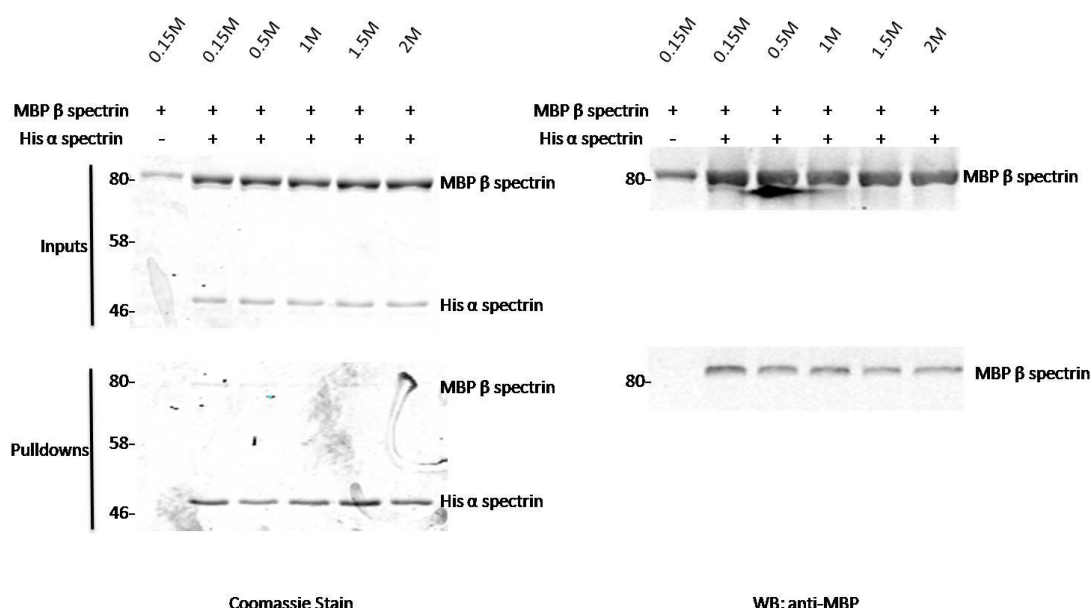


Figure 3.32: Stability of the Truncated Spectrin Heterodimeric Domain under High Salt

Concentrations:

MBP β -r1r2r3r4 and His α -r18r19r20r21 were co-expressed in *E. coli* cells, resulting heterodimers were purified using sequential affinity chromatography and subjected to a His tag pull-down assay under various NaCl concentrations, between 150mM to 2M. A control assay involving purified MBP β -r1r2r3r4 monomers only was undertaken in parallel in all NaCl concentrations. (Full data not shown). Resulting input and pull-down fractions were analysed using SDS protein gel electrophoresis followed by Coomassie Brilliant Blue staining, in conjunction with western blotting using anti-MBP. Pull-down assays demonstrated interaction between MBP β -r1r2r3r4 and His α -r18r19r20r21 under all salt conditions and no non-specific MBP β -r1r2r3r4 interactions. As the NaCl concentration is increased, a weakening of association is observed. Proteins of interest and the sizes (in kDa) of the relevant molecular weight markers are indicated. n=1

3.4.7.2 The Investigation of the Thermostability of Spectrin r1-r4/r18-21

Heterodimers

The thermal stabilities of all 36 single spectrin repeats has been determined by An et al. (2006). They reported that the unfolding transition midpoints for each repeat varies from 21-72°C. This variability between repeats may supplement findings by MacDonald & Cummings (2004) they find that certain repeat pairings are less thermodynamically stable than others, and that these pairings may acts as “hinges”, supplying the spectrin complex with elastic properties (discussed in section 1.1.2.3.2). Here, I investigate the thermal stability of four repeat spectrin proteins α -r18r19r20r21 and β -r1r2r3r4.

Purified truncated α -/ β -spectrin truncated heterodimers (His α -r18r19r20r21:MBP β -r1r2r3r4) were incubated for 30 min in increasing temperatures, from 4°C - 70°C. This short incubation period was to allow for

possible dissociation of the heterodimers to occur. Each heterodimer sample at each temperature was then mixed with nickel beads and allowed to further incubate for 1 hour at its sample temperature. All wash steps were carried out at each samples required temperature.

MBP β -r1r2r3r4 was detected in samples pulled-down with His α -r18r19r20r21 that were incubated at 4°C. A smaller amount of MBP β -r1r2r3r4 was detected in samples pulled-down with His α -r18r19r20r21 that were incubated at 37°C. In all temperatures unsatisfactory pulldowns are obtained – coomassie staining is weak and inconsistent across all samples. This inconsistency is worsened in samples at 50°C and over. Coomassie stain reveals very faint bands, unequal in intensity to those bands observed for lower temperatures for His α -r18r19r20r21, while the corresponding western blot detects a large amount of MBP β r1r2r3r4. This may suggest that, at higher temperatures, protein aggregation is occurring (Fig. 3.33).

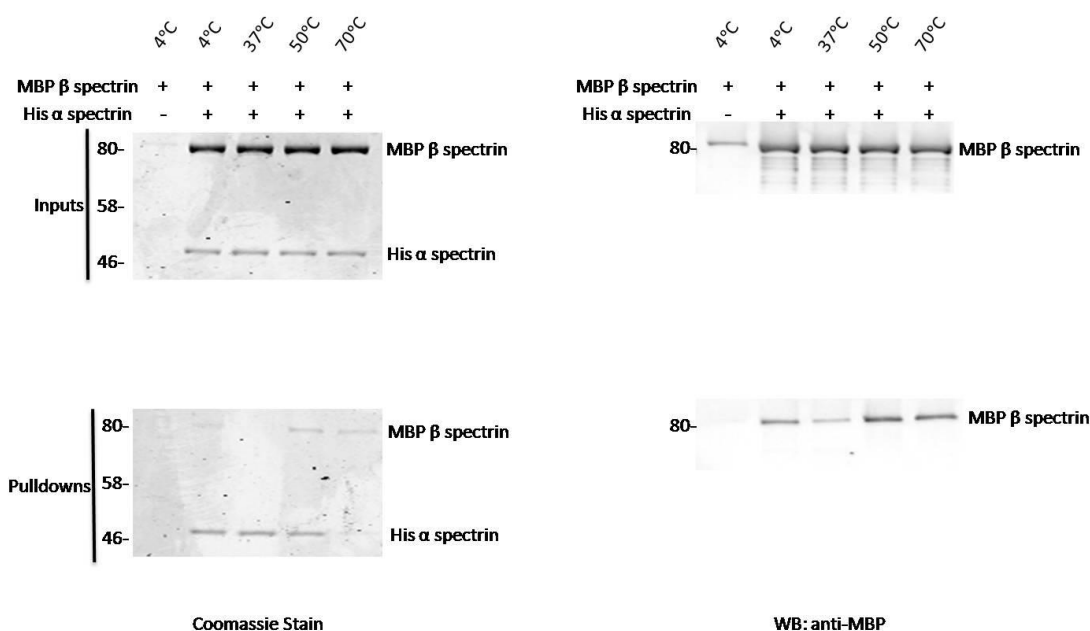


Figure 3.33: Stability of the Truncated Spectrin Heterodimeric Domain under Increasing Temperatures.

MBP β -r1r2r3r4 and His α -r18r19r20r21 were co-expressed in *E. coli* cells, resulting heterodimers were purified using sequential affinity chromatography and subjected to a His tag pull-down assay under various temperatures of between 4 and 70°C. Control assay involving purified MBP β -r1r2r3r4 monomers only was undertaken in parallel in all temperatures. (Full data not shown). Resulting input and pull-down fractions were analysed using SDS protein gel electrophoresis followed by Coomassie Brilliant Blue staining, in conjunction with western blotting using anti-MBP. Pull-down assays demonstrated a maintained interaction between MBP β -r1r2r3r4 and His α -r18r19r20r21 heterodimers at a temperature of 4°, and dissociation of these pseudoheterodimers at 37°C. No non-specific MBP β -r1r2r3r4 interactions were detected. Proteins of interest and the sizes (in kDa) of the relevant molecular weight markers are indicated. n=2

3.5 Discussion

The overall aim of the research presented in this chapter was to examine the dimeric interactions between the spectrin-like repeats of actinin and the spectrin repeats of α -/ β -spectrin in view of assessing their appropriateness as building blocks in the construction of protein nanostructures.

To generate these dimers, I made use of a co-expression and purification system that I developed that would allow me to co-express and co-purify an assortment of proteins.

3.5.1 Co-expression System

In the benchmarking study comparing expression from three different co-expression strategies (bicistronic, two-promoter-one-plasmid and two-plasmid), both the two-promoter-one-plasmid and the two-plasmid strategies performed well in expressing each protein. The bicistronic strategy yielded very low expression of one protein, actinin S-tag r1r2r3r4, whose gene sequence was positioned furthest from the promoter. When using the bicistronic system it is very normal to only get expression of one gene, usually that gene closest to the promoter (Kim et al. 2004). These observations suggested that either the two-promoter-one-plasmid strategy or the two plasmid strategy would have been an acceptable option with which to continue.

While the initial aim was to generate a co-expression system to produce actinin dimers and α -/ β -spectrin heterodimers, going forward, I wanted to be able to utilise and manipulate this system with respect to the nanosynthetic aspect of the project. When designing and creating any form of structure there is always more than one type of building block and, each building block is present in varying amounts. With this in mind, I wanted to create a system in which one could control and independently regulate the expression of each target construct. For this reason, I decided to progress with the two-plasmid strategy, rather than the two-promoter-one-plasmid strategy. In addition, this one-plasmid-one-protein co-expression method would allow me to “mix and match” different protein combinations quite simply and easily.

While making use of the two-plasmid strategy, it was observed that, in practice, co-expressing two proteins, each under the control of a different promoter (P_{BAD} or $T7\ lac$ promoters), on a different plasmid, was not very straightforward. To carry out the actinin spectrin-like repeat interaction assays (section 3.4.4.1) it was imperative that the actinin spectrin-like repeat proteins were co-expressed, to allow them the best opportunity to form dimers, if they were so inclined. A combination of IPTG and arabinose concentrations that produced relatively equimolar amounts of actinin four- and three-spectrin-like repeat proteins was identified, but, it was very difficult to establish a set of IPTG and arabinose concentrations that would produce equimolar amounts of actinin two-spectrin-like repeat proteins. A study, undertaken by Lee et al. (2007), prompted the consideration that maybe the two promoters ($T7\ lac$ and P_{BAD}) were not working independently of each other. In their study, they found that both of these promoters had a strong tendency to involve themselves in a type of promoter crosstalk where the inducer of one promoter disturbs expression from the other promoter; i.e. where IPTG was found to inhibit expression from the P_{BAD} system. These findings reflected my own observations; expression from the P_{BAD} system only seemed to occur in the presence of very low IPTG concentrations. This study found their mutated version of the P_{BAD} system to be much more appropriate for use where the presence of IPTG was also required. I was able to re-affirm this observation using the MBP protein expressed from either the WT P_{BAD} system or the C280* P_{BAD} system in the presence or absence of IPTG.

In expanding this study, comparing the WT and C280* P_{BAD} systems, and determining the robustness of this C280* P_{BAD} system in a co-expression situation, i.e. where MBP was expressed from the C280* P_{BAD} system in the presence of arabinose, together with YFP expression from the $T7\ lac$ system in the presence of IPTG, it was observed that high concentrations of arabinose were affecting expression of YFP from the $T7\ lac$ promoter, the opposite of what was seen in co-expression trials using the WT P_{BAD} system and the $T7\ lac$ system. In fact, it was observed that as the concentration of arabinose in the culture increased, expression from the C280* P_{BAD} system also increased, while expression from the $T7\ lac$ system decreased. Further investigation suggested that, this time, promoter crosstalk was not responsible; addition of increasing concentrations of arabinose to cultures containing only, and

therefore expressing only, from the T7/*lac* system did not exhibit any decline in expression. The actual presence of the arabinose inducer was not affecting expression from the T7/*lac* system, but rather expression from the C280* P_{BAD} system was affecting expression from the T7/*lac* system. This study suggests that perhaps the C280* P_{BAD} system is much more selfish system than the T7/*lac* system, monopolising the protein synthesis machinery of the bacterial cell leaving the cell deficient in its ability to produce protein from the T7/*lac* system.

Overall, the combination of the WT P_{BAD} system with the T7/*lac* system appeared to be very “inflexible” with varied combinations of IPTG and arabinose inducers yielding “all-or-nothing” expression patterns for the protein of interest. This makes it very difficult to uncover optimal inducer concentrations for balanced co-expression. By contrast, while I revealed some previously unreported issues with use of the C280* pBAD system with the T7/*lac* system, it was found that the concentrations of inducers were much more titratable with C280* pBAD system, compared to the WT version. Thus the C280* pBAD system does represent an improvement in terms of achieving independent control of the expression of two proteins.

3.5.2 Heterodimer Purification

I speculated that a heterodimer purification system, involving the double-tagging system followed by sequential affinity chromatography, would be useful not only in relation to this project, but to other protein-based projects. Some proteins require the presence of a chaperone protein to help them fold correctly and remain stable (Georgiou & Valax 1996). By differentially tagging the protein of interest and the chaperone, and co-expressing them together in the one cell, I envisioned the use of this optimised co-expression and purification strategy to produce soluble, stable and correctly folded native proteins, which, for example, could then be further studied for structural determination. Previous work in our lab has shown through *in vitro* binding assays that actinin-1 and actinin-4 can form heterodimers (Foley & Young 2013). The properties of these actinin-1/-4 heterodimers have not yet been

completely studied. With the use of this co-expression and co-purification technique, it should be possible to purify these heterodimers and analyse them further.

Originally, the purification strategy was a two-day procedure, consisting of an overnight dialysis to remove the imidazole from the semi-pure protein elution, prior to loading onto the second chromatography column. In efforts to streamline the procedure, thus making it more attractive, it was noted that the presence of imidazole does not affect the binding of MBP to the amylose column. This observation made the overnight dialysis step in between purification from both columns unnecessary, turning the two-day procedure into a one-day process.

The added advantage of using a purification strategy involving sequential affinity chromatography is that it should always yield a 1:1 ratio of each protein. An equal ratio of each protein was imperative when carrying out the salt stability and thermostability assays in sections 3.4.5 and 3.4.7. The use of double tag sequential affinity chromatography procedure slightly attenuated the pressures of trying to achieve equal co-expression of each protein. As previously mentioned and shown, the crosstalk that was observed between the two initial promoters that were chosen, *T7lac* and WT pBAD promoters made equal co-expression of each protein very complex and difficult to accomplish. However, use of the *T7lac* promoter with the C280* pBAD promoter, made co-expression a less formidable task.

3.5.3 Actinin Spectrin-like Repeats and α -/ β -Spectrin Spectrin Repeats:

Dimerisation Studies

The actinin spectrin-like repeats (r1r2r3r4) and the α -/ β - (r18r19r20r21)/(r1r2r3r4) spectrin spectrin repeats have the ability to self-assemble into dimers and, as a result, were to be my main building blocks. I made use of MBP pulldown assays and native protein gel electrophoresis to confirm this dimerisation.

Native protein gel electrophoresis uses non-denaturing conditions meaning that the proteins maintain their higher-order structure (Fanarraga et al. 2010). All spectrin repeat recombinant proteins (from both actinin and spectrin proteins) had low pI values, meaning they all had net negative charges at neutral pH, and so, migrated readily into the native gels. The rate of migration will be influenced by their

exact charge, as well as their molecular weight and shape. When analyzing these native gels, I assumed that, when disposed to do so, dimers would form between protein pairings and they would run as one band and, when indisposed to do so, non-interacting monomeric proteins would run as two separate bands. The appearance of a third band would indicate another type of dimeric interaction. Using these guidelines, it was confirmed that actinin rod domain proteins (r1r2r3r4) interact with themselves forming homodimers, where both of the actinin rod domain proteins contributing to the dimer have the same tag, and pseudoheterodimers, where both the actinin rod domain proteins contributing to the dimer have a different tag.

These guidelines were also used to study possible dimerisation between the α -/ β -spectrin truncated proteins (α -r18r19r20r21/ β -r1r2r3r4). β -r1r2r3r4 constructs migrate much more slowly than α -r18r19r20r21 constructs. This might be explained by charge differences. α -r18r19r20r21 has a much lower pI than β -r1r2r3r4, 4.90 and 6.06 respectively. This means it has a much greater negative charge density and so will migrate at a faster rate. However, an alternative explanation could be that β -r1r2r3r4 possesses a tendency to homodimerise with itself. This observation may explain the conflicting results obtained from these native gels regarding dimerisation between α -r18r19r20r21 and β -r1r2r3r4; complete dimerisation is observed between His mCherry α -r18r19r20r21 and His β -r1r2r3r4, but not between His mCherry β -r1r2r3r4 and His α -r18r19r20r21. It may be that the His mCherry β -r1r2r3r4 is not available for complete heterodimerisation with His α -r18r19r20r21, due to its homodimerisation with itself, or it may simply be that, when present on β -r1r2r3r4 protein, the mCherry tag sterically prevents complete heterodimerisation to His α -r18r19r20r21. It may also be that His α -r18r19r20r21 and His mCherry β -r1r2r3r4 did interact, mCherry fluorescence did reveal an altered migration pattern of His mCherry β -r1r2r3r4 between lanes 1 and 2. The presence of two bands may mean that not all of the His α -r18r19r20r21 interacted with the His mCherry β -r1r2r3r4.

This would not be the first study to report associations between spectrin spectrin repeats. A three spectrin repeat α -spectrin molecule comprising spectrin repeats 15-17 crystallised as an anti-parallel homodimer (Kusunoki et al. 2004b). It is unclear if the lateral interactions that occur between spectrin repeats outside of the

dimer initiation site are specific, or if they occur due to proximity after initial alignment of α 20-21 and β 1-2 (Li et al. 2007). Li et al. (2007) have suggested that monomeric spectrin proteins can homodimerise with weak affinity. Considering the β -spectrin proteins used in this study contained two of the dimer initiation sites, β 1 and β 2, which always precisely align with α 20 and α 21 (Li et al. 2007), it is unlikely, that non-specific pairing occurred. However, the presence of spectrin repeats β 3 and β 4 may have induced homodimerisation, especially in samples not containing the α -spectrin protein. These possible homodimers may provide information on the pairing of spectrin repeats outside of the dimer initiation site.

Nevertheless, heterodimerisation between His α -r18r19r20r21 and MBP β -r1r2r3r4 was verified with a MBP pull-down.

In assessing the dimerisation and self-assembly capability of truncated actinin rod-domain constructs, I found both the three-spectrin-like repeat proteins (r1r2r3 and r2r3r4) to offer the most potential. Agreeing with previous studies involving chicken gizzard actinin carried out by Flood et al. (1997) and Flood et al. (1995), homodimerisation occurred between the equivalent truncated three-repeat constructs, r1r2r3. Heterodimerisation also occurred between two different three-repeat constructs, r1r2r3 and r2r3r4. Densiometric analysis suggested that this heterodimerisation between r1r2r3 and r2r3r4 constructs was tighter and stronger than the homodimerisation between two r1r2r3 constructs. This observation was not surprising. In the aligned actinin dimer model, the abrogation of one pairwise alignment still leaves three available to mediate heterodimerisation between r1r2r3 and r2r3r4, however homodimerisation between two r1r2r3 monomers involves only two pairwise alignments. This study lends further support to the aligned actinin dimer model. Only one of the actinin two-spectrin-like repeat proteins offered the possibility of self-assembly; r2r3. This result was anticipated, given that the crystal structure of the r2r3 protein had determined it to be a dimer, however an interaction between r1r2 and r3r4 was also expected, based on previous work carried out by Young & Gautel (2000) using a yeast 2 hybrid system. Also, with this protein combination, under the aligned actinin dimer model, two pairwise interactions are available, making dimerisation very probable. The fact that dimerisation was not

reported here could be due to a number of reasons, the use of different expression systems, the possibility that the MBP tag may have interfered with dimerisation, or, alternatively, maybe the interaction was very weak and, was therefore difficult to detect. However, speculative conclusions can be drawn from the observation that r1r2 proteins failed to interact with r3r4 proteins, while r2r3 was found to readily form dimers with itself, so substantially in fact, that differentially tagged r2r3 proteins had to be co-expressed, rather than singly expressed in the hope of producing pseudoheterodimers over homodimers. It has already been suggested that r2r3 represents the structural foundation that determines the architecture of the entire rod domain and indeed, the complete actinin protein (Djinović-Carugo et al. 1999). Results presented here indicate that perhaps dimerisation of r2r3 may represent the minimum requirement necessary to induce dimerisation; this interaction may create the context allowing for the co-operative binding of repeats one and four. Dimerisation of actinin molecules might occur from the middle outwards. This is in contrast to the zipper-like model of heterodimerisation between spectrin molecules, which begins with the alignment of α - and β -spectrin repeats at one end of the molecule followed by the lateral association of remaining spectrin repeats (Speicher et al. 1992; Ursitti et al. 1996; Harper et al. 2001)

3.5.4 Actinin Spectrin-like Repeat Dimers and α/β -Spectrin Spectrin Repeat Heterodimers: Stability Assays

In sections 3.4.5.1 and 3.4.7.1, both actinin spectrin-like repeat dimers and α/β -spectrin spectrin repeat heterodimers displayed remarkable stability under all high salt concentrations. The electrostatic static interactions contributing to the dimer formation (Kusunoki et al. 2004b; Djinović-Carugo et al. 1999) must be buried deep within the dimer interface and are therefore protected from the screening effects of NaCl. Since salts differ in their ability to screen charges, it might be interesting to observe the effect with a more chaotropic salt (Perez-Jimenez et al. 2004). Although, a weakening of association between truncated α - and β -spectrin constructs was observed as the concentration of NaCl increased. This is in agreement with Begg et al. (2000) who also reported a reduced association between these

truncated spectrin constructs as the NaCl concentration increased from 0.1-1M in sedimentation equilibrium experiments. Older studies have found that the secondary structure of spectrin repeats is not disrupted with increased ionic strength, but rather dissociation of dimers is induced by disruption of electrostatic attractions between repeats (LaBrake et al. 1993; DeSilva et al. 1997).

Thermostability investigations of actinin rod domain dimers yielded interesting results. Up to temperatures of 37°C, the actinin rod domain dimer remains intact. Beyond this temperature dissociation is induced. However, upon cooling, these monomers can apparently be enticed to re-associate and re-form the dimer. These characteristics are reminiscent of the DNA double helix, the formation of which makes use of complementary strand base-pair alignments between guanine and cytosine, adenine and thymine. Under conditions of high heat, DNA strands contributing to the helix separate and upon cooling, re-anneal. This process has been greatly exploited in the field of synthetic nanoconstruction (Nangreave et al. 2010). These disassociation and re-association properties of actinin could be useful in terms of building large and complex structures with actinin based building blocks as it provides an extra layer of control over the assembly process. Through manipulation of temperature, structures can be induced to assemble or dis-assemble. This new found property should also it may make it easier to facilitate attachment of biological molecules, such as enzymes or motor proteins, to the actinin-based structure, making it functional. It would be interesting to study if temperatures inducing dis-association and re-association between actinin spectrin-like repeats would be different depending on the amount of spectrin-like repeats present in the building block. If so, assembly of structures formed from actinin building blocks made up of different numbers of spectrin-like repeats could be enticed to occur hierarchically, over a number of different temperatures, which might lead to the formation of a more detailed structure. Apart from the above, this property also suggests that the monomeric actinin rod domain is quite stable too, being able to maintain its structural integrity in high temperature conditions.

Thermostability investigations of truncated α -/ β -spectrin spectrin repeat heterodimers indicated that these dimers may not be as heat resilient as the actinin rod domain homodimer; truncated spectrin heterodimers dissociated at 37°C, while

actinin rod domain pseudoheterodimers dissociated at a higher temperature. It maybe that full length α -/ β -spectrin heterodimers are more heat resilient. Indeed, spectrin is believed to be dimeric in vivo, so the additional spectrin repeats in full length spectrin must provide additional thermostability. The physiological body temperature is 37°C. It may not be unusual to observe some spectrin heterodimer dissociation at this temperature as it may contribute to making the RBC more elastic. The interpretations gathered from these assays are credible considering the thermostability of the MBP protein has reported to have a T_m , the temperature at which a protein starts to denature, of 63°C at a pH of 7.4 (Ganesh et al. 1997). Spectrin repeat thermostability assays were carried out at a max temperature of 70°C at a pH of 7.5. This may explain the possible protein aggregation that was observed in assays carried out at 70°C. In assays carried out at lower temperatures however, the MBP tag should have remained folded. These thermal characteristics make MBP protein a suitable protein tag for such assays.

3.6 Conclusion

Although the goal of much of this work was to re-confirm what was already known in the field, it was important to do so. I needed to be able to relay this information in terms of my constructs, expression systems and lab techniques before proceeding further with the project, in the hope of using these constructs as components in the construction of a protein nanostructure. In my opinion, it was imperative for me to become familiar with my own tools and building blocks first, and then focus on the design and composition of my protein nanostructures.

However, along the way I have devised and optimised a protein co-expression and purification strategy that, for this study, has been successful in generating actinin and spectrin building blocks, but has the potential for use in any study requiring the generation of protein complexes. I have also gleaned a few novel insights with regard to spectrin-like and spectrin repeat interactions that should not only be helpful in designing protein building blocks and protein nanostructures going forward, but should also contribute to the large volume of information already known about these proteins; the central repeats of the actinin rod domain, r2r3, appear to an essential minimum requirement for actinin dimer formation; within reasonable temperatures the actinin rod domain behaves in a similar fashion to the DNA double helix insofar as it can be enticed to dissociate and re-associate; and β -spectrin spectrin repeats 1-4 may have a slight tendency to homodimerise.

The overall conclusion from the work carried out for this chapter is that spectrin repeats from both actinin and spectrin proteins make strong candidates as nanostructure building blocks with which to go forward with in attempts to design and build a protein nanostructure.

Chapter 4:

Using Actinin and Spectrin Dimerisation Domains to Generate Nanostructure Building Blocks

4.1 Abstract

Proteins have enormous potential as building blocks, as has been evident with the creation of protein cages, lattices and nano-scaffolds. However, cytoskeletal proteins have been under-represented in this field. Considering their important mechanical and physical properties, I propose that cytoskeletal proteins have potential applications in this area. In this study, I assess the possibility of using Spectrin Family proteins, particularly their spectrin repeat domains (dimerisation domains), as building blocks for protein-based nanostructures. Through a fusion-based assembly strategy, I create homodimeric and heterodimeric bivalent building blocks and demonstrate their potential for future application in Bionanotechnology.

4.2 Introduction

In the last number of years, a type of molecular biology revolution has taken place with the rise of bionanotechnology, a discipline dedicated to, not only identifying and describing biological macromolecules, but also using them to create nanoscale structures. Self-assembly is the instinctive automatic association of modules or components into organized structures and is the main approach used by nature to bring about the biological complexity that makes up the cell and its inner workings (Ryadnov 2007; Alberts 1998). Researchers, through bottom-up assembly techniques, exploit this intrinsic self-assembly ability of biomolecules to both gain a better understanding of living systems and their natural biological complexes, and to generate nanostructures that have practical “real-world” applications. DNA, for example has been used to create various complex 2D and 3D shapes and structures (Nangreave et al. 2010). However, proteins might make a more effective building block. They are principally used by nature to form great and complex structures (Alberts 1998). In fact, the bulk dry mass of a cell is made up by proteins and nearly every process carried out in a cell, is carried out through the collaboration and assembly of many proteins (Alberts 1998). Therefore, in terms of their functional properties, proteins are extremely diverse and versatile. This versatility can be extended to their physical and structural properties too because their functionality is determined through their tertiary structure (Nelson & Cox 2005b).

For this particular study, I considered the cytoskeleton to be a considerably attractive toolbox as a source of building components. Cytoskeletal proteins are known to have very dynamic mechanical properties. They provide stability to the cell and maintain cell shape, behaving rather like an internal scaffolding system, while, somewhat paradoxically, they co-ordinate forces that allow the cell to move and change shape (Fletcher & Mullins 2010). These functions indicate properties of great versatility and strength; important properties that I would consider to be necessary in a building block.

From this cytoskeletal toolbox, I choose two proteins to construct with; α -actinin 2 and erythroid α - and β -spectrin, particularly their spectrin repeats that make up

their central region (dimerisation domains). As an important architectural member of the sarcomeric Z-disc and the red cell membrane respectively (Gautel & Djinojic-Carugo 2016; Gratzner 1981; Luther 1991), I propose that both actinin and spectrin proteins could also act as such in an unnatural synthetic structure.

4.2.1 Approaches and Principles for Designing Protein Nanostructures

There are many ways in which proteins can be manipulated into forming higher order complex structures. Ligand-mediated assembly is one such approach, it exploits the high affinity interaction between small molecules and their receptor to bring about protein assembly (Fegan et al. 2010; King & Lai 2013). Metal-directed protein assembly is another approach, this method gains from metal co-ordination and the ability of certain metal ions to bind to specific proteins and, for example, direct their folding or link proteins together in multiprotein complexes (Salgado et al. 2010). The fusion-based assembly method is another technique that has been very successful in the creation of protein nanostructures. It involves the creation of protein chimeras, through the fusion of two protein oligomerisation domains into the one protein chain (Padilla et al. 2001; King & Lai 2013) (see section 1.2.5).

Taking advantage of the ability of telethonin to crosslink and associate with titin, Bruning et al. (2010) used the fusion-protein strategy to create a protein nanoscaffold, with the potential to display particular nanoparticles. Assembly was brought about through the use of two building blocks; one being a fusion protein consisting of two copies of the two N-terminal telethonin binding Ig-domains of titin, Z1Z2, separated from each other with a rationally designed linker (Z1Z2-Z1Z2), and the other building block being a truncated variant of the telethonin protein; made up of only its titin interacting region. The availability of two titin domains for telethonin binding on the one protein molecule made it possible for telethonin to crosslink these fusion proteins in a staggered fashion that lead to the formation of a long nanofibre.

Another study also used the fusion-based strategy to create a protein cage (Padilla et al. 2001). This study exploited the self-associative properties of two proteins, bromoperoxidase, a protein which forms trimers with itself, and the M1

matrix protein of the influenza virus, a protein which forms dimers with itself. A protein cage was assembled from the interaction between fusion proteins made up of one of each of these protein domains separated with a helical linker.

Although the functions of actinin-2 in the sarcomeric Z-disc imply that this protein has great structural strength, this was not my only reason for choosing this protein as my first building block, although both reasons are inherently linked (discussed below). Actinin has the ability to form dimers with itself, a dimerisation which is mediated by its central rod domain (Ylänne et al. 2001; Djinović-Carugo et al. 1999). This means that the actinin dimer exhibits two-fold symmetry (Ylänne et al. 2001). In nature, the majority of assembled protein complexes are symmetrical, meaning that through evolution, they have acquired self-complementary shapes (King & Lai 2013; Villar et al. 2009; Goodsell & Olson 2000). The large volume of naturally symmetrical protein complexes in the present day cell would suggest that symmetrical complexes offer an evolutionary advantage over asymmetrical complexes, or simple single protein monomers (Goodsell & Olson 2000). Apart from the obvious advantages of symmetric assemblies to the cell or organism; better coding efficiency, greater translational error control, and an improved regulation over the assembly process, one of the main advantages offered to the protein, or protein complex itself, is stability (Goodsell & Olson 2000). It has been said that the lowest energy state of an assembly is a symmetrical one (Goodsell & Olson 2000). A symmetrical complex is said to be more stable because its folding requires less interaction interfaces than the folding of asymmetric complexes (Lai et al. 2012). This means that there are less kinetic barriers to overcome during the folding process (Goodsell & Olson 2000). Also, large protein complexes tend to have a reduced surface area, which is said to protect them from degradation (Goodsell & Olson 2000).

From a design perspective, it seemed logical that my protein based nanostructure should take into account the principles of symmetry, and from a practical point of view, this made sense. Symmetry would allow the possible creation of a large structure using only a small number of proteins, or interaction interfaces.

4.2.2 Objectives

In the first part of this study I evaluate a fusion-based strategy for assembling protein complexes involving the fusion of two homodimeric proteins domains, that would naturally oligomerise with each other, into a single protein molecule, in this case, the fusion of two actinin-2 rod domains.

In the second part of this study, I evaluate a fusion-based strategy for assembling protein complexes involving the fusion of homodimeric and heterodimeric protein domains, domains that would not naturally oligomerise with each other, in a single protein molecule, in this case, fusion of the actinin rod domain with either a truncated α -spectrin protein or a truncated β -spectrin protein, each consisting of only four spectrin repeats.

Ultimately, through the use of a fusion-based assembly strategy that leads to the creation of very promising bivalent and tetravalent building blocks, I demonstrate the possibility of using spectrin-like and spectrin repeats from actinin and spectrin respectively to build large complex protein assemblies, that might, one day, have the potential to be utilised in the synthetic biology discipline.

4.3 Materials and Methods

4.3.1 cDNA constructs and Plasmid Construction

4.3.1.1 Actinin and Spectrin cDNA Constructs

All actinin constructs in this chapter correspond to residues 274-746 of the human muscle actinin-2 (calcium insensitive) isoform, GeneBank sequence NM_001103. This region contains spectrin-like repeats 1-4.

All α -spectrin constructs correspond to residues 1818-2259 of the human erythrocytic α -spectrin, GeneBank sequence NM_003126. This region contains spectrin repeats 18-21.

All β -spectrin constructs correspond to residues 293-743 of the human erythrocytic β -spectrin transcript variant 1, GeneBank sequence NM_001024858. This region contains spectrin repeats 1-4.

Two sets of primers (Integrated DNA Technologies, Inc., Leuven, Belgium) were designed for actinin r1-r4 construct amplification; one set to yield a product with an EcoRI site at its 5' end, and XhoI and HindIII sites at its 3' end. The other set, to yield a product with EcoRI and SacII sites at its 5' end, and KpnI and Sall sites at its 3' end (Fig. 4.1)

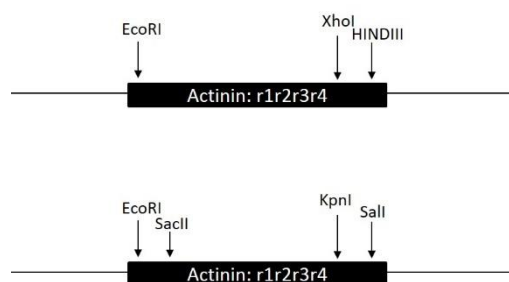


Figure 4.1: Strategy for Cloning Actinin cDNA Constructs. Restriction sites employed for the cloning of actinin-2 constructs.

The primers to amplify the α -spectrin: r18-r21 construct were designed to yield a product with BglII and Ascl sites at its 5' end and Sall and XhoI sites at its 3' end.

The primers to amplify the β -spectrin: r1-r4 construct were designed to yield a product with a EcoRI site at its 5' end, and Sall and HindIII sites at its 3' end (Fig 4.2).

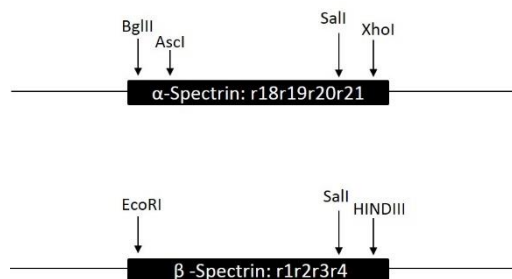


Figure 4.2: Strategy for Cloning Spectrin Constructs. Restriction sites employed for the cloning of α -Spectrin and β -Spectrin constructs.

4.3.1.2 Homodimeric Fusion Protein Construction

Homodimeric fusion proteins containing two actinin rod domains (r1r2r3r4) joined by a linker region were constructed through sequential cloning steps. Initially, actinin r1r2r3r4 was introduced into the commercially available pCDF-Duet plasmid (see appendix for plasmid map) twice as two separate preparations, as follows: MCS1 (EcoRI and HindIII) and MCS2 of the pCDF-Duet plasmid (EcoRI and Sall; making use of compatible cohesive end ligation with plasmid sites Mfe I and XhoI, respectively). Using EcoRI and HindII restriction sites, actinin r1r2r3r4 was then excised from the first plasmid preparation, and sub-cloned into the second, using the same restriction sites.

In respect to designing linker regions, the PBD file 1HCL was examined. This file exhibited two extra serine residues in the N-terminus of actinin's spectrin-like repeat 1 and one extra aspartic acid in the C-terminus of its spectrin-like repeat 4, that are not encoded for in the gene sequence. Linkers in Section 4.4.1.1.1 accommodated these extra residues, but linkers designed thereafter only continually accommodated the aspartic acid residue.

Oligonucleotides encoding for desired linker sequence (Integrated DNA Technologies, Inc., Leuven, Belgium) were designed to contain XhoI and SacII overhangs so to allow for introduction to the pCDF-Duet plasmid containing actinin r1r2r3r4 in each MCS. All linkers were designed as such, excepting the four short

linkers in section 4.4.1.1.2; -no linker-, -D- and -DS-. These three linkers were created through XhoI enzymatic plasmid digestion of the longer, rigid linkers of the that section; -DIPPR-, -DISRD- and -DISRDS, with subsequent re-ligation.

All construct design strategies incorporated the N-terminal 6xHis tag encoded by its gene sequence located in MCS1 of both pCDF/pRSF plasmids.

4.3.1.3 Orthogonal Homodimeric Fusion-Protein Construction

Actinin rod domain proteins with one, two or three amino acid insertions between repeat 2 and repeat 3 were generated using site directed mutagenesis with primer extension. Three mutagenic primers were designed, each encoding for one of the three desired amino acid insertions; p.L238_E239insL, p.L238_E239insLL and p.L238_E239insKLL. For each mutational insertion, three PCR reactions were carried out. Two nested PCR reactions; one reaction with the EcoRI actinin r1r4 forward primer and mid-actinin reverse primer, the next reaction with the SalIKpnI actinin r1r4 R primer and one of the three forward mutational primers, generated two DNA fragments with overlapping ends. Hybridisation between the complementary overlapping 3' ends of each fragment in the subsequent PCR fusion reaction, with the EcoRI actinin r1r4 forward primer and the SalIKpnI actinin r1r4 R primer generated the final full length product.

Orthogonal homodimeric fusion-proteins, containing one of these p.L238_E239insL, p.L238_E239insLL or p.L238_E239insKLL actinin rod domains and one WT actinin rod domain, were created through replacement of one of the WT actinin rod domains in constructs containing the -DSS- linker and -D9xGSS- linker, using restriction sites EcoRI and HindIII.

4.3.1.4 Heterodimeric-to-Homodimeric Fusion Protein Construction

Heterodimeric-to-Homodimeric fusion-proteins with flexible linkers (section 4.4.2.1) containing truncated spectrin proteins (four spectrin repeats; α -r18r19r20r21/ β -r1r2r3r4) and an actinin rod domain (r1r2r3r4) were created through sub-cloning steps in which actinin r1r2r3r4 in MCS1 of constructs containing the -D12xGSS- linker was replaced with either spectrin α -r18r19r20r21; using compatible cohesive end ligation involving BglII and XhoI with BamHI and SalI

respectively, or spectrin β -r18r19r21r22; using the EcoRI site, and compatible cohesive end ligation between Sall and XhoI sites.

11 heterodimeric-to-homodimeric fusion proteins with rigid helical linkers (Section 4.4.2.2) containing truncated spectrin proteins (four spectrin repeats; α -r18r19r20r21/ β -r1r2r3r4) and actinin rod domains (r1r2r3r4) were created through sequential cloning steps. Using PCR amplification, 11 different actinin r1r2r3r4 constructs were produced each juxtaposed to a XhoI site, followed by a sequence encoding for helical linkers of varying length, by use of 11 different forward primers. One of these forward primers was designed to produce a direct fusion between α -/ β -spectrin and actinin. A common reverse primer placed XmaI, PaeI and HindIII site at the 3' end of these actinin r1r2r3r4 constructs. Using XhoI and PaeI sites, each of the 11 actinin constructs were cloned into Sall and Pac I digested pCDF and pRSF Duet plasmids containing either α -spectrin r18r19r20r21 or β -spectrin r1r2r3r4 their MCS1. The cohesive annealing of XhoI and Sall sites encoded for a short two amino acid sequence consisting of serine and arginine. All helical linker sequences started with this short sequence, including the construct presumed to be a direct fusion.

All construct design strategies incorporated the N-terminal 6xHis tag encode in MCS1 of both pCDF/pRSF plasmids

Constructs containing one actinin rod domain centred between two spectrin rod domains were created through several cloning steps. α -r18r19r20r21 and β -r1r2r3r4 with 6xGly N-terminal linker sequences and appropriate flanking restriction sites were first synthesised (Integrated DNA Technologies).

A 6xHis- α -spectrin r18r19r20r21-actinin r1r2r3r4- α -spectrin r18r19r20r21 construct was created by cloning the 6xGly- α -Spectrin r18r19r20r21 sequence at the 3' end of an 6xHis- α -spectrin r18r19r20r21-6xGly-actinin r1r2r3r4 construct in the pCDF Duet plasmid using the sites KpnI and PaeI.

A 6xHis- β -spectrin r1r2r3r4-actinin r1r2r3r4- β -spectrin r1r2r3r4 construct was created by first cloning the 6xGly- β -spectrin r1r2r3r4 at the 3' end of a 6xHis- β -spectrin r1r2r3r4 construct in the pRSF Duet plasmid using Sall and PaeI sites. Actinin r1r2r3r4 with 8xGly C-terminal linkers were then cloned in between the two β -spectrin r1r2r3r4 regions using Sall and SacI restriction sites.

4.3.2 Protein Expression and Purification

All constructs were transformed into *E. coli* [DE3] (Novagen, Quintin, France). Protein expression were induced at 37 °C by addition of 0.2mM IPTG and cells were harvested, through centrifugation, 4 hours post induction. Cell pellets were resuspended in PBS, 0.2% triton, 20mM β -mercaptoethanol and 1mM phenylmethylsulfonyl fluoride (PMSF). Cells were lysed by sonication and addition of 0.1mg/ml lysozyme for 30min at 4 °C. Lysates were cleared by centrifugation at 39,000xg for 40min at 4 °C.

All purifications were based on nickel immobilised metal affinity chromatography, as all constructs were designed to have a 6xHis tag on their N-terminal. Proteins were loaded onto a Ni-column pre-equilibrated with Ni-wash buffer (0.5M NaCl, 50mM KPO_4 pH 8.0, 20mM β -mercaptoethanol, 5mM imidazole, 0.1% triton). Columns were washed three times with 10ml wash buffer. Bound proteins were eluted in 200mM imidazole pH7, with 20mM β -mercaptoethanol.

4.3.3 Size Exclusion Chromatography

Size exclusion chromatography was performed on an AKTA FPLC system. A Supradex 200 column (GE Healthcare) was used, equilibrated with buffer A (20mM Tris pH 7.5, 150mM NaCl and 0.5mM DTT) at a flow rate of 0.2ml/min. Samples were injected at a volume of 0.4ml.

4.3.4 Native Gel Electrophoresis

Native protein gel electrophoresis set up was as per the standard polyacrylamide gel electrophoresis protocol, with the exception that SDS, β -mercaptoethanol and boiling steps were omitted.

Section 4.4.2.2 required the mixing of corresponding heterodimeric to homodimeric fusion proteins prior to native gel electrophoresis. 0.5 μ M of each protein in each pair was mixed and left to incubate overnight at 4 °C.

Gel loading buffer (without β -mercaptoethanol and SDS) was added to all proteins and protein mixes on ice. Samples were then loaded onto 5% native gels

(prepared without SDS). Samples were run in native gel running buffer (without SDS) at 4 °C. Both the separating gel and gel running buffer were designed to have an approx. pH of 8-9, and stacking gel was designed to have a pH of 6.8 as per standard denaturing protocol.

4.3.5 Transmission Electron Microscopy

Protein solutions (between 0.1 and 1mg/ml) were deposited onto carbon grids. The loaded grids were blotted with filter paper and then negatively stained using 2% uranyl acetate or 2% phosphotungstic acid. Grids were then blotted again with filter paper, and allowed to air dry. Electron microscopy was carried out with a Jeol 2000FXII transmission electron microscope.

4.4 Results

4.4.1 Evaluation of Fusion-based Assembly Strategy Employing Two Homodimeric Oligomerisation Domains

This first strategy consisted of two components; the protein building blocks, i.e. repeated actinin rod domains (r1r2r3r4), and a linker peptide, designed to connect the two rod domains to each other, ultimately creating homodimeric actinin rod fusion proteins.

In this section I set out to assess the fusion-based assembly strategy with actinin rod domain proteins, and determine which type linker, flexible or short/rigid, would best suit this type of protein assembly approach.

With this strategy, two homodimeric actinin rod domains are genetically fused into a single protein chain (Fig. 4.3A). Staggered interaction between the actinin rod domains in different proteins chains should produce symmetrical bivalent building blocks (Fig. 4.3B). These building blocks are desirable; concatenation of many of these building blocks would bring about the assembly of higher order oligomers or polymers. However, aligned interactions between the actinin rod domains in different proteins chains could also occur. (Fig. 4.3C), or, the actinin rod domains in the same protein chain could fold back on each other and form a monomeric unit (Fig. 4.3D). These interactions are not desirable as the structures formed are not capable of any further self-assembly. Optimisation of linker design was necessary to prevent the formation of such structures.

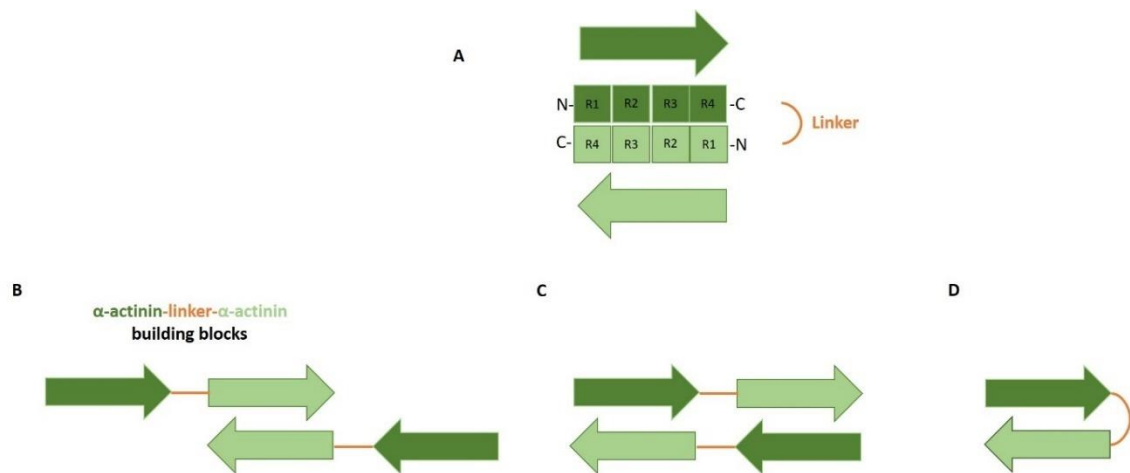


Figure 4.3: Fusion-based Strategy Employing Two Homodimeric Actinin Rod Domains.

(A) In nature, actinin dimerises with itself through its spectrin-like rod domain. Two actinin rod domains (r1r2r3r4) would be connected to each other using a designed linker peptide that would connect to the C-terminus of one rod domain and to the N-terminus of the next, thereby connecting the two actinin rod domains.

(B) Staggered homodimerisation between actinin rod domains in different protein chains is desirable as it would produce symmetrical bivalent building blocks.

(C) Aligned homodimerisation between two actinin rod domains in two different protein chains could also occur. These are not desirable

(D) Interactions between actinin rod domains in the same protein chain would bring about formation of the monomeric unit. This is not desirable.

4.4.1.1 Assessment of Fusion-protein Linkers

Linkers are short peptide sequences that are commonly employed by nature to separate the domains in single protein molecules. Generally, these linkers can take two forms; flexible or rigid (Reddy Chichili et al. 2013).

4.4.1.1.1 Connection of Two Homodimeric Oligomerisation Domains using Flexible Linkers

Five flexible linkers (Fig.4.4) that were each made up of varying numbers of glycine residues were designed. The objective was to see if varying linker length could favour staggered homodimers (Fig. 4.3B) over other possibilities, such as aligned dimers (Fig. 4.3C).

The use of a flexible glycine linker might allow the adjacent actinin rod domains to be able to move and manoeuvre relative to each other and assemble into structures that are compatible with the symmetry that is inherent to its natural quaternary structure. Glycine-rich linkers are known to be quite flexible; glycine is very small in size as it lacks a bulky R group, as a result, it experiences a large

amount of conformational freedom about its backbone. Consequently, glycine linkers are known not to interfere with the functional or physical properties of the proteins to which they are attached (Reddy Chichili et al. 2013).

One very short linker was designed to contain no glycine residues, but the presence of two serine residues might invoke a certain degree of flexibility due to their small size (Chen et al. 2014).

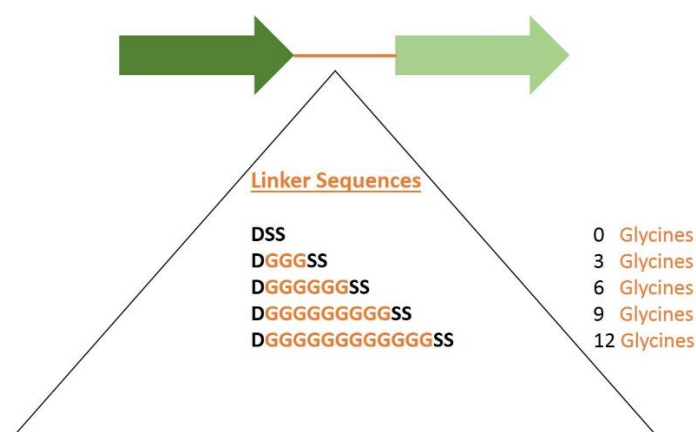


Figure 4.4: Design Strategy for Homodimeric Fusion Proteins with Glycine Flexible Linkers.

A number of homodimeric fusion proteins were designed. Each consisted of two actinin rod domains (r1r2r3r4) separated from each other through one of a number of flexible linkers. These flexible linkers were made up of varying amounts of glycine residues, from none at all up to 12. The PDB file (1HCL) which was used to study the 3D structure of the actinin-2 rod domain contained two extra serine residues in the N-terminus of its spectrin-like repeat 1 and one extra aspartic acid residue in the C-terminus of spectrin-like repeat 4, that are not encoded for in the gene sequence. Linkers in this section were designed to accommodate these three extra residues.

Constructs were designed to contain a 6xHis-tag, and were created through three sequential cloning steps; intermediate plasmid containing one actinin rod domain to intermediate plasmid containing two actinin rod domains to, finally, plasmid containing two actinin rod domains separated with a flexible glycine linker. All homodimeric actinin rod domain fusion proteins were expressed and purified in soluble form with a reasonably high yield. Mild degradation was noted (Fig. 4.5A).

Fusion proteins were analysed using native gel electrophoresis. (Fig. 4.5B). In native gel electrophoresis, protein samples are prepared in non-denaturing, non-reducing conditions, allowing the protein retain its folded conformation. Native gel electrophoresis was used to determine if new higher order structures were being

formed through assembly of the homodimeric actinin rod fusion proteins, and to characterise the homogeneity of these possible structures.

As a type of protein marker (Fig 4.5B; lane 1), a protein mix of His actinin rod domain (His r1r2r3r4; ~50kDa) and His MBP actinin rod domain (HIS MBP r1r2r3r4; ~100kDa) were loaded together. The three bands observed represent the three different types of assemblies that can form from this protein mix in non-denaturing conditions; homodimers made up of His r1r2r3r4:His r1r2r3r4 (~100kDa) or His MBP r1r2r3r4:His MBP r1r2r3r4 (~200kDa) and pseudoheterodimers made up of His r1r2r3r4:His MBP r1r2r3r4 (~150kDa).

In non-reducing, non-denaturing conditions the actinin rod domain retains the ability to interact with itself to form a homodimer. These homodimers are represented by the single band in (Fig. 4.5B; lane 2). Homodimeric actinin rod fusion proteins with long flexible glycine linkers (Fig. 4.5B; lanes 4-7) migrate to this same region expected for dimers. This suggests that they are forming the monomeric unit, as depicted in Fig. 4.3D. An alternative migration pattern is observed for the homodimeric actinin rod fusion protein containing no glycine residues (Fig. 4.5B; lane 3). These proteins migrate at a much slower pace, which is suggestive of the formation of higher order protein assemblies. The presence of two slowly migrating bands for this sample was indicative that the possible protein assemblies were not homogenous; at least two different types of protein complex were forming.

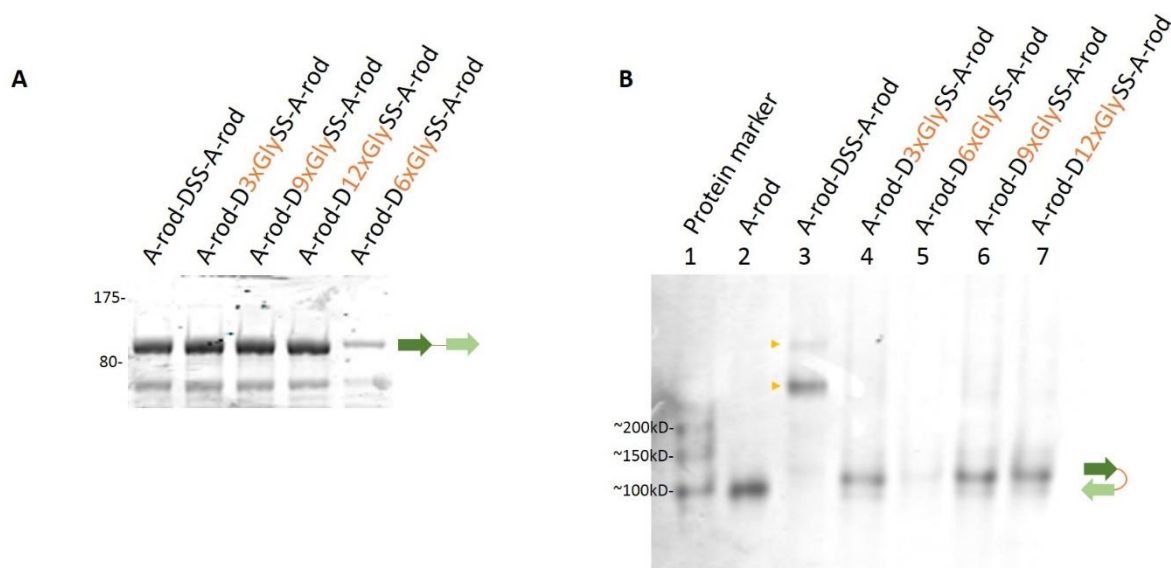


Figure 4.5: PAGE Analysis of Homodimeric Actinin rod Fusion Proteins with Flexible Linkers.

(A) Ni-column purification of fusion proteins was assessed using SDS protein gel electrophoresis followed by Coomassie Brilliant Blue staining.

Proteins of interest and the sizes (in kDa) of the relevant molecular weight markers are indicated.

(B) Purified homodimeric fusion proteins were analysed using native gel electrophoresis, followed by GelCode™ Blue Staining. A purified mix of His actinin rod domain and His MBP actinin rod domain proteins acts as a molecular weight marker (lane 1), and single actinin rod domain protein (lane 2) act as a maker of homodimer migration pattern.

Fusion proteins that contain glycine linkers of various lengths (3-12 residues; lanes 4-7) migrate to the same region as single actinin rod domain proteins (lane 2) i.e. migrating to the region expected for dimers. An altered migration pattern is observed for the fusion protein with a short linker comprised of the residues -DSS- (lane 3).

▶ symbol indicates migration of possible higher order structures.

n=3 (-DSS- proteins)

n=2 (-D3xGlySS-, -D6xGlySS-, -D9xGlySS-, -D12xGlySS- proteins)

4.4.1.1.2. Connection of two Homodimeric Oligomerisation Domains using Short and Rigid Linkers

Seven more different linkers (Fig. 4.6) were designed, three of which were intended to be rigid enough to prevent the actinin rod domains in one protein chain folding back to form the monomeric unit.

Two of these seven linkers made use of amino acids that have a strong tendency to form rigid alpha-helical structures, amino acids such as aspartic acid, serine, arginine and glutamic acid. These amino acids are also commonly seen in nature as separators of domains in multi-domain proteins. Each spectrin repeat is comprised of a triple helical coiled-coil bundle (Yan et al. 1993), meaning that in the actinin rod domain, repeat 1 begins and repeat 4 ends with a helical structure. Designing linkers that also adopt a helical structure would result in a continuous

alpha-helix running from one domain to the next, the result of which might mean a more stable and rigid conformation.

One of these linkers incorporated two prolines. Proline is a very unique amino acid that is commonly found in many natural linkers where it is known to cause the formation of rigid structural linkers, without impinging on the natural functions of the proteins. With such a bulky cyclic side chain, the possible number of conformations that can form in its presence are limited. Also, it has a reduced capacity to form hydrogen bonds with other amino acids, its presence therefore reduces the likelihood of an interaction between the linker and the protein domains, which, altogether, should increase the stiffness of the linker (Chen et al. 2014; Reddy Chichili et al. 2013).

The remaining four, of the seven linkers, were designed to be very short, and while two of them contained serine and/or glycine residues, making them slightly more flexible than the rest, it was anticipated that their shorter length might inhibit interaction between the two actinin rod domains in the same protein chain, overall, making the protein more rigid. Results from section 4.4.1.1.1 indicated that a linker length of between three and six amino acids might be short and rigid enough to do so. In fact, in hindsight, the homodimeric actinin rod-DSS-actinin rod fusion protein described in section 4.4.1.1.1 would be better categorised here as a short/rigid linker.

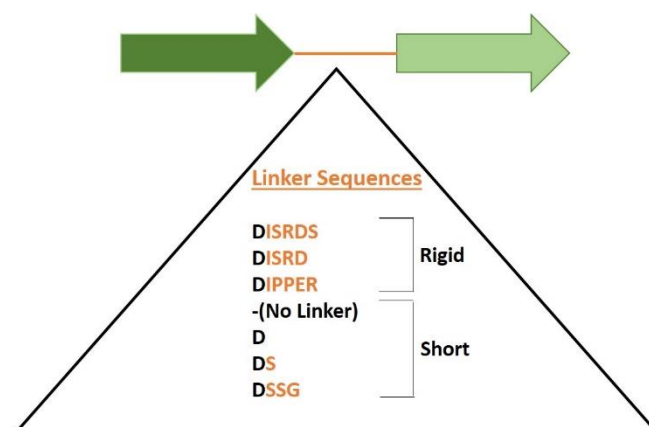


Figure 4.6: Design Strategy Homodimeric Fusion Proteins with Rigid and Short Linkers.

A number of homodimeric fusion proteins, each consisting of two actinin rod domains (r1r2r3r4) separated from each other through one of a number of rigid or short linkers. Three rigid linkers each consisting of a number of amino acids with a high tendency to form alpha-helical or coiled-coil structures and four short linkers, one being a direct fusion of one actinin rod domain to the next were designed.

In the set of flexible linkers (section 4.4.1.1.1) the two extra serine residues in the N-terminus of the actinin rod domain and the one extra aspartic acid in its C-terminus, that were contained in the PDB file (1HCL), were accommodated. For this set of rigid and short linkers, the two serine residues were not accommodated in all the linkers; serine is a small amino acid, and therefore exhibits great conformational flexibility (Chen et al. 2014). It was thought that the presence of serine in these linkers might encourage interaction between the actinin rod domains in a single polypeptide chain.

Constructs were designed to contain a 6xHis-tag, and were created through sequential cloning steps. All but one construct, actinin rod-DISRDS-actinin rod, expressed well, in soluble form in *E. coli* cells. All homodimeric actinin rod fusion proteins that expressed were purified using nickel column purification with a reasonable yield. Mild degradation was noted. (Fig. 4.7A).

Fusion proteins were subjected to native gel electrophoresis (Fig. 4.7B) to assess their assembly state and to characterise their homogeneity. In native gel images in Fig. 4.7B, homodimers formed through the interaction of single actinin rod domains are represented with the single band in lane 1. Fusion protein samples in remaining lanes (lanes 2-4 and 5-7) do not appear as clearly resolved. The presence of an increasing smear may be suggestive that the samples are very heterogeneous, perhaps an increasing amount of polymerisation is occurring within the samples. The presence of a few slowly migrating sharp bands within these samples are noted. These bands may be indicative of a more definite structure formation. However, the monomeric unit predominates with the majority of the

homodimeric fusion proteins within each sample migrating in the region expected for homodimer formation.

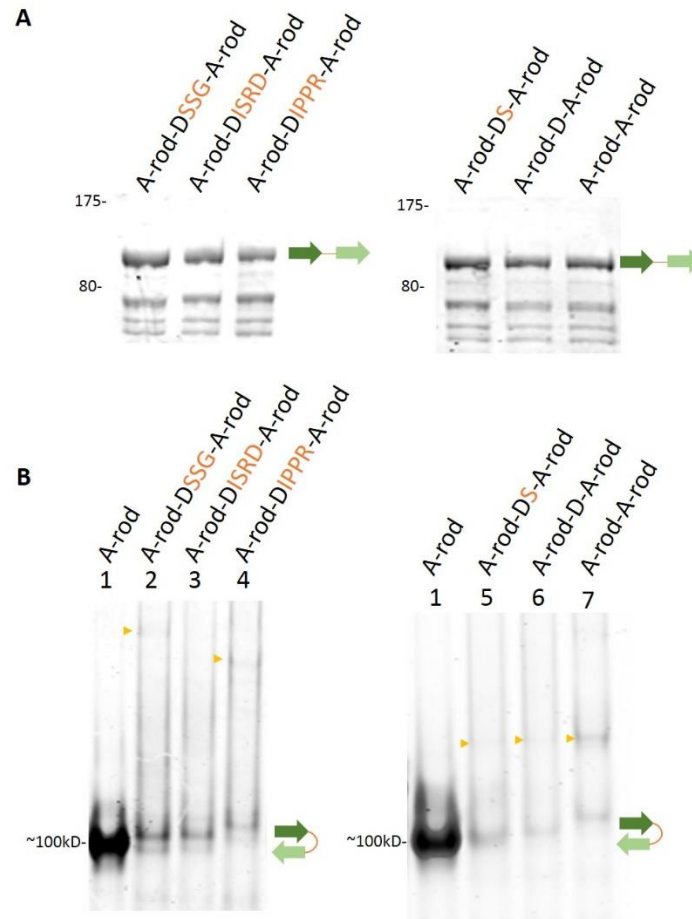


Figure 4.7: PAGE Analysis of Homodimeric Fusion Proteins with Rigid/Short linkers.

(A) Ni-column purification of fusion proteins was assessed using SDS protein gel electrophoresis, followed by Coomassie Brilliant Blue staining

Proteins of interest and the sizes (in kDa) of the relevant molecular weight markers are indicated.

(B) Purified fusion proteins were analysed using native gel electrophoresis followed by GelCode™ Blue Staining. Single actinin rod domain acts as a molecular weight marker, migrating at ~ 100kDa, and also acts as a marker of homodimer migration pattern.

For all fusion protein samples, sharp bands are noted to be migrating to the region expected for dimers. Smearing suggests that these fusion protein samples are not homogenous. Slowly migrating sharp bands are highlighted.

▶ symbol indicates migration of possible higher order structures.

A-rod = actinin rod domain (r1r2r3r4)

n=2 (-DISRD-, -DIPPR-, -no linker- proteins)

n=1 (-DSSG-, DS-, -D- proteins)

4.4.1.2 Analysis of Possible Protein Assemblies using Electron Microscopy

Native gel electrophoresis and the presence of slowly migrating bands in the fusion protein samples was evidence that some of these homodimeric actinin rod fusion proteins, particularly those with the shorter linkers, might be assembling into some form of higher order complex, and not just folding back on themselves, forming a monomeric unit. Fig. 4.8 is a schematic of the possible structures that could be forming through assembly of these fusion protein samples, depending on the properties of the linker peptide.

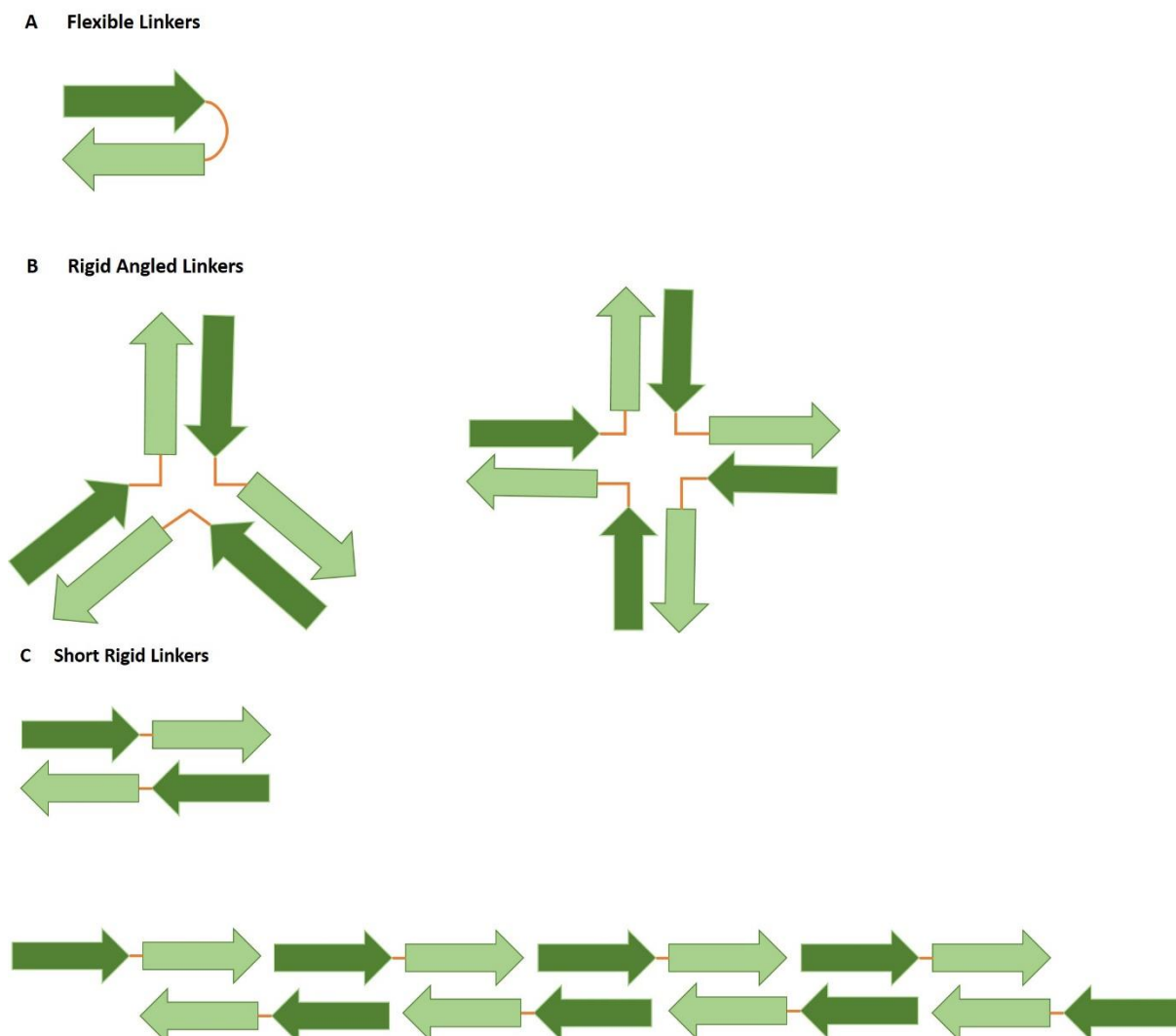


Figure 4.8: Graphic Representation of Possible Homodimeric Actinin Rod Fusion-Protein Assemblies.

(A) Long, flexible linkers might allow the actinin rod domains in one protein chain to fold back and interact with each other, forming a dimer.

(B) Linkers designed with a bend or kink, such as those containing the proline amino acid, -DIPPR-linker, might induce the formation of such trimeric and tetrameric structures.

(C) Short rigid filaments might allow the homodimeric actinin rod fusion proteins to concatamerise into long polymeric filaments.

In order to assess the shape or pattern of possible protein complexes, three of the 12 different homodimeric actinin rod fusion proteins, actinin rod-DSS-actinin rod, actinin rod-DIPPR-actinin rod and actinin rod-actinin rod, were chosen to be further analysed using negative-stain electron microscopy.

Prior to staining, a sample of each protein preparation was subjected to SDS and native gel electrophoresis to verify their behaviour, i.e. the presence of slowly

migrating bands on native gels confirmed that they were still forming higher order structures (Fig. 4.9)

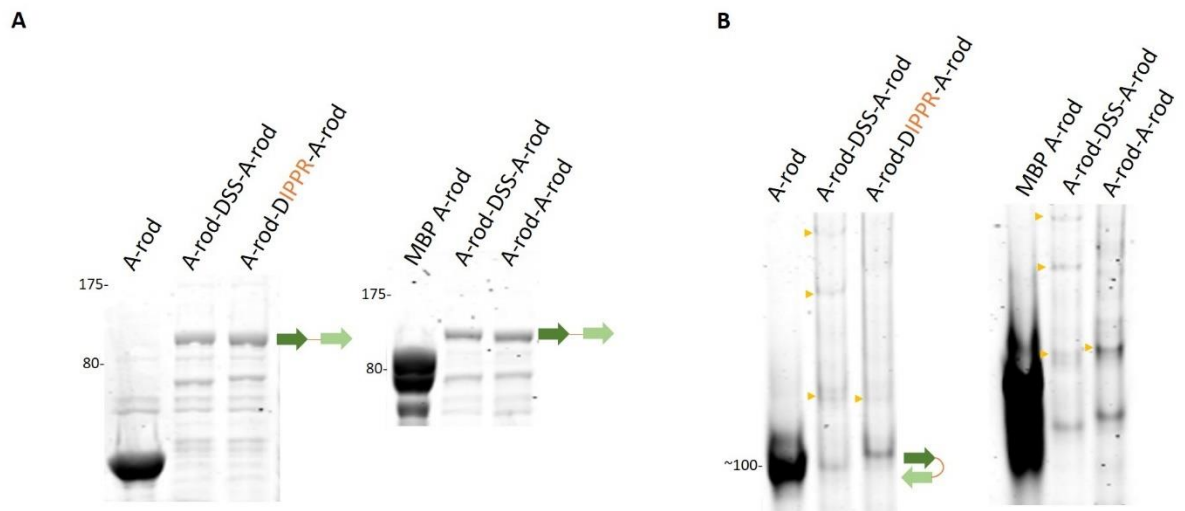


Figure 4.9: PAGE Analysis of Homodimeric Actinin Rod Fusion Proteins.

Prior to negative staining all proteins were assessed using protein gel electrophoresis.

(A) SDS protein gel electrophoresis followed by Coomassie Brilliant Blue staining.

Mild degradation is noted for all fusion protein samples.

Proteins of interest and the sizes (in kDa) of the relevant marker bands are indicated.

(B) Native gel electrophoresis followed by GelCode™ Blue Staining. Single actinin rod domain acts as a molecular weight marker, migrating at ~ 100kDa, and also acts as a marker of homodimer migration pattern.

For all fusion-protein samples, sharp bands are noted to be migrating to the region expected for dimers. Slowly migrating sharp bands are highlighted.

▶ symbol indicates migration of possible higher order structures.

A-rod = actinin rod domain (r1r2r3r4).

Previous studies had documented the staining of the Actinin rod domain with the uranyl acetate (UA) negative stain (Winkler et al. 1997).

In UA samples the protein appears light against a dark background of stain. (Fig. 4.10). Negatively stained His tagged actinin rod domain and negatively stained MBP tagged actinin rod domain acted as the controls.

Long filamentous-type structures are noted for the actinin rod domain controls. Homodimeric actinin rod fusion protein with short linker, comprised of amino acid residues -DSS-, also appears to be forming these structures, however they are not as widespread. Remaining two homodimeric actinin rod fusion protein samples, fusion protein with long linker comprised of amino acid residues -DIPPR- and fusion protein with no linker, appear to be very heterogeneous. Proteins are collected in small aggregates and structures do not appear to be as distinct as those seen for control samples.

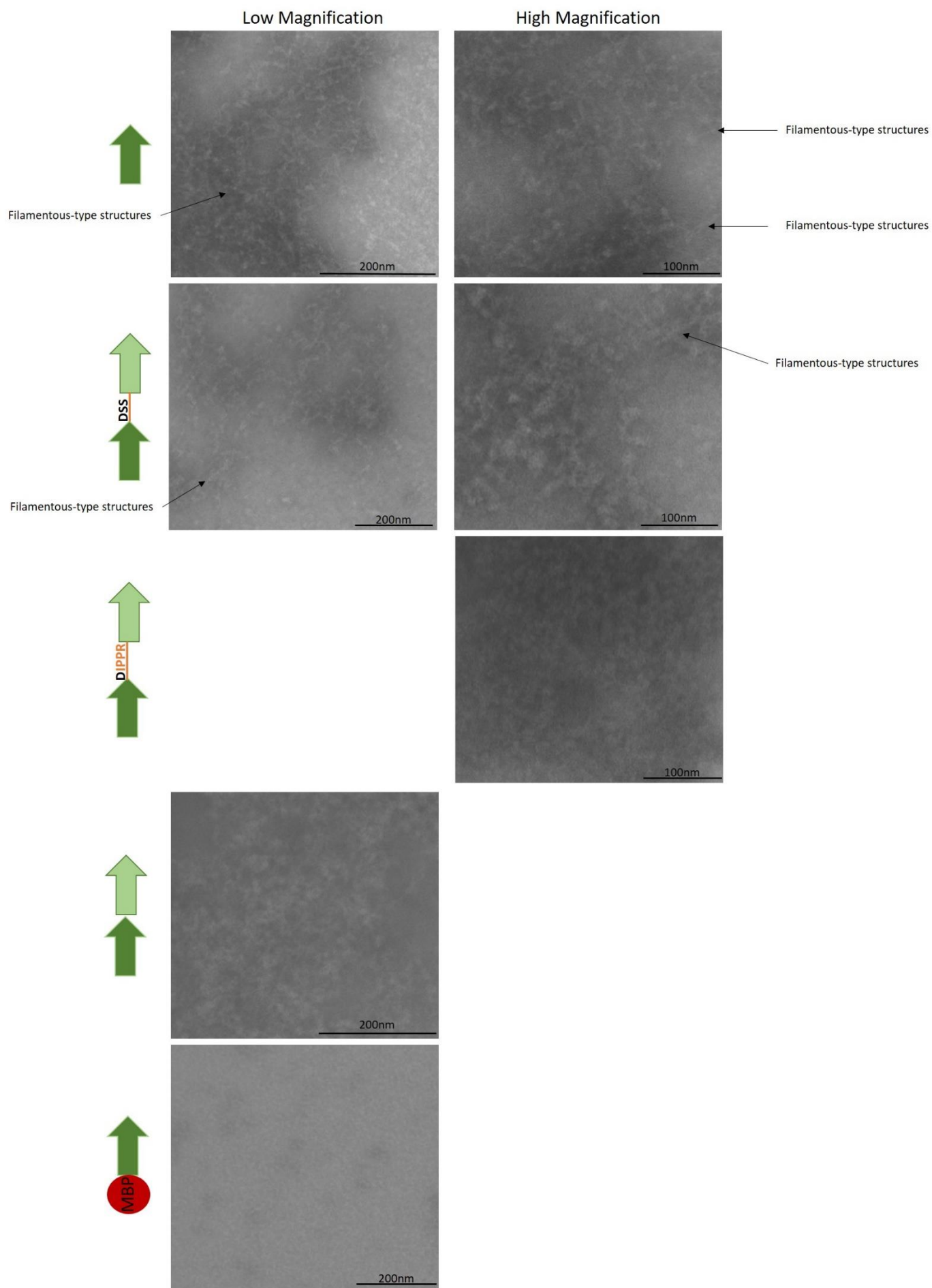


Figure 4.10: Representative Electron Micrographs from Analysis of UA Negatively Stained Homodimeric Fusion Protein Assemblies.

Distinct filamentous structures are observed in actinin rod control samples. Similar type structures are observed in homodimeric fusion protein sample with short linker comprised of amino acid residues -DSS-. Homodimeric fusion protein sample with long linker comprised of amino acids residues -DIPPR- and homodimeric fusion protein sample with no linker both appear to be very heterogeneous, with small collections of protein aggregates.

Arrows point to a few observable filamentous-type structures.

Low magnification: 100-150k

High Magnification: 200-250k

n=3

To investigate the contribution of the UA stain to the heterogeneity observed, another round of EM was undertaken, this time using the negative stain phosphotungstic acid (PTA). Previous studies had also documented the staining of the actinin rod domain with the PTA negative stain (Suzuki et al. 1976).

Negatively stained His tagged actinin rod domain and negatively stained MBP tagged actinin rod domain acted as the controls. In PTA stained samples proteins appear light against a dark background of stain (Fig. 4.11). Images obtained with PTA staining were quite similar to those obtained with UA staining. Long filamentous type structures are again noted for the actinin rod control. Homodimeric fusion protein samples appear to be heterogeneous, but it is possible to discern a few filamentous-type structures in these samples too.

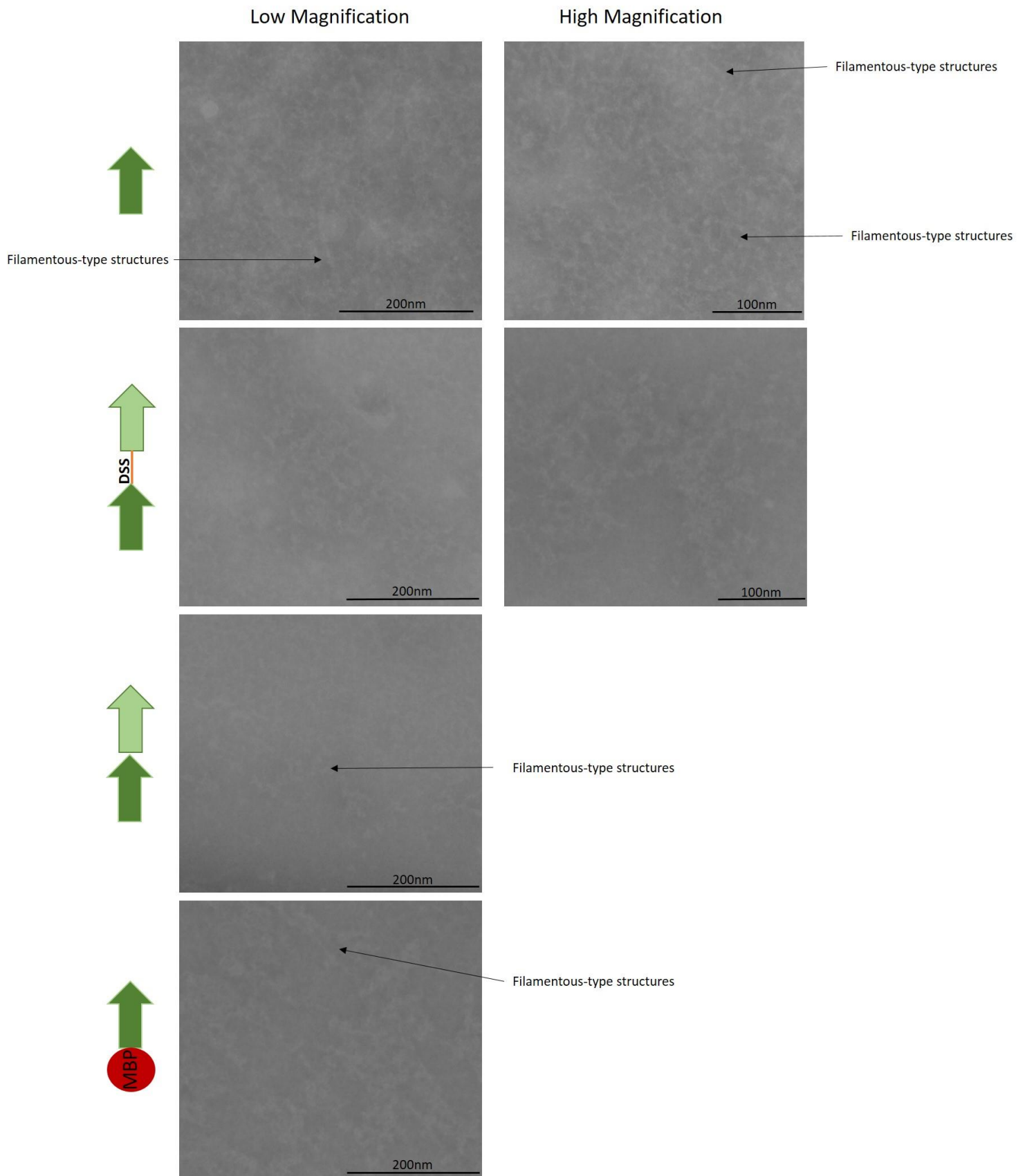


Figure 4.11: Representative Electron Micrographs from Analysis of PTA Negatively Stained Homodimeric Fusion Proteins Assemblies.

Distinct filamentous structures are observed in actinin rod control samples. Homodimeric fusion protein sample with short linker comprised of amino acids residues -DSS- and homodimeric fusion protein sample with no linker both appear to be very heterogeneous, with small collections of protein aggregates and a limited number of filamentous type structures.

Arrows point to a few filamentous-type structures.

Low magnification: 100-150k

High Magnification: 200-250k

n=2

Both the length and the diameter of the actinin rod domain have already been determined as being 25nm and 4nm respectively (Imamura et al. 1988). The filamentous structures observed in this study, especially those in the actinin rod domain controls, are both wider and longer than these reported molecular measurements.

4.4.1.3. Generation of Orthogonal Homodimeric Actinin Rod Fusion Proteins

Up to this point, the homodimeric fusion proteins, two actinin rod domains separated with a series of different linkers, all had a very high tendency to fold back and form a monomeric unit, making them unavailable to interact with copies of themselves. The formation of this monomeric unit greatly limited the number and type of other protein complexes that could assemble.

In this section, I aimed to create a series of actinin rod fusion proteins that could not form this monomeric unit (i.e. the actinin rod domains within the same protein chain would be orthogonal to each other in terms of their ability to dimerise) and therefore, would be forced to interact with copies of themselves in a staggered arrangement to produce a long concatemer (Fig. 4.13B), rather the monomeric unit (Fig. 4.13A).

The helical linker region connecting repeat 2 to repeat 3 (Fig. 4.12) in the centre region of the actinin rod domain is known to be its centre of symmetry and it defines the orientation of these two repeats (Djinović-Carugo et al. 1999). I sought to alter the orientation of these repeats, and in doing so alter the orientation of the entire rod domain, in such a way that these mutant actinin rod domains could no longer interact with WT actinin rod domains, but could interact with copies of themselves. The actinin rod domain exhibits a twist of $\sim 90^\circ$. I anticipated that by inserting extra amino acids into this helical linker region I would alter the twist of

the rod. The presence of an altered twist, and the fact that repeats two and three would now be separated from each other by a greater distance, should change the orientation of the repeats within the actinin rod domain in such a way that the mutated rod domains would dimerise with themselves but not with the WT actinin rod domain.

The insertional amino acids were chosen to be lysine (K) and leucine (L) residues. A portion of the natural helical linker between repeats 2 and 3 is made up of one K residue and two L residues. These two L residues make up a hydrophobic bundle. Interactions between this hydrophobic bundle and repeats 2 and 3 are known to have a stabilising effect on the actinin homodimer (Djinović-Carugo et al. 1999). By choosing these same amino acids to insert into the linker the stabilising interactions should be maintained, and the ability of the mutant rod domains to interact with themselves should also be maintained.

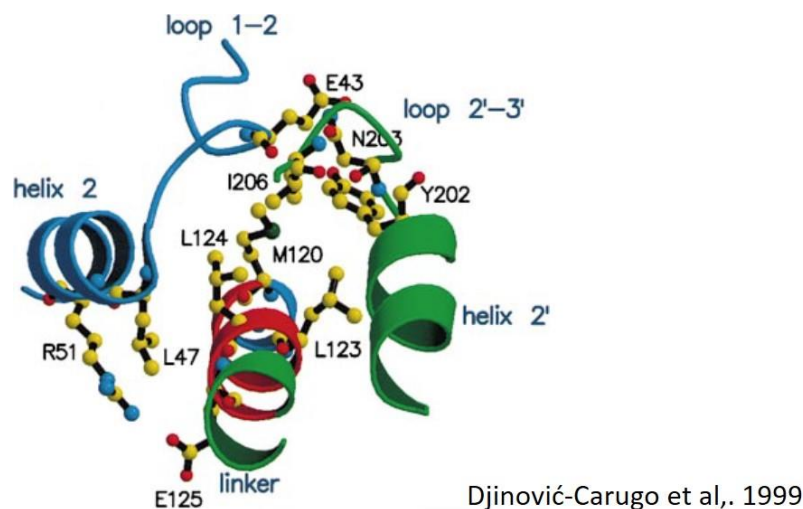


Figure 4.12: Helical Linker Region Between Spectrin-like Repeats Two and Three.

In respect to this image, amino acid insertions of L, LL, or KLL were between residues L124 and E125. Stabilising Interactions between the linker and repeats two and three are centred at the hydrophobic cluster consisting of leucine residues 123 and 124.

Amino acids are drawn in a ball and stick representation. Protein backbone is drawn in a ribbon formation of which the helical linker is coloured red, while repeats two and three are coloured blue and green respectively.

Using site directed mutagenesis, three modified actinin rod domain proteins were created, each differing from each other with the insertion of one, two or three amino acids, lysine (K), lysine and leucine (KL) or lysine, leucine and leucine (KLL),

p.L238_E239insL, p.L238_E239insLL and p.L238_E239insKLL. Each of the mutant actinin rod domains were fused to the WT actinin rod domain by means of either the short -DSS- linker or the flexible -D9xGlySS- linker (from section 4.4.1.1.1). The short -DSS linker had proven itself to already be conducive to the possible formation of higher order assemblies involving homodimeric actinin rod fusion proteins (Fig. 4.5B) and the -D9xGlySS- linker might be flexible enough to allow for the formation of higher order assemblies.



Figure 4.13: Schematic of Possible Outcome with Orthogonal Homodimeric Actinin Rod Fusion Proteins.

(A) Fusion-proteins created up to this point had a high tendency to fold back on themselves.
(B) Through fusing two orthogonal homodimeric actinin rod domains together with a previously designed linker (section 4.4.1.1) it was hoped that the actinin rod domains in one protein chain would be unable to interact with themselves, being orthogonal to each other, and be forced to interact with other fusion proteins in the sample.

All unfused single mutant actinin rod domains were expressed and purified (Fig. 4.14A) to high yields in soluble form. Analysis through native gel electrophoresis suggested that they still retained the ability to form dimers with themselves (Fig. 4.14B; lanes 2-4) they migrated to the same region as that for unfused WT single actinin rod domain (Fig. 4.14B; lane 1). The slightly slower migrating band for p.L238_E239insKLL actinin rod domain (lane 2) may be due to the presence of the extra charged lysine residue.

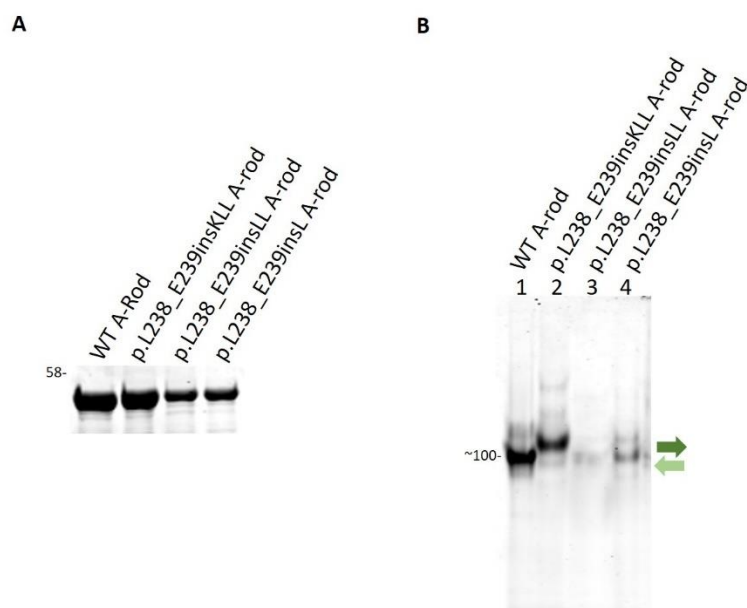


Figure 4.14: PAGE-Analysis of Unfused Single WT and Unfused Single Mutant Actinin Rod Domains.

(A) Ni-column purification of unfused single WT or mutant actinin rod domains were assessed using SDS protein gel electrophoresis, followed by Coomassie Brilliant Blue staining. Sizes (in kDa) of the relevant molecular weight markers are indicated.

(B) Purified unfused single WT or unfused single mutant actinin rod domains were analysed using native gel electrophoresis followed by GelCode™ Blue Staining. Unfused single WT actinin rod domain acts as a molecular weight marker, migrating at ~ 100kDa, and also acts as a marker of dimer migration pattern.

Each of the unfused single mutant actinin rod domain proteins migrate to the region expected for dimers. Slightly altered migration pattern for p.L238_E239insKLL actinin rod, lane 2, but this may be due to the presence of an extra charged lysine residue.

A-rod = actinin rod domain (r1r2r3r4).

n=1

Through several cloning steps each of these mutated actinin rod domains, p.L238_E239insL, p.L238_E239insLL and p.L238_E239insKLL, were fused to the WT actinin rod domain by way of a linker that was previously designed and used in section 4.4.1.1.1, the -DSS- linker and the -D9xGlySS- linker.

All orthogonal homodimeric actinin rod fusion proteins were expressed in soluble form in *E. coli* cells and were purified with a high yield using nickel column purification. Mild degradation was noted (Fig. 4.15A).

Fusion proteins were subjected to native gel electrophoresis (Fig. 4.15B) to assess their assembly state and to characterise their homogeneity. In native gel images, dimers formed from the interaction of single WT actinin rod domains are represented with the single band in lane 1. The presence of slowly migrating bands for orthogonal homodimeric actinin rod fusion proteins with -DSS- linker (Fig. 4.15B; lanes 2-5) is evidence of higher order protein assembly formation. No higher

order protein assembly is noted for orthogonal homodimeric actinin rod fusion proteins with longer, more flexible -D9xGlySS- linker. The monomeric unit predominates as these orthogonal homodimeric fusion proteins migrate to the region expected for dimers. This suggests that the mutant actinin rod domains still retain the capacity to interact with the WT actinin rod domain, and this long flexible linker allows then to do so. Thus the goal of generating rod domains that have orthogonal dimerisation capacity seems not to have been achieved. Nevertheless, these mutant rod domains may be useful based on their putative altered degree of twist.

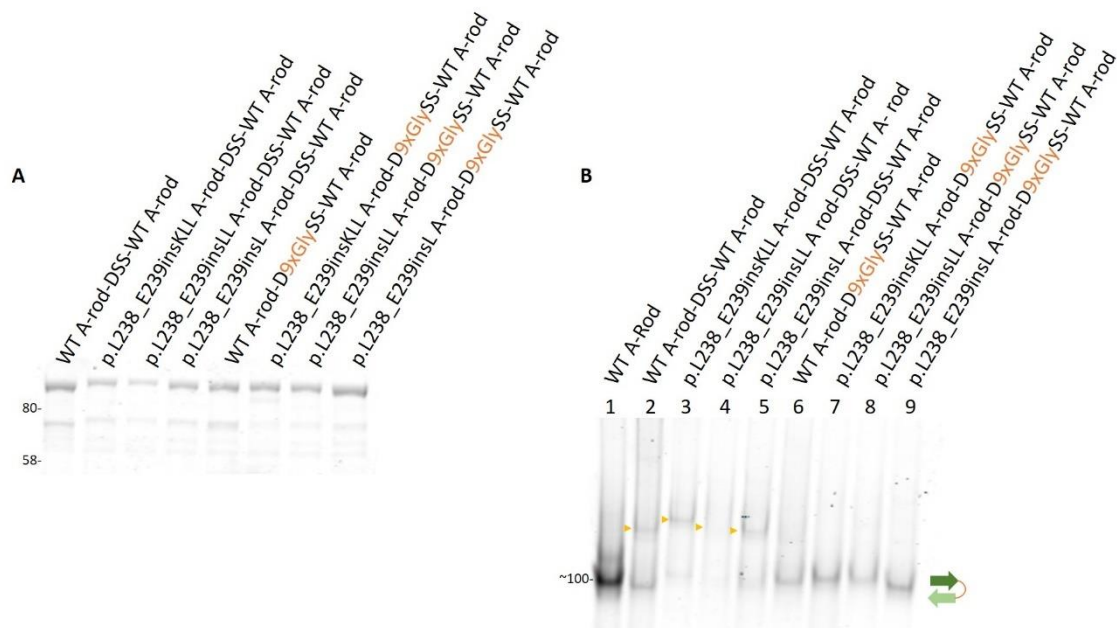


Figure 4.15: PAGE Analysis of Orthogonal Homodimeric Actinin rod Fusion Proteins:

(A) Ni-column purification of fusion proteins was assessed using SDS protein gel electrophoresis, followed by Coomassie Brilliant Blue staining.

The sizes (in kDa) of the relevant molecular weight markers are indicated.

(B) Purified fusion proteins were analysed using native gel electrophoresis, followed by GelCode™ Blue staining. Single actinin rod domain acts as a molecular weight marker, migrating at ~ 100kDa, and also as a maker of dimer migration pattern.

Orthogonal homodimeric actinin rod fusion proteins with a short linker comprised of the residues -DSS- migrate at a slower pace than the actinin rod domain sample. This bands are highlighted.

Orthogonal homodimeric fusion proteins with a longer linker comprising -D9xGlySS- migrate at the same pace as those proteins known to be forming dimers.

▶ symbol indicates migration of possible higher order structures.

A-rod = actinin rod domain (r1r2r3r4).

n=1

4.4.2 Evaluation of Fusion-based Strategy Employing Heterodimeric and Homodimeric Oligomerisation Domains

This second strategy consisted of two components; the protein building blocks, i.e. actinin rod domain (r1r2r3r4), truncated α - and β -spectrin proteins, each consisting of four spectrin repeats, and a linker peptide, designed to connect the truncated α - or β -spectrins to the actinin rod domain.

In this section I set out to assess the fusion-based assembly strategy with both heterodimeric and homodimeric oligomerisation domains through determination of the type of linker, flexible or short and rigid, that would best suit this type of protein assembly approach.

Two different oligomeric protein domains are genetically fused together; either a truncated α -spectrin protein, i.e. spectrin repeats 18-22, or a truncated β -spectrin protein, i.e. spectrin repeats 1-4 (hereafter referred to as spectrin heterodimerisation domains) are fused to the actinin rod domain (r1r2r3r4) (hereafter referred to as homodimerisation domain) in a single protein chain to create heterodimeric-to-homodimeric fusion proteins.

Ultimately, two different heterodimeric-to-homodimeric fusion-proteins are created; α -spectrin r18r19r20r21-linker-actinin r1r2r3r4, and β -spectrin r1r2r3r4-linker-actinin r1r2r3r4 (Fig. 4.16B). Each of these heterodimeric-to-homodimeric fusion proteins should be unable to fold back and interact with themselves through their actinin homodimeric and spectrin heterodimeric domains, but homodimerisation between the actinin dimerisation domains on separate protein chains should produce two symmetrical and bivalent building blocks (Fig. 4.16C). Upon mixing, these building blocks should be able to interact with each other, through heterodimerisation between the α - and β -spectrin heterodimerisation domains (Fig. 4.16D), to possibly form larger, more complex protein assemblies.

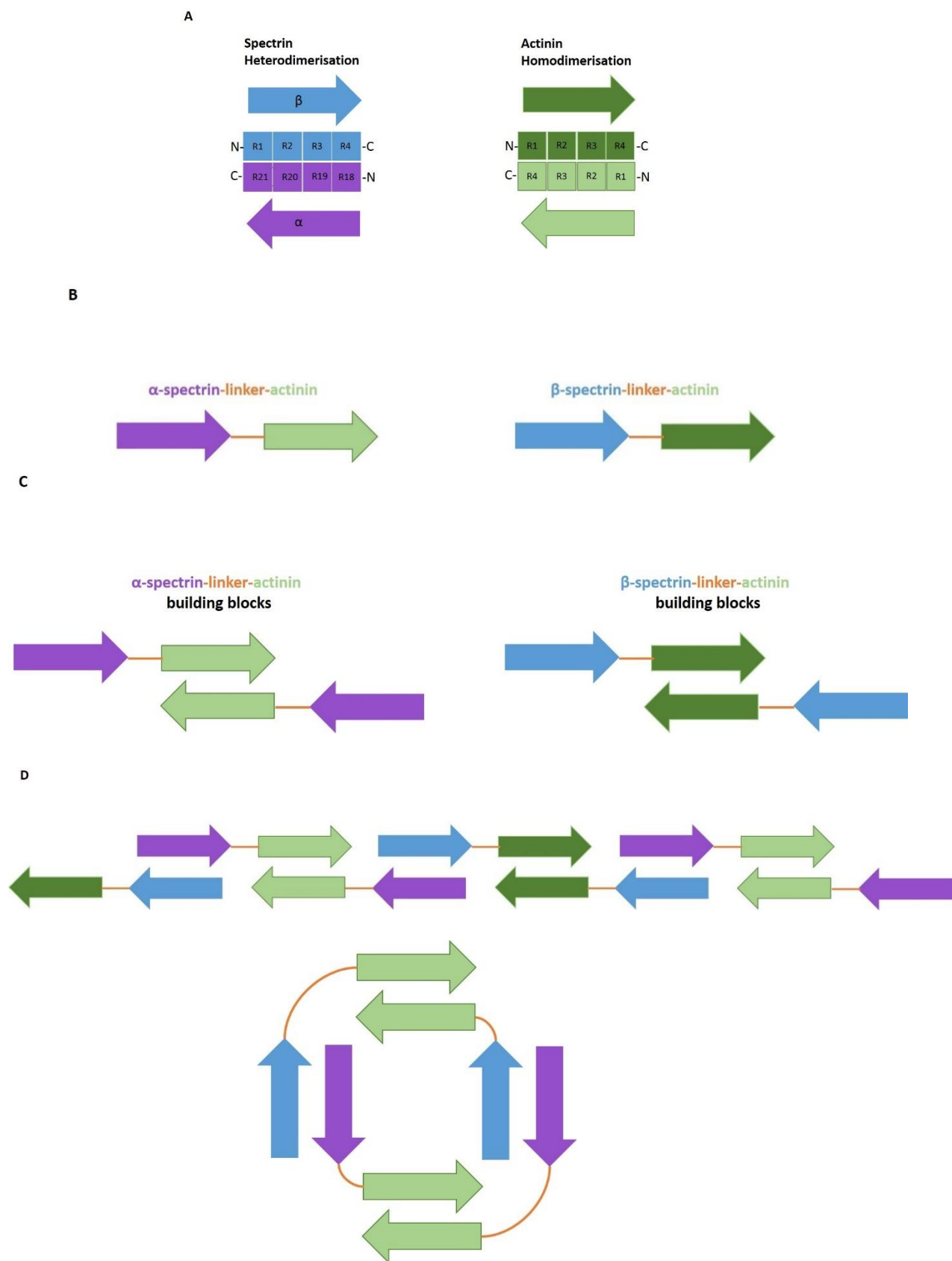


Figure 4.16: Fusion Based Strategy Employing Heterodimeric Truncated Spectrins and Homodimeric Actinin Proteins with Schematic of Possible Outcomes.

(A) Heterodimerisation between spectrin heterodimerisation domains and homodimerisation between actinin homodimerisation domains.

(B) Two heterodimeric-to-homodimeric fusion proteins were designed, one consisting four spectrin repeats from α -spectrin, r18r19r20r21, fused to the four actinin spectrin-like repeats (r1r2r3r4), and the other consisting of four spectrin repeats from β -spectrin, r1r2r3r4, fused to the four actinin spectrin-like repeats (r1r2r3r4).

(C) Homodimerisation between the actinin homodimerisation domains to create two bivalent building blocks.

(D) Heterodimerisation between spectrin heterodimerisation domains upon mixing of these building blocks to bring about the formation of large protein assemblies such as a 2D square, or a long filamentous type structure.

4.4.2.1 Connection of Heterodimeric and Homodimeric Oligomerisation Domains with Flexible Linkers

It was anticipated that a flexible linker would be best suited to separate the α -/ β -spectrin heterodimerisation domains from the actinin homodimerisation domain. A flexible linker would offer great freedom of movement and should therefore not constrain the ability of the heterodimeric-to-homodimeric fusion proteins to assemble, providing the most potential for the formation of higher order structures. It was thought that the -D12xGlySS- linker would provide the greatest conformational flexibility.

Both constructs were designed to contain a 6xHis-tag, and were created through sequential cloning steps. Both were expressed in soluble form in *E. coli* cells and purified with reasonable yield (Fig. 4.17A). High levels of degradation were noted.

Prior to native gel electrophoresis equal amounts of both purified heterodimeric-to-homodimeric fusion proteins were incubated together overnight to allow possible interactions to occur. Native gel electrophoresis analysis of the mixed heterodimeric-to-homodimeric fusion protein samples revealed the migration of a slowly migrating band (Fig. 4.17B; lanes 2 and 4), that is not observed in the independent (unmixed) heterodimeric-to-homodimeric fusion protein samples (Fig. 4.17B; lanes 1 and 3). These slowly migrating bands indicate that higher order structures might be forming.

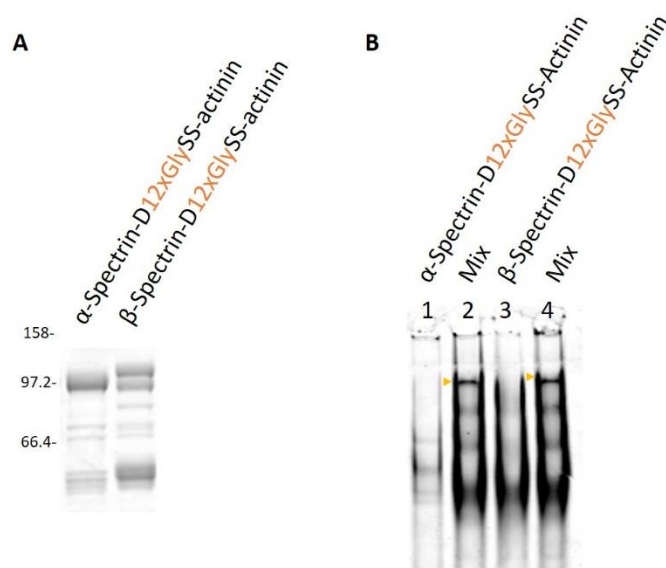


Figure 4.17: PAGE Analysis of Heterodimeric-to-Homodimeric Fusion-proteins with Flexible Linker.

(A) Ni-column purification of fusion proteins was assessed using SDS protein gel electrophoresis, followed by Coomassie Brilliant Blue staining.

Both proteins exhibited high amounts degradation.

The sizes (kDa) of the relevant molecular weight markers are indicated.

(B) Purified heterodimeric-to-homodimeric fusion proteins were analysed using native gel electrophoresis, followed by GelCode™ Blue Staining.

Slowly migrating bands in mixed fusion-protein samples (lanes 2 and 4) that are not present in individual fusion protein samples (lanes 1 and 3) are highlighted.

► symbol indicates migration of possible higher order structures.

n=3

4.4.2.2 Connection of Heterodimeric and Homodimeric Oligomerisation Domains with Rigid Helical Linkers

The heterodimeric-to-homodimeric spectrin heterodimerisation domain-D12xGlySS-actinin homodimerisation domain fusion proteins demonstrated great potential as nanostructure building blocks, however their high tendency to degrade upon purification was unfavourable. To overcome this, alternative linkers known to have a high propensity to form alpha helical secondary structures (Arai et al. 2001) were used. These linkers were each of different lengths, from one amino acid residue to ten and were comprised of amino acids glutamic acid, alanine and lysine, all of which have been noted to have a high helical propensity, with alanine having the highest propensity out of all 20 amino acids (Pace & Scholtz 1998). The exact composition of each linker is outlined in table 4.1. These helical linkers were used in a previous study (Arai et al., 2001).

Actinin and spectrin spectrin-like and spectrin repeats are each made up of a triple helical coiled-coil bundle (Yan et al. 1993) meaning that (in relation to the fusion proteins generated for this study), for α - and β -spectrin, repeat 21 and repeat 4 respectively both end with a helical structure and, for actinin, repeat 1 begins a helical structure. Linkers known to adopt a helical structure would result in a continuous alpha-helix running from one domain, i.e. the α - or β -spectrin heterodimerisation domain, to the next, i.e. the actinin homodimerisation domain, the result of which might mean a more stable and rigid conformation.

While 10 helical linkers were designed, 11 fusion proteins were created. The 0HelLinker construct (Fig. 4.18) represents a direct fusion of the actinin homodimerisation domain to the α -/ β -spectrin heterodimerisation domain. All constructs were designed to contain a 6xHis-tag, and were created through sequential cloning steps. All fusion-proteins were expressed as soluble products with a high yield.

Rigid Helical Linker Amino Acid Composition	
1HelLinker	E
2HelLinker	EA
3HelLinker	EAA
4HelLinker	EAAA
5HelLinker	EAAAK
6HelLinker	EAAAKE
7HelLinker	EAAAKEA
8HelLinker	EAAAKEAA
9HelLinker	EAAAKEAAA
10HelLinker	EAAAKEAAK

Table 4.1: Linker Design to Join Spectrin Heterodimerisation Domain to Actinin Rod Domain. Listed are the amino acid residues that make up each of the Helical Linkers.

All heterodimeric-to-homodimeric fusion proteins were purified using nickel column chromatography. Both heterodimeric-to-homodimeric fusion proteins were prone to degradation, but more so the β -spectrin heterodimerisation domain-helical linker-actinin homodimerisation fusion proteins, especially around the linker region. (Fig. 4.18).

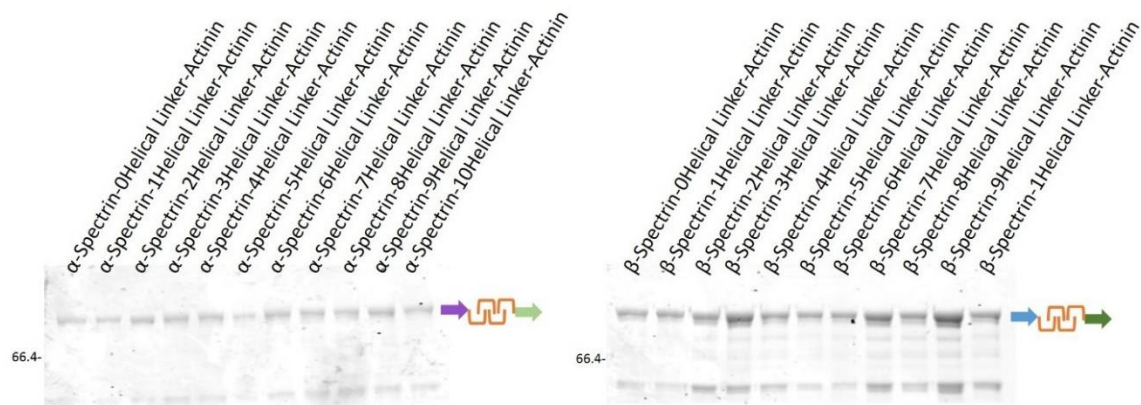


Figure 4.18: Purification of Heterodimeric-to-Homodimer Fusion proteins with Helical Linker

Ni-column purification of fusion proteins was assessed using SDS protein gel electrophoresis, followed by Coomassie Brilliant Blue staining.

All proteins exhibited varying degrees of protein degradation.

Proteins of interest and the sizes (in kDa) of the relevant molecular weight markers are indicated.

Spectrin refers to spectrin (α -r18r19r20r21/ β -r1r2r3r4) heterodimerisation domain. Actinin refers to actinin dimerisation domain (r1r2r3r4).

Prior to native gel electrophoresis equal amounts of both heterodimeric-to homodimeric-fusion proteins; α -spectrin heterodimerisation domain-helical linker-actinin homodimerisation domain with corresponding β -spectrin heterodimerisation domain-helical linker-actinin homodimerisation domain, in which both proteins contained a helical linker of the same length, were incubated together overnight, to allow possible interactions to occur. Native gel analysis of these mixed heterodimeric-to-homodimeric fusion protein samples (Fig. 4.19B) revealed a protein smear effect that was not present in the individual protein samples. A more discernible slowly migrating band can be seen in some of these mixed protein samples, indicated in Figure.

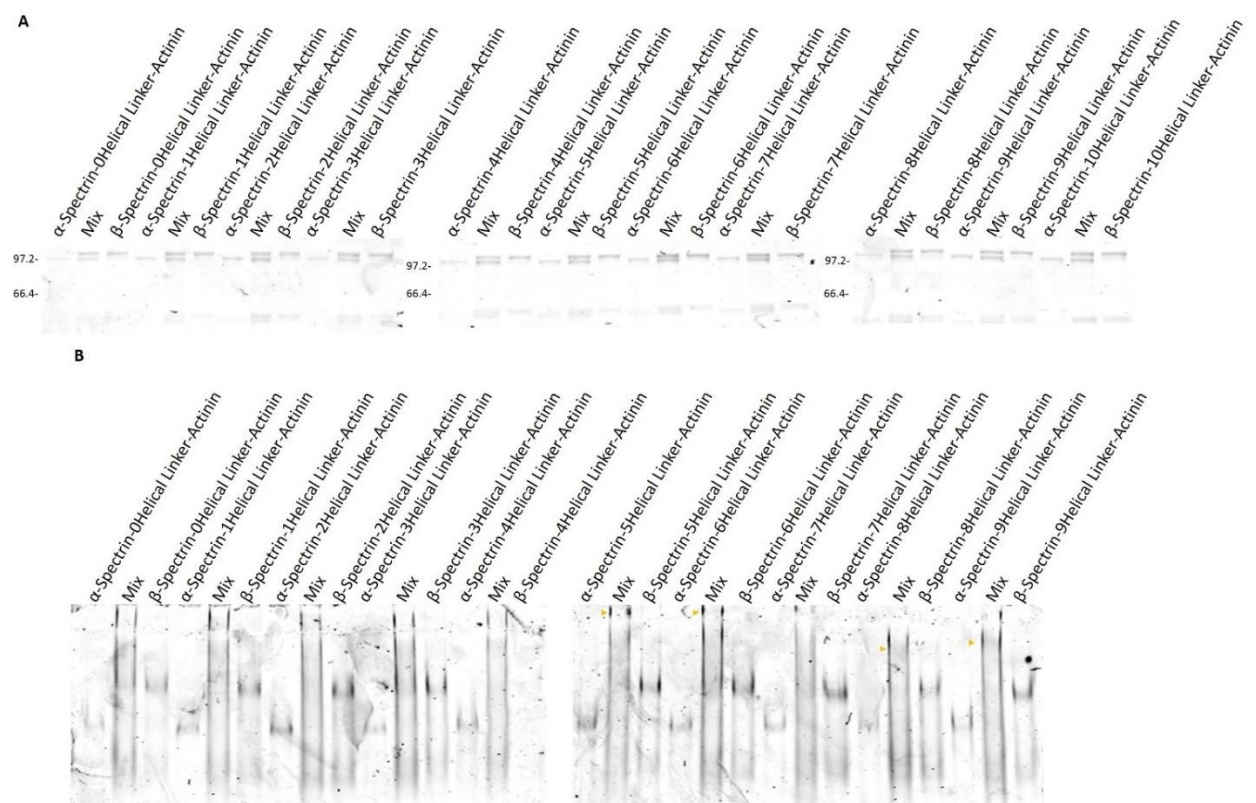


Figure 4.19: PAGE Analysis of Both Individual and Mixed Heterodimeric-to-Homodimeric Spectrin Heterodimerisation Domain-Helical Linker-Actinin Homodimerisation Domain Fusion Proteins.

Corresponding heterodimeric-to-homodimeric fusion proteins, with helical linker of the same length were mixed and incubated together to allow possible interactions to occur.

Individual and mixed samples were analysed through

(A) SDS, and.

(B) native gel electrophoresis, followed by GelCode™ Blue Staining.

Native gels displayed a protein smear effect for mixed protein samples. Slowly migrating bands are also observed, and are highlighted. Individual protein samples displayed no protein smear.

► symbol indicates migration of possible higher order structures.

Spectrin refers to spectrin (α-r18r19r20r21/β-r1r2r3r4) heterodimerisation domain. Actinin refers to actinin dimerisation domain (r1r2r3r4).

n=2

For all combinations; the mixing of corresponding heterodimeric-to-homodimeric fusion proteins with equivalent helical linker lengths gave a strong indication that higher order protein assemblies were forming. To assess if protein assemblies could form between corresponding heterodimeric-to-homodimeric fusion proteins with different length helical linkers the heterodimeric-to-homodimeric β-spectrin heterodimerisation domain-9 residue helical linker-actinin homodimerisation domain was mixed and incubated with all heterodimeric-to-homodimeric α-spectrin heterodimerisation domain-helical linker-actinin homodimerisation domain proteins. The outcome of all mixes was assessed through native gel electrophoresis.

All mixed protein samples in Fig. 4.20 exhibited the protein smear effect, suggestive of heterogeneous higher order protein assembly.

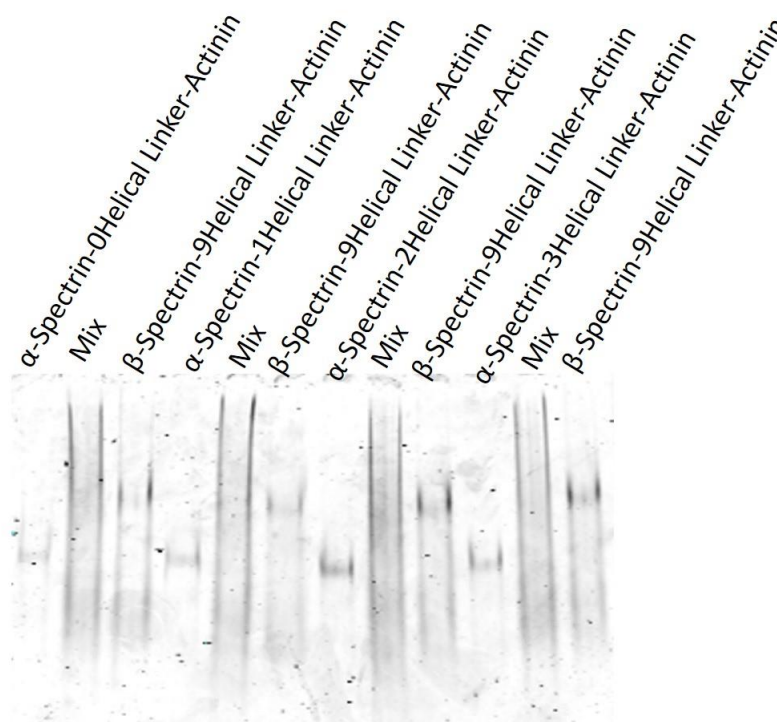


Figure 4.20: Native Gel Electrophoresis Analysis of Both Individual and Mixed Corresponding Heterodimeric-to-Homodimeric Fusion Proteins with Different Length Helical Linkers.

β -spectrin heterodimerisation domain-9 residue helical linker-actinin homodimerisation domain was mixed and incubated with all α -spectrin heterodimerisation domain-helical linker-actinin dimerisation domain proteins.

A protein smear effect is observed for all protein mixes. No protein smear is observed for individual proteins.

Proteins were stained with GelCode™ Blue Stain Reagent.

Representative image, all combinations not shown, but all gave similar result.

Spectrin refers to spectrin (α -r18r19r20r21/ β -r1r2r3r4) heterodimerisation domain. Actinin refers to actinin dimerisation domain (r1r2r3r4).

n=1

4.4.2.2.1 Analysis of Possible Protein Assemblies from Helical Linker Based Heterodimeric Fusion Strategy using Electron Microscopy

In order to assess the shape or pattern of these complexes, I chose one heterodimeric-to-homodimeric fusion protein mix; the heterodimeric-to-homodimeric α -spectrin heterodimerisation domain-7 residue helical linker-actinin homodimerisation domain and the heterodimeric-to-homodimeric β -spectrin heterodimerisation domain-7 residue helical linker-actinin homodimerisation domain, to be further analysed through negative-stain electron microscopy.

These proteins, as already shown (Fig.4.18), were very prone to degradation, leading to a very heterogeneous protein sample. In order to ensure a clean, homogenous sample for EM analysis, after nickel column chromatography, they were further purified to homogeneity with size exclusion chromatography.

Prior to UA negative staining, heterodimeric-to-homodimeric fusion proteins were mixed and incubated overnight before being subjected to SDS (Fig. 4.21A) and native (Fig. 4.21B) gel electrophoresis to verify their behaviour, i.e. the presence of slowly migrating bands on native gels confirmed that they were still forming higher order structures.

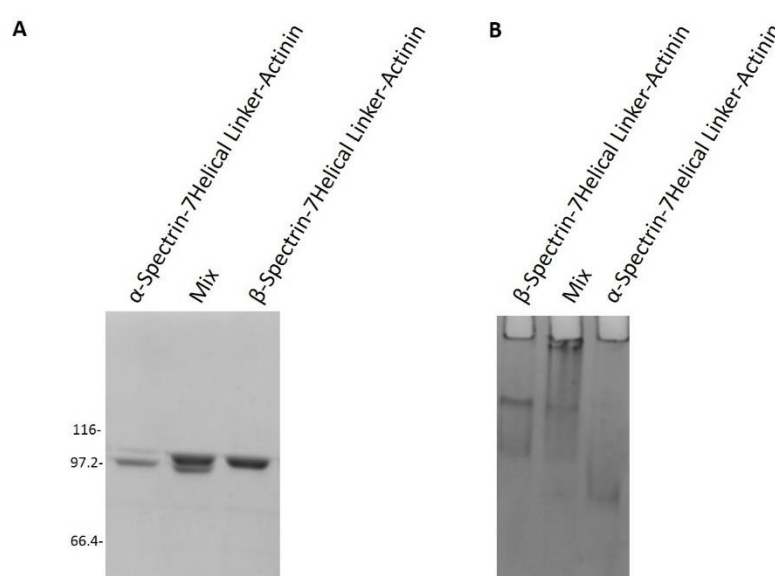


Figure 4.21: PAGE Analysis of Heterodimeric-to Homodimeric Fusion Proteins.

Prior to negative staining all proteins were assessed using protein gel electrophoresis.

(A) SDS protein gel electrophoresis, followed by Coomassie Brilliant Blue staining.

Size exclusion chromatography was successful in removing all degradation products.

The sizes (in kDa) of the relevant molecular weight markers are indicated.

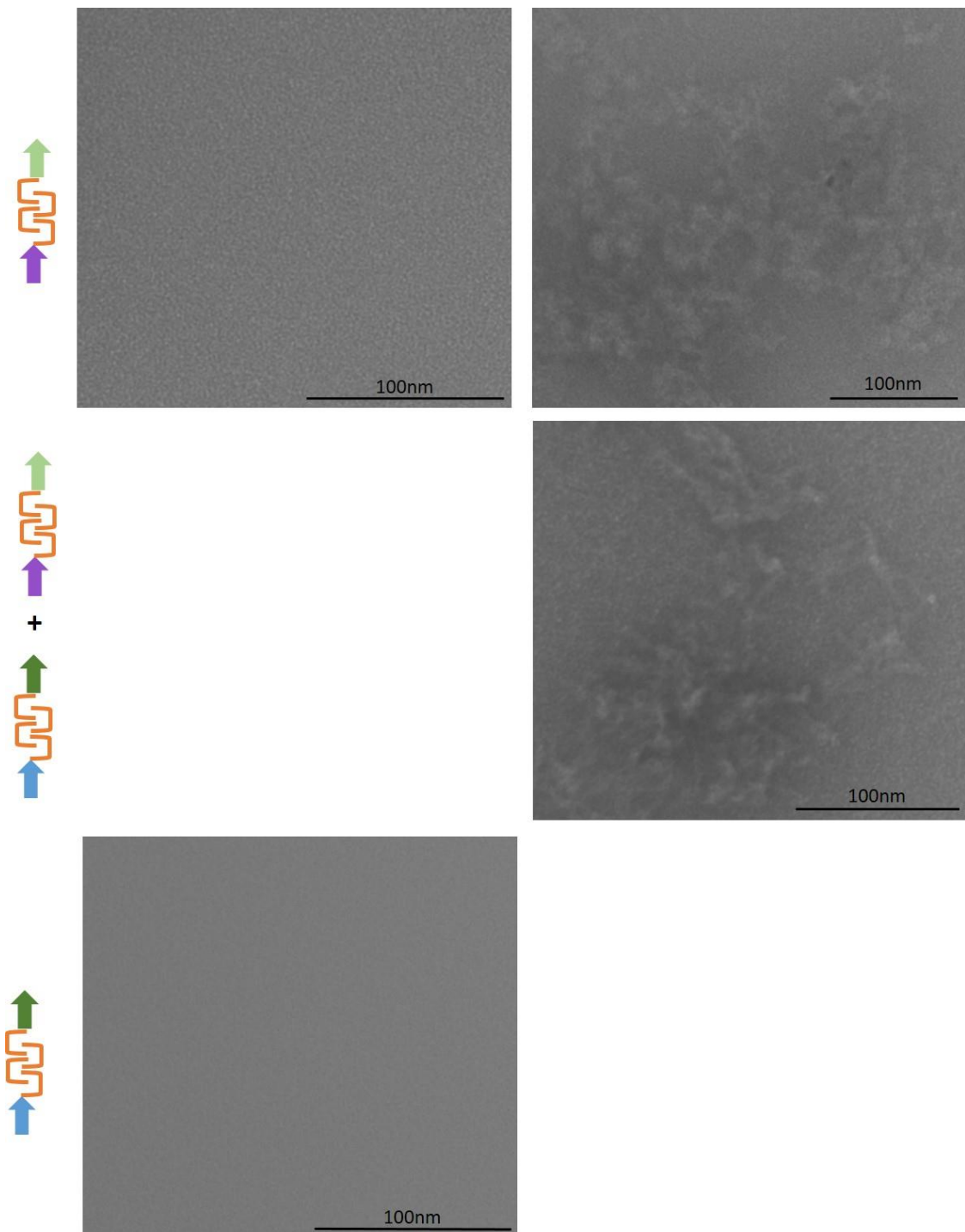
(B) Native gel electrophoresis, followed by GelCode™ Blue staining.

The usual protein smear effect is observed for the protein mix sample, with slowly migrating band.

Both are absent from individual protein samples.

Electron micrographs (Fig. 4.22) display a dense collection of proteins staining light against a dark background. Large heterogeneous protein aggregates were consistently observed for the heterodimeric-to-homodimeric α -spectrin heterodimerisation domain-7 residue helical linker-actinin homodimerisation domain with the heterodimeric-to-homodimeric β -spectrin heterodimerisation domain-7 residue helical linker-actinin homodimerisation domain protein mix.

While protein aggregates were observed in the heterodimeric-to-homodimeric α -spectrin heterodimerisation domain-7 residue helical linker-actinin homodimerisation domain only samples, they were not as frequent, and no protein aggregates were observed for heterodimeric-to-homodimeric β -spectrin heterodimerisation domain-7 residue helical linker-actinin homodimerisation domain only sample. The high quantity of protein loaded onto the grids makes it difficult to identify independent isolated structures.



	Heterodimeric to homodimeric α -spectrin heterodimerisation domain-7 residue helical linker-actinin dimerisation domain
	Heterodimeric to homodimeric β -spectrin heterodimerisation domain-7 residue helical linker-actinin dimerisation domain

Figure 4.22: Representative Electron Micrographs from Analysis of UA Negatively Stained Heterodimeric-to-Homodimeric Fusion Protein Assemblies.

Protein aggregates were consistently observed in the heterodimeric-to-homodimeric fusion protein mix; heterodimeric to homodimeric α -spectrin heterodimerisation domain-7 residue helical linker-actinin homodimerisation domain mixed with heterodimeric-to-homodimeric β -spectrin heterodimerisation domain-7 residue helical linker-actinin homodimerisation domain (one micrograph, centre, represents these aggregates). Aggregates were less frequently observed in the heterodimeric-to-homodimeric α -spectrin heterodimerisation domain-7 residue helical linker-actinin homodimerisation domain only sample (top two micrographs displaying frequently observed dense collection of proteins with no aggregates, and less frequently observed protein aggregates). No protein aggregates were observed in the heterodimeric-to-homodimeric β -spectrin heterodimerisation domain-7 residue helical linker-actinin homodimerisation domains only sample (one micrograph, bottom, displaying consistently observed dense collection of proteins with no protein aggregates).

Magnification range: 200-300k.

n=1

4.4.3 Evaluation of Fusion-based Strategy Employing Three Protein

Oligomerisation Domains

Building upon the last two sections (section 4.4.1 and section 4.4.2), this third and final section involves the creation of two fusion proteins containing three protein oligomerisation domains; two α -spectrin or β -spectrin heterodimerisation domains (r18r19r20r21 or r1r2r3r4 respectively) and one actinin homodimerisation domain. It was anticipated that these could be used as tetravalent building blocks (Fig.4.23A), that could self-assemble into complicated structures (Fig. 4.23B).

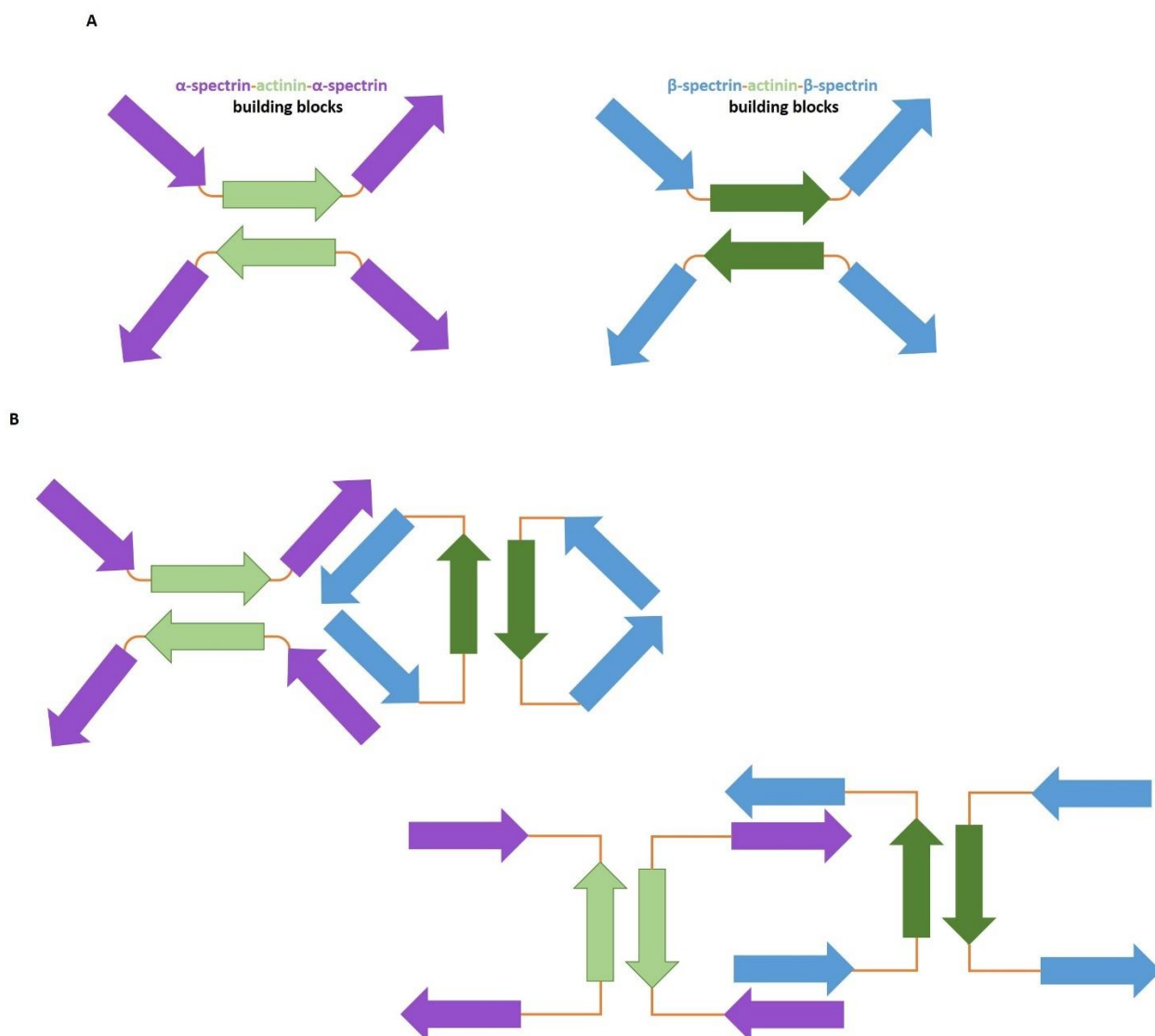


Figure 4.23: Schematic of Possible Outcome with Fusion Proteins made up of Two Spectrin Heterodimerisation Domains and One Actinin Rod Domain.

(A) Homodimerisation between the actinin homodimerisation domains to create two tetravalent building blocks.

(B) Mixing of these building blocks to bring about the formation of complex protein assemblies.

Fusion proteins consisting of: two α -spectrin proteins, each made up of four spectrin repeats, with an intervening actinin homodimerisation domain, or two β -spectrin proteins, each made up of four spectrin repeats, with an intervening actinin homodimerisation domain (Fig. 4.23A) were designed. For both types of fusion protein in this section, each domain was separated by use of a flexible linker consisting of six or eight glycine residues (see Materials and Methods section 4.3.1.4). These glycine-based linkers were expected to yield the flexibility required to produce complex protein assemblies, such as those in Fig. 4.23B. Constructs were designed to contain a 6xHis-tag and were expressed in soluble form in *E. coli* cells

(Fig. 4.24A). These proteins proved themselves to be very unstable and rapidly degraded throughout the purification process (Fig. 4.24B). Due to their instability, no further study was undertaken with these particular fusion proteins.

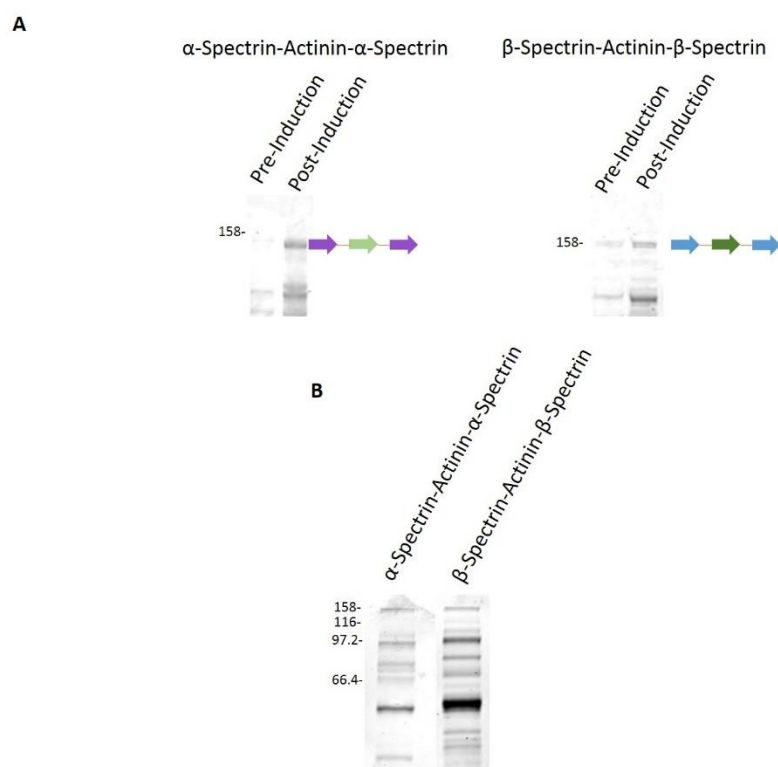


Figure 4.24: Expression and Purification of Spectrin Heterodimerisation Domain - linker- Actinin Homodimerisation Domain-linker-Spectrin Heterodimerisation Domain Fusion Proteins.

(A) Total cell protein lysates, both pre- and post- induction of protein expression with 0.2mM IPTG, were analysed using SDS protein gel electrophoresis, followed by Coomassie Brilliant Blue Staining.

(B) Ni-column purification of fusion proteins was assessed using SDS protein gel electrophoresis, followed by Coomassie Brilliant Blue Staining.

Proteins experienced rapid degradation

Proteins of interest and the sizes (in kDa) of the relevant molecular weight markers are indicated.

4.5 Discussion

Of all the different approaches that can be used to direct the formation of higher order protein assemblies and protein nanostructures, I decided to adopt the fusion-based assembly approach, an approach which involves the introduction of two or more oligomerisation protein domains into one protein chain, with each domain separated by way of a rationally designed linker (King & Lai 2013; Padilla et al. 2001). This approach appealed to me because it allowed for exploitation of the symmetry that arises in the quaternary structure of dimeric actinin. Taking advantage of this symmetry would provide an additional level of geometrical control that the other two aforementioned approaches, ligand-mediated and metal-directed protein assembly (see section 1.2.5), did not offer without additional modification. The fusion-based assembly strategy therefore consisted of fewer design steps. Also, I knew that I had the knowledge and ability to be able to connect each protein domain with a linker of a desired composition, and that careful design of this linker would inhibit it from interfering with the folding and activity of the protein domains it was separating.

4.5.1 Homodimeric Actinin Rod Fusion Proteins

As a starting point in the design of large protein assemblies, focus was initially placed on fusion proteins consisting of two homodimeric oligomerisation domains; the actinin rod domain-r1r2r3r4 (section 4.4.1). The aim of these early experiments was twofold; to demonstrate proof of principle; that Spectrin Family protein members could be manipulated to form higher order protein assemblies, and to determine which type of linker would best suit the formation of these higher order structures. Initially, therefore, rather than rigorously trying to influence the formation of a particular shape or structure with these Spectrin Family proteins, I was asking the question: given the ability of these proteins to self-assemble, what structures will form when I link them together with a series of different linkers?

Despite the potential flexibility of the glycine linkers, native gel analysis revealed that the homodimeric actinin rod fusion proteins containing them self-

assembled in a very limited number of conformations, most frequently the monomeric unit (section 4.4.1.1.1).

Analysis of the homodimeric actinin rod fusion proteins with linkers designed to have a more helical and, therefore, rigid disposition also exposed that they also had a strong tendency to fold into the monomeric unit. However, the slower migration of protein bands for the homodimeric actinin rod fusion proteins containing short linkers of four amino acid residues or less, or containing the proline amino acid, known to bring about the formation of rigid structures, was evidence of the formation of higher order assemblies (section 4.4.1.1.2)

4.5.2 Orthogonal Actinin Rod Fusion Proteins

Attempts to inhibit the formation of the monomeric unit were made with the creation of orthogonal homodimeric actinin rod domain fusion proteins (section 4.4.1.3). These consisted of a natural WT actinin rod domain fused to an actinin rod domain that had been altered in such a way so that it would no longer dimerise with the WT actinin rod domain.

Considering alpha helices only have 3.6 amino acid residues per helical turn, it was anticipated that the insertion of extra amino acids (1-3 amino acid residues) into the helical linker region between repeats 2 and 3 would introduce an additional twist, or at least alter the twist in this helical linker, and, as a result, force the actinin rod domain to acquire a different orientation to that of the natural WT actinin rod domain. With this new orientation, it was hoped that these actinin rod domains would be able to interact with themselves, but not with the WT actinin rod domain.

While p.L238_E239insL, p.L238_E239insLL and p.L238_E239insKLL actinin rod domains were shown to be able to interact with themselves, they also retained the capacity to interact with the WT actinin rod domain. It has been suggested that repeats 2 and 3 underpin the structural architecture of the entire actinin molecule (Djinović-Carugo et al. 1999). Also, results from Chapter 3 of this study suggests that the presence of repeats 2 and 3 are required to induce dimerisation, and that they allow for the co-operative binding of repeats 1 and 4. Therefore, considering

the structural importance of repeats 2 and 3, it seems plausible that three insertional mutations were not enough to alter its ability to dimerise. Perhaps a more stringent strategy would be necessary to alter actinin rod dimerisation. Such a strategy might involve creating two different actinin rod domain proteins, each consisting of several mutations across the entire length of the dimerisation interface. These mutations would be designed to be accommodating, meaning that mutant actinin rod domains would be able to accommodate dimerisation between themselves, but not with the WT actinin rod domain. A simple example of such an accommodating mutation might be replacing a positively charged amino acid residue with a negatively charged amino acid residue on one mutant actinin rod domain, and vice versa for its complementary amino acid partner on the other mutant actinin rod domain. These mutated rod domains could then be fused to the WT actinin rod domain to achieve the same goal that was attempted in section 4.4.1.3.

In order to identify those amino acids contributing to dimerisation, and to identify those amino acids that, when mutated might lead to loss of protein structure and function, 3D modelling of the actinin rod protein structure would be required. However, results obtained using this process should be more desirable.

4.5.3 Major Findings from Fusion-Protein Strategy: Using Homodimeric Protein Oligomerisation Domains

These preliminary studies were beneficial in the amount of information gathered from them; not only was linker composition an important factor to consider, but so too was linker length, after all, linker length would play a role in controlling the spatial organisation or alignment of the actinin rod domains. The presence of slowly migrating bands on native gels for both homodimeric- and orthogonal homodimeric-actinin rod domain fusion proteins containing the short -DSS- linker, and for homodimeric-actinin rod domain fusion proteins containing the rigid linker with proline residues, -DIPPR-, was evidence that actinin proteins could be manipulated to form protein assemblies and that possibly short and slightly rigid

linkers might be best suited to the formation of these protein assemblies. The fact that the actinin rod domains, despite them being tethered together in a single protein molecule, still retained the ability to dimerise and form the monomeric unit, was a very important observation. The presence of the linker was not disturbing their functional and physical properties such as their ability to dimerise and self-assemble. These properties underpinned the design of the whole project.

4.5.4 Heterodimeric to Homodimeric Fusion Proteins and Their Major Findings

Next I wanted to take a more direct approach towards the assembly of higher order protein structures using the Spectrin Family proteins. The creation of two heterodimeric-to-homodimeric fusion proteins would allow for greater control over the assembly process because, ultimately, no structure should form until both heterodimeric-to-homodimeric proteins are present. Although the approach was first adopted with the creation of the orthogonal homodimeric-actinin rod domain fusion proteins, and was proven unsuccessful, these new heterodimeric-to-homodimeric fusion proteins had much greater potential because each fusion protein was made up of protein domains not known to interact; heterodimeric-to-homodimeric fusion proteins were made up of either a truncated α -spectrin or β -spectrin, each containing 4 spectrin repeats, α -r18r19r20r21 and β -r1r2r3r4 (referred to as heterodimerisation domains in this section), and the entire actinin rod domain-r1r2r3r4 (referred to as homodimerisation domain in this section). This strategy involved the exploitation of the symmetry that arises in the quaternary structure of the actinin dimerisation domain. This symmetry, i.e. the homodimerisation between the actinin rod domains, should align the spectrin heterodimerisation domains along the same axis of symmetry, thereby providing restraint on the orientation of these spectrin heterodimerisation domains. This would create two bivalent building blocks, that, following mixing and heterodimerisation between the aligned spectrin heterodimerisation domains would bring about higher order assembly.

Initially, flexible linkers were used with this strategy (section 4.4.2.1). I thought that actinin homodimerisation alone would provide enough control to maintain the orientation of both spectrin heterodimerisation domains and actinin homodimerisation domains along the same axis, despite the flexibility of the linker region. However, heterodimeric- to-homodimeric fusion proteins containing flexible linkers were very prone to degradation.

Those designed to have a rigid helical linker were found to be a slightly better choice appearing to be more stable (section 4.4.2.2). This may be because the inclusion of a helical linker in between the spectrin heterodimerisation domains and actinin homodimerisation domain results in a continuous alpha helix extending from the coiled coil from either repeat 22 or repeat 4 from α - or β - spectrin respectively, to the coiled coil from repeat 1 of actinin. Another reason as to why different levels of degradation were observed for the heterodimeric-to-homodimeric fusion proteins with flexible linkers and heterodimeric-to-homodimeric fusion proteins with rigid linkers may be because protein regions of high flexibility are normally more prone to proteolysis. With the ability to adopt a wide range of conformations there is a great possibility that one of these conformations will fit the active site of a proteolytic enzyme. Rigid regions of a protein however normally show great resistance to proteolysis. Having only one definite conformation, the likelihood of it being complementary to the active site of the proteolytic enzyme is very low (Tsai et al. 2002). Results observed therefore suggest that the alpha helical linkers designed were near fit for purpose; to be rigid.

Nevertheless, evidence for the formation of higher order structures between complementary heterodimeric-to-homodimeric fusion proteins with flexible or helical linkers is provided with the migration of slowly migrating bands during native gel analysis. While these slowly migrating bands are discernible, the protein lanes themselves consist largely of a protein smeared effect. This may be an indication that a number of different higher order structures are forming, suggesting that the protein samples themselves were very heterogeneous. This heterogeneity could be occurring because the orientation of the fused protein domains was not always correct, hence definite structures could not form, or at least large amount of these definite structures could not form. The protein smear

was also observed for protein mixes of heterodimeric-to-homodimeric fusion proteins that had been further purified using HPLC. This indicated that the protein smearing observed in the native gel images was not due to protein degradation. For whatever reason, this observation is common in the first iteration steps of a design strategy. The heterogeneous structures that form usually do so due to steric conflict between amino acids that would not normally be in such close proximity in the natural structure and due to the fact that protein surfaces are very reactive and are therefore known to partake in indiscriminate and random interactions and associations (Lai et al. 2013; Bruning et al. 2010). However, just as nature, through evolution, has created complementary interfaces to bring about protein assembly (Goodsell & Olson 2000), a synthetic biologist must also manipulate the protein interface to bring about controlled assembly. Indeed, the formation of the protein cage generated by Padilla et al. (2001) (discussed above in section 4.2.1), was not brought about until two amino acid changes were made to the helical linker region of the fusion-proteins (Lai et al. 2013). Up until these changes were made, the protein cages that formed were extremely heterogeneous and could not be characterised very well.

4.5.5 Negative Stain Electron Microscopy for Homodimeric Actinin Rod Fusion-Proteins and Heterodimeric-to-Homodimeric Fusion Proteins

The most obvious and simplest structure that could be forming with the actinin rod domain bivalent building blocks, i.e. the homodimeric actinin rod fusion proteins containing a short linker, -DSS-, or rigid linker, -DIPPR-, or no linker at all, is that of a filamentous type structure, brought about through polymerisation at both ends of these bivalent building blocks.

Unfortunately, EM analysis (section 4.4.1.2) revealed no satisfactory insight into whether this type of structure, or indeed any other type of structure could be forming. Previous EM analysis of full length actinin or the isolated rod domain carried out by other groups had reported observing discrete rod shaped particles, with an approx. length and width of 25nm x 4nm, respectively (Winkler et al. 1997; Imamura et al. 1988). Similar results were anticipated, but were not observed. Long

filamentous type structures were observed for the actinin rod domain controls. To a lesser extent, these were also observed in homodimeric actinin rod fusion proteins containing the short -DSS-linker. Remaining homodimeric actinin rod fusion proteins containing the rigid -DIPPR-linker, or no linker, appeared very heterogeneous. Attempts to reduce this heterogeneity by changing the negative stain from UA to PTA gave only slight improvement; it was now possible to observe these long filamentous type structures in all protein samples. This filamentous structure observed is both too long and too wide to suggest that it is a actinin rod domain homodimer.

As already mentioned, I did not have a particular protein structure in mind when designing these fusion proteins. As a result, I did not anticipate the observation of a particular structure upon EM analysis. I did, however, expect the homodimeric actinin rod fusion proteins to differ in their structural appearance to the actinin rod domain control sample. Ultimately, no dramatic structural difference was observed between the two.

The most obvious structure that could be forming from a mix of the heterodimeric-to-homodimeric α -/ β -spectrin heterodimerisation domain-helical linker-actinin homodimerisation domain fusion proteins is that of another filamentous type structure through polymerisation at both ends of the bivalent building blocks. The heterogeneity observed in the homodimeric actinin rod domain fusion proteins prompted the inclusion of an extra size exclusion chromatography step prior to EM analysis of the heterodimeric-to-homodimeric fusion proteins (section 4.4.2.2.1).

Still, all images detailed a very heterogeneous mix of possible protein structures. However, control samples, consisting of only one heterodimeric-to-homodimeric fusion protein, either the heterodimeric α -spectrin heterodimerisation domain-7 residue helical linker-actinin homodimerisation domain, or the heterodimeric β -spectrin heterodimerisation domain-7 residue helical linker-actinin homodimerisation domain, differed from the heterodimeric-to-homodimeric fusion protein mix, consisting of both of these heterodimeric-to-homodimeric fusion proteins. Large protein aggregates were consistently observed for the heterodimeric-to-homodimeric fusion protein mix. These aggregates were

also observed for the heterodimeric-to-homodimeric α -spectrin heterodimerisation domain-7 residue helical linker-actinin homodimerisation domain only sample, but only one time, and they were not observed at all for the heterodimeric-to-homodimeric β -spectrin heterodimerisation domain-7 residue-helical linker-actinin homodimerisation only sample. While these protein aggregates give no indication of the type of structure that could be forming, their presence suggests that there is an interaction between the two complementary heterodimeric-to-homodimeric fusion proteins. This is in agreement to results obtained from native gel analysis.

As previously documented by Winkler et al. (1997) one reason for the heterogeneity observed in all EM samples may simply be brought about by the many different orientations that the proteins can adopt upon adsorption onto the carbon grids. Another reason might be that the technique has not been fully optimised for these fusion proteins. Both the pH of the negative stain and salt concentration of the protein buffer are known to affect the dimensions of actinin (Winkler et al. 1997; Suzuki et al. 1976). Also, staining time can affect actinin dimensions (Suzuki et al. 1976). Additionally, my EM images suggest a dense quantity of protein is present on the grids, a more dilute protein concentration, and further optimisation of pH and salt concentration might make it easier to recognise the formation of possible structures.

Previous studies have carried out EM and rotary shadowing to further characterise the overall arrangement of the actinin structure (Pollard et al. 1986; Mabuchi et al. 1985; Winkler et al. 1997). EM in combination with rotary shadowing might help in better characterising the sizes of these homodimeric fusion proteins and these heterodimeric-to-homodimeric fusion proteins, and the possible protein assemblies that might be forming between them.

4.5.6 Molecular Modelling

Despite the recent progress in computational molecular modelling programs (Liu & Kuhlman 2006), apart from visual inspection of the molecular structure of the actinin-2 using USCF Chimera program, at no other point was molecular modelling used to design the linkers or to describe the orientation of the of the actinin rod

domains (dimerisation domains) or the spectrin heterodimerisation domains. Similar to the study carried out by Grueninger et al. (2008), linkers were designed using a few general rules regarding interactions between amino acids, and any alterations made to the actinin rod domain were based on observations taken from the literature.

A medium throughput screening approach, involving cloning, protein expression, protein purification and native gel analysis, was used to determine which linkers or which fusion-based assembly strategy worked best.

This study represents the first iteration of a complex protein engineering bionanotechnology project, and although this approach is simplistic, it was necessary as it allowed for the determination of how far the project would progress without any molecular modelling. This approach could be adopted in any lab, and through it, I had hoped to make protein engineering more accessible.

4.6 Conclusions

In general, the synthetic creation of large protein assemblies or nanostructures is difficult owing to our incomplete understanding of the sequence-to-structure relationship in proteins and of the rules that proteins follow when folding into particular tertiary structures, or assembling into certain quaternary structures (Boyle et al. 2012; Bromley et al. 2008). However, this study nicely demonstrates the proof of principle of this project, that Spectrin Family protein members, particularly their spectrin repeat domains, can be manipulated to form protein assemblies. I have shown that the use of *de-novo* designed short, rigid or helical linkers to connect two protein domains result in the creation homodimeric and heterodimeric-to-homodimeric fusion proteins, which exhibit great potential as bivalent building blocks. These linkers do not appear to affect the quaternary structure of the domains that they separate, and could possibly have the potential to be used in a wide variety of fusion proteins made up of different protein oligomerisation domains. Without the use of molecular modelling I have designed and created both homodimeric and heterodimeric building blocks, however, molecular modelling may be required to yield a precise structural arrangement using these building blocks.

5. Bibliography

- Alberts, B., 1998. The cell as a collection of protein machines: preparing the next generation of molecular biologists. *Cell*, 92(3), pp.291–294.
- Alfred, T., Ben-Shlomo, Y., Cooper, R., Hardy, R., Cooper, C., Deary, I.J., Gunnell, D., Harris, S.E., Kumari, M., Martin, R.M., Moran, C.N., Pitsiladis, Y.P., Ring, S.M., Sayer, A.A., Smith, G.D., Starr, J.M., Kuh, D., Day, I.N.M. et al., 2011. *ACTN3* genotype, athletic status, and life course physical capability: meta-analysis of the published literature and findings from nine studies. *Human Mutation*, 32(9), pp.1008–1018.
- An, X. Debnath, G., Guo, X., Liu, S., Lux, S.E., Baines, A., Gratzer, W. & Mohandas, N., 2005. Identification and functional characterization of protein 4.1R and actin-binding sites in erythrocyte beta spectrin: regulation of the interactions by phosphatidylinositol-4,5-bisphosphate. *Biochemistry*, 44(31), pp.10681–10688.
- An, X., Guo, X., Sum, H., et al., 2004a. Phosphatidylserine binding sites in erythroid spectrin: location and implications for membrane stability. *Biochemistry*, 43(2), pp.310–315.
- An, X., Guo, X., Wu, Y. & Mohandas, N., 2004b. Phosphatidylserine binding sites in red cell spectrin. *Blood Cells, Molecules, and Diseases*, 32(3), pp.430–432.
- An, X., Guo, X., Zhang, X., Baines, J.A., Debnath, G., Moyo, D., Salomao, M., Bhasin, N., Johnson, C., Discher, D., Gratzer, W.B. & Mohandas, N., 2006. Conformational stabilities of the structural repeats of erythroid spectrin and their functional implications. *The Journal of Biological Chemistry*, 281(15), pp. 10527-10532.
- An, X., Lecomte, C., Chasis, J.A., Mohandas, N. & Gratzer, W., 2002. Shear-response of the spectrin dimer-tetramer equilibrium in the red blood cell membrane. *The Journal of Biological Chemistry*, 277(35), pp.31796–31800.
- Andersen, E.S., Dong, M., Nielsen, M.M., Jahn, K., Lind-Thomsen, A., Mamdouh, W., Gothelf, K.V., Besenbacher, F. & Kjems, J., 2008. DNA origami design of

dolphin-shaped structures with flexible tails. *ACS Nano*, 2(6), pp.1–7.

Andersen, E.S., Dong, M., Nielsen, M.M., Jahn, K., Subramani, R., Mamdouh, W., Golas, M.M., Sander, B., Stark, H., Oliveira, C.L.P., Pedersen, J.S., Birkedal, V., Besenbacher, F., Gothelf, K.V. & Kjems, J., 2009. Self-assembly of a nanoscale DNA box with a controllable lid. *Nature*, 459(7243), pp.73–6.

Arai, R., Ueda, H., Kitayama, A., Kamiya, N. & Nagamune, T., 2001. Design of the linkers which effectively separate domains of a bifunctional fusion protein. *Protein Engineering*, 14(8), pp.529–532.

Araki, N., Hatae, T., Yamada, T. & Hirohashi, S., 2000. Actinin-4 is preferentially involved in circular ruffling and macropinocytosis in mouse macrophages: analysis by fluorescence ratio imaging. *Journal of Cell Science*, 113(1), pp.3329–3340.

Armstrong, C.T., Bolye, A.L., Bromley, E.C.H., Mahmoud, Z.N., Smith, L., Thomson, A.R. & Woolfson, D.N., 2009. Rational design of peptide-based building blocks for nanoscience and synthetic biology. *Faraday Discussions*, 143(19), pp. 305–317.

Bagnall, R.D., Molloy, L.K., Kalman, J.M. & Semsarian, C., 2014. Exome sequencing identifies a mutation in the *ACTN2* gene in a family with idiopathic ventricular fibrillation, left ventricular noncompaction, and sudden death. *BMC Medical Genetics*, 15(99).

Bai, Y., Luo, Q., Zhang, W., Miao, L., Xu, J., Li, H. & Liu, J., 2013. Highly ordered protein nanorings designed by accurate control of glutathione S-transferase self-assembly. *Journal of the American Chemical Society*, 135(30), pp.10966–10969.

Baines, A.J., 2009. Evolution of spectrin function in cytoskeletal and membrane networks. *Biochemical Society Transactions*, 37(Pt 4), pp.796–803.

Balduini, A., Pallotta, I., Malara, A., Lova, P., Pecci, A., Viarengo, G., Balduini, C.L. & Torti, M., 2008. Adhesive receptors, extracellular proteins and myosin IIA orchestrate proplatelet formation by human megakaryocytes. *Journal of*

Thrombosis and Haemostasis, 6(11), pp.1900–1907.

Balduini, C.L., Pecci, A. & Savoia, A., 2011. Recent advances in the understanding and management of MYH9-related inherited thrombocytopenias. *British Journal of Haematology*, 154(2), pp.161–174.

Balduini, C.L. & Savoia, A., 2012. Genetics of familial forms of thrombocytopenia. *Human Genetics*, 131(12), pp.1821–1832.

Bañuelos, S., Saraste, M. & Djinoić Carugo, K., 1998. Structural comparisons of calponin homology domains: implications for actin binding. *Structure*, 6(11), pp.1419–1431.

Barral, J.M. & Epstein, H.F., 1999. Protein machines and self assembly in muscle organization. *BioEssays*, 21(10), pp.813–823.

Bearer, E.L., Prakash, J.M. & Li, Z., 2002. Actin dynamics in platelets. *International Review of Cytology*, 217, pp. 137-182.

Begg, G.E. Harper, S.L., Morris, M.B. & Speicher, D.W., 2000. Initiation of spectrin dimerization involves complementary electrostatic interactions between paired triple-helical bundles. *The Journal of Biological Chemistry*, 275(5), pp.3279–3287.

Begg, G.E., Morris, M.B. & Ralston, G.B., 1997. Comparison of the salt-dependent self-association of brain and erythroid spectrin. *Biochemistry*, 36(23), pp.6977–6985.

Beggs, A.H., Byers, T.J., Knoll, J.H.M., Boyce, F.M., Bruns, G.A.P. & Kunkel, L.M., 1992. Cloning and characterization of two human skeletal muscle alpha-actinin genes located on chromosomes 1 and 11. *The Journal of Biological Chemistry*, 267(13), pp.9281–9288.

Benner, S. & Sismour, A., 2005. Synthetic biology. *Nature Reviews. Genetics.*, 6(July), pp.533–543.

Bennett, V. & Baines, A.J., 2001. Spectrin and ankyrin-based pathways: metazoan inventions for integrating cells into tissues. *Physiological Reviews*, 81(3),

pp.1353–1392.

Berman, Y. & North, K.N., 2010. A gene for speed: the emerging role of α -actinin-3 in muscle metabolism. *Physiology*, 25(4), pp.250–259.

Berrou, E., Adam, F., Lebre, M., Fergelot, P., Kauskot, A., Couprie, I., Jandrot-Perrus, M., Nurden, A., Favier, R., Rosa, J-P., Goizet, C., Nurden, P. & Bryckaert, M., 2013. Heterogeneity of platelet functional alterations in patients with filamin A mutations. *Arteriosclerosis, Thrombosis, and Vascular Biology*, 33(1), pp.e11–e18.

Beumer, S., Heijnen, H.F.G., IJsseldijk, M.J.W., Orlando, E., de Groot, P.G. & Sixma, J.J., 1995. Platelet adhesion to fibronectin in flow: the importance of von Willebrand factor and glycoprotein Ib. *Blood*, 86(9), pp.3452–60.

Bialkowska, K., Saido, T.C. & Fox, J.E.B., 2004. SH3 domain of spectrin participates in the activation of Rac in specialised calpain-induced integrin signalling complexes. *Journal of Cell Science*, 118 (Pt 2), pp. 381-395.

Birkedal, V., Dong, M., Golas, M., Sander, B., Andersen, E.B., Gothelf, K.V., Besenbacher, F. & Kjems, J., 2011. Single molecule microscopy methods for the study of DNA origami structures. *Microscopy Research and Technique*, 74(7), pp.688–698.

Blanchard, A., Ohanian, V. & Critchley, D., 1989. The structure and function of α -actinin. *Journal of Muscle Research and Cell Motility*, 260(10), pp.280–289.

Bolton-Maggs, P.H.B., Chalmers, E.A., Collins, P.W., Harrison, P., Kitchen, S., Liesner, R.J., Minford, A., Mumford, A.D., Parapia, L.A., Perry, D.J., Watson, S.P., Wilde, J.T. & Williams, M.D., 2006. A review of inherited platelet disorders with guidelines for their management on behalf of the UKHCDO. *British Journal of Haematology*, 135(5), pp.603–633.

Borrego-Diaz, E., Kerff, F., Lee, S.H., Ferron, F., Li, Y. & Dominguez, R., 2006. Crystal structure of the actin-binding domain of α -actinin 1: evaluating two competing actin-binding models. *Journal of Structural Biology*, 155(2), pp.230–238.

- Bottega, R., Marconi, C., Faleschini, M., Baj, G., Cagioni, C., Pecci, A., Pippucci, T., Ramenghi, U., Pardini, S., Ngu, L., Baronci, C., Kunishima, S., Balduini, C.L. Seri, M., Savoia, A. & Noris, P., 2015. ACTN1-related thrombocytopenia : identification of novel families for phenotypic characterisation. *Blood* , 125(5), pp.869–873.
- Boyle, A.L., Bromley, E.H.C., Bartlett, G.J., Sessions, R.B., Sharp, T.H., Williams, C.L., Curmi, P.M.G., Forde, N.R., Linke, H. & Woolfson, D.N., 2012. Squaring the circle in peptide assembly: From fibers to discrete nanostructures by de novo design. *Journal of the American Chemical Society*, 134(37), pp.15457–15467.
- Brass, L.F., 2003. Thrombin and platelet activation. *CHEST*, 134(3), p.18S–25S.
- Broderick, M.J.F. & Winder, S.J., 2005. Spectrin, α -actinin, and dystrophin. *Advances in protein chemistry*, 70(04), pp.203–246.
- Broderick, M.J.F., Bobkov, A., Winder, S.J., 2012. Utrophin ABD binds to F-actin in an open conformation. *Federation of European Biochemical Societes*, 2, pp. 6-11
- Bromley, E.H.C., Channon, K., Moutevelis, E. & Woolfson D.N., 2008. Peptide and protein building blocks for synthetic biology: from programming biomolecules to self-organized biomolecular systems. *ACS Chemical Biology*, 3(1), pp.38–50.
- Bruning, M., Kreplak, L., Leopoldseder, S., Muller, S.A., Ringler, P., Duchesne, L., Fernig, D.G., Engel, A., Ucurum-Fotiadis, Z. & Mayans, O., 2010. Bipartite design of a self-fibrillating protein copolymer with nanopatterned peptide display capabilities. *Nano Letters*, 10(11), pp.4533–4537.
- Burgueño, J., Blake, D.J., Benson, M.A., Tinsley, C.L., Esapa, C.T., Canela, E.I., Penela, P., Mallol, J., Mayor F., Lluís, C., Franco, R. & Ciruela, F., 2003. The adenosine A2A receptor interacts with the actin-binding protein α -actinin. *The Journal of Biological Chemistry*, 278(39), pp.37545–37552.
- Burridge, K. & Chrzanowska-Wodnicka, M., 1996. Focal adhesions, contractility, and signaling. *Annual Review of Cell and Developmental Biology*, 12, pp.463–518.
- Busso, D., Peleg, Y., Heidebrecht, T., Romier, C., Jacobovitch, Y., Dantes, A., Salim, L.,

- Troesch, E., Schuetz, A., Heinemann, U., Folkers, G.E., Geerlof, A., Wilmanns, M., Polewacz, A., Quedenau, C., Bussow, K., Adamson, R., Blagova, E., Walton, J., Cartwright, J.L., Bird, L.E., Owens, R.J., Berrow, N.S., Wilson, K.S. Sussman, J.L., Perrakis, A. & Celie, P.H.N., 2011. Expression of protein complexes using multiple *Escherichia coli* protein co-expression systems: a benchmarking study. *Journal of Structural Biology*, 175(2), pp.159–170.
- Bustos, S.A. & Schleif, R.F., 1993. Functional domains of the AraC protein. *Proceedings of the National Academy of Sciences of the United States of America*, 90(12), pp. 5638-5642.
- Byers, T.J., Husain-Chishti, A., Dubreuil, R.R., Branton, D. & Goldstein, L.S.B., 1989. Sequence similarity of the amino-terminal domain of *Drosophila* beta spectrin to alpha actinin and dystrophin. *The Journal of Cell Biology*, 109(October), pp.1633–1641.
- Carlson, J.C.T., Jena, S.S., Flenniken, M., Chou, T-F, Siegel, R.A., Wagner, C.R., 2006. Chemically controlled self-assembly of protein nanorings. *Journal of the American Chemical Society*, 128(23), pp.7630–7638.
- Carra, J.H. & Schleif, R.F., 1993. Variation of half-site organisation and DNA looping by AraC protein. *The EMBO Journal*, 12(1), pp.35-44.
- Carpén, O., Pallai, P., Staunton, D.E. & Springer, T.A., 1992. Association of intercellular adhesion molecule-1 (ICAM-1) with actin-containing cytoskeleton and alpha-actinin. *The Journal of Cell Biology*, 118(5), pp.1223–34.
- Celli, L., Ryckewaert, J-J., Delachanal, E. & Duperray, A., 2006. Evidence of a functional role for interaction between ICAM-1 and nonmuscle α -actinins in leukocyte diapedesis. *Journal of Immunology*, 177(6), pp.4113–4121.
- Chen, X., Zaro, J. & Shen, W-C., 2014. Fusion protein linkers: property, design and functionality. *Advanced Drug Delivery Reviews*, 65(10), pp.1357–1369.
- Chin., Olson, E.N., Richardson, J.A., Yang, Q., Humphries, C., Shelton, J.M., Wu, H., Zhu, W., Bassel-Duby, R. & Williams R.S., 1998. A calcineurin-dependent transcriptional pathway controls skeletal muscle fiber type. *Genes &*

Development, 12(16), pp.2499–2509.

Chiu, C., Bagnall, R.D., Ingles, J., Yeates, L., Kennerson, M., Donald, J.A., Jormakka, M., Lind, J.M., Semsarian, C., 2010. Mutations in alpha-actinin-2 cause hypertrophic cardiomyopathy. A genome-wide analysis. *Journal of the American College of Cardiology*, 55(11), pp.1127–1135.

Choi, S., Kelber, J., Jiang, X., Strnadel, J., Fujimura, K., Pasillas, M., Coppinger, J. & Klemke, R., 2014. Procedures for the biochemical enrichment and proteomic analysis of the cytoskeleton. *Analytical Biochemistry*, 446(1), pp.102–107.

Chworos, A., Severcan, I., Koyfman, A.Y., Weinkam, P., Oroujev, E., Hansma, H.G., Jaeger L., 2004. Building programmable jigsaw puzzles with RNA. *Science*, 306(5704), pp.2068–2072.

Clainche, C. Le & Carlier, M-F.F., 2008. Regulation of actin assembly associated with protrusion and adhesion in cell migration. *Physiological Reviews*, 88(2), pp.489–513.

Clapham, D.E., 2007. Calcium signaling. *Cell*, 131(6), pp.1047–1058.

Clark, A.R., Sawyer, G.M., Robertson, S.P. & Sutherland-Smith, A.J., 2009. Skeletal dysplasias due to filamin A mutations result from a gain-of-function mechanism distinct from allelic neurological disorders. *Human Molecular Genetics*, 18(24), pp.4791–4800.

Cohen, C.M. & Langley, R.C., 1984. Functional characterisation of human erythrocyte spectrin alpha and beta chains: association with actin and erythrocyte protein 4.1. *American Chemical Society*, 23(19), pp.4488–4495.

Colombo, G., Soto, P. & Gazit, E., 2007. Peptide self-assembly at the nanoscale: a challenging target for computational and experimental biotechnology. *Trends in Biotechnology*, 25(5), pp.211–218.

Condeelis, J. & Vahey, M., 1982. A calcium- and pH-regulated protein from *Dictyostelium discoideum* that cross-links actin filaments. *The Journal of Cell Biology*, 94(2), pp.466–471.

- Corgan, A-M., Singleton, C-A., Santoso, C.B. & Greenwood, J.A., 2004. Phosphoinositides differentially regulate α -actinin flexibility and function. *Biochemical Journal*, 378(3), pp. 1067-1072.
- Crawford, A.W., Michelsen, J.W. & Beckerle, M.C., 1992. An interaction between zyxin and alpha actinin. *The Journal of Cell Biology*, 116(6), pp.1381–1393.
- Crawford, A.W., Pino, J.D. & Beckerle, M.C.D.A-J., 1994. Biochemical and molecular characterization of the chicken cysteine-rich protein, a developmentally-regulated lim-domain protein that is associated with the actin cytoskeleton. *The Journal of Cell Biology*, 124(1), pp.117–127
- Cybulsky, A. V & Kennedy, C.R.J., 2011. Podocyte injury associated with mutant α -actinin-4. *Journal of Signal Transduction*, 2011, p.563128.
- Dandapani, S. V., Sugimoto, H., Matthews, B.D., Kolb, R.J., Sinha, S., Gerszten, R.E., Zhou, J., Ingber, D.E., Kalluri, R, & Pollak, M.R., 2007. α -Actinin-4 is required for normal podocyte adhesion. *The Journal of Biological Chemistry*, 282(1), pp.467–477.
- Das, A., Base, C., Manna, D., Cho, W. & Dubreuil, R.R., 2008. Unexpected complexity in the mechanisms that target assembly of the spectrin cytoskeleton. *The Journal of Biological Chemistry*, 283(18), pp. 12643-12653.
- Delaunay, J., 1995. Genetic disorders of the red cell mebrane. *Federation of European Biochemical Societies*, 369(1), pp. 34-37.
- Delling, U., Tureckova, J., Lim, H.W., De Windt, L.J., Rotwein, P. & Molkentin, J.D., 2000. A calcineurin-NFATc3-dependent pathway regulates skeletal muscle differentiation and slow myosin heavy-chain expression. *Molecular and Cellular Biology*, 20(17), pp.6600–11.
- DeSilva, T.M., Harper, S.L., Kotula, L., Hensley, P., Curtis, P.J., Otvos, L. & Speicher, D.W., 1997. Physical properties of a single-motif erythrocyte spectrin peptide: A highly stable independently folding unit. *Biochemistry*, 36(13), pp. 3991-3997.

- Dhermy, D., Lecomte, M.C., Garbarz, M., Bournier, O., Galand, C., Gautero, H., Feo, C., Alloisio, N., Delaunay, J. & Boivin, P., 1982. Spectrin β -chain variant associated with Hereditary Elliptocytosis. *The Journal of Clinical Investigation*, 70(4), pp. 707-715.
- Djinovic-Carugo, K., Gautel, M., Ylanne, J. & Young, P., 2002. The spectrin repeat: A structural platform for cytoskeletal protein assemblies. *FEBS Letters*, 513(1), pp.119–123.
- Djinović-Carugo, K., Young, P., Gautel, M. & Saraste, M., 1999. Structure of the alpha-actinin rod: molecular basis for cross-linking of actin filaments. *Cell*, 98(4), pp.537–546.
- Djinovic-Carugo, K., Banuelos, S. & Saraste, M., 1997. Crystal structure of a calponin homology domain. *Nature Structural Biology*, 4(3), pp.686–689.
- Doles, T., Bozic, S., Gradisar, H. & Jerala, R., 2012. Functional self-assembling polypeptide bionanomaterials. *Biochemical. Society. Transactions.*, 40(4), pp.629–634.
- Dubois, C., Panicot-Dubois, L., Merrill-Skoloff, G., Furie, B. & Furie, B.C., 2006. Glycoprotein VI – dependent and – independent pathways of thrombus formation in vivo. *Blood*, 107(10), pp.3902–3906.
- Dubreuil, R.R. et al., 1989. The Complete sequence of Drosophila alpha-spectrin: conservation of structural domains between alpha-spectrins and alpha-actinin. *The Journal of Biological Chemistry*, 109(November), pp.2197–2205.
- Dumetz, A.C., Snellinger-O'Brien, A.M., Kaler, E.W. & Lenhoff, A.M., 2007. Patterns of protein – protein interactions in salt solutions and implications for protein crystallization. *Protein Science*, 16(9), pp.1867–1877.
- Durand, D., 2003. Vertebrate Evolution: Doubling and shuffling with a full deck. *Trends in Genetics*, 19(1), pp. 2-5.
- Dwir, O., Kansas, G.S. & Alon, R., 2001. Cytoplasmic anchorage of L-selectin controls leukocyte capture and rolling by increasing the mechanical stability of the

- selectin tether. *The Journal of Cell Biology*, 155(1), pp.145–156.
- Edlund, M., Lotano, M.A. & Otey, C.A., 2001. Dynamics of alpha-actinin in focal adhesions and stress fibers visualized with alpha-actinin-green fluorescent protein. *Cell Motility and the Cytoskeleton*, 48(3), pp.190–200.
- Ehrlicher, A.J., Krishnan, R., Guo, M., Bidan, C.M., Weitz, D.A. & Pollak, M.R., 2015. Alpha-actinin binding kinetics modulate cellular dynamics and force generation. *Proceedings of the National Academy of Sciences of the United States of America*, 112(21), pp.6619–24.
- Ellis, R.J. & Teresa J. T. Pinheiro, 2002. Danger — misfolding proteins. *Nature*, 416(April), p.483.
- Endo, M., Katsuda, Y., Hidaka, K. & Sugiyama, H., 2010. A versatile DNA nanochip for direct analysis of DNA base-excision repair. *Angewandte Chemie International Edition*, 49(49), pp.9412–9416.
- Eynon, N., Ruiz, J.R., Femia, P., Pushkarev, V.P., Cieszczyk, P., Maciejewska-Karlowska, A., Sawczuk, M., Dyatlov, D.A., Lekontsev, E.V., Kulikov, L.M., Birk, R., Bishop, D.J. & Lucia, A., 2012. The *ACTN3* R577X polymorphism across three groups of elite male European athletes. *PLoS ONE*, 7(8), pp.1–7.
- Fairman, R., Chao, H-G., Lavoie, T.B., Villafranca, J.J., Matsueda, G.R. & Novotny, J., 1996. Design of heterotetrameric coiled coils: Evidence for increased stabilization by Glu--Lys⁺ ion pair interactions. *Biochemistry*, 35(9), pp.2824–2829.
- Falet, H., Pollitt, A.Y., Begonja, A.J., Weber, S.E., Duerschmied, D., Wagner, D.D., Watson, S.P. & Hartwig, J.H., 2010. A novel interaction between FlnA and Syk regulates platelet ITAM-mediated receptor signaling and function. *The Journal of Experimental Medicine*, 207(9), pp.1967–1979.
- Fanarraga, M.L., Carranza, G., Castano, R., Nolasco, S., Avila, J. & Zabala, J.C., 2010. Nondenaturing electrophoresis as a tool to investigate tubulin complexes. *Methods in Cell Biology*, 95(10), pp.59–75.

- Fegan, A., White, B., Carlson, J.C.T. & Wagner, C.R., 2010. Chemically controlled protein assembly: techniques and applications. *Chemical Reviews*, 110(6), pp.3315–3336.
- Fegan, A., Kumarapperuma, S.C. & Wagner, C.R., 2012. Chemically self-assembled antibody nanostructures as potential drug carriers. *Molecular Pharmaceutics*, 9(11), pp.3218–3227.
- Feng, D., DuMontier, C. & Pollak, M.R., 2015. The role of alpha-actinin-4 in human kidney disease. *Cell & Bioscience*, 5(44).
- Fernandez-Lopez, S., Kim, H-S., Choi, E.C., Delgado, M., Granja, J.R., Khasanov, A., Kraehenbuehl, K., Long, G., Weinberger, D.A., Wilcoxon, K.M., & Ghadiri, M.R., 2001. Antibacterial agents based on the cyclic D,L- α -peptide architecture. *Nature*, 412(6845), pp.452–455.
- Fletcher, D.A. & Mullins, R.D., 2010. Cell mechanics and the cytoskeleton. *Nature*, 463(7280), pp.485–492.
- Flood, G., Kahana, E., Gilmore, A.P., Rowe, A.J., Gratzer, W.B. & Critchley, D.R., 1995. Association of structural repeats in the alpha-actinin rod domain. Alignment of inter-subunit interactions. *Journal of Molecular Biology*, 252(2), pp.227–234.
- Flood, G., Rowe, A.J., Critchley, D.R. & Gratzer, W.B., 1997. Further analysis of the role of spectrin repeat motifs in alpha-actinin dimer formation. *European Biophysics Journal*, 25(5), pp.431–435.
- Foley, K.S. & Young, P.W., 2013. An analysis of splicing, actin-binding properties, heterodimerization and molecular interactions of the non-muscle α -actinins. *Biochemical Journal*, 452(3), pp.477–88.
- Foley, K.S. & Young, P.W., 2014. The non-muscle functions of α -actinin. *Biochemical Journal*, 459(1), pp.1–13.
- Fraleigh, T.S., Tran, T.C., Corgan, A.M., Nash, C.A., Hao, J., Critchley, D.R., Greenwood, J.A., 2003. Phosphoinositide binding inhibits alpha-actinin bundling activity.

The Journal of Biological Chemistry, 278(26), pp.24039–24045.

Fraleigh, T.S., Pereira, C.B., Tran, T.C., Singleton, C.A. & Greenwood, J.A., 2005.

Phosphoinositide binding regulates alpha-actinin dynamics: mechanism for modulating cytoskeletal remodeling. *The Journal of Biological Chemistry*, 280(15), pp.15479–15482.

Francis, D.M. & Page, R., 2010. Strategies to Optimize Protein Expression in *E. coli*.

Current Protocols in Protein Science, 5(24), pp.1–29.

Franco, A.T., Corken, A. & Ware, J., 2015. Review Article Platelets at the interface of thrombosis , inflammation, and cancer. *Blood*, 126(5), pp.582–589.

Franzot, G., Sjoeblo, B., Gautel, M. & Djinoic-Carugo, K., 2005. The crystal structure of the actin binding domain from alpha-actinin in its closed conformation: Structural insight into phospholipid regulation of alpha-actinin. *Journal of Molecular Biology*, 348(1), pp.151–165.

Friedlander, S.M., Herrmann, A.L., Lowry, D.P., Meph, E.R., Lek, M., North, K.N. & Organ, C.L., 2013. *ACTN3* allele frequency in humans covaries with global latitudinal gradient. *PLoS ONE*, 8(1), pp.6–9.

Fu, T.-J. & Seeman, N.C., 1993. Dna double-crossover molecules. *Biochemistry*, 32(13), pp.3211–3220.

Fukami, K., Furuhashi, K., Inagaki, M., Endo, T., Hatano, S. & Takenawa, T., 1992.

Requirement of a phosphatidylinositol 4,5-bisphosphate for α -actinin function. *Nature*, 359(6391), pp. 150-152.

Fukami, K., Sawada, N., Endo, T., Takenawa, T., 1996. Identification of a phosphatidylinositol 4,5-bisphosphate -binding site in chicken skeletal muscle α -actinin. *The Journal of Biological Chemistry*, 271(5), pp. 2646-2650.

Furie, B. & Furie, B.C., 2008. Mechanisms of thrombus formation. *The New England Journal of Medicine*, 359(9), pp.938–949.

Galkin, V.E., Orlova, A., Salmazo, A., Djinoic-Carugo, K. & Egelman, E.H., 2010.

Opening of tandem calponin homology domains regulates their affinity for F-

- actin. *Nature Structural & Molecular Biology*, 17(5), pp.614–6.
- Ganesh, C., Shah, A.N., Swaminaththan, C.P., Surolia, A. and Varadarajan, R., 1997. Thermodynamic characterisation of the reversible, two-state unfolding of the maltose binding protein, a large two-domain protein. *Biochemistry*, 36(16), pp. 5020-5028.
- Gautel, M., Goulding D., Bullard, B., Weber, K. & Furst, D.O., 1996. The central Z-disk region of titin is assembled from a novel repeat in variable copy numbers. *Journal of Cell Science*, 109(Pt 1), pp.2747–54.
- Gautel, M. & Djinoovic-Carugo, K., 2016. The sarcomeric cytoskeleton: from molecules to motion. *Journal of Experimental Biology*, 219(2), pp.135–145.
- Georgiou, G. & Valax, P., 1996. Expression of correctly folded proteins in *Escherichia coli*. *Current Opinion in Biotechnology*, 7(2), pp.190–197.
- Ghazarian, H., Idoni, B. & Oppenheimer, S.B., 2011. A glycobiology review: carbohydrates, lectins, and implications in cancer therapeutics. *Acta Histochemica*, 113(3), pp.236–247.
- Gilead, S. & Gazit, E., 2005. Self-organization of short peptide fragments: from amyloid fibrils to nanoscale supramolecular assemblies. *Supramolecular Chemistry*, 17(1-2), pp.87–92.
- Gimona, M., Djinoovic-Carugo, K., Kranewitter, W.J. & Winder, S.W., 2002. Functional plasticity of CH domains. *FEBS Letters*, 513(1), pp.98–106.
- Girolami, F., Iascone, M., Tomberli, B., Bardi, S., Benelli, M., Marseglia, G., Pescucci, C., Pezzoli, L., Sana, M.E., Basso, C., Marziliano, N., Merlini, P.A., Fornaro, A., Cecchi, F., Torricelli, F. & Olivotto, I., 2014. Novel α -actinin-2 variant associated with familial hypertrophic cardiomyopathy and juvenile atrial arrhythmias: a massively parallel sequencing study. *Circulation: Cardiovascular Genetics*, 7(6), pp.741–750.
- Goldsmith, S.C., Pokala, N., Shen, W., Fedorov, A.A., Matsudaira, P. & Almo, S.C., 1997. The structure of an actin-crosslinking domain from human fimbrin.

Nature Structural and Molecular Biology, 4(9), pp.708–712.

Goldstein, M.A., Michael, L.H., Schroeter, J. P. & Sass, R.L., 1988. Structural states in the Z-band of skeletal muscle correlate with states of active and passive tension. *The Journal of General Physiology*, 92(1), pp. 113-119.

Goodsell, D.S. & Olson, A.J., 2000. Structural symmetry and protein function. *Annual Review of Biophysics and Biomolecular Structure*, 29, pp.105–53.

Goubau, C., Buyse, G.M., Van Geet, C. & Freson, K., 2014. The contribution of platelet studies to the understanding of disease mechanisms in complex and monogenetic neurological disorders. *Developmental Medicine and Child Neurology*, 56(8), pp.724–731.

Gradišar, H., Bozic, S., Doles, T., Vengust, D., Hafner-Bratkovic, I., Mertelj, A., Webb, B., Sali, A., Klavzar, S. & Jerala, R., 2013. Design of a single-chain polypeptide tetrahedron assembled from coiled-coil segments. *Nature Chemical Biology*, 9(6), pp. 362-366.

Gradišar, H. & Jerala, R., 2014. Self-assembled bionanostructures: proteins following the lead of DNA nanostructures. *Journal of Nanobiotechnology*, 12(4), p.4.

Gratzner, W.B., 1981. The red cell membrane and its cytoskeleton. *Biochemical Journal*, 198(1), pp.1–8.

Greenwood, J.A., Theibert, A.B., Prestwich, G.D. & Murphy-Ullrich, J.E., 2000. Restructuring of focal adhesion plaques by PI 3-kinase: regulation by ptdIns (3,4,5)-P3 binding to alpha-actinin. *The Journal of Cell Biology*, 150(3), pp.627–641.

Gregg, D., 2003. Platelets and cardiovascular disease. *Circulation*, 108(13), p.88–90.

Grueninger, D., Treiber, N., Ziegler, M.O.P., Koetter, J.W.A., Schulze, M-S. & Schulz, G.E., 2008. Designed protein-protein association. *Science*, 319(January), pp.206–210.

- Grum, V.L., Li, D., MacDonald, R.I. & Mondragon, A., 1999. Structures of two repeats of spectrin suggest models of flexibility. *Cell*, 98(4), pp.523–535.
- Guéguen, P., Rouault, K., Chen, J-M., Raguene, O., Fichou, Y., Hardy, E., Gobin, E., Pan-petes, B., Kerbirou, M., Trouve, P., Marcorelles, P., Abgrall, J-F., Le Marechal, C. & Ferec, C., 2013. A missense mutation in the alpha-actinin-1 gene (*ACTN1*) is the cause of autosomal dominant macrothrombocytopenia in a large french family. *PLoS ONE*, 8(9), pp.1–8.
- Gunay-Aygun, M., Falik-Zaccai, T.C., Vilboux, T., Zivony-Elboun, Y., Gumruk, F., Cetin, M., Khayat, M., Boerkoel, C.F., Kfir, N., Huang, Y., Maynard, D., Doward, H., Berger, K., Kleta, R., Anikster, Y., Arat, M., Freiberg, A.S., Kehrel, B.E., Jurk, K., Cruz, P., Mullikin, J.C., White, J.G., Huizing, M. & Gahl, W.A., 2011. NBEAL2 is mutated in gray platelet syndrome and is required for biogenesis of platelet alpha-granules. *Nature Genetics*, 43(8), pp.732–734.
- Guo, P., 2010. The emerging field of RNA nanotechnology. *Nature Nanotechnology*, 5(12), pp.833–842.
- Guzman, L.M., Belin, D., Carson, M.J. & Beckwith., 1995. Tight regulation, modulation, and high-level expression by vectors containing the arabinose P_{BAD} promoter. *Journal of Bacteriology*, 177(14), pp.4121–4130.
- Han, X., Zheng, Y., Munro, C.J., Ji, Y. & Braunschweig, A.B., 2015. Carbohydrate nanotechnology: hierarchical assembly using nature's other information carrying biopolymers. *Current Opinion in Biotechnology*, 34, pp.41–47.
- Hanein, D., Volkmann, N., Goldsmith, S., Michon, A-M., Lehman, W., Craig, R., DeRosier, D., Almo, S. & Matsudaira, P., 1998. An atomic model of fimbrin binding to F-actin and its implications for filament crosslinking and regulation. *Nature Structural and Molecular Biology*, 5(9), pp. 787-792.
- Harbury, P.B., Zhang, T., Kim, P.S. & Alber, T., 1993. A switch between two-, three- and four-stranded coiled-coils in GCN4 leucine zipper mutants. *Science*, 262(5138), pp. 1401-1407.
- Harper, S.L., Begg, G.E. & Speicher, D.W., 2001. Role of terminal nonhomologous

- domains in initiation of human red cell spectrin dimerization. *Biochemistry*, 40(33), pp.9935–9943.
- Harris, A.S., Croall, D.E. & Morrow, J.S., 1988. The calmodulin binding site in α -fodrin is near the calcium dependent protease-I cleavage site. *The Journal of Biological Chemistry*, 263(30), pp. 15754-15761.
- Harris, A.S. & Morrow, J.S., 1988. Proteolytic processing of human brain alpha spectrin (fodrin): identification of a hypersensitive site. *The Journal of Neuroscience*, 8(7), pp. 2640-2651.
- Hartwig, J. & Italiano, J., 2003. The birth of the platelet. *Journal of Thrombosis and Haemostasis*, 1(7), pp.1580–1586.
- Hartwig, J.H. & Italiano, J.E., 2006. Cytoskeletal mechanisms for platelet production. *Blood Cells, Molecules, and Diseases*, 36(2), pp.99–103.
- Hayashida, Y., Honda, K., Idogawa, M., Ino, Y., Ono, M., Tsuchida, A., Aoki, T., Hirohashi, S. & Yamada, T., 2005. E-cadherin regulates the association between beta-catenin and actinin-4. *Cancer Research*, 65(19), pp.8836–8845.
- Hayes, N.V.L., Scott, C., Heerkens, E., Ohanian, V., Maggs, A.M., Pinder, J.C., Kordeli, E. & Baines, J.A., 2000. Identification of a novel C-terminal variant of β II spectrin: two isoforms of β II spectrin have distinct intracellular locations and activities. *Journal of Cell Science*, 113(Pt 11), pp. 2023-2034.
- He, D. & Marles-Wright, J., 2015. Ferritin family proteins and their use in bionanotechnology. *New Biotechnology*, 32(6), pp. 651-657.
- Head, S.I., Chan, S., Houweling, P.J., Quinlan, K.G.R., Murphy, R., Wagner, S., Friedrich, O. & North, K.N., 2015. Altered calcium kinetics associated with alpha-actinin-3 deficiency may explain positive selection for *ACTN3* null allele in human evolution. *PLoS Genetics*, 11(1), pp.1–18.
- Heemskerk, J.W.M., Bevers, E.M. & Lindhout, T., 2002. Platelet activation and blood coagulation. *Thrombosis and haemostasis*, 88(2), pp.186–193.
- Hemmings, L., Kuhlman, P.A. & Critchley, D.R., 1992. Analysis of the actin-binding

domain of alpha-actinin by mutagenesis and demonstration that dystrophin contains a functionally homologous domain. *The Journal of Cell Biology*, 116(6), pp.1369–1380.

Heng, Y-W. & Koh, C-G., 2010. Actin cytoskeleton dynamics and the cell division cycle. *The International Journal of Biochemistry & Cell Biology*, 42(10), pp.1622–33.

Holmes, T.C., De Lacalle, S., Su, X., Liu, G., Rich, A. & Zhang, S., 2000. Extensive neurite outgrowth and active synapse formation on self-assembling peptide scaffolds. *Proceedings of the National Academy of Sciences of the United States of America*, 97(12), pp.6728–6733.

Holterhoff, C.K., Saunders, R.H., Brito, E.E. & Wagner, D.S., 2009. Sequence and expression of the zebrafish alpha-actinin gene family reveals conservation and diversification among vertebrates. *Developmental Dynamics*, 238(11), pp.2936–2947.

Honda, K., Yamada, T., Hayashida, Y., Idogawa, M., Sato, S., Hasegawa, F., Ino, Y., Ono, M. & Hirohashi, S., 2005. Actinin-4 increases cell motility and promotes lymph node metastasis of colorectal cancer. *Gastroenterology*, 128(1), pp.51–62.

Honda, K., Yamada, T., Endo, R., Ino, Y., Gotoh, M., Tsuda, H., Yamada, Y., Chiba, H. Hirohashi, S., 1998. Actinin-4, a novel actin-bundling protein associated with cell motility and cancer invasion. *The Journal of Cell Biology*, 140(6), pp.1383–1393.

Honda, K., Yamada, T., Seike, M., Hayashida, Y., Idogawa, M., Kondo, T., Ino, Y. & Hirohashi, S., 2004. Alternative splice variant of actinin-4 in small cell lung cancer. *Oncogene*, 23(May), pp.5257–5262.

Honda, K., 2015. The biological role of actinin-4 (ACTN4) in malignant phenotypes of cancer. *Cell & Bioscience*, 5(41).

Hotulainen, P. & Lappalainen, P., 2006. Stress fibers are generated by two distinct actin assembly mechanisms in motile cells. *The Journal of Cell Biology*, 173(3),

pp.383–394.

- Hughes, A.L., 1999. Phylogenies of developmentally important proteins do not support the hypothesis of two rounds of genome duplication early in vertebrate history. *Journal of Molecular Evolution*, 48(5), pp. 565-576.
- Hyvonen, M., Macias, M.J., Nilges, M., Oschkinat, H., Saraste, M. & Wilmanns, M., 1995. Structure of the binding site for inositol phosphates in a PH domain. *The EMBO Journal*, 14(19), pp. 4676-4685.
- Ikura, M., 1996. Calcium binding and conformational response in EF-hand proteins. *Trends in Biochemical Sciences*, 21(1), pp.14–17.
- Imamura, M., Endo, T., Kuroda, M., Tanaka, T. & Masaki, T., 1988. Substructure and higher structure of chicken smooth muscle alpha-actinin molecule. *The Journal of Biological Chemistry*, 263(16), pp.7800–7805.
- Ipsaro, J.J., Harper, S.L., Messick, T.E., Marmorstein, R., Mondragon, A. & Speicher, D.W., 2010. Crystal structure and functional interpretation of the erythrocyte spectrin tetramerization domain complex. *Blood*, 115(23), pp.4843–4852.
- Italiano, J.E., Lecine, P., Shivdasani, R.A. & Hartwig, J.H., 1999. Blood platelets are assembled principally at the ends of proplatelet processes produced by differentiated megakaryocytes. *The Journal of Cell Biology*, 147(6), pp.1299–1312.
- Izaguirre, G., Aguirre, L., Hu, Y-P., Lee, H.Y., Schlaepfer, D.D., Aneskievich, B.J. & Haimovich, B., 2001. The cytoskeletal/non-muscle isoform of alpha-actinin is phosphorylated on its actin-binding domain by the focal adhesion kinase. *The Journal of Biological Chemistry*, 276(31), pp.28676–28685.
- Jennings, L.K., 2009. Mechanisms of platelet activation: need for new strategies to protect against platelet-mediated atherothrombosis. *Thrombosis and Haemostasis*, 102(2), pp.248–257.
- Jiang, G-B., Quan, D., Liao, K. & Wang, H., 2006. Novel polymer micelles prepared from chitosan grafted hydrophobic palmitoyl groups for drug delivery.

Molecular Pharmaceutics, 3(2), pp.152–160.

Jungmann, R., Renner, S. & Simmel, F.C., 2008. From DNA nanotechnology to synthetic biology. *HFSP Journal*, 2(2), pp.99–109.

Kamath, S., Blann, A.D. & Lip, G.Y.H., 2001. Platelet activation: assessment and quantification. *European Heart Journal*, 22(17), pp.1561–1571.

Kaplan, J.M., Kim, S.H., North, K.N., Rennke, H., Correia, L.A., Tong, H-Q., Mathis, B.J., Rodriguez-Perez, J-C., Allen, P.G., Beggs, A.H. & Pollak, M.R., 2000. Mutations in *ACTN4*, encoding alpha-actinin-4, cause familial focal segmental glomerulosclerosis. *Nature Genetics*, 24(March), pp.251–256.

Ke, Y., Sharma, J., Liu, M., Jahn, K., Liu, Y. & Yan, H., 2009. Scaffolded DNA origami of a DNA tetrahedron molecular container. *Nano Letters*, 9(6), pp.2445–2447.

Ke, Y., Lindsay, S., Chang, Y., Liu, Y. & Yan, H., 2008. Self-assembled water-soluble nucleic acid probe tiles for label-free RNA hybridization assays. *Science*, 319(180), pp.180–183.

Keep, N.H., Winder, S.J., Moores, C.A., Walke, S., Norwood, F.L.M. & Kendrick-Jones, J., 1999. Crystal structure of the actin-binding region of utrophin reveals a head-to-tail dimer. *Structure*, 7(12), pp.1539–1546.

Kelley, M.J., Jawien, W., Ortel, T.L. & Korczak, J.F., 2000. Mutation of MYH9, encoding non-muscle myosin heavy chain A, in May-Hegglin anomaly. *Nature Genetics*, 26(1), pp.106–108.

Kennedy, S.P., Warren, S.L., Forget, B.G. & Morrow, J.S., 1991. Ankyrin binds to the 15th repetitive unit of erythroid and non-erythroid β -spectrin. *The Journal of Cell Biology*, 115(1), pp. 267-277.

Khurana, S., Chakraborty, S., Cheng, X., Su, Y-T. & Kao, H-Y., 2011. The actin-binding protein, actinin alpha 4 (*ACTN4*), is a nuclear receptor coactivator that promotes proliferation of MCF-7 breast cancer cells. *The Journal of Biological Chemistry*, 286(3), pp.1850–1859.

Kim, K-J., Kim, H-E., Lee, K-H., Han, W., Yi, M-J., Jeong, J. & Oh, B-H., 2004. Two-

promoter vector is highly efficient for overproduction of protein complexes.

Protein science, 13(6), pp.1698–1703.

King, N.P. & Lai, Y.T., 2013. Practical approaches to designing novel protein assemblies. *Current Opinion in Structural Biology*, 23(4), pp.632–638.

King, S.M. & Reed, G.L., 2002. Development of platelet secretory granules. *Seminars in Cell & Developmental Biology*, 13(6), pp.507–513.

Kisiday, J., Jin, M., Kurz, B., Hung, H., Semino, C., Zhang, S. & Grodzinsky., 2002. Self-assembling peptide hydrogel fosters chondrocyte extracellular matrix production and cell division: implications for cartilage tissue repair. *Proceedings of the National Academy of Sciences*, 99(15), pp.9996–10001.

Knudsen, K.A., Soler, A.P., Johnson, K.R. & Wheelock, M.J., 1995. Interaction of alpha-actinin with the cadherin/catenin cell-cell adhesion complex via alpha-catenin. *The Journal of Cell Biology*, 130(1), pp.67–77.

Korsgren, C. & Lux, S.E., 2010. The carboxyterminal EF domain of erythroid alpha-spectrin is necessary for optimal spectrin-actin binding. *Blood*, 116(14), pp.2600–2607.

Korsgren, C., Peters, L.L. & Lux, S.E., 2010. Protein 4.2 binds to the carboxyl-terminal EF-hands of erythroid α -spectrin in a calcium- and calmodulin-dependent manner. *The Journal of Biological Chemistry*, 285(7), pp.4757–4770.

Kos, C.H., Le, T.C., Sinha, S., Henderson, J.M., Kim, S.H., Sugimoto, H., Kalluri, R., Gerszten, R.E. & Pollak, M.R., 2003. Mice deficient in alpha-actinin-4 have severe glomerular disease. *The Journal of Clinical Investigation*, 111(11), pp.1683–1690.

Krishnan, Y. & Bathe, M., 2012. Designer nucleic acids to probe and program the cell. *Trends in Cell Biology*, 22(12), pp.624–633.

Kuhlman, P. A., Hemmings, L. & Critchley, D.R., 1992. The identification and characterisation of an actin-binding site in alpha-actinin by mutagenesis. *FEBS letters*, 304(2), pp.201–206.

- Kunishima, S., Okuna, Y., Yosida, K., Shiraishi, Y., Sanada, M., Muramatsu, H., Chiba, K., Tanaka, H., Miyazaki, K., Sakai, M., Ohtake, M., Kobayashi, R., Iguchi, A., Niimi, G., Otsu, M., Takahashi, Y., Miyano, S., Saito, H., Kojima, S. & Ogawa, S., 2013. *ACTN1* mutations cause congenital macrothrombocytopenia. *American Journal of Human Genetics*, 92(3), pp.431–438.
- Kunishima, S. & Saito, H., 2006. Congenital macrothrombocytopenias. *Blood Reviews*, 20(2), pp.111–121.
- Kusunoki, H., Minasov, G., et al., 2004a. Independent movement, dimerization and stability of tandem repeats of chicken brain α -spectrin. *Journal of Molecular Biology*, 344(2), pp.495–511.
- Kusunoki, H., MacDonald, R.I. & Mondragon, A., 2004b. Structural insights into the stability and flexibility of unusual erythroid spectrin repeats. *Structure*, 12(4), pp.645–656.
- Kuwahara, M., Sugimoto, M., Tsuji, S., Matsui, H., Mizuno, T., Miyata, S. & Yoshioka, A., 2002. Platelet shape changes and adhesion under high shear flow. *Arteriosclerosis, Thrombosis, and Vascular Biology*, 22(2), pp.329–334.
- LaBrake, C.C., Wang, L., Keiderling, T.A. & Fung, L.W-M., 1993. Fourier transform infrared spectroscopic studies of the secondary structure of spectrin under different ionic strengths. *Biochemistry*, 32(39), pp. 10296–10302.
- Lai, Y-T., Tsai, K-L., Sawaya, M.R., Asturias, F.J., Yeates, T.O., et al., 2013. Structure and flexibility of nanoscale protein cages designed by symmetric self-assembly. *Journal of the American Chemical Society*, 135(20), pp.7738–7743.
- Lai, Y.T., King, N.P. & Yeates, T.O., 2012. Principles for designing ordered protein assemblies. *Trends in Cell Biology*, 22(12), pp.653–661.
- Langanger, G., Moeremans, M., Daneels, G., Sobieszek, A., De Brabander, M. & De Mey, J., 1986. The molecular organization of myosin in stress fibers of cultured cells. *The Journal of Cell Biology*, 102(January), pp.200–209.
- Larsen, H.B., 2003. Kenyan dominance in distance running. *Comparative*

Biochemistry and Physiology 136(3), pp.161–170.

Lee, J., Choi, Y.J. & Lim, Y., 2010. Self-assembled filamentous nanostructures for drug/gene delivery applications. *Expert Opinion on Drug Delivery*, 7(3), pp.341–351.

Lee, S.H., Weins, A., Hayes, D.B., Pollak, M.R. & Dominguez, R., 2008. Crystal structure of the actin-binding domain of alpha-actinin-4 Lys255Glu mutant implicated in focal segmental glomerulosclerosis. *Journal of Molecular Biology*, 376(2), pp.317–324.

Lee, S.K., Chou, H.H., Pflieger, B.F., Newman, J.D., Yoshikuni, Y. & Keasling, J.D., 2007. Directed evolution of AraC for improved compatibility of arabinose- and lactose-inducible promoters. *Applied and Environmental Microbiology*, 73(18), pp.5711–5715.

Lek, M., Quinlan, K.G.R. & North, K.N., 2010. The evolution of skeletal muscle performance: gene duplication and divergence of human sarcomeric alpha-actinins. *BioEssays*, 32(1), pp.17–25.

Lemmon, M.A. & Ferguson, K.M., 2000. Signal-dependent membrane targeting by pleckstrin homology (PH) domains. *Biochemical Journal*, 350(1), pp. 1-18.

Lemmon, M.A., Ferguson, K.M. & Abrams, C.S., 2002. Pleckstrin homology domains and the cytoskeleton. *Federation of European Biochemical Societies*, 513(1), pp. 71-76.

LeRoy, C. & Wrana, J.L., 2005. Clathrin and non-clathrin mediated endocytic regulation of cells signalling. *Nature Reviews*, 112(6), pp. 112-126.

Levine, B.A., Moir, A.J.G., Patchell, V.B. & Perry, S.V., 1992. Binding sites involved in the interaction of actin with the N-terminal region of dystrophin. *FEBS Letters*, 298(1), pp.44–48.

Levine, B.A., Moir, A.J.G., Patchell, V.B. & Perry, S.V., 1990. The interaction of actin with dystrophin. *FEBS Letters*, 263(1), pp.159–162.

Li, D., Harper, S. & Speicher, D.W., 2007. Initiation and propagation of spectrin

heterodimer assembly involves distinct energetic processes. *Biochemistry*, 46(37), pp.10585–10594.

Li, D., Tang, H.Y. & Speicher, D.W., 2008. A structural model of the erythrocyte spectrin heterodimer initiation site determined using homology modeling and chemical cross-linking. *The Journal of Biological Chemistry*, 283(3), pp.1553–1562.

Li, H., Lee, T., Dziubla, T., Pi, F., Guo, S., Xu, J., Li, C., Haque, F., Liang, X-J. & Guo, P., 2016. RNA as a stable polymer to build controllable and defined nanostructures for material and biomedical applications. *Nano Today*, 10(5), pp.631–655.

Li, Q., So, C.R., Fegan, A., Cody, V., Sarikaya, M., Vallera, D.A. & Wagner, C.R., 2010. Chemically self-assembled antibody nanorings (CSANs): design and characterization of an anti-CD3 IgM biomimetic. *Journal of the American Chemical Society*, 132(48), pp.17247–17257.

Lim, P. J. & Gleeson, P.A., 2011. Macropinocytosis: an endocytic pathway for internalising large gulps. *Immunology and Cell Biology*, 89(8), pp. 836-843.

Liu, J., Taylor, D.W. & Taylor, K.A., 2004. A 3-D reconstruction of smooth muscle alpha-actinin by CryoEm reveals two different conformations at the actin-binding region. *Journal of Molecular Biology*, 338(1), pp.115–125.

Liu, S.C., Derick, L.H. & Palek, J., 1987. Visualization of the hexagonal lattice in the erythrocyte membrane skeleton. *Journal of Cell Biology*, 104(3), pp.527–536.

Liu, S.C., Palek, J., Prchal, J.T., Defective spectrin dimer-dimer association in hereditary elliptocytosis. *Proceedings of the National Academy of Sciences of the United States of America*, 79(6), pp. 2072-2076.

Liu, Y. & Kuhlman, B., 2006. RosettaDesign server for protein design. *Nucleic Acids Research*, 34(Web Server Issue), pp.235–238.

Lobell, R.B. & Schleif, R.F., DNA looping and unlooping by AraC protein. *Science*, 250(4980), pp. 528-532.

Lodish, H., Berk, A., Kaiser, C.A., Krieger, M., Scott, M.P., Bretcher, A., Ploegh, H. &

- Matsudaira, P., 2008a. Cell organisation and movement. Ahr, K., Tontono, M., Pantges-Frost, E., Rice, E., Tymoczko, N. & Varas, C., *Molecular Cell Biology*. New York: W.H. Freeman and Company, pp. 713–754.
- Lodish, H., Berk, A., Kaiser, C.A., Krieger, M., Scott, M.P., Bretcher, A., Ploegh, H. & Matsudaira, P., 2008b. Integrating cells into tissues. Ahr, K., Tontono, M., Pantges-Frost, E., Rice, E., Tymoczko, N. & Varas, C., *Molecular Cell Biology*. New York: W.H. Freeman and Company, pp. 801–847.
- Long, Y.C., Glund, S., Garcia-Roves, P.M. & Zierath, J.R., 2007. Calcineurin regulates skeletal muscle metabolism via coordinated changes in gene expression. *The Journal of Biological Chemistry*, 282(3), pp.1607–1614.
- Luther, P.K., 2009. The vertebrate muscle Z-disc: sarcomere anchor for structure and signalling. *Journal of Muscle Research and Cell Motility*, 30(5), pp.171–185.
- Luther, P.K., 1991. Three-dimensional reconstruction of a simple Z-band in fish muscle. *The Journal of Cell Biology*, 113(5), pp.1043–1055.
- Luther, P.K., Barry, J.S. & Squire, J.M., 2002. The three-dimensional structure of a vertebrate wide (slow muscle) Z-band: lessons on Z-band assembly. *Journal of Molecular Biology*, 315(1), pp.9–20.
- Mabuchi, I., Hamaguchi, Y., Kobayashi, T., Hosoya, H., Tsukita, S. & Tsukita, S., 1985. Alpha-actinin from sea urchin eggs: biochemical properties, interaction with actin, and distribution in the cell during fertilization and cleavage. *The Journal of Cell Biology*, 100(2), pp.375–383.
- MacArthur, D.G., Seto, J.T., Raftery, J.M., Quinlan, K.G., Huttley, G.A., Hook, J.W., Lemckert, F.A., Kee, A.J., Edwards, M.R., Berman, Y., Hardeman, E.C., Gunning, P.W., Eastal, S., Yang, N. & North, K.N., 2007. Loss of *ACTN3* gene function alters mouse muscle metabolism and shows evidence of positive selection in humans. *Nature Genetics*, 39(10), pp.1261–1265.
- MacArthur, D.G. & North, K.N., 2007. ACTN3: A genetic influence on muscle function and athletic performance. *Exercise and Sport Sciences Reviews*, 35(1), pp.30–34.

- MacDonald, R.I., & Cummings, J.A., 2004. Stabilities of folding of clustered, two-repeat fragments of spectrin reveal a potential hinge in the human erythroid spectrin tetramer. *Proceedings of the National Academy of Sciences of the United States of America*, 101(6), pp. 1502-1507.
- Machesky, L.M., 2008. Lamellipodia and filopodia in metastasis and invasion. *FEBS Letters*, 582(14), pp.2102–2111.
- Machlus, K.R. & Italiano, J.E., 2013. The incredible journey: from megakaryocyte development to platelet formation. *The Journal of Cell Biology*, 201(6), pp.785–796.
- Machlus, K.R., Thon, J.N. & Italiano, J.E., 2014. Interpreting the developmental dance of the megakaryocyte: a review of the cellular and molecular processes mediating platelet formation. *British Journal of Haematology*, 165(2), pp.227–236.
- Machnicka, B., Czogalla, A., Hryniewicz-Jankowska, A., Boguslawska, D.M., Grochowalska, R., Heger, E. & Sikorski, A.F., 2014. Spectrins: a structural platform for stabilization and activation of membrane channels, receptors and transporters. *Biochimica et Biophysica Acta - Biomembranes*, 1838(2), pp.620–634.
- MaHam, A., Tang, Z., Wu, H., Wang, J. & Lin Y., 2009. Protein-based nanomedicine platforms for drug delivery. *Small*, 5(15), pp. 1706-1721.
- Mashaghi, S., Jadidi, T., Koenderink, G. & Maghaghi, A., 2013. Lipid nanotechnology. *International Journal of Molecular Sciences*, 14(2), pp.4242–4282.
- Mason, J.M. & Arndt, K.M., 2004. Coiled coil domains: stability, specificity, and biological implications. *ChemBiochem: A European Journal of Chemical Biology*, 5(2), pp. 170-176.
- De Matteis, M.A. & Morrow, J.S., 2000. Spectrin tethers and mesh in the biosynthetic pathway. *Journal of Cell Science*, 113 (Pt 13), pp.2331–2343.
- Matthews, K.S., 1992. DNA looping. *Microbiological Reviews*, 56(1), pp.123–36.

- Mayer, B.J., 2001. SH3 domains: complexity in moderation. *Journal of Cell Science*, 114 (Pt 7), pp. 1253-1263.
- McNeil, S.E., 2005. Nanotechnology for the biologist. *Journal of Leukocyte Biology*, 78(3), pp.585–594.
- Michaud, J-L.R., Hosseini-Abardeh, M., Farah, K. & Kennedy, C.R.J., 2009. Modulating alpha-actinin-4 dynamics in podocytes. *Cell Motility and the Cytoskeleton*, 66(3), pp.166–78.
- Mills, M., Yang, N., Weinberger, R.P., Vander Woude, D.L., Beggs, A.H., Easteal, S. & North, K.N., 2001. Differential expression of the actin-binding proteins, alpha-actinin-2 and -3, in different species: implications for the evolution of functional redundancy. *Human Molecular Genetics*, 10(13), pp.1335–46.
- Mishra, D.R., 2015. Some breakthroughs in nanoelectronics in the last decade. *International Journal of Engineering Research and General Science*, 3(2), pp.1340–1357.
- Miyanaga, A., Honda, K., Tsuta, K., Masuda, M., Yamaguchi, U., Fujii, G., Miyamoto, A., Shinagawa, S., Miura, N., Tsuda, H., Sakuma, T., Asamura, H., Gemma, A. & Yamada, T., 2013. Diagnostic and prognostic significance of the alternatively spliced *ACTN4* variant in high-grade neuroendocrine pulmonary tumours. *Annals of Oncology*, 24(1), pp.84–90.
- Mohandas, N. & Gallagher, P.G., 2009. Red cell membrane : past, present and future. *Blood*, 112(10), pp.3939–3948.
- Mohapatra, B., Jimenez, S., Lin, J.H., Bowles, K.R., Coveler, K.J., Marx, J.G., Chrisco, M.A., Murphy, R.T., Lurie, P.R., Schwartz, R.J., Elliot, P.M., Vatta, M., McKenna, W., Towbin, J.A. & Bowles, N.E., 2003. Mutations in the muscle LIM protein and α -actinin-2 genes in dilated cardiomyopathy and endocardial fibroelastosis. *Molecular Genetics and Metabolism*, 80(1-2), pp.207–215.
- Monroe, D.M., Hoffman, M. & Roberts, H.R., 2002. Platelets and thrombin generation. *Arteriosclerosis, Thrombosis, and Vascular Biology*, 22(9), pp.1381–1389.

- Moore, C.A., Keep, N.H. & Kendrick-Jones, J., 2000. Structure of the utrophin actin-binding domain bound to F-actin reveals binding by an induced fit mechanism. *Journal of Molecular Biology*, 297(2), pp. 465-480.
- Moore, C.A. & Kendrick-Jones, J., 2000. Biochemical characterisation of the actin-binding properties of utrophin. *Cytoskeleton*, 46(2), pp. 116-128.
- Morrow, J.S. & Marchesi, V.T., 1981. Self-assembly of spectrin oligomers *in vitro*: a basis for a dynamic cytoskeleton. *The Journal of Cell Biology*, 88(2), pp. 463-468.
- Mukhina, S., Wang, Y.-L. & Murata-Hori, M., 2007. α -Actinin is required for tightly regulated remodelling of the actin cortical network during cytokinesis. *Developmental Cell*, 13(4), pp. 554-565.
- Mundel, P. & Shankland, S.J., 2002. Podocyte biology and response to injury. *Journal of the American Society of Nephrology*, 13(12), pp.3005–3015.
- Murphy, A.C.H. & Young, P.W., 2015. Congenital macrothrombocytopenia-linked mutations in the actin-binding domain of α -actinin-1 enhance F-actin association. *FEBS Letters*, 590(6), pp. 685-695.
- Nakamura, F., Pudas, R., Heikkinen, O., Permi, P., Kilpelainen, I., Munday, A.D., Hartwig, J.H., Stossel, T.P. & Ylanne, J., 2006. The structure of the GPIIb-filamin A complex. *Blood*, 107(5), pp.1925–1932.
- Nangreave, J., Han D., Liu, Y. & 2010. DNA origami: A history and current perspective. *Current Opinion in Chemical Biology*, 14(5), pp.608–615.
- Nans, A., Mohandas, N. & Stokes, D.L., 2011. Native ultrastructure of the red cell cytoskeleton by cryo-electron tomography. *Biophysical Journal*, 101(10), 2341-2350.
- Nayak, S. & Andrew Lyon, L., 2005. Soft nanotechnology with soft nanoparticles. *Angewandte Chemie. International Edition*, 44(47), pp.7686–7708.
- Nelson, D.L. & Cox, M.M., 2005a. Nucleotides and nucleic acids. Ahr, K., Ryan, M., O'Neill, J., Wong, V., Ciprioni, J., Tymoczko, N., *Lehninger's Principles of*

Biochemistry. New York: W.H. Freeman and Company, pp. 273–306.

Nelson, D.L. & Cox, M.M., 2005b. The three dimensional structure of proteins. Ahr, K., Ryan, M., O'Neill, J., Wong, V., Ciprioni, J., Tymoczko, N., *Lehninger's Principles of Biochemistry*. New York: W.H. Freeman and Company, pp. 116–156.

Nelson, David L & Cox, M.M., 2005c. Lipids. Ahr, K., Ryan, M., O'Neill, J., Wong, V., Ciprioni, J., Tymoczko, N., *Lehninger's Principles of Biochemistry*. New York: W.H. Freeman and Company, pp. 343–368.

Nelson, D. & Cox, M.M., 2005d. Biological membranes and transport. Ahr, K., Ryan, M., O'Neill, J., Wong, V., Ciprioni, J., Tymoczko, N., *Lehninger's Principles of Biochemistry*. New York: W.H. Freeman and Company, pp. 369–420.

Nicolas, G., Pedroni, S., Fournier, C., Gautero, H., Craescu, C., Dhermy, D. & Lecomte, M.C., 1998. Spectrin self-association site: characterisation and study of β -spectrin mutations associated with hereditary elliptocytosis. *Biochemical Journal*, 332(1), pp.81-89.

Niemeyer, C.M., 2001. Nanoparticles, proteins and nucleic acids: biotechnology meets materials science. *Angewandte Chemie. International Edition*, 40(22), pp.4128–4158.

Nieset, J.E., Redfield, A.R., Jin, F., Knudson, K.A., Johnson, K.R., Wheelock, M.J., 1997. Characterization of the interactions of α -catenin with α -actinin and β -catenin/plakoglobin. *Journal of Cell Science*, 110(Pt 8), pp.1013–1022.

Ning, Y.M., He, K., Dagher, R., Sridhara, R., Farrell, A., Justice R. & Pazdur, R., 2007. Liposomal doxorubicin in combination with bortezomib for relapsed or refractory multiple myeloma. *Oncology*, 21(1), pp.1503–1508.

North, K., Yang, N., Wattanasirichaigoon, D., Mills, M., Easteal, S., & Beggs, A.H., 1999. A common nonsense mutation results in α -actinin-3 deficiency in the general population. *Nature*, 21(April), pp.353–354.

Norwood, F.L.M., Suderland-Smith, A.J., Keep, N.H. & Kendrick-Jones, J., 2000. The

structure of the N-terminal actin-binding domain of human dystrophin and how mutations in this domain may cause Duchenne or Becker muscular dystrophy. *Structure*, 8(5), pp.481–491.

Nurden, A. & Nurden, P., 2011. Advances in our understanding of the molecular basis of disorders of platelet function. *Journal of Thrombosis and Haemostasis*, 9(1), pp.76–91.

Nurden, A.T., Fiore, M., Nurden, P. & Pillois, X., 2011. Glanzmann thrombasthenia: a review of ITGA2B and ITGB3 defects with emphasis on variants, phenotypic variability, and mouse models. *Blood*, 118(23), pp.5996–6005.

Nurden, P., Debili, N., Coupry, I., Bryckaert, M., Youlyouze-Marfak, I., Sole, G., Pons, A-C., Berrou, E., Adam, F., Kauskot, A., Lamaziere, J-M.D., Rameau, P., Fergelot, P., Rooryck, C., Cailley, D., Arveiler, B., Lacombe, D., Vainchenker, W., Nurden, A. & Goizet, C., 2011. Thrombocytopenia resulting from mutations in filamin A can be expressed as an isolated syndrome. *Blood*, 118(22), pp.5928–5937.

O’Shea, E.K., Klemm, J.D., Kim, P.S. & Alber, T., 1991. X-ray structure of the GCN4 leucine zipper, a two-stranded, parallel coiled-coil. *Science*, 254(5031), pp.539–544.

Otey, C.A, Pavalko, F.M. & Burridge, K., 1990. An interaction between alpha-actinin and the beta 1 integrin subunit in vitro. *The Journal of Cell Biology*, 111(2), pp.721–729.

Otey, C. & Carpen, O., 2004. Alpha-actinin revisited: a fresh look at an old player. *Cell Motility and the Cytoskeleton*, 58(February), pp.104–111.

Pace, C.N. & Scholtz, J.M., 1998. A helix propensity scale based on experimental studies of peptides and proteins. *Biophysical Journal*, 75(1), pp.422–427.

Padilla, J.E., Colovos, C. & Yeates, T.O., 2001. Nanohedra: using symmetry to design self assembling protein cages, layers, crystals, and filaments. *Proceedings of the National Academy of Sciences of the United States of America*, 98(5), pp.2217–2221.

- Park, J.W., Hong, K., Kirpotin, D.B., Colbern G., Shalaby, R., Baselga, J., Shao, Y., Nielsen, U.B., Marks, J.D., Moore, D., Papahadjopoulos, D, Benz, C.C., 2002. Anti-HER2 immunoliposomes: enhanced anticancer efficacy due to targeted delivery. *Clinical Cancer Research*, 8(April), pp.1172–1181.
- Park, S.H., Yin, P., Liu, Y., Reif, J.H., LaBean T.H. and Yan H., 2005. Programmable DNA self-assemblies for nanoscale organization of ligands and proteins. *Nano Letters*, 5(4), pp.729–733.
- Pascual, J., Pfuhl, M., Walther, D., Saraste, M, & Nilges M., 1997. Solution structure of the spectrin repeat: a left-handed antiparallel triple-helical coiled-coil. *Journal of Molecular Biology*, 273(3), pp.740–751.
- Pascual, J., Castresana, J. & Saraste, M., 1997. Evolution of the spectrin repeat. *BioEssays*, 19(9), pp.811–817.
- Pavalko, F.M., Walker, D.M., Graham, L., Goheen, M., Doerschuk, C.M. & Kansas, G.M., 1995. The cytoplasmic domain of L-selectin sinteracts with cytoskeletal proteins via alpha actinin: Receptor positioning in microvilli does not require interaction with alpha actinin. *The Journal of Cell Biology*, 129(4), pp.1155–1164.
- Pavalko, F.M. & Burridge, K., 1991. Disruption of the actin cytoskeleton after microinjection of proteolytic fragments of alpha-actinin. *The Journal of Cell Biology*, 114(3), pp.481–491.
- Pavenstädt, H., Kriz, W. & Kretzler, M., 2003. Cell biology of the glomerular podocyte. *Physiological Reviews*, 83(1), pp.253–307.
- Pecci, A., Panza, E., Pujol-Moix, N., Klersy, C., Di Bari, F., Bozzi, V., Gresele, P., Lethagen, S., Fabris, F., Dufour, C., Granata, A., Doubek, M., Pecoraro, C., Koivisto, P.A., Heller, P.G., Iolascon, A., Alvisi, P., Schwabe, D., De Candia, E., Rocca, B., Rosso, U., Ramenghi, U., Noris, P., Seri, M., Balduini, C.L. & Savoia, A., 2008. Position of nonmuscle myosin heavy chain IIA (NMMHC-IIA) mutations predicts the natural history of MYH9-related disease. *Human Mutation*, 29(3), pp.409–417.

- Perez-Jimenez, R., Godoy-Ruiz, R., Ibarra-Molero, B. & Sanchez-Ruiz, J.M. 2004. The efficiency of different salts to screen charge interactions in proteins: a Hofmeister effect? *Biophysical Journal*, 86(4), pp.2414–2429.
- Pertuy, F., Eckly, A., Weber, J., Proamer, F., Rinckel, J-Y., Lanza, F., Gachet, C. & Leon, C., 2014. Myosin IIA is critical for organelle distribution and F-actin organization in megakaryocytes and platelets. *Blood*, 123(8), pp.1261–1269.
- Peterson, L.J., Rajfur, Z., Maddoz, A.S., Freel, C.D., Chen, Y., Edlund, M., Otey, C., Burridge, K., 2004. Simultaneous stretching and contraction of stress fibers in vivo. *Molecular Biology of the Cell*, 15(April), pp.3497–3508.
- Pinheiro, A. V., Han, D., Shih, W.M. & Yan H., 2011. Challenges and opportunities for structural DNA nanotechnology. *Nature Nanotechnology*, 6(12), pp.763–772.
- Pollard, T.D., Tseng, P.C-H., Rimm, D.L., Bichell, D.P., Williams, R.C., Sinard, J. & Sato, M., 1986. Characterization of alpha-actinin from *Acanthamoeba*. *Cell Motility Cytoskeleton*, 6(6), pp.649–661.
- Pomies, P., Louis, H.A. & Beckerle, M.C., 1997. CRP1, a LIM domain protein implicated in muscle differentiation, interacts with alpha-actinin. *The Journal of Cell Biology*, 139(1), pp.157–168.
- Poulter, N.S. & Thomas, S.G., 2015. Cytoskeletal regulation of platelet formation: coordination of F-actin and microtubules. *International Journal of Biochemistry and Cell Biology*, 66, pp.69–74.
- Quinlan, K.G.R., Seto, J.C., Turner, N., Vandebrouck, A., Floetenmeyer, M., MacArthur, D.G., Raftery, J.M., Lek, M., Yang, N., Parton, R.G., Cooney, G.J. & North, K.N., 2010. α -Actinin-3 deficiency results in reduced glycogen phosphorylase activity and altered calcium handling in skeletal muscle. *Human Molecular Genetics*, 19(7), pp.1335–1346.
- Rajfur, Z., Roy, P., Otey, C., Romer, L & Jacobson, K., 2002. Dissecting the link between stress fibres and focal adhesions by CALI with EGFP fusion proteins. *Nature Cell Biology*, 4(4), pp.286–293.

- Ramaekers, F.C.S. & Bosman, F.T., 2004. The cytoskeleton and disease. *Journal of Pathology*, 204(4), pp.351–354.
- Rambaran, R.N. & Serpell, L.C., 2008. Amyloid fibrils: abnormal protein assembly. *Prion*, 2(3), pp.112–117.
- Raynaud, F., Bonnal, C., Fernandez, E., Bremaud, L., Cerutti, M., Lebart, M-C., Roustan, C., Ouali, A. & Benyamin, Y., 2003. The calpain 1- α -actinin interaction: resting complex between the calcium-dependant protease and its target in cytoskeleton. *European Journal of Biochemistry*, 270(23), pp.4662–4670.
- Reches, M., 2003. Casting metal nanowires within discrete self-assembled peptide nanotubes. *Science*, 300(5619), pp.625–627.
- Reches, M. & Gazit, E., 2004. Formation of closed-cage nanostructures by self-assembly of aromatic dipeptides. *Nano Letters*, 4(4), pp.581–585.
- Reches, M. & Gazit, E., 2006. Molecular self-assembly of peptide nanostructures: mechanism of association and potential uses. *Current Nanoscience*, 2(2), pp.105–111.
- Reddy Chichili, V.P., Kumar, V. & Sivaraman, J., 2013. Linkers in the structural biology of protein-protein interactions. *Protein Science*, 22(2), pp.153–167.
- Reinhard, M., Zumbunn, J., Jaquemar, D., Kuhn, M., Walter, U & Trueb, B., 1999. An α -actinin binding site of zyxin is essential for subcellular zyxin localization and α -actinin recruitment. *The Journal of Biological Chemistry*, 274(19), pp.13410–13418.
- Rendu, F. & Brohard-Bohn, B., 2001. The platelet release reaction: granules' constituents, secretion and functions. *Platelets*, 12(5), pp.261–273.
- Ribeiro, E. de A., Pinotsis, N., Ghisleni, A., Salmazo, A., Konarev, P.V., Kostan, J., Sjoblom, B., Schreiner, C., Polyansky, A.A., Gkougkoulia, E.A., Holt, M.R., Aachmann, F.L., Zagrovic, B., Bordignon, E., Pirker, K.F., Svergun, D.I., Gautel, M. Djinoovic-Carugo, K., 2014. The structure and regulation of human muscle α -

- actinin. *Cell*, 159(6), pp.1447–1460.
- Ridely, A.J., Schwartz, M.A., Burridge, K., Firtel, R.A., Ginsberg, M.H., Borisy, G., Parsons, T.J. & Horwitz, A.R., 2003. Cell migration: integrating signals from front to back. *Science*, 302(5651), pp. 1704-1709.
- Roca-Cusachs, P., Del Rio, A., Puklin-Faucher, E., Gauthier, N.C., Biais, N. & Sheetz, M.P., 2013. Integrin-dependent force transmission to the extracellular matrix by α -actinin triggers adhesion maturation. *Proceedings of the National Academy of Sciences*, 110(15), pp.E1361–E1370.
- Rothemund, P.W.K., 2006. Folding DNA to create nanoscale shapes and patterns. *Nature*, 440(7082), pp.297–302.
- Rothemund, P.W.K. & Andersen, E.S., 2012. The importance of being modular. *Nature*, 485(7400), pp.7–8.
- Rotter, B., Kroviarski, Y., Nicolas, G., Dhermy, D. & Lecomte, M-C., 2004. α -II spectrin is an *in vitro* target for caspase-2, and its cleavage is regulated by calmodulin binding. *Biochemical Journal*, 378(1), pp. 161-168.
- Le Rumeur, E., Hubert, J. & Winder, S.J., 2012. A new twist to coiled coil. *FEBS Letters*, 586(17), pp.2717–2722.
- Ryadnov, M.G., 2007. Peptide α -helices for synthetic nanostructures. *Biochemical Society Transactions*, 35(Pt 3), pp.487–91.
- Salgado, E.N., Radford, R.J. & Tezcan, F.A., 2010. Metal-directed protein self assembly. *Accounts of Chemical Research*, 43(5), pp.661–672.
- Sanger, J.W., Wang, J., Fan, Y., White, J. & Sanger J.M., 2010. Assembly and dynamics of myofibrils. *Journal of Biomedicine and Biotechnology*, 2010.
- Savoia, A., De Rocco, D., Panza, E., Bozzi, V., Scandellari, R., Loffredo, G., Mumford, A., Heller, P.G., Noris, P., De Groot, M.R., Giani, M., Freddi, P., Scognamiglio, F., Riondino, S., Pujol-Moix, N., Fabris, F., Seri, M, Balduini, C.L. & Pecci, A., 2010. Heavy chain myosin 9-related disease (MYH9-RD): Neutrophil inclusions of myosin-9 as a pathognomonic sign of the disorder. *Thrombosis and*

Haemostasis, 103(4), pp.826–832.

Sawyer, W.H. & Puckridge, J., 1973. The dissociation of proteins by chaotropic salts. *The Journal of Biological Chemistry*, 248(24), pp.8429–8433.

Schachtner, H., Calaminus, S.D.J., Sinclair, A., Monypenny, J., Blundell, M.P., Leon, C., Holyoake, T.L., Thrasher, A.J., Michie, A.M., Vukovic, M., Gachet, C., Jones, G.E., Thomas, S.G., Watson, S.P. & Machesky, L.M., 2013. Megakaryocytes assemble podosomes that degrade matrix and protrude through basement membrane. *Blood*, 121(13), pp.2542–2552.

Scheibel, T., Parthasarathy, R., Sawicki G., Lin, X-M., Jaeger, H. & Lindquist, S., 2003. Conducting nanowires built by controlled self-assembly of amyloid fibers and selective metal deposition. *Proceedings of the National Academy of Sciences of the United States of America*, 100(8), pp.4527–32.

Schleif, R., 2003. AraC protein: a love-hate relationship. *BioEssays*, 25(3), pp.274–282.

Schleif, R., 2010. AraC protein, regulation of the l-arabinose operon in *Escherichia coli* , and the light switch mechanism of AraC action. *FEMS Microbiology Reviews*, 34(5), pp.779–796.

Schwartz, H., Koster, S., Kahr, W.H., Michetti, N., Kraemer, B.F., Weitz, D.A., Blaylock, R.C., Kraiss, L.W., Greinacher, A., Zimmerman G.A. & Weyrich, A.S., 2010. Anucleate platelets generate progeny. *Blood*, 115(18), pp.3801–3809.

Seeman, N.C., 2003. DNA in a material world. *Nature*, 421(6921), pp.427–431.

Selliah, N. & Brooks, W.H., 1996. Proteolytic cleavage of α -actinin by calpain in T-cells stimulated with Anti-CD3 monoclonal antibody. *The Journal of Immunology*, 156(9), pp.3215–3221.

Semple, J.W., Italiano, J.E. & Freedman, J., 2011. Platelets and the immune continuum. *Nature Reviews Immunology*, 11(4), pp.264–74.

Seto, J.T., Quinlan, K.G.R., Lek, M., Zheng, X.F., Garton, F., MacArthur, D.G., Hogarth, M.W., Houweling, P.J., Gregorevic, P., Turner, N., Cooney, G.J., Yang,

- N. & North, K.N., 2013. *ACTN3* genotype influences muscle performance through the regulation of calcineurin signaling. *The Journal of Clinical Investigation*, 123(10), pp.4255–4263.
- Shao, H., Travers, T., Camacho, C.J. & Wells, A., 2013. The carboxyl tail of alpha-actinin-4 regulates its susceptibility to m-calpain and thus functions in cell migration and spreading. *International Journal of Biochemistry and Cell Biology*, 45(6), pp.1051–1063.
- Shao, H., Wu, C. & Wells, A., 2010. Phosphorylation of alpha-actinin 4 upon epidermal growth factor exposure regulates its interaction with actin. *Journal of Biological Chemistry*, 285(4), pp.2591–2600.
- Shen, Z., Yan, H., Wang, T & Seeman, N.C., 2004. Paranemic crossover DNA: a generalized Holliday structure with applications in nanotechnology. *Journal of the American Chemical Society*, 126(6), pp.1666–1674.
- Sinclair, J.C., Davies, K.M., Venien-Bryan, C. Noble, M.E.M., 2011. Generation of protein lattices by fusing proteins with matching rotational symmetry. *Nature Nanotechnology*, 6(9), pp.558–62.
- Singh, S.M. & Mallela, K.M.G., 2012. The N-terminal actin binding tandem calponin homolgy (CH) domain of dystrophin is in a closed conformation in solution and when bound to F-actin. *Biophysical Journal*, 103(9), pp. 1970-1978.
- Sjöblom, B., Salmazo, A. & Djinić-Carugo, K., 2008. α -Actinin structure and regulation. *Cellular and Molecular Life Sciences*, 65(17), pp.2688–2701.
- Smyth, S.S., McEver, R.P., Weyrich, A.S., Morrell, C.N., Hoffman, M.R., Arepally, G.M., French, P.A., Dauerman, H.L. & Becker, R.C., 2009. Platelet functions beyond hemostasis. *Journal of Thrombosis and Haemostasis*, 7(11), pp.1759–1766.
- Speicher, D.W., DeSilva, T.M., Speicher, K.D., Ursitti, J.A., Hembach, P. & Weglarz, L., 1993. Location of the human red cell spectrin tetramer binding site and detection of a related ‘closed’ hairpin loop dimer using proteolytic footprinting. *The Journal of Biological Chemistry*, 268(6), pp.4227–4235.

- Speicher, D.W., Weglarz, L. & Desilva, T.M., 1992. Properties of human red cell spectrin heterodimer (side-to-side) assembly and identification of an essential nucleation site. *The Journal of Biological Chemistry*, 267(21), pp.14775–14782.
- Sprague, C.R., Fraley, T.S., Jang, H.S., Lal, S. & Greenwood, J.A., 2008. Phosphoinositide binding to the substrate regulates susceptibility to proteolysis by calpain. *The Journal of Biological Chemistry*, 283(14), pp.9217–9223.
- Squire, J.M., 1997. Architecture and function in the muscle sarcomere. *Current Opinion in Structural Biology*, 7(2), pp.247–257.
- Stossel, T.P., Condeelis, J., Cooley, L., Hartwig, J.H., Noegel, A., Schleicher, M. & Shapiro, S.S., 2001. Filamins as integrators of cell mechanics and signalling. *Nature Reviews. Molecular Cell Biology*, 2(2), pp.138–145.
- Studier, F.W. & Moffatt, B. A., 1986. Use of bacteriophage T7 RNA polymerase to direct selective high-level expression of cloned genes. *Journal of Molecular Biology*, 189(1), pp.113–130.
- Sung, L.A., Chien, S., Fan, Y-S., Lin, C.C., Lambert, K., Zhu, L., Lam, J.S. & Chang, L-S., 1992. Human erythrocyte protein 4.2: isoform expression, differential splicing, and chromosomal assignment. *Blood*, 79(10), pp.2763–2771.
- Suzuki, A., Goll, D.E., Singh, I., Allen, R.E., Robson, R.M. & Stromer, M.H., 1976. Some properties of purified skeletal muscle alpha-actinin. *The Journal of Biological Chemistry*, 251(21), pp.6860–6870.
- Swierczewska, M., Han, H.S., Kim, K., Park, J.H. & Lee, S., 2016. Polysaccharide-based nanoparticles for theranostic nanomedicine. *Advanced Drug Delivery Reviews*, 99(Pt A), pp.70–84.
- Tadokoro, S., Nakazawa, T., Kamae, T., Kiyomizu, K., Kashiwagi, H., Honda, S., Kanakura, Y. & Tomiyama, Y., 2011. A potential role for alpha-actinin in inside-out $\alpha\text{IIb}\beta\text{3}$ signaling. *Blood*, 117(1), pp.250–258.
- Tang, J., Taylor, D.W. & Taylor, K. A., 2001. The three-dimensional structure of

- alpha-actinin obtained by cryoelectron microscopy suggests a model for calcium-dependent actin binding. *Journal of Molecular Biology*, 310(4), pp.845–58.
- Tatarnikova, O.G., Orlov, M.A. & Bobkova, N. V, 2015. Beta-amyloid and tau-protein: structure, interaction, and prion-like properties. *Biochemistry*, 80(13), pp.1800–1819.
- Taylor, K. A. & Taylor, D.W., 1993. Projection image of smooth muscle alpha-actinin from two-dimensional crystals formed on positively charged lipid layers. *Journal of Molecular Biology*, 230(1), pp.196–205.
- Theis, J.L., Bos, J.M., Bartleson, V.B., Will, M.L., Binder, J., Vatta, M., Towbin, J.A., Gersh, B.J., Ommen, S.R. & Ackerman, M.J., 2006. Echocardiographic-determined septal morphology in Z-disc hypertrophic cardiomyopathy. *Biochemical and Biophysical Research Communications*, 351(4) pp.896–902.
- Thomas, G.H., Newbern, E.C., Korte, C.C., Bales, M.A., Muse, S. V., Clark, A.G. & Kiehart, D.P., 1997. Intragenic duplication and divergence in the spectrin superfamily of proteins. *Molecular Biology and Evolution*, 14(12), pp.1285–95.
- Thon, J.N., Montalvo, A., Patel-Hett, S., Devine M.T., Richardson, J.L., Ehrlicher, A., Larson, M.K., Hoffmesiter, K., Hartwig, J.H. & Italiano J.E. Jr., 2010. Cytoskeletal mechanics of proplatelet maturation and platelet release. *Journal of Cell Biology*, 191(4), pp.861–874.
- Thon, J.N. & Italiano, J.E., 2012. Does size matter in platelet production? *Blood*, 120(8), pp.1552–61.
- Tojkander, S., Gateva, G. & Lappalainen, P., 2012. Actin stress fibers - assembly, dynamics and biological roles. *Journal of Cell Science*, 125(Pt 8), pp.1855–1864.
- Trave, G., Pastore, A., Hyvonen, M. & Saraste, M., 1995. The C-terminal domain of alpha-spectrin is structurally related to calmodulin. *European Journal of Biochemistry*, 227(1-2), pp.35–42.
- Tsai, C-J., Polverino de Laureto, P., Fontana, A. & Nussinov, R., 2002. Comparison of

protein fragments identified by limited proteolysis and by computational cutting of proteins. *Protein science*, 11(7), pp.1753–1770.

Tyler, J.M., Anderson, J.M. & Branton, D., 1980. Structural comparison of several actin-binding macromolecules. *The Journal of Cell Biology*, 85(May), pp.489–495.

Ugwu, S.O. & Apte, S.P., 2004. The effect of buffers on protein conformational stability. *Pharmaceutical Technology*, March, pp.1387–1395.

Ursitti, J. A., Kotula, L., DeSilva, T.M., Curtis, P.J. & Speicher, D.W., 1996. Mapping the human erythrocyte beta-spectrin dimer initiation site using recombinant peptides and correlation of its phasing with the alpha-actinin dimer site. *The Journal of Biological Chemistry*, 271(12), pp.6636–6644.

Uzoigwe, C., 2006. The human erythrocyte has developed the biconcave disc shape to optimise the flow properties of the blood in the large vessels. *Medical Hypotheses*, 67(5), pp.1159–1163.

Vallenius, T., Luukko, E. & Makela, T.P., 2000. CLP-36 PDZ-LIM protein associates with nonmuscle alpha -actinin-1 and alpha -actinin-4. *The Journal of Biological Chemistry*, 275(15), pp.11100–11105.

Vallenius, T. & Mäkelä, T.P., 2002. Clk1: a novel kinase targeted to actin stress fibers by the CLP-36 PDZ-LIM protein. *Journal of Cell Science*, 115(Pt 10), pp.2067–73.

te Velthuis, A.J.W., Isogai, T., Gerrits, L. & Bagowski, C.P., 2007. Insights into the molecular evolution of the PDZ/LIM family and identification of a novel conserved protein motif. *PLoS ONE*, 2(2).

Viel, A., 1999. Alpha-actinin and spectrin structures: an unfolding family story. *FEBS Letters*, 460(3), pp.391–394.

Viel, A. & Branton, D., 1994. Interchain binding at the tail end of the *Drosophila* spectrin molecule. *Proceedings of the National Academy of Sciences of the United States of America*, 91(23), pp.10839–10843.

- Vigoreaux, J.O., 1994. The muscle Z band: lessons in stress management. *Journal of Muscle Research and Cell Motility*, 15(3), pp.237–55.
- Villar, G., Wilber, A.W., Williamson, A.J., Thiara, P., Doye, J.P.K., Louis, A.A., Jochum M.N., Lewis, A.C.F. & Levy, E.D., 2009. Self-assembly and evolution of homomeric protein complexes. *Physical Review Letters*, 102(11), pp.4–7.
- Virel, A. & Backman, L., 2004. Molecular evolution and structure of α -actinin. *Molecular Biology and Evolution*, 21(6), pp.1024-1031
- Wang, P., Ko, S.H., Tian, C., Hao, C. & Mao, C., 2013. RNA-DNA hybrid origami: folding of a long RNA single strand into complex nanostructures using short DNA helper strands. *Chemical Communications*, 49(48), pp.5462–4.
- Wasenius, V-M., Saraste, M., Salven, P., Eramaa, M., Holm, L. & Lehto, V-P., 1989. Primary structure of brain α -spectrin. *The Journal of Cell Biology*, 108(1), pp. 79-93.
- Way, M., Pope, B. & Weeds, A.G., 1992. Evidence for functional homology in the F-actin binding domains of gelsolin and α -actinin: implications for the requirements of severing and capping. *The Journal of Cell Biology*, 119(4), pp.835–842.
- Weins, A., Schlondorff, J.S., Nakamura, F., Denker, B.M., Hartwig, J.H., Stossel, T.P. & Pollak, M.R., 2007. Disease-associated mutant alpha-actinin-4 reveals a mechanism for regulating its F-actin-binding affinity. *Proceedings of the National Academy of Sciences of the United States of America*, 104(41), pp.16080–16085.
- Weins, A., Kenlan, P., Herbert, S., Le, T.C., Villegas, I., Kaplan, B.S., Appel, G.B. & Pollak, M.R., 2005. Mutational and biological analysis of alpha-actinin-4 in focal segmental glomerulosclerosis. *Journal of the American Society of Nephrology*, 16(12), pp.3694–3701.
- White, J., Barro, M.V., Makarenkova, H.P., Sanger, J.W. Sanger, J.M., 2014. Localization of sarcomeric proteins during myofibril assembly in cultured mouse primary skeletal myotubes. *Anatomical Record*, 297(9), pp.1571–1584.

- Whitesides, G.M., Mathias, J.P. & Seto, C.T., 1991. Molecular self-assembly and nanochemistry. A chemical strategy for the synthesis of nanostructures. *Science*, 254(5036), pp.1312–1319.
- Williamson, D., Pikovski, I., Cranmer, S.L., Mangin, P., Mistry, N., Domagala, T., Chehab, S., Lanza, F., Salem, H.H. & Jackson, S.P., 2002. Interaction between platelet glycoprotein Iba and filamin-1 is essential for glycoprotein Ib/IX receptor anchorage at high shear. *The Journal of Biological Chemistry*, 277(3), pp.2151–2159.
- Willis, M.S., Schliser, J.C., Portbury, A.L. & Patterson, C., 2009. Build it up-Tear it down: protein quality control in the cardiac sarcomere. *Cardiovascular Research*, 81(3), pp.439–448.
- Winder, S.J., Hemmings, L., Maciver, S.K., Bolton, S.J., Tinslet, J.M., Davies, K.E., Critchley, D.R. & Kendrick-Jones, J., 1995. Utrophin actin binding domain: analysis of actin binding and cellular targeting. *Journal of Cell Science*, 108 (Pt 1), pp. 63-71.
- Winder, S.J. & Ayscough, K.R., 2005. Actin-binding proteins. *Journal of Cell Science*, 118(4), pp.651–654.
- Winkelmann, J.C., Costa, F.F., Linzie, B.L. & Forget, B.G., 1990. β -spectrin in human skeletal muscle. *The Journal of Biological Chemistry*, 265(33), pp. 20449-20454.
- Winkelmann, J.C. & Forget, B.G., 1993. Erythroid and nonerythroid spectrins. *Blood*, 81(12), pp.3173–85.
- Winkler, J., Lünsdorf, H. & Jockusch, B.M., 1997. Flexibility and fine structure of smooth-muscle alpha-actinin. *European Journal of Biochemistry*, 248(1), pp.193–199.
- Woolfson, D.N., Bartlett, G.J., Bruning, M. & Thomson, A.R., 2012. A new currency for old rope: from coiled-coil assemblies to α -helical barrels. *Current Opinion in Structural Biology*, 22(4), pp. 432-441.
- Woolfson, D.N., 2005. The design of coiled-coil structures and assemblies. *Advances*

in Protein Chemistry, 70, pp. 79-112.

Workman, R.F. & Low, P.S., 1998. Biochemical analysis of potential sites for protein 4.1 mediated anchoring of the spectrin-actin skeleton to the erythrocyte membrane. *The Journal of Biological Chemistry*, 273(11), pp. 6171-6173.

Xia, Y. & Whitesides, G.M., 1998. Soft Lithography. *Angewandte Chemie. International Edition*, 28, pp.153–184.

Yamada, S., Yanamoto, S., Yoshida, H., Yoshitomi, I., Kawasaki, G., Mizuno, A. & Nemoto, T.K., 2010. RNAi-mediated down-regulation of α -actinin-4 decreases invasion potential in oral squamous cell carcinoma. *International Journal of Oral and Maxillofacial Surgery*, 39(1), pp.61–67.

Yamaguchi, H. & Condeelis, J., 2007. Regulation of the actin cytoskeleton in cancer cell migration and invasion. *Biochimica et Biophysica Acta - Molecular Cell Research*, 1773(5), pp.642–652.

Yamamoto, S., Tsuda, H., Honda, K., Onozato, K., Takano, M., Tamai, S., Imoto, I., Inazawa, J., Yamada, T. & Matsubara, O., 2009. Actinin-4 gene amplification in ovarian cancer: a candidate oncogene associated with poor patient prognosis and tumor chemoresistance. *Modern pathology*, 22(4), pp.499–507.

Yamamoto, S., Tsuda, H., Honda, K., Takano, M., Tamai, S., Imoto, I., Inazawa, J., Yamada, T. & Matsubara, O., 2012. *ACTN4* gene amplification and actinin-4 protein overexpression drive tumour development and histological progression in a high-grade subset of ovarian clear-cell adenocarcinomas. *Histopathology*, 60(7), pp.1073–1083.

Yan, H., Park, S.H., Finkelstein G., Reif, J.H. & LaBean, T.H., 2003. DNA-templated self-assembly of protein arrays and highly conductive nanowires. *Science*, 301(5641), pp.1882–1884.

Yan, Y., Winograd, E., Viel, A., Cronin, T., Harrison, S.C. & Branton, D., 1993. Crystal structure of the repetitive segments of spectrin. *Science*, 262(5142), pp.2027–2030.

- Yang, N., MacArthur, D.G., Gulbin, J.P., Hahn, A.G., Beggs, A.H., Easteal, S. & North, K., 2003. *ACTN3* genotype is associated with human elite athletic performance. *American Journal of Human Genetics*, 73(3), pp.627–631.
- Yang, N., MacArthur, D.G., Wolde, B., Onywera, V.O., Boit, M.K., Lau, S.Y.M-A., Wilson, R.H., Scott, R.A., Pitsiladis Y.P. & North, K., 2007. The *ACTN3* R577X polymorphism in east and west African athletes. *Medicine and Science in Sports and Exercise*, 39(11), pp.1985–1988.
- Yao, J., Le, T.C., Kos, C.H., Henderson J.M., Allen, P.G., Benker, B.M. & Pollak, M.R., 2004. Alpha-actinin-4-mediated FSGS: An inherited kidney disease caused by an aggregated and rapidly degraded cytoskeletal protein. *PLoS Biology*, 2(6), pp.787–794.
- Yao, N.Y., Becker, D.J., Broedersz, C.P., Depken, M., MacKintosh F.C., Pollak, M.R. & Weitz, D.A., 2011. Nonlinear viscoelasticity of actin transiently cross-linked with mutant alpha-actinin-4. *Journal of Molecular Biology*, 411(5), pp.1062–1071.
- Yasutomi, M., Kunishima, S., Okazaki, S., Tanizawa, A., Tsuchida, S. & Ohshima, Y., 2016. *ACTN1* rod domain mutation associated with congenital macrothrombocytopenia. *Annals of Hematology*, 95(1), pp.141–144.
- Ye, N., Verma, D., Meng, F., Davidson, M.W., Suffoletto, K. & Hua, S.Z., 2014. Direct observation of α -actinin tension and recruitment at focal adhesions during contact growth. *Experimental Cell Research*, 327(1), pp.57–67.
- Ylännä, J., Scheffzek, K., Young, P. & Saraste, M., 2001. Crystal structure of the alpha-actinin rod reveals an extensive torsional twist. *Structure*, 9(1), pp.597–604.
- Yoshino, H. & Marchesi, V.T., 1984. Isolation of spectrin subunits and reassociation *in vitro*. *The Journal of Biological Chemistry*, 259(7), pp. 4496-4500.
- Young, P., Ferguson, C., Banuelos, S. & Gautel, M., 1998. Molecular structure of the sarcomeric Z-disk: two types of titin interactions lead to an asymmetrical sorting of α -actinin. *The EMBO Journal*, 17(6), pp.1614–1624.

- Young, P. & Gautel, M., 2000. The interaction of titin and alpha-actinin is controlled by a phospholipid-regulated intramolecular pseudoligand mechanism. *The EMBO Journal*, 19(23), pp.6331–40.
- Zadegan, R.M. & Norton, M.L., 2012. Structural DNA nanotechnology: from design to applications. *International Journal of Molecular Sciences*, 13(6), pp.7149–7162.
- Zhang, P., Talluri, S., Deng, H., Branton, D. & Wagner, G., 1995. Solution structure of the pleckstrin homology domain of *Drosophila* β -spectrin. *Structure*, 3(11), pp.1185-1195.
- Zhang, R., Zhang, C.Y., Zhao, Q. & Li, D.H., 2013. Spectrin: structure, function and disease. *Science China Life Sciences*, 56(12), pp.1076–1085.
- Zhang, S., 2003. Fabrication of novel biomaterials through molecular self-assembly. *Nature Biotechnology*, 21(10), pp.1171–8.
- Zhang, S., Holmes, T.C., DiPersio, C.M., Hynes, R.O., Su, X. & Rich, A., 1995. Self Complimentary oligopeptide support mammalian cell attachment. *Biomaterials*, 16(18), pp.1385–1393.
- Zhao, X., 2009. Design of self-assembling surfactant-like peptides and their applications. *Current Opinion in Colloid and Interface Science*, 14(5), pp.340–348.
- Zhao, X. & Zhang, S., 2007. Designer self-assembling peptide materials. *Macromolecular Bioscience*, 7(5), pp.13–22.

6. Appendix

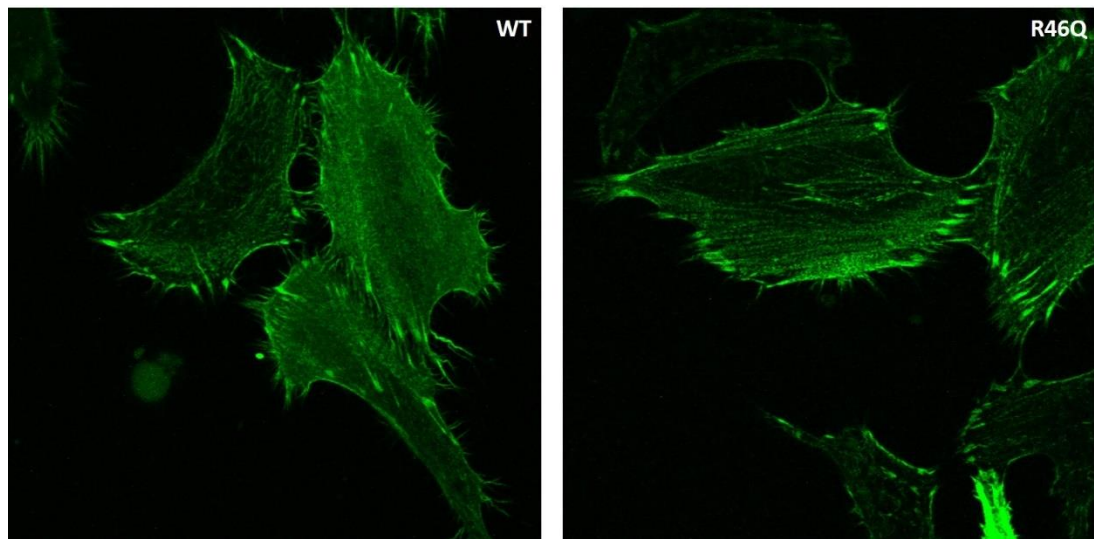


Figure 6.1: Projection confocal z-stack of HeLa cells overexpressing GFP-tagged WT or p.Arg46Gln actinin-1 proteins. No major disruption of the cytoskeleton was observed in cells overexpressing GFP-WT-actinin-1 or GFP-p.Arg46Gln-actinin-1; all cells show similar actinin organisation.